

# Innate sensing of $\beta$ -glucans in plants: insights into the role of host $\beta$ -glucanases and fungal cell surface glycans in plant-fungal interactions



Inaugural-Dissertation  
zur Erlangung des Doktorgrades  
der Mathematisch-Naturwissenschaftlichen Fakultät  
der Universität zu Köln

Vorgelegt von

**Alan Wanke**  
aus Zabrze (Polen)

Köln, 23. Februar 2023

**Advisory committee**

**First supervisor**

Prof. Dr. Alga Zuccaro

**Second supervisor**

Prof. Dr. Jane Parker

**Third supervisor**

Dr. Ruben Garrido-Oter

**Thesis committee**

**First supervisor**

Prof. Dr. Alga Zuccaro

**Second supervisor**

Prof. Dr. Bart Thomma

**Chair of thesis committee**

Prof. Dr. Jan Riemer

The presented research was conducted under the auspices of the Graduate School of Biological Sciences (University of Cologne) and the Max Planck Research School (Max Planck Institute for Plant Breeding Research)

“Denn so wie ihr Augen habt, um das Licht zu sehen und Ohren, um Klänge zu hören, so habt ihr ein Herz, um damit die Zeit wahrzunehmen. Und alle Zeit, die nicht mit dem Herzen wahrgenommen wird, ist so verloren wie die Farben des Regenbogens für einen Blinden oder das Lied eines Vogels für einen Tauben.”

Michael Ende (*Momo*, 1973)

Parts of this thesis were published in following articles:

**Chandrasekar, B.\***, **Wanke, A.\***, **Wawra, S.\***, **Saake, P.**, **Mahdi, L.**, **Charura, N.**, **Neidert, M.**, **Poschmann, G.**, **Malisic, M.**, **Thiele, M.**, **Stühler, K.**, **Dama, M.**, **Pauly, M.**, & **Zuccaro, A. (2022)**. Fungi hijack a ubiquitous plant apoplastic endoglucanase to release a ROS scavenging  $\beta$ -glucan deca-saccharide to subvert immune responses. *The Plant Cell*, 34(7), 2765–2784. <https://doi.org/10.1093/plcell/koac114>

**Wanke, A.**, **Malisic, M.**, **Wawra, S.**, & **Zuccaro, A. (2021)**. Unraveling the sugar code: the role of microbial extracellular glycans in plant-microbe interactions. *Journal of Experimental Botany*, 72(1), 15–35. <https://doi.org/10.1093/jxb/eraa414>

**Wanke, A.\***, **Rovenich, H.\***, **Schwanke, F.**, **Velte, S.**, **Becker, S.**, **Hehemann, J.-H.**, **Wawra, S.**, & **Zuccaro, A. (2020)**. Plant species-specific recognition of long and short  $\beta$ -1,3-linked glucans is mediated by different receptor systems. *The Plant Journal*, 102(6), 1142–1156. <https://doi.org/10.1111/tpj.14688>

Further publications published in framework of this thesis (not included):

**Vanacore, A.**, **Vitiello, G.**, **Wanke, A.**, **Cavasso, D.**, **Clifton, L. A.**, **Mahdi, L.**, **Campanero-Rhodes, M. A.**, **Solís, D.**, **Wuhrer, M.**, **Nicolardi, S.**, **Molinaro, A.**, **Marchetti, R.**, **Zuccaro, A.**, **Paduano, L.**, & **Silipo, A. (2022)**. Lipopolysaccharide O-antigen molecular and supramolecular modifications of plant root microbiota are pivotal for host recognition. *Carbohydrate Polymers*, 277, 118839. <https://doi.org/10.1016/j.carbpol.2021.118839>



# Content

	Abstract (Zusammenfassung)	<b>1</b>
<b>Chapter 1</b>	General Introduction	<b>5</b>
<b>Chapter 2</b>	Unravelling the sugar code: the role of microbial extracellular glycans in plant–microbe interactions	<b>25</b>
<b>Chapter 3</b>	Plant species-specific recognition of long and short $\beta$ -1,3-linked glucans is mediated by different receptor systems	<b>48</b>
<b>Chapter 4</b>	Fungi hijack a ubiquitous plant apoplastic endoglucanase to release a ROS scavenging $\beta$ -glucan deca-saccharide to subvert immune responses	<b>74</b>
<b>Chapter 5</b>	A GH81-type $\beta$ -glucan-binding protein facilitates colonization by mutualistic fungi in barley	<b>119</b>
<b>Chapter 6</b>	Concluding discussion	<b>169</b>
	List of abbreviations	<b>190</b>
	Author contributions	<b>192</b>
	Acknowledgements	<b>194</b>
	Eidesstattliche Erklärung	<b>197</b>
	About the author	<b>198</b>

## Abstract

As plants constantly interact with living organisms from all kingdoms of life, they deploy receptor-based surveillance systems to assess their immediate surroundings and adapt accordingly. Glycans, a major component of cell surfaces in microbes and plants, represent a central class of ligands for these receptors, enabling plants to effectively interpret their biotic environment. Upon enzymatic attack, hydrolytically released fragments inform the host about putative invaders and self-damage. Moreover, some microbes actively secrete glycan-based molecules as symbiotic messenger to initiate host symbiotic programs. In most cases, it is not the perception of a single molecule but rather the continuous integration of an array of signals, creating a complex and intertwined signaling network that shapes the host response.

Fungal cell wall  $\beta$ -glucans represent an important class of glycans in plant-fungal interactions. Although it has long been known that  $\beta$ -glucans can elicit plant immunity, our understanding of the molecular principles underlying this process has been hindered by technical challenges. With the recent advances in glycan biochemistry and plant immunity research, new tools and resources emerged to readdress the fundamental questions underpinning innate sensing of  $\beta$ -glucans in plants.

To establish a comprehensive literature-based foundation for this thesis, we conducted an extensive review of our current understanding on the impact of glycans in various plant-microbial interactions (**Chapter 2**). Furthermore, we spotlight how the use of secreted fungal lectins as microscopic probes can advance our view on fungal cell wall architectures. Based on recent literature and our own microscopic observations, we present a *three-layer cell wall model* for plant-associated fungi.

We performed a systematic study on the perception of short-chain and long-chain  $\beta$ -glucans in different plants which revealed striking species-specific differences in  $\beta$ -glucan perception based on  $\beta$ -glucan polymer length (**Chapter 3**). We demonstrate that perception of these two classes of  $\beta$ -glucan substrates is mediated by different receptor systems, unveiling a previously unknown, CERK1-independent glucan perception pathway in plants.

Although recent studies emphasized the presence of a  $\beta$ -glucan-rich extracellular polysaccharide matrix surrounding fungal hyphae, only little is known on the function of this outer most cell wall layer. In **Chapter 4**, we isolated cell walls from the root

mutualistic fungus *Serendipita indica* and the hemibiotrophic pathogen *Bipolaris sorokiniana*, separating the outer, amorphous polysaccharide matrix from the rigid inner cell wall core. We show that these two layers are separate but interconnected compartments with distinct glycomic and proteomic signatures. Moreover, we demonstrate that fungi hijack the host hydrolytic machinery to release an antioxidative  $\beta$ -glucan deca-saccharide from their extracellular polysaccharide matrix to facilitate plant colonization. This mechanism represents a conserved strategy in phylogenetically distant fungi with different plant-associated lifestyles.

In **Chapter 5**, we applied a proteomic pull-down approach with biotinylated laminarin to identify host components involved in  $\beta$ -glucan-mediated immunity pathways. This identified a GH81-type  $\beta$ -1,3-endoglucanase that acts a tissue-independent compatibility factor for mutualistic and pathogenic fungi.

Overall, the findings presented in this thesis contribute several novel aspects with regards to fungal cell wall architecture as well as the processing and perception of  $\beta$ -1,3-glucans by plants. These concepts not only directly impact our understanding of plant-fungal interactions, but furthermore highlight the role of glycans in the context of complex microbial communities.

## Zusammenfassung

Da Pflanzen permanent mit lebenden Organismen in ihrer Umwelt interagieren, setzen sie rezeptorbasierte Überwachungssysteme ein um ihre unmittelbare Umgebung zu bewerten und sich ihr entsprechend anzupassen. Glykane sind ein wichtiger Bestandteil von Zelloberflächen vieler Mikroben und Pflanzen und stellen hierbei eine zentrale Klasse von Liganden für diese Rezeptoren dar, die es Pflanzen ermöglichen, ihre belebte Umgebung zu bewerten. Pflanzen und Pilze sekretieren hydrolytische Enzyme in den Apoplasten; die hierdurch freigesetzten Glykanfragmente informieren den Wirt über vermeintliche Eindringlinge und kolonisierungsbedingte Schäden an der eigenen Zellwand. Darüber hinaus scheiden einige Mikroben Glykan-basierte Moleküle als symbiotische Botenstoffe aus. Die Entscheidung, wie Pflanzen auf ihre Umwelt reagieren, wird in den meisten Fällen nicht durch die Wahrnehmung eines einzelnen Moleküls entschieden, sondern basiert auf der kontinuierlichen Integration vieler Stimuli, die ein verwobenes Signalnetzwerk schaffen.

Pilzliche Zellwand- $\beta$ -Glukane stellen eine wichtige Gruppe von Glykanen in Interaktionen zwischen Pflanzen und Pilzen dar. Obwohl bekannt ist, dass  $\beta$ -Glukane eine pflanzliche Immunität auslösen können, ist unser Verständnis über die molekularen Grundlagen, die diesem Prozess zugrunde liegen, unbekannt. Mit den jüngsten Fortschritten in der Glykanbiochemie und der Forschung zur pflanzlichen Immunität sind neue Werkzeuge und Ressourcen entstanden, um die grundlegenden Fragen zur Erkennung von  $\beta$ -Glukanen in Pflanzen neu zu betrachten.

Um eine literaturbasierte Grundlage für diese Arbeit zu schaffen, haben wir eine umfassende Zusammenfassung unseres aktuellen Verständnisses über die Rolle von Glykanen in verschiedenen pflanzlich-mikrobiellen Interaktionen erstellt (**Kapitel 2**). Darüber hinaus erläutern wir, wie der Einsatz von sekretierten Pilzlektinen als mikroskopische Sonden unser Verständnis von pilzlichen Zellwänden vorantreiben kann. Basierend auf aktueller Literatur und unseren eigenen mikroskopischen Beobachtungen präsentieren wir ein dreischichtiges Zellwand-Modell für pflanzen-assoziierte Pilze.

Wir haben eine systematische Studie zur Erkennung von kurzkettigen und langkettigen  $\beta$ -Glukanen in verschiedenen Pflanzen durchgeführt, die artenspezifische Unterschiede in der Wahrnehmung von  $\beta$ -Glukanen aufgrund der

Polymerlänge aufgedeckt hat (**Kapitel 3**). Wir zeigen, dass die Wahrnehmung dieser beiden Klassen von  $\beta$ -Glukanen durch verschiedene Rezeptorsysteme vermittelt wird, was einen zuvor unbekanntem, CERK1-unabhängigen Signalweg für die Erkennung von  $\beta$ -Glukanen enthüllt.

Obwohl neuste Studien die Anwesenheit einer  $\beta$ -Glukan-reichen extrazellulären Polysaccharidmatrix um Pilzhyphen betonen, ist wenig über die Funktion dieser äußersten Zellwandschicht bekannt. In **Kapitel 4** haben wir Zellwände des mutualistischen Wurzelpilzes *Serendipita indica* und des hemibiotrophen Pathogens *Bipolaris sorokiniana* isoliert und diese mobile  $\beta$ -Glukanschicht vom starren inneren Zellwandkern getrennt. Wir zeigen, dass diese beiden Schichten separate, aber miteinander verbundene Kompartimente mit unterschiedlichen glykomischen und proteomischen Signaturen sind. Darüber hinaus demonstrieren wir, dass Pilze die hydrolytische Maschinerie des Wirts nutzen um ein antioxidatives  $\beta$ -Glukan-Decasaccharid aus ihrer extrazellulären Polysaccharidmatrix freizusetzen, das die Kolonisierung ihrer Wirte fördert. Dieser Mechanismus stellt eine konservierte Strategie in phylogenetisch unverwandten Pilzen mit unterschiedlichen pflanzen-assoziierten Lebensstilen dar.

In **Kapitel 5** haben wir einen *Pull-Down*-Ansatz mit biotinyliertem Laminarin angewendet um Wirtskomponenten zu identifizieren, die an  $\beta$ -Glukan-vermittelter Immunität beteiligt sind. Hierbei wurde eine GH81-Typ  $\beta$ -1,3-Endoglucanase identifiziert, die als gewebsunabhängiger Kompatibilitätsfaktor für Pilze agiert.

Die in dieser Arbeit vorgestellten Ergebnisse tragen mehrere neue Aspekte zur Pilzzellwandarchitektur sowie zur Verarbeitung und Wahrnehmung von  $\beta$ -1,3-Glukanen durch Pflanzen bei. Diese Konzepte bereichern nicht nur unser Verständnis von Pflanze-Pilz-Interaktionen, sondern heben auch die Rolle von Glykanen im Kontext komplexer mikrobieller Gemeinschaften hervor.

# **Chapter 1**

## **General Introduction**

## A schematic overview of the plant immune system

### The plant microbiome and plant immunity

Plants are constantly exposed to a multitude of microbes living inside (i.e. endophytically) and outside (i.e. epiphytically) their tissues. Collectively, these microbial consortia are known as the plant microbiome. The microbiome consists of bacteria, archaea, fungi, oomycetes and other protists that can act as commensals, pathogens or mutualists (Schlaeppli & Bulgarelli, 2015). It significantly impacts plant fitness due to its contributions to nutrient and water acquisition (Rolli *et al.*, 2015; Hacquard *et al.*, 2015; Hiruma *et al.*, 2016; Almario *et al.*, 2017; Finkel *et al.*, 2020), pathogen defense (Berendsen *et al.*, 2012; Vannier *et al.*, 2019; Sarkar *et al.*, 2019; Mahdi *et al.*, 2021) and resilience against abiotic stress (Vorholt *et al.*, 2017; Khare *et al.*, 2018; Xu *et al.*, 2018; Liu *et al.*, 2020a). Plants actively shape their microbiome through different means, including the presence of physical barriers like cell walls (CWs), the secretion of root exudates containing nutrients, plant hormones, signaling molecules and antimicrobials as well as through their immune system (Bais *et al.*, 2006; Sasse *et al.*, 2018; Fitzpatrick *et al.*, 2020; Kawa & Brady, 2022). In particular, host immune receptors are crucial surveillance tools to monitor the microbiome composition. Mutations of central immune-related gene networks hubs in plants destabilize and alter microbial compositions, a condition referred to as microbiota dysbiosis (Chen *et al.*, 2020). Dysbiotic microbiomes exhibit either an overrepresentation of pathogenic microbes or a reduced microbial diversity, both associated with detrimental impacts on plant health and yield (Liu *et al.*, 2020b).

Two classes of receptors mediate scrutiny of the microbiome composition: membrane-integral pattern recognition receptors (PRRs) with extracellular recognition domains, and intracellular nucleotide-binding leucine-rich repeat receptors (NLRs) (Jones & Dangl, 2006). Due to the evolutionary arms race between microbes and their hosts, receptor gene families for both PRRs and NLRs have massively expanded in many land plant lineages (Ngou *et al.*, 2022). Although these receptors are tightly intertwined and form a complex, continuous signaling network, they were classically separated into two tiers of immunity. While membrane receptors mediate pattern-triggered immunity (PTI, Figure 1A), intracellular receptors are responsible for effector-triggered immunity (ETI, Figure 1B) (Jones & Dangl, 2006). However, rigid use of terminology as well as the observation that PRRs could bind apoplastic effectors have led to

controversies about this categorization of plant immunity (Thomma *et al.*, 2011). This debate gave rise to several approaches to conceptualize plant immunity (Cook *et al.*, 2015; van der Burgh & Joosten, 2019; Lacaze & Joly, 2020; Ding *et al.*, 2021). To stay consistent with the terminology used in the upcoming chapters, I will adhere to the traditional PTI/ETI concept.

### Pattern-triggered immunity

Most PRRs are receptor-like kinases (RLKs) consisting of an intracellular kinase domain, a hydrophobic transmembrane stretch, and an extracellular ligand-binding recognition domain (Boutrot & Zipfel, 2017). Receptor-like proteins (RLPs) lack the intracellular kinase domain, for which reason they constitutively associate with a RLK to form a functional dimeric receptor complex (Gust & Felix, 2014). Activation of PTI is triggered by the binding of microbe-associated molecular patterns (MAMPs) or damage-associated molecular patterns (DAMPs) to their corresponding PRRs (Jones & Dangl, 2006). MAMPs are typically small, conserved molecules that are maintained through evolution due to their essential role for microbial fitness, *e.g.* bacterial flagellin peptides (flg22) (Jones & Dangl, 2006). Other PRRs are specialized to detect DAMPs, which are modified versions of host molecules that were produced upon microbial colonization, *e.g.* plant CW-derived oligogalacturonides that were hydrolytically or mechanically released by microbial enzymes (Tanaka & Heil, 2021).

The specificity between receptor and ligand is determined by the extracellular domain of each PRRs. These domains can be classified as leucine-rich repeat (LRR), lysin motif (LysM), lectin, malectin and epidermal growth-factor-like domains (Boutrot & Zipfel, 2017). Upon ligand binding, PRRs associate with other co-receptors and form a multimeric receptor complex which initiates signaling cascades, finally culminating in PTI (Ma *et al.*, 2016; Hohmann *et al.*, 2017). Initial auto- and transphosphorylation cascades between PRRs and receptor-like cytoplasmic kinases (RLCK) transmit the signal from the site of ligand binding to plasma membrane-located calcium channels and NADPH oxidases, triggering cytosolic calcium influx and apoplastic production of reactive oxygen species (ROS) (Schwessinger *et al.*, 2011; Kadota *et al.*, 2014; Liang & Zhou, 2018; Bi *et al.*, 2018; Tian *et al.*, 2019; Thor *et al.*, 2020). Ion fluxes lead to immediate closure of stomata, thereby restricting further pore-mediated entry of microbes (Thor *et al.*, 2020). Furthermore, cytosolic calcium influx activates calcium-dependent protein kinases (CDPKs) in the cytosol (Liu *et al.*, 2019). RLCKs



additionally activate mitogen-activated protein kinase (MAPK) cascades (Asai *et al.*, 2002; Bi *et al.*, 2018). Concerted phosphorylation cascades by RLCKs, MAPKs and CDK activate transcription factors (e.g. WRKY transcription factors) that will transcriptionally reprogram the host to produce defense hormones, secrete antimicrobials and physically fortify its CW through deposition of callose and crosslinking of phenolic compounds (Boudsocq *et al.*, 2010; Voigt, 2014; Bigeard *et al.*, 2015; Guan *et al.*, 2015; Lal *et al.*, 2018; Bjornson *et al.*, 2021). PTI provides a basal level of immunity to avert colonization by non-adapted microbes (Jones & Dangl, 2006; Yu *et al.*, 2017).

PTI signaling and the triggered immune response are costly; their constitutive activation can lead to growth inhibition or even autoimmunity (Huot *et al.*, 2014). Since roots are permanently exposed to a vast number of microbes at the soil-root interface, mechanisms must be in place to avoid these adverse effects. A recent study has identified a “damage-gating” mechanism in *Arabidopsis thaliana* (hereafter *Arabidopsis*) that prevents plants from perpetual activation of PTI in their roots. In the first place, epidermal and outer cortex cell layers of differentiated root regions do not sufficiently express PRR genes and are therefore unresponsive to MAMPs. When these cell layers experience physical damage, for example through a penetrating fungus or a feeding insect, PRR gene expression is induced in directly neighboring cell layers, thereby sensitizing them to MAMPs (Zhou *et al.*, 2020). Additionally, many microbes stay initially undiscovered by the host as they have evolved strategies to evade recognition by the PTI or suppress PTI-triggered signaling (reviewed in **Chapter 2** for chitin perception). For this purpose, microbes often secrete small effector proteins that can either act in the apoplast or within the host cell, creating a scenario referred to as effector-triggered susceptibility (ETS). To intercept the microbial efforts to bypass plant immunity, plants can detect apoplastic effectors through PRRs and intracellular effectors through NLRs, both events leading to the activation of immune responses. Traditionally, perception of effectors that were translocated into the host cytoplasm is referred to as ETI (Jones & Dangl, 2006). Although PTI and ETI have been considered as two separable tiers of the plant immune system for a long time, recent evidence shows that these two pathways converge onto similar downstream response and reciprocally potentiate each other’s dynamics and immune response amplitudes (Ngou *et al.*, 2021; Yuan *et al.*, 2021).

### Effector-triggered immunity

The activation of ETI by NLRs triggers a robust and prolonged immune response that often culminates in localized cell death programs, also referred to as hypersensitive response (HR). NLRs can be subdivided into three subclass depending on their N-terminal domain, which are Toll/Interleukin-1 receptor/Resistance protein (TIR) domains (TIR domain NLRs, TNLs), coiled-coil (CC) domains (CC-domain NLRs, CNLs) or RESISTANCE TO POWDERY MILDEW 8-like (RPW8) CC domains (RPW8-CC-domain NLRs, RNLs) (Pan *et al.*, 2000; Shao *et al.*, 2014). Although the N-terminus can fulfill different functions, a common pattern among NLRs is its involvement in different mechanisms of signal transduction (Bentham *et al.*, 2017). Most of these types of NLRs share a central conserved nucleotide binding site and ARC (present in Apaf-1, R proteins, and CED-4) domain (short: NB-ARC) as ADP/ATP-binding functional switch and a C-terminal stretch of LRRs involved in ligand binding and autoinhibition (Bentham *et al.*, 2017).

Similar to PRRs, microbial perception through NLRs can be either direct through binding of a microbial effector, or indirect by recognizing modification of another host component as a consequence of effector action (Kourelis & van der Hoorn, 2018). NLRs can either work as singletons, combining sensing and initiation of signaling in one protein, as pairs of NLRs with divided functions (sensor and helper/executor NLRs) or in interlaced networks as found in asterid plants (e.g. tobacco and tomato) (Adachi *et al.*, 2019; Saile *et al.*, 2020).

In the last three years, cryo-electron microscopy and high resolution mass spectrometry gave us important insights into NLR-mediated immunity (Wang *et al.*, 2023). Upon ligand binding, conformational changes initiate NLR oligomerization, triggering the formation of so-called resistosomes (Wang *et al.*, 2019; Ma *et al.*, 2020; Martin *et al.*, 2020; Zhao *et al.*, 2022; Förderer *et al.*, 2022). Subsequent downstream responses depend on the type of NLR. Resistosomes composed of CNLs like the Arabidopsis HOPZ-ACTIVATED RESISTANCE 1 (ZAR1) form a funnel-like structure at their N-terminus that can integrate into plant membranes, attributing non-canonical Ca<sup>2+</sup> channel properties to these complexes (Wang *et al.*, 2019; Bi *et al.*, 2021).

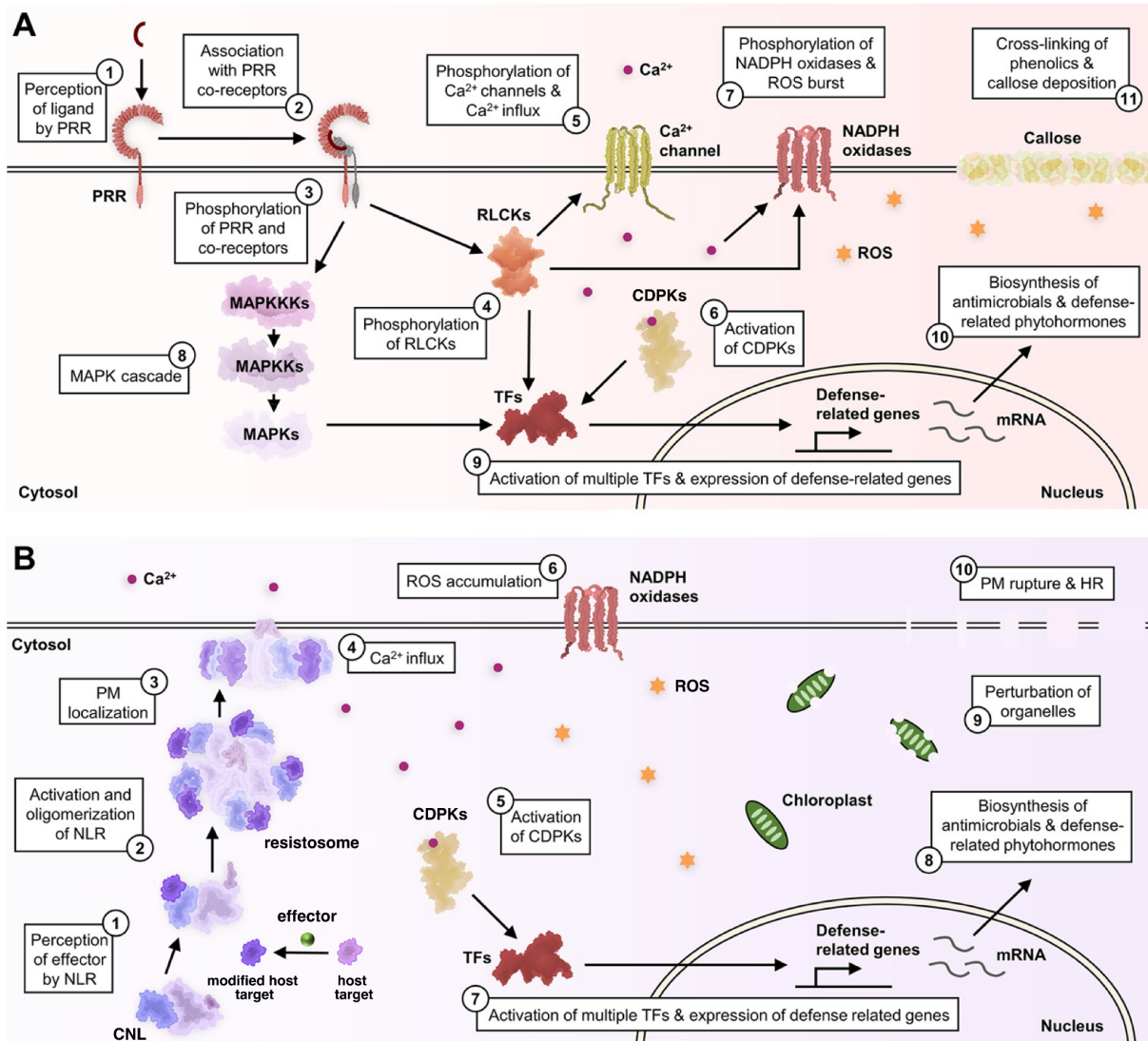


**Figure 1: Schematic overview of PTI and ETI signaling.** (A) PRR-mediated immunity, PTI. Perception of MAMP (ligand) by corresponding PRR leads to oligomerization of PRR with co-receptors. PRR complex formation initiates auto- and transphosphorylation cascades, transmitting the signal from the plasma membrane (PM) *via* RLCK to calcium channels and NADPH oxidases. CDPK- and MAPK-mediated signaling cascades activate TFs and instruct transcriptional reprogramming, leading to phytohormone signaling, secretion of antimicrobials and callose depositions. (B) CNL-mediated immunity, ETI. Modification of guarded host protein leads to host protein binding and subsequent formation of CNL resistosome. Resistosome inserts into PM and forms cation channels. The resulting calcium influx further triggers ROS production, transcriptional reprogramming, organelle perturbation, phytohormone signaling, antimicrobial synthesis and HR. Modified figure from Ngou *et al.*, 2022.

In contrast, TNL resistosomes exhibit nicotinamide adenine dinucleotide nucleosidase activity (Ma *et al.*, 2020; Martin *et al.*, 2020). Together with other TIR domain-

containing proteins, TNL resistosomes form second messengers that stimulate the formation of downstream complexes between helper RNLs (ACTIVATED DISEASE RESISTANCE 1 [ADR1] and N REQUIREMENT GENE 1 [NRG1]) and ENHANCED DISEASE SUSCEPTIBILITY 1 (EDS1) family proteins (EDS1/ PHYTOALEXIN DEFICIENT 4 [PAD4]/ SENESCENCE- ASSOCIATED GENE 101 [SAG101]) in *Arabidopsis* (Jia *et al.*, 2022). While the EDS1-SAG101-NRG1 module mediates the downstream cell death response, the EDS1-PAD4-ADR1 module confers pathogen resistance via salicylic acid-dependent basal immunity pathways (Dongus & Parker, 2021). In both cases, the helper NLRs ADR1 and NRG1 are activated by interaction with the respective EDS1 family heterodimers, forming RNLs resistosomes that - similarly to CNL resistosomes - function as nonselective cation channels (Jacob *et al.*, 2021).

It is not fully understood how resistosome-mediated pore formation translates into downstream restriction of pathogens and HR (Wang *et al.*, 2023). The current experimental evidence suggests that - similarly to PTI - calcium fluxes activate CDPKs and initiate phosphorylation cascades triggering ROS production and transcriptional reprogramming of the host (Gao *et al.*, 2013; Kadota *et al.*, 2019; Bi *et al.*, 2021). Further perturbation of the chloroplasts, vacuoles, and membrane integrity finally causes cell rupture, which is responsible for the macroscopically visible HR response (Bi *et al.*, 2021).

## Rationale and main objectives of this thesis

Our current understanding of how PRRs mediate the perception of microbes is largely focused on proteinaceous MAMPs. Among these, a few bacterial proteins, such as the flagellin peptide flg22, have been extensively studied, leading to a comprehensive overview of PRR complex formation, PRR distribution in nano-scale membrane environments, intracellular signaling cascades, PTI regulation as well as canonical immune response repertoires (Couto & Zipfel, 2016; Zipfel & Oldroyd, 2017; Bjornson *et al.*, 2021; Gronnier *et al.*, 2022; Ngou *et al.*, 2022). Despite this skewed focus, studies have revealed that a subset of PTI signaling is conserved among different MAMPs (Couto & Zipfel, 2016; Bjornson *et al.*, 2021). Therefore, knowledge gained from the study of one MAMP can be partially transferred to others. While the main principles of PRR-mediated perception also apply to many glycans, symbiosis research has shown that very similar glycan oligomers (e.g. bacterial extracellular polysaccharides [EPS], chitooligomers) can be involved in the initiation of immunity- and symbiosis-related host programs (Zipfel & Oldroyd, 2017; Feng *et al.*, 2019). Microbial perception undergoes several compatibility checkpoints as microbial colonization progresses, constantly supplying informational cues to the host (Kawaharada *et al.*, 2015). In these networks, the same glycan-binding PRRs - depending on their co-receptors - can act as switches between contrasting transcriptional responses (Feng *et al.*, 2019). Studying the function and perception of more glycans will help to dissect these complex regulatory systems underlying glycan perception.

In plant-fungal interactions, the CW polymer chitin represents the best studied MAMP. Chitin is a linear glycan polymer consisting of  $\beta$ -1,4-linked N-acetylglucosamine monomers, forming rigid crystalline chitin fibrils at the plasma membrane-adjacent side of fungal CWs. While its conserved presence across fungi underpins its suitability as MAMP, chitin and chitin-derived oligomers additionally function as symbiosis messengers (reviewed in more detail in **Chapter 2**). However, chitin represents only a minor component in most plant-colonizing fungi (Fesel & Zuccaro, 2016). Fungal  $\beta$ -1,3-linked glucose polymers (i.e.  $\beta$ -1,3-glucans) constitute the most abundant CW component (50-60% dry weight), yet their implications for plant-microbe interactions are largely unexplored (Fesel & Zuccaro, 2016; Gow *et al.*, 2017). Fungal  $\beta$ -glucans form highly connected meshes comprising  $\beta$ -1,3/1,4/1,6 linkages that scaffolds fungal

CWs (Gow *et al.*, 2017). Furthermore, fungi produce a gelatinous,  $\beta$ -glucans-rich EPS sheath surrounding fungal hyphae (Wawra *et al.*, 2019). The structural diversity and the reactivity of the numerous hydroxyl groups on each individual sugar monomer impedes the *de novo* synthesis of sufficient amounts of defined  $\beta$ -glucans (Guberman & Seeberger, 2019). The biochemical complexity also poses a challenge to obtain contamination-free isolation of  $\beta$ -glucans from fungal CW glucans. While many studies have shown that  $\beta$ -glucans activate plant immune responses, inconsistencies in the substrates utilized, the surveyed plant species, and the monitored immune responses have made it challenging to draw definitive conclusions from the available literature (Fesel & Zuccaro, 2016). The fact that fungi and oomycetes developed strategies to surpass  $\beta$ -glucan-related immunity emphasizes the relevance of these glycans in plant-microbe interactions (reviewed in more detail in **Chapter 2**).

The availability of homogenous  $\beta$ -1,3-glucan substrates, and novel molecular approaches for studying plant immunity have created an opportunity to reexamine the role of innate sensing of  $\beta$ -glucans in plants. Consequently, this thesis seeks to address the following research questions throughout the course of this thesis:

- I. Do different plant species mount a similar set of immune responses when treated with short-chain and long-chain  $\beta$ -1,3-glucans?
- II. Which host components contribute to the perception of short-chain and long-chain  $\beta$ -1,3-glucans in different plant model systems?
- III. Do host  $\beta$ -1,3-glucanases release glycan oligomers from fungal CWs and are these oligomers relevant to plant-fungal interactions?

To address these research questions, we utilized various experimental systems, which I will introduce in the subsequent sections.

## Experimental systems

### Fungal $\beta$ -glucans and their surrogate substrates: laminarioligomers, laminarin and native $\beta$ -glucans

Fungal  $\beta$ -1,3-linkage type glucans represent 65-90% of all fungal CW  $\beta$ -glucans (Bowman & Free, 2006). Most CW  $\beta$ -1,3-glucans are decorated with  $\beta$ -1,6-branches, some of them connecting adjacent  $\beta$ -1,3-glucan strands. The frequency of  $\beta$ -1,6-substitutions is influenced by environmental conditions and the developmental stage of the fungus (Bowman & Free, 2006; Oliveira-Garcia & Deising, 2016).

Here, we have used two types of commercially available  $\beta$ -1,3-glucan substrates: short-chain laminarioligomers and branched, long-chain laminarins (Figure 2). Throughout the course of this study, linear  $\beta$ -1,3-glucans with a degree of polymerization (DP) between two and seven are referred to as **short-chain laminarioligomers**. The major laminarioligomers used in this study are laminarihexaose (glucose hexamer, DP=6) and laminariheptaose (glucose heptamer, DP=7).

Complementarily, we used the **long-chain  $\beta$ -1,3/1,6-glucan** laminarin isolated from brown algae. Laminarin is commonly used in human and plant immunity studies as a substitute for fungal CW  $\beta$ -glucans (Xie *et al.*, 2010; Fesel & Zuccaro, 2016). Laminarins have an average DP of 20-30 with varying branching patterns depending on the algal species (Becker *et al.*, 2020). Laminarin from *Laminaria digitata* is the major long-chain  $\beta$ -1,3-glucan used in this study. It is decorated with  $\beta$ -1,6-linked glucose moieties every seven to ten backbone units (Pang *et al.*, 2005; Becker *et al.*, 2020). In contrast, laminarin from *Eisenia bicyclis* is highly substituted with side branches, exhibiting a  $\beta$ -1,6-substitution on every other backbone unit (Maeda & Nishizawa, 1968; Usui *et al.*, 1979; Pang *et al.*, 2005). The spatial orientation of  $\beta$ -1,3-linked glucose units creates a helical pitch in  $\beta$ -1,3-backbones which becomes pronounced at high DPs (Okobira *et al.*, 2008). This triggers the formation of triple helices (i.e. triplex) consisting of three intertwined  $\beta$ -1,3-glucan chains. The supramolecular aggregation of laminarins is important for enzyme binding and immunological properties (Takahasi *et al.*, 2009; Kanagawa *et al.*, 2011; Hanashima *et al.*, 2014; Qin *et al.*, 2017; Pluvinage *et al.*, 2017). Triplex formation proportionally decreases with increasing frequency of  $\beta$ -1,6-substitutions on the backbone (Okobira

*et al.*, 2008). To separate the effects of  $\beta$ -1,3-glucan length from their branching pattern, we deployed a bacterial glucanase (glycoside hydrolase 30 family) that specifically removes  $\beta$ -1,6-branches from  $\beta$ -1,3-backbones to debranch laminarin (Becker *et al.*, 2017).

In addition to our set of short- and long-chain  $\beta$ -1,3-glucans, we established fungal CW extraction protocols that discriminate between the rigid inner CW layers and the mobile  $\beta$ -glucan-rich EPS layer surrounding fungal hyphae, expanding our investigations to native fungal  $\beta$ -glucans (**Chapter 4**). The immunogenic potential of these distinct CW fractions was tested either directly without pretreatment or after digestion with plant glucanases.

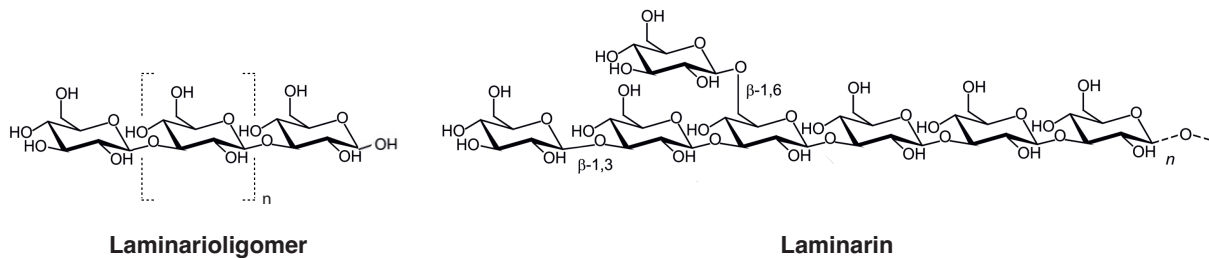


**Figure 2: Structures of the utilized  $\beta$ -glucan substrates.** Throughout the study, we have used the commercially available laminarioligomers (linear  $\beta$ -1,3-glucans) and laminarin (branched  $\beta$ -1,3/1,6-glucans).

### Plant model species used to dissect $\beta$ -glucan-triggered immunity

Our understanding of plant immunity is primarily based on tremendous efforts performed on the plant model species **Arabidopsis** (thale cress) (Couto & Zipfel, 2016; Zipfel & Oldroyd, 2017). *Arabidopsis* belongs to the mustard family (*Brassicaceae*) and is native to Eurasia and North Africa (Koornneef & Meinke, 2010). Its sequenced diploid genome, available transformation techniques, as well as a large collection of mutants and natural accessions render *Arabidopsis* an excellent model for molecular genetic studies, including forward- and reverse-genetic approaches and genome-wide association studies (Koornneef & Meinke, 2010). Recent work has demonstrated that perception of laminarihexaose in *Arabidopsis* is mediated by the central carbohydrate LysM-RLK CERK1 (Mélida *et al.*, 2018; Hierro *et al.*, 2021). However, the responses to short-chain  $\beta$ -1,3-glucans in the standard *Arabidopsis* accession Columbia-0 (Col-0) are comparatively weak, and long-chain  $\beta$ -1,3-glucans like laminarin are not perceived at all (Wawra *et al.*, 2016). Moreover, members of the



*Brassicaceae* family have a reduced repertoire of glycan-binding LysM-RLKs compared to other dicotyledonous families (Buendia *et al.*, 2018). The lack of compatibility for  $\beta$ -glucan substrates in the central model species of plant biology partially explains the striking knowledge gap on  $\beta$ -glucan-triggered immunity in plants. We included the tobacco relative ***Nicotiana benthamiana*** as a complementary dicot model species in this study. Despite the complex allotetraploid genome, a comprehensive toolkit including *Agrobacterium*-mediated transient expression systems in leaves, virus-induced gene silencing and CRISPR/Cas9 promoted *N. benthamiana* to a common model system for molecular studies (Goodin *et al.*, 2002; Senthil-Kumar & Mysore, 2014; Stuttmann *et al.*, 2021). *N. benthamiana* has been successfully used in numerous immunity related studies (Goodin *et al.*, 2008). Its relative *Nicotiana tabacum* was previously shown to mount immune responses upon treatment with different  $\beta$ -glucan substrates (Klarzynski *et al.*, 2000; Ménard *et al.*, 2004, 2005).

Despite a high degree of homology between the immunity pathways of monocots and dicots, comparative studies are needed to discover lineage-specific features, such as for example the loss of an entire ETI receptor class in the monocots (Tarr & Alexander, 2009). To explore  $\beta$ -1,3-glucan-triggered immunity in monocots, we mainly focused on ***Hordeum vulgare*** (hereafter barley). Barley belongs to the *Poaceae*, a grass family which includes agronomically relevant cereal crops like maize, wheat, rice, and millet. Despite its large and complex genome (5 Gbp, > 80% repetitive elements), its diploid chromosome set makes it more accessible to genetic studies than hexaploid wheat (International Barley Genome Sequencing Consortium, 2012; Mascher *et al.*, 2017). Recent advances in multiplexed CRISPR/Cas protocols for barley made reverse-genetic approaches more feasible for research (Kumar *et al.*, 2018). To make use of published mutants, we additionally included ***Brachypodium distachyon*** and the agriculturally important cereal ***Oryza sativa*** (rice) in our analyses.

#### Fungal species used in this study

Most parts of this work focus on the interaction between the mutualistic root endophyte ***Serendipita indica*** and barley as host. *S. indica* belongs to the fungal order Sebaciales (Basidiomycota), a phylogenetically diverse and geographically ubiquitous group of fungi (Weiss *et al.*, 2011; Garnica *et al.*, 2013; Weiß *et al.*, 2016).

Sebacinales exhibit a wide range of different lifestyles, including saprotrophic, endophytic, ectomycorrhizal and endomycorrhizal species (Weiß *et al.*, 2016). The root mutualist *S. indica* has emerged as a well-established model system for endophytism, owing to its broad host range, easy axenic cultivation, and genetic tractability. Intra- and extracellular fungal colonization is restricted to the epidermal and cortex cell layers of the root (Deshmukh *et al.*, 2006; Jacobs *et al.*, 2011). *S. indica* incorporates saprotrophic traits into an endophytic lifestyle: while initial colonization is characterized by a biotrophic phase, colonized areas transition to a cell-death associated phase at later stages. This mutualistic host cell death phase is required for the beneficial outcomes of this interaction, such as for example growth promotion (Deshmukh *et al.*, 2006; Jacobs *et al.*, 2011; Lahrman *et al.*, 2013). Several recent discoveries promoted *S. indica* as an interesting system to study the role of innate  $\beta$ -glucan sensing in plant-fungal interactions. *S. indica* secretes several  $\beta$ -glucan-binding lectins into the apoplastic space, including the  $\beta$ -glucan-binding effector (FGB1) that can suppress  $\beta$ -glucan-triggered immunity in different plant species. Moreover, *S. indica* hyphae are surrounded by an extensive  $\beta$ -glucan-enriched EPS layer (Wawra *et al.*, 2019).

For selected parts of this work, we additionally included phylogenetically distant fungi with diverse lifestyles. Specifically, we included four additional species: ***Serendipita vermifera*** (Basidiomycota), another root endophyte from the Sebacinales order; ***Bipolaris sorokiniana*** (Ascomycota), a hemibiotrophic pathogen; ***Blumeria graminis forma specialis hordei*** (Ascomycota), an obligate biotrophic fungus that infects barley; and ***Rhizophagus irregularis*** (Glomeromycotina), a mutualistic arbuscular mycorrhizal fungus with an obligate biotrophic lifestyle.

## Thesis outline

Glycans are a structurally diverse group of biomolecules with an inherently large potential for chemical communication. They not only decorate the various cell surface layers of most microbes, but also are actively secreted as interkingdom signaling molecules.

To cover the current body of literature, **Chapter 2** summarizes our knowledge on glycans from bacteria, fungi, and oomycetes, their perception by the plant host, and their wider implications in plant-microbial interactions. Beyond this, this chapter highlights how fluorescently tagged fungal lectins can be employed as glycan probes to study fungal cell wall architecture.

Among fungal cell surface glycans,  $\beta$ -glucans represent the most abundant glycan class in most fungi. While many previous studies reported on the immunogenic properties of  $\beta$ -glucans in plants, a high variability in the experimental setup used across those studies makes it difficult to draw general conclusions. In **Chapter 3**, we have systematically tested two commercially available  $\beta$ -glucans with different length and branching profiles in representative monocot and dicot species.

To obtain more detailed insights on the perception of native, fungal  $\beta$ -glucans, we focused on the interaction between barley and the mutualistic root endophyte *S. indica* (**Chapter 4**). We established a method to separate the amorphous extracellular polysaccharide layer from the more inner rigid cell wall layers and characterized these two CW compartments using glycomic and proteomic approaches. Moreover, we digested CW preparations with a fungal-induced host glucanase to look for the release of oligomers relevant for plant-fungal interactions.

While there is limited knowledge on the perception of short  $\beta$ -1,3-glucans in *Arabidopsis*, we do not have any information on molecular components involved in the processing and perception of long-chain  $\beta$ -1,3-glucans like laminarin. In **Chapter 5**, we have used a pull-down approach with biotinylated laminarin to identify novel components involved in host defense against fungi.

Finally, **Chapter 6** discusses the different aspects of  $\beta$ -glucan immunity discovered in this thesis and places them into the broader context of plant-microbial interactions.

## References

- Adachi, H., Derevnina, L. and Kamoun, S.** (2019) NLR singletons, pairs, and networks: evolution, assembly, and regulation of the intracellular immunoreceptor circuitry of plants. *Curr. Opin. Plant Biol.*, **50**, 121–131.
- Almario, J., Jeena, G., Wunder, J., Langen, G., Zuccaro, A., Coupland, G. and Bucher, M.** (2017) Root-associated fungal microbiota of nonmycorrhizal *Arabidopsis thaliana* and its contribution to plant phosphorus nutrition. *Proc. Natl. Acad. Sci. U. S. A.*, **114**, E9403–E9412.
- Asai, T., Tena, G., Plotnikova, J., Willmann, M.R., Chiu, W.-L., Gomez-Gomez, L., Boller, T., Ausubel, F.M. and Sheen, J.** (2002) MAP kinase signalling cascade in Arabidopsis innate immunity. *Nature*, **415**, 977–983.
- Bais, H.P., Weir, T.L., Perry, L.G., Gilroy, S. and Vivanco, J.M.** (2006) The role of root exudates in rhizosphere interactions with plants and other organisms. *Annu. Rev. Plant Biol.*, **57**, 233–266.
- Becker, S., Scheffel, A., Polz, M.F. and Hehemann, J.-H.** (2017) Accurate Quantification of Laminarin in Marine Organic Matter with Enzymes from Marine Microbes. *Appl. Environ. Microbiol.*, **83**. Available at: <http://dx.doi.org/10.1128/AEM.03389-16>.
- Becker, S., Tebben, J., Coffinet, S., Wiltshire, K., Iversen, M.H., Harder, T., Hinrichs, K.-U. and Hehemann, J.-H.** (2020) Laminarin is a major molecule in the marine carbon cycle. *Proc. Natl. Acad. Sci. U. S. A.*, **117**, 6599–6607.
- Bentham, A., Burdett, H., Anderson, P.A., Williams, S.J. and Kobe, B.** (2017) Animal NLRs provide structural insights into plant NLR function. *Ann. Bot.*, **119**, 827–702.
- Berendsen, R.L., Pieterse, C.M.J. and Bakker, P.A.H.** (2012) The rhizosphere microbiome and plant health. *Trends Plant Sci.*, **17**, 478–486.
- Bigeard, J., Colcombet, J. and Hirt, H.** (2015) Signaling Mechanisms in Pattern-Triggered Immunity (PTI). *Mol. Plant*, **8**, 521–539.
- Bi, G., Su, M., Li, N., et al.** (2021) The ZAR1 resistosome is a calcium-permeable channel triggering plant immune signaling. *Cell*, **184**, 3528–3541.e12.
- Bi, G., Zhou, Z., Wang, W., et al.** (2018) Receptor-Like Cytoplasmic Kinases Directly Link Diverse Pattern Recognition Receptors to the Activation of Mitogen-Activated Protein Kinase Cascades in Arabidopsis. *Plant Cell*, **30**, 1543–1561.
- Bjornson, M., Pimprikar, P., Nürnbergger, T. and Zipfel, C.** (2021) The transcriptional landscape of Arabidopsis thaliana pattern-triggered immunity. *Nature Plants*, **7**, 579–586.
- Boudsocq, M., Willmann, M.R., McCormack, M., Lee, H., Shan, L., He, P., Bush, J., Cheng, S.-H. and Sheen, J.** (2010) Differential innate immune signalling via Ca<sup>2+</sup> sensor protein kinases. *Nature*, **464**, 418–422.
- Boutrot, F. and Zipfel, C.** (2017) Function, Discovery, and Exploitation of Plant Pattern Recognition Receptors for Broad-Spectrum Disease Resistance. Available at: <https://www.annualreviews.org/doi/abs/10.1146/annurev-phyto-080614-120106>.
- Bowman, S.M. and Free, S.J.** (2006) The structure and synthesis of the fungal cell wall. *Bioessays*, **28**, 799–808.
- Buendia, L., Girardin, A., Wang, T., Cottret, L. and Lefebvre, B.** (2018) LysM Receptor-Like Kinase and LysM Receptor-Like Protein Families: An Update on Phylogeny and Functional Characterization. *Front. Plant Sci.*, **9**, 1531.
- Burgh, A.M. van der and Joosten, M.H.A.J.** (2019) Plant Immunity: Thinking Outside and Inside the Box. *Trends Plant Sci.*, **24**, 587–601.

- Chen, T., Nomura, K., Wang, X., et al.** (2020) A plant genetic network for preventing dysbiosis in the phyllosphere. *Nature*, **580**, 653–657.
- Cook, D.E., Mesarich, C.H. and Thomma, B.P.H.** (2015) Understanding Plant Immunity as a Surveillance System to Detect Invasion. *Annual Review of Phytopathology*, **53**, 541–563.
- Couto, D. and Zipfel, C.** (2016) Regulation of pattern recognition receptor signalling in plants. *Nat. Rev. Immunol.*, **16**, 537–552.
- Deshmukh, S., Hückelhoven, R., Schäfer, P., Imani, J., Sharma, M., Weiss, M., Waller, F. and Kogel, K.-H.** (2006) The root endophytic fungus *Piriformospora indica* requires host cell death for proliferation during mutualistic symbiosis with barley. *Proc. Natl. Acad. Sci. U. S. A.*, **103**, 18450–18457.
- Ding, P., Sakai, T., Krishna Shrestha, R., et al.** (2021) Chromatin accessibility landscapes activated by cell-surface and intracellular immune receptors. *J. Exp. Bot.*, **72**, 7927–7941.
- Dongus, J.A. and Parker, J.E.** (2021) EDS1 signalling: At the nexus of intracellular and surface receptor immunity. *Curr. Opin. Plant Biol.*, **62**, 102039.
- Feng, F., Sun, J., Radhakrishnan, G.V., et al.** (2019) A combination of chitooligosaccharide and lipochitooligosaccharide recognition promotes arbuscular mycorrhizal associations in *Medicago truncatula*. *Nat. Commun.*, **10**, 1–12.
- Fesel, P.H. and Zuccaro, A.** (2016)  $\beta$ -glucan: Crucial component of the fungal cell wall and elusive MAMP in plants. *Fungal Genet. Biol.*, **90**, 53–60.
- Finkel, O.M., Salas-González, I., Castrillo, G., et al.** (2020) A single bacterial genus maintains root growth in a complex microbiome. *Nature*, **587**, 103–108.
- Fitzpatrick, C.R., Salas-González, I., Conway, J.M., Finkel, O.M., Gilbert, S., Russ, D., Teixeira, P.J.P.L. and Dangl, J.L.** (2020) The Plant Microbiome: From Ecology to Reductionism and Beyond. *Annu. Rev. Microbiol.*, **74**, 81–100.
- Förderer, A., Li, E., Lawson, A.W., et al.** (2022) A wheat resistosome defines common principles of immune receptor channels. *Nature*, **610**, 532–539.
- Gao, X., Chen, X., Lin, W., et al.** (2013) Bifurcation of Arabidopsis NLR Immune Signaling via Ca<sup>2+</sup>-Dependent Protein Kinases. *PLoS Pathog.*, **9**, e1003127.
- Goodin, M.M., Dietzgen, R.G., Schichnes, D., Ruzin, S. and Jackson, A.O.** (2002) pGD vectors: versatile tools for the expression of green and red fluorescent protein fusions in agroinfiltrated plant leaves. *Plant J.*, **31**, 375–383.
- Goodin, M.M., Zaitlin, D., Naidu, R.A. and Lommel, S.A.** (2008) *Nicotiana benthamiana*: Its History and Future as a Model for Plant–Pathogen Interactions. *Mol. Plant. Microbe. Interact.*, **21**, 1015–1026.
- Guan, R., Su, J., Meng, X., Li, S., Liu, Y., Xu, J. and Zhang, S.** (2015) Multilayered Regulation of Ethylene Induction Plays a Positive Role in Arabidopsis Resistance against *Pseudomonas syringae*. *Plant Physiol.*, **169**, 299–312.
- Guberman, M. and Seeberger, P.H.** (2019) Automated Glycan Assembly: A Perspective. *J. Am. Chem. Soc.*, **141**, 5581–5592.
- Gust, A.A. and Felix, G.** (2014) Receptor like proteins associate with SOBIR1-type of adaptors to form bimolecular receptor kinases. *Curr. Opin. Plant Biol.*, **21**, 104–111.
- Hacquard, S., Garrido-Oter, R., González, A., et al.** (2015) Microbiota and Host Nutrition across Plant and Animal Kingdoms. *Cell Host Microbe*, **17**, 603–616.

- Hanashima, S., Ikeda, A., Tanaka, H., Adachi, Y., Ohno, N., Takahashi, T. and Yamaguchi, Y.** (2014) NMR study of short  $\beta(1-3)$ -glucans provides insights into the structure and interaction with Dectin-1. *Glycoconj. J.*, **31**, 199–207.
- Hierro, I. del, Hierro, I. del, Mérida, H., Broyart, C., Santiago, J. and Molina, A.** (2021) Computational prediction method to decipher receptor–glycoligand interactions in plant immunity. *Plant J.*, **105**, 1710–1726.
- Hiruma, K., Gerlach, N., Sacristán, S., et al.** (2016) Root Endophyte Colletotrichum tofieldiae Confers Plant Fitness Benefits that Are Phosphate Status Dependent. *Cell*, **165**, 464–474.
- Hohmann, U., Lau, K. and Hothorn, M.** (2017) The Structural Basis of Ligand Perception and Signal Activation by Receptor Kinases. *Annu. Rev. Plant Biol.*, **68**, 109–137.
- Huot, B., Yao, J., Montgomery, B.L. and He, S.Y.** (2014) Growth–Defense Tradeoffs in Plants: A Balancing Act to Optimize Fitness. *Mol. Plant*, **7**, 1267–1287.
- International Barley Genome Sequencing Consortium** (2012) A physical, genetic and functional sequence assembly of the barley genome. *Nature*, **491**, 711–716.
- Jacob, P., Kim, N.H., Wu, F., et al.** (2021) Plant “helper” immune receptors are  $\text{Ca}^{2+}$ -permeable nonselective cation channels. *Science*, **373**, 420–425.
- Jacobs, S., Zechmann, B., Molitor, A., Trujillo, M., Petutschnig, E., Lipka, V., Kogel, K.-H. and Schäfer, P.** (2011) Broad-Spectrum Suppression of Innate Immunity Is Required for Colonization of Arabidopsis Roots by the Fungus *Piriformospora indica*. *Plant Physiol.*, **156**, 726–740.
- Jia, A., Huang, S., Song, W., et al.** (2022) TIR-catalyzed ADP-ribosylation reactions produce signaling molecules for plant immunity. *Science*, **377**, eabq8180.
- Jones, J.D.G. and Dangl, J.L.** (2006) The plant immune system. *Nature*, **444**, 323–329.
- Kadota, Y., Liebrand, T.W.H., Goto, Y., et al.** (2019) Quantitative phosphoproteomic analysis reveals common regulatory mechanisms between effector- and PAMP-triggered immunity in plants. *New Phytologist*, **221**, 2160–2175.
- Kadota, Y., Sklenar, J., Derbyshire, P., et al.** (2014) Direct regulation of the NADPH oxidase RBOHD by the PRR-associated kinase BIK1 during plant immunity. *Mol. Cell*, **54**, 43–55.
- Kanagawa, M., Satoh, T., Ikeda, A., Adachi, Y., Ohno, N. and Yamaguchi, Y.** (2011) Structural Insights into Recognition of Triple-helical  $\beta$ -Glucans by an Insect Fungal Receptor. *J. Biol. Chem.*, **286**, 29158–29165.
- Kawa, D. and Brady, S.M.** (2022) Root cell types as an interface for biotic interactions. *Trends Plant Sci.*, **27**, 1173–1186.
- Kawaharada, Y., Kelly, S., Nielsen, M.W., et al.** (2015) Receptor-mediated exopolysaccharide perception controls bacterial infection. *Nature*, **523**, 308–312.
- Klarzynski, O., Plesse, B., Joubert, J.-M., Yvin, J.-C., Kopp, M., Kloareg, B. and Fritig, B.** (2000) Linear  $\beta$ -1,3 Glucans Are Elicitors of Defense Responses in Tobacco. *Plant Physiol.*, **124**, 1027–1038. Available at: [Accessed February 21, 2023].
- Koornneef, M. and Meinke, D.** (2010) The development of Arabidopsis as a model plant. *Plant J.*, **61**, 909–921.
- Kourelis, J. and Hoorn, R.A.L. van der** (2018) Defended to the Nines: 25 Years of Resistance Gene Cloning Identifies Nine Mechanisms for R Protein Function. *Plant Cell*, **30**, 285–299.
- Kumar, N., Galli, M., Ordon, J., Stuttmann, J., Kogel, K.-H. and Imani, J.** (2018) Further analysis of barley MORC1 using a highly efficient RNA-guided Cas9 gene-editing system. *Plant Biotechnol. J.*, **16**, 1892–1903.

- Lacaze, A. and Joly, D.L.** (2020) Structural specificity in plant-filamentous pathogen interactions. *Mol. Plant Pathol.*, **21**, 1513–1525.
- Lahrman, U., Ding, Y., Banhara, A., Rath, M., Hajirezaei, M.R., Döhlemann, S., Wirén, N. von, Parniske, M. and Zuccaro, A.** (2013) Host-related metabolic cues affect colonization strategies of a root endophyte. *Proc. Natl. Acad. Sci. U. S. A.*, **110**, 13965–13970.
- Lal, N.K., Nagalakshmi, U., Hurlburt, N.K., et al.** (2018) The Receptor-like Cytoplasmic Kinase BIK1 Localizes to the Nucleus and Regulates Defense Hormone Expression during Plant Innate Immunity. *Cell Host & Microbe*, **23**, 485–497.e5. Available at: <http://dx.doi.org/10.1016/j.chom.2018.03.010>.
- Liang, X. and Zhou, J.-M.** (2018) Receptor-Like Cytoplasmic Kinases: Central Players in Plant Receptor Kinase-Mediated Signaling.
- Liu, H., Brettell, L.E., Qiu, Z. and Singh, B.K.** (2020) Microbiome-Mediated Stress Resistance in Plants. *Trends Plant Sci.*, **25**, 733–743.
- Liu, H., Brettell, L.E. and Singh, B.** (2020) Linking the Phyllosphere Microbiome to Plant Health. *Trends Plant Sci.*, **25**, 841–844.
- Liu, Y., Maierhofer, T., Rybak, K., et al.** (2019) Anion channel SLAH3 is a regulatory target of chitin receptor-associated kinase PBL27 in microbial stomatal closure. *Elife*, **8**.
- Maeda, M. and Nishizawa, K.** (1968) Fine structure of laminaran of *Eisenia bicyclis*. *J. Biochem.*, **63**, 199–206.
- Mahdi, L.K., Miyauchi, S., Uhlmann, C., et al.** (2021) The fungal root endophyte *Serendipita vermifera* displays inter-kingdom synergistic beneficial effects with the microbiota in *Arabidopsis thaliana* and barley. *ISME J.*, **16**, 876–889.
- Martin, R., Qi, T., Zhang, H., Liu, F., King, M., Toth, C., Nogales, E. and Staskawicz, B.J.** (2020) Structure of the activated ROQ1 resistosome directly recognizing the pathogen effector XopQ. *Science*, **370**.
- Mascher, M., Gundlach, H., Himmelbach, A., et al.** (2017) A chromosome conformation capture ordered sequence of the barley genome. *Nature*, **544**, 427–433.
- Ma, S., Lapin, D., Liu, L., et al.** (2020) Direct pathogen-induced assembly of an NLR immune receptor complex to form a holoenzyme. *Science*, **370**.
- Mélida, H., Sopena-Torres, S., Bacete, L., Garrido-Arandia, M., Jordá, L., López, G., Muñoz-Barrios, A., Pacios, L.F. and Molina, A.** (2018) Non-branched  $\beta$ -1,3-glucan oligosaccharides trigger immune responses in *Arabidopsis*. *Plant J.*, **93**, 34–49.
- Ménard, R., Alban, S., Ruffray, P. de, Jamois, F., Franz, G., Fritig, B., Yvin, J.-C. and Kauffmann, S.** (2004)  $\beta$ -1,3 Glucan Sulfate, but Not  $\beta$ -1,3 Glucan, Induces the Salicylic Acid Signaling Pathway in Tobacco and *Arabidopsis*. *Plant Cell*, **16**, 3020–3032.
- Ngou, B.P.M., Ahn, H.-K., Ding, P. and Jones, J.D.G.** (2021) Mutual potentiation of plant immunity by cell-surface and intracellular receptors. *Nature*, **592**, 110–115.
- Ngou, B.P.M., Ding, P. and Jones, J.D.G.** (2022) Thirty years of resistance: Zig-zag through the plant immune system. *Plant Cell*, **34**, 1447–1478.
- Okobira, T., Miyoshi, K., Uezu, K., Sakurai, K. and Shinkai, S.** (2008) Molecular dynamics studies of side chain effect on the beta-1,3-D-glucan triple helix in aqueous solution. *Biomacromolecules*, **9**, 783–788.
- Oliveira-Garcia, E. and Deising, H.B.** (2016) Attenuation of PAMP-triggered immunity in maize requires down-regulation of the key  $\beta$ -1,6-glucan synthesis genes KRE5 and KRE6 in biotrophic hyphae of *Colletotrichum graminicola*. *Plant J.*, **87**, 355–375.

- Pang, Z., Otaka, K., Maoka, T., Hidaka, K., Ishijima, S., Oda, M. and Ohnishi, M.** (2005) Structure of beta-glucan oligomer from laminarin and its effect on human monocytes to inhibit the proliferation of U937 cells. *Biosci. Biotechnol. Biochem.*, **69**, 553–558.
- Pan, Q., Wendel, J. and Fluhr, R.** (2000) Divergent evolution of plant NBS-LRR resistance gene homologues in dicot and cereal genomes. *J. Mol. Evol.*, **50**, 203–213.
- Pluvinage, B., Fillo, A., Massel, P. and Boraston, A.B.** (2017) Structural Analysis of a Family 81 Glycoside Hydrolase Implicates Its Recognition of  $\beta$ -1,3-Glucan Quaternary Structure. *Structure*, **25**, 1348–1359.e3.
- Qin, Z., Yang, D., You, X., Liu, Y., Hu, S., Yan, Q., Yang, S. and Jiang, Z.** (2017) The recognition mechanism of triple-helical  $\beta$ -1,3-glucan by a  $\beta$ -1,3-glucanase. *Chem. Commun.*, **53**, 9368–9371.
- Rolli, E., Marasco, R., Vigani, G., et al.** (2015) Improved plant resistance to drought is promoted by the root-associated microbiome as a water stress-dependent trait. *Environmental Microbiology*, **17**, 316–331.
- Saile, S.C., Jacob, P., Castel, B., Jubic, L.M., Salas-González, I., Bäcker, M., Jones, J.D.G., Dangl, J.L. and El Kasmi, F.** (2020) Two unequally redundant “helper” immune receptor families mediate *Arabidopsis thaliana* intracellular “sensor” immune receptor functions. *PLoS Biol.*, **18**, e3000783.
- Sarkar, D., Rovenich, H., Jeena, G., et al.** (2019) The inconspicuous gatekeeper: endophytic *Serendipita vermifera* acts as extended plant protection barrier in the rhizosphere. *New Phytol.*, **224**, 886–901.
- Sasse, J., Martinoia, E. and Northen, T.** (2018) Feed Your Friends: Do Plant Exudates Shape the Root Microbiome? *Trends Plant Sci.*, **23**, 25–41.
- Schlaeppli, K. and Bulgarelli, D.** (2015) The Plant Microbiome at Work. *Molecular Plant-Microbe Interactions* **28**, 212–217 .
- Schwessinger, B., Roux, M., Kadota, Y., Ntoukakis, V., Sklenar, J., Jones, A. and Zipfel, C.** (2011) Phosphorylation-Dependent Differential Regulation of Plant Growth, Cell Death, and Innate Immunity by the Regulatory Receptor-Like Kinase BAK1. *PLoS Genetics*, **7**, e1002046.
- Senthil-Kumar, M. and Mysore, K.S.** (2014) Tobacco rattle virus–based virus-induced gene silencing in *Nicotiana benthamiana*. *Nat. Protoc.*, **9**, 1549–1562.
- Shao, Z.-Q., Zhang, Y.-M., Hang, Y.-Y., et al.** (2014) Long-term evolution of nucleotide-binding site-leucine-rich repeat genes: understanding gained from and beyond the legume family. *Plant Physiol.*, **166**, 217–234.
- Stuttman, J., Barthel, K., Martin, P., et al.** (2021) Highly efficient multiplex editing: one-shot generation of 8× *Nicotiana benthamiana* and 12× *Arabidopsis* mutants. *Plant J.*, **106**, 8–22.
- Takahasi, K., Ochiai, M., Horiuchi, M., Kumeta, H., Ogura, K., Ashida, M. and Inagaki, F.** (2009) Solution structure of the silkworm  $\beta$ GRP/GNBP3 N-terminal domain reveals the mechanism for  $\beta$ -1,3-glucan-specific recognition. *Proceedings of the National Academy of Sciences*, **106**, 11679–11684.
- Tarr, D.E.K. and Alexander, H.M.** (2009) TIR-NBS-LRR genes are rare in monocots: evidence from diverse monocot orders. *BMC Res. Notes*, **2**, 197.
- Thomma, B.P.H.J., Nürnberger, T. and Joosten, M.H.A.J.** (2011) Of PAMPs and effectors: the blurred PTI-ETI dichotomy. *Plant Cell*, **23**, 4–15.
- Thor, K., Jiang, S., Michard, E., et al.** (2020) The calcium-permeable channel OSCA1.3 regulates plant stomatal immunity. *Nature*, **585**, 569–573.
- Tian, W., Hou, C., Ren, Z., et al.** (2019) A calmodulin-gated calcium channel links pathogen patterns to plant immunity. *Nature*, **572**, 131–135.



- Usui, T., Toriyama, T. and Mizuno, T.** (1979) Structural investigation of laminaran of *Eisenia bicyclis*. *Agric. Biol. Chem.*, **43**, 603–611.
- Vannier, N., Agler, M. and Hacquard, S.** (2019) Microbiota-mediated disease resistance in plants. *PLoS Pathog.*, **15**, e1007740.
- Voigt, C.A.** (2014) Callose-mediated resistance to pathogenic intruders in plant defense-related papillae. *Front. Plant Sci.*, **5**.
- Vorholt, J.A., Vogel, C., Carlström, C.I. and Müller, D.B.** (2017) Establishing Causality: Opportunities of Synthetic Communities for Plant Microbiome Research. *Cell Host Microbe*, **22**, 142–155.
- Wang, J., Hu, M., Wang, J., et al.** (2019) Reconstitution and structure of a plant NLR resistosome conferring immunity. *Science*, **364**.
- Wang, J., Song, W. and Chai, J.** (2023) Structure, biochemical function, and signaling mechanism of plant NLRs. *Mol. Plant*, **16**, 75–95.
- Wawra, S., Fesel, P., Widmer, H., et al.** (2016) The fungal-specific  $\beta$ -glucan-binding lectin FGB1 alters cell-wall composition and suppresses glucan-triggered immunity in plants. *Nat. Commun.*, **7**, 1–11.
- Wawra, S., Fesel, P., Widmer, H., Neumann, U., Lahrmann, U., Becker, S., Hehemann, J.-H., Langen, G. and Zuccaro, A.** (2019) FGB1 and WSC3 are in planta-induced  $\beta$ -glucan-binding fungal lectins with different functions. *New Phytol.*, **222**, 1493–1506.
- Weiss, M., Sýkorová, Z., Garnica, S., Riess, K., Martos, F., Krause, C., Oberwinkler, F., Bauer, R. and Redecker, D.** (2011) Sebaciales everywhere: previously overlooked ubiquitous fungal endophytes. *PLoS One*, **6**, e16793.
- Xie, J., Guo, L., Ruan, Y., Zhu, H., Wang, L., Zhou, L., Yun, X. and Gu, J.** (2010) Laminarin-mediated targeting to Dectin-1 enhances antigen-specific immune responses. *Biochem. Biophys. Res. Commun.*, **391**, 958–962.
- Xu, L., Naylor, D., Dong, Z., et al.** (2018) Drought delays development of the sorghum root microbiome and enriches for monoderm bacteria. *Proc. Natl. Acad. Sci. U. S. A.*, **115**, E4284–E4293.
- Yuan, M., Jiang, Z., Bi, G., et al.** (2021) Pattern-recognition receptors are required for NLR-mediated plant immunity. *Nature*, **592**, 105–109.
- Yu, X., Feng, B., He, P. and Shan, L.** (2017) From Chaos to Harmony: Responses and Signaling upon Microbial Pattern Recognition. *Annu. Rev. Phytopathol.*, **55**, 109–137.
- Zhao, Y.-B., Liu, M.-X., Chen, T.-T., et al.** (2022) Pathogen effector AvrSr35 triggers Sr35 resistosome assembly via a direct recognition mechanism. *Sci Adv*, **8**, eabq5108.
- Zhou, F., Emonet, A., Déneraud Tendon, V., Marhavy, P., Wu, D., Lahaye, T. and Geldner, N.** (2020) Co-incidence of Damage and Microbial Patterns Controls Localized Immune Responses in Roots. *Cell*, **180**, 440–453.e18.
- Zipfel, C. and Oldroyd, G.E.D.** (2017) Plant signalling in symbiosis and immunity. *Nature*, **543**, 328–336.

## Chapter 2

### Unraveling the sugar code: the role of microbial extracellular glycans in plant-microbe interactions

Alan Wanke<sup>1,2</sup>, Milena Malisic<sup>1</sup>, Stephan Wawra<sup>1</sup>, Alga Zuccaro<sup>1</sup>

<sup>1</sup> University of Cologne, Cluster of Excellence on Plant Sciences (CEPLAS), 50679 Cologne, Germany

<sup>2</sup> Max Planck Institute for Plant Breeding Research, 50829 Cologne, Germany

This article was published in *Journal of Experimental Botany*, **72**: 15-35 (2021).  
DOI: <https://doi.org/10.1093/jxb/eraa414>



*Journal of Experimental Botany*, Vol. 72, No. 1 pp. 15–35, 2021  
doi:10.1093/jxb/eraa414 Advance Access Publication 15 September 2020

This paper is available online free of all access charges (see <https://academic.oup.com/jxb/pages/openaccess> for further details)



## REVIEW PAPER

# Unraveling the sugar code: the role of microbial extracellular glycans in plant–microbe interactions

Alan Wanke<sup>1,2</sup>, Milena Malisic<sup>1</sup>, Stephan Wawra<sup>1</sup> and Alga Zuccaro<sup>1,\*</sup>

<sup>1</sup> University of Cologne, Cluster of Excellence on Plant Sciences (CEPLAS), Institute for Plant Sciences, D-50674 Cologne, Germany

<sup>2</sup> Max Planck Institute for Plant Breeding Research, D-50829 Cologne, Germany

\* Correspondence: [azuccaro@uni-koeln.de](mailto:azuccaro@uni-koeln.de)

Received 20 May 2020; Editorial decision 1 September 2020; Accepted 14 September 2020

Editor: Andreas Weber, Heinrich-Heine-Universität Düsseldorf, Germany

## Abstract

To defend against microbial invaders but also to establish symbiotic programs, plants need to detect the presence of microbes through the perception of molecular signatures characteristic of a whole class of microbes. Among these molecular signatures, extracellular glycans represent a structurally complex and diverse group of biomolecules that has a pivotal role in the molecular dialog between plants and microbes. Secreted glycans and glycoconjugates such as symbiotic lipochitooligosaccharides or immunosuppressive cyclic  $\beta$ -glucans act as microbial messengers that prepare the ground for host colonization. On the other hand, microbial cell surface glycans are important indicators of microbial presence. They are conserved structures normally exposed and thus accessible for plant hydrolytic enzymes and cell surface receptor proteins. While the immunogenic potential of bacterial cell surface glycoconjugates such as lipopolysaccharides and peptidoglycan has been intensively studied in the past years, perception of cell surface glycans from filamentous microbes such as fungi or oomycetes is still largely unexplored. To date, only few studies have focused on the role of fungal-derived cell surface glycans other than chitin, highlighting a knowledge gap that needs to be addressed. The objective of this review is to give an overview on the biological functions and perception of microbial extracellular glycans, primarily focusing on their recognition and their contribution to plant–microbe interactions.

**Keywords:** Cell wall, chitin, extracellular polysaccharides, glucan, immunity, matrix, microbes, symbiosis.

## Introduction

Plants are immobile organisms that constantly sense and integrate information from biotic and abiotic cues in order to adapt to a dynamic environment. Monitoring of the microbial surrounding can be achieved by perception of molecular patterns that are either microbe-derived compounds [including structural microbe-associated molecular patterns (MAMPs)]

Abbreviations: AM, arbuscular mycorrhiza; CbG, cyclic  $\beta$ -glucan; CO, chitooligomer; DP, degree of polymerization; EPS, extracellular polysaccharide; GAG, galactosaminogalactan; GlcNAc, *N*-acetylglucosamine; GXM, glucuronoxylomannan; GalXM, glucuronoxylomanogalactan; GPI, glycosylphosphatidylinositol; Kdo, 2-keto-3-deoxy-octonate; LCO, lipochitooligosaccharide; LPS, lipopolysaccharide; LysM, lysin motif; MAPK, mitogen-activated protein kinase; MurNAc, *N*-acetylmuramic acid; PGN, peptidoglycan; PRR, pattern recognition receptor; pv, pathovar; RLS, rhizobium–legume symbiosis; ROS, reactive oxygen species; SA, salicylic acid; Xcc, *Xanthomonas campestris* pv. *campestris*.

© The Author(s) 2020. Published by Oxford University Press on behalf of the Society for Experimental Biology.

This is an Open Access article distributed under the terms of the Creative Commons Attribution License (<http://creativecommons.org/licenses/by/4.0/>), which permits unrestricted reuse, distribution, and reproduction in any medium, provided the original work is properly cited.

and microbial effectors] or host-specific molecules released or modified upon microbial activities, also referred to as damage-associated molecular patterns (DAMPs). Pattern sensing occurs via extracellular, membrane-integral pattern recognition receptors (PRRs) or intracellular receptors such as nucleotide-binding domain leucine-rich repeat-containing (NLR) proteins (Dodds and Rathjen, 2010; Cook *et al.*, 2015). Upon recognition of these cues, subsequent receptor activation leads to signaling cascades that enable the plant to readjust its own physiological status towards defense (including pattern-triggered immunity and effector-triggered immunity) or symbiotic (i.e. mutualistic) programs (Zipfel and Oldroyd, 2017). Common features of microbe-triggered signaling are transphosphorylation cascades, ionic fluxes and membrane depolarization, apoplastic production of reactive oxygen species (ROS), transcriptional reprogramming, phytohormone signaling, production of secondary metabolites, and initiation of developmental programs (Couto and Zipfel, 2016; Zipfel and Oldroyd, 2017). Furthermore, these plant responses also hold the potential to influence and reshape the microbial composition in above- and below-ground tissues (Xin *et al.*, 2016; Hacquard *et al.*, 2017; Teixeira *et al.*, 2019; Chen *et al.*, 2020). However, the mechanisms governing the processing and integration of information obtained from the remarkable number of signaling events into an outcome that is overall favorable for the plant remain largely unclear and are under intensive investigation.

The nature of molecular patterns acting as indicators of microbial presence is highly diverse. It covers the most important classes of biopolymers, such as proteins and peptides, fatty acids, nucleic acids, and purine derivatives, as well as glycan-based substances (Gallucci and Maffei, 2017; Saijo *et al.*, 2018; Nizam *et al.*, 2019; Albert *et al.*, 2020). Plants can sense an extremely wide spectrum of glycan substrates consisting of homo- and heteromeric polysaccharides and glycoconjugates. This includes endogenous sugar metabolites derived from carbon assimilation, plant cell wall components released upon damage, microbial glycoconjugate messengers dedicated to plant-microbe communication, as well as fibrous cell surface glycans involved in microbial biofilm and cell wall formation (Bolouri Moghaddam and Van den Ende, 2013; Limpens *et al.*, 2015; Fesel and Zuccaro, 2016). Cell surface glycans in particular represent conserved and abundant targets for the plant's surveillance system (Fesel and Zuccaro, 2016). On the other hand, microbes have evolved a plethora of tools and strategies to evade plant recognition (Rocafort *et al.*, 2020).

The widespread potential for communication mediated by glycans lies in their structural complexity. While many biological polymers (e.g. polypeptides) are of linear nature, glycans are often built from small repeating basic units of monosaccharides that assemble into different three-dimensional flexible structures with a myriad of possible linkage types and branching patterns (Guberman and Seeberger, 2019). Chain length [also referred to as degree of polymerization (DP)], chemical modifications, and supramolecular structures have been shown to

constitute relevant characteristics for specific recognition by the host (Ménard *et al.*, 2004; Takahashi *et al.*, 2009; Kanagawa *et al.*, 2011; Zipfel and Oldroyd, 2017; Wanke *et al.*, 2020).

This review provides an overview of the most important microbial glycan-derived patterns that are either directly perceived by plants or indirectly manipulate plant responses. Based on the diverse portfolio of biological and biophysical properties of microbe-derived polysaccharides, we highlight their potential to transmit information on the microbial composition (bacteria, fungi, and oomycetes) surrounding plant tissues.

### Judging a microbe by its 'cover': cell surface glycans and glycan-binding proteins in plant-microbe interactions

Cell walls from bacteria and filamentous microbes are multi-layered structures of fibrous homo- and heteropolysaccharides (Geoghegan *et al.*, 2017; Gow *et al.*, 2017) (Fig. 1). They act as mechanical support maintaining the cell turgor and determining cell shape and development (Shockman and Barrett, 1983; Money, 2008; Silhavy *et al.*, 2010; Samalova *et al.*, 2017). Although cell walls provide mechanical protection against adverse conditions and external aggressors, they can also be considered as an 'Achilles' heel' in terms of their immunological potential (Supplementary Table S1 at JXB online). Upon colonization of the plant, they are one of the very first microbial components to be in contact with plant cells, either via direct physical contact or through the release of oligomers by a fleet of plant-secreted hydrolases (Rovenich *et al.*, 2016). The basic functional principles of cell walls are comparable between different kingdoms; however, their molecular composition can be species specific (Coronado *et al.*, 2007; Mérida *et al.*, 2013; Gow *et al.*, 2017). For that reason, plants evolved a broad surveillance system to recognize structurally different carbohydrate signatures (Albert *et al.*, 2020). In the following sections we will describe the cell surface glycan compositions of bacteria and filamentous microbes (fungi and oomycetes) and highlight those glycan structures relevant for interaction with their hosts.

#### Cell surface glycans in bacteria

Plants are able to perceive a complex array of glycan-based molecules that can be found in different layers of bacterial cell walls. Two major representatives are the glycoconjugates peptidoglycan (PGN) and lipopolysaccharide (LPS) (Fig. 1). PGN consists of a polymeric glycan-based backbone composed of alternating  $\beta$ -1,4-glycosidic-linked *N*-acetylglucosamine (GlcNAc) and *N*-acetylmuramic acid (MurNAc) residues (Vollmer *et al.*, 2008). Oligopeptide bridges cross-link MurNAc residues of separate backbone polymers resulting in a multi-layered structure (Vollmer *et al.*, 2008). LPS, the second key building block, is composed of three covalently linked parts:

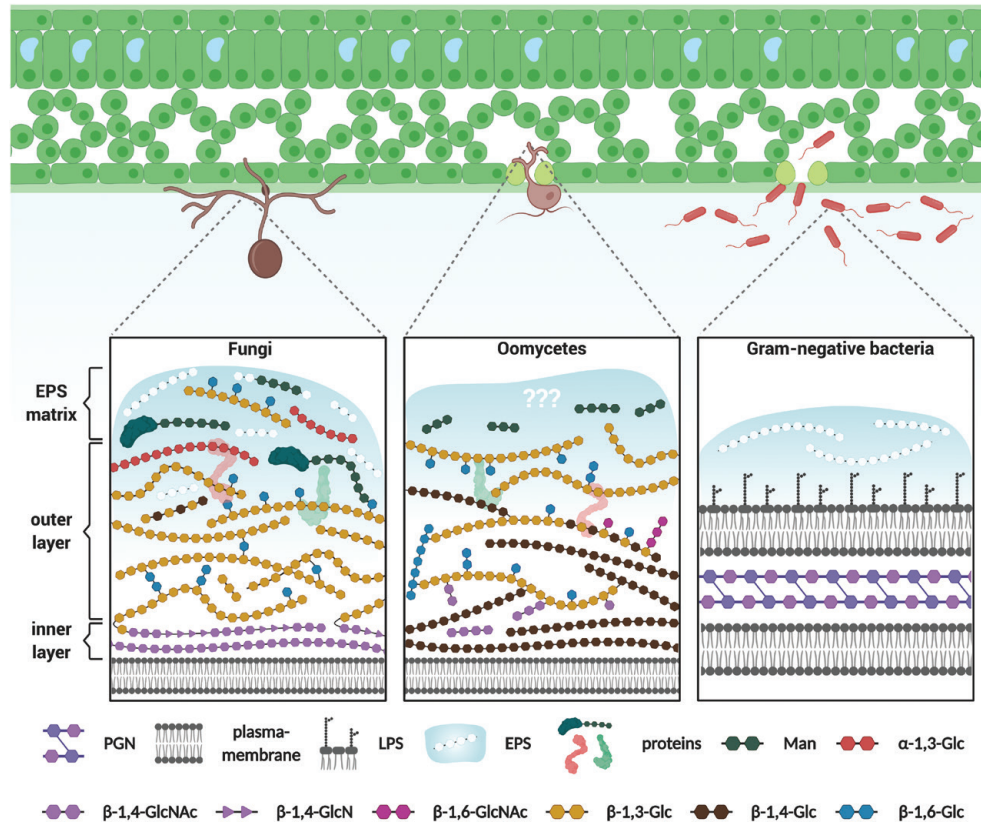


**Fig. 1.** Schematic overview of microbial cell surface glycans. Recognition of microbe-derived cell wall polysaccharides represents an important mechanism by which plants surveil their microbial surrounding. Since cell wall structure and function are highly interlocked, core polysaccharides are conserved within different microbial groups. This scheme illustrates these core polysaccharides and their linkage types without representing exact quantitative proportions. Cell walls of filamentous fungi and oomycetes are network-like structures consisting of highly interconnected polysaccharide fibrils. In fungi, the inner cell wall layer consists of chitin ( $\beta$ -1,4-GlcNAc) and chitosan polymers ( $\beta$ -1,4-GlcN). It is covalently linked to the outer cell wall layer, which is mainly composed of  $\beta$ -1,3/1,6-glucans ( $\beta$ -1,3/1,6-Glc) with minor amounts of  $\beta$ -1,4-glucose ( $\beta$ -1,4-Glc). The outer layer is concealed by  $\alpha$ -1,3-glucans ( $\alpha$ -1,3-Glc) and mixed-linkage mannose (Man) polymers. Mannose polymers often occur as heterosaccharides with minor amounts of additional sugar types (e.g. rhamnose and galactose). A highly mobile, gel-like extracellular polysaccharide (EPS) matrix is loosely attached to the outer cell wall of many fungi. In contrast to fungi, no detailed studies on the cell wall architecture of oomycetes have been performed. Cross-linked cellulose ( $\beta$ -1,4-Glc) and  $\beta$ -1,3/1,6-glucans are major components of the inner part of oomycete cell walls. Chitin ( $\beta$ -1,4- and  $\beta$ -1,6-GlcNAc) only occurs in minute amounts; most of it is assumed to be connected to  $\beta$ -glucan polymers. The cellulose content is reduced in the external parts of the cell wall. Instead, branched  $\beta$ -glucans and mannose oligomers are present in that layer. To our knowledge, no detailed information on the architecture of an EPS matrix in oomycetes has been reported. Peptidoglycan (PGN) is a conserved part of bacterial cell walls present in Gram-positive and Gram-negative bacteria. The main heteropolysaccharides consist of alternating *N*-acetylglucosamine (GlcNAc) and *N*-acetylmuramic acid residues, which are interconnected through peptide chains. In Gram-negative bacteria, PGN is embedded between an inner (plasma membrane) and outer membrane layer. The outer membrane layer is decorated with lipid-linked polysaccharides, so-called lipopolysaccharides (LPSs). An amorphous matrix made of EPSs (e.g. xanthan and succinoglycan) encases many bacterial species. A more detailed overview on microbial cell surface glycans and their implications on plant–microbe interactions can be found in [Supplementary Table S1](#).

Lipid A, the core oligosaccharide, and the O-antigen polysaccharide ([Whitfield and Trent, 2014](#)). Lipid A anchors LPS to the outer membrane via glucosamine-linked fatty acid chains. It is linked via 2-keto-3-desoxy-octonat (Kdo) to the core oligosaccharide which is composed of various sugar moieties. Lipid A and the core oligosaccharide together are also referred to as lipooligosaccharide and can be attached to a terminal O-antigen polysaccharide that is variable in size ([Whitfield and Trent, 2014](#)). While LPS is specific to Gram-negative bacteria,

PGN exists in both Gram-positive and Gram-negative bacteria. Additionally, some bacterial species have capsular polysaccharides, which are tightly associated with the bacterial membrane and contain neutral or acidic polysaccharides ([D’Haeze and Holsters, 2004](#)). The composition of capsular polysaccharides varies among bacterial species and strains, but the presence of Kdo residues is commonly observed ([Lopez-Baena \*et al.\*, 2016](#)). Moreover, a highly hydrated layer of polymeric substances, often referred to as extracellular matrix, surrounds bacterial

cells. This layer includes proteins, extracellular DNA, and polysaccharides (Flemming and Wingender, 2010). Bacterial biofilm formation is supported by the extracellular matrix and creates a three-dimensional microenvironment where cell–cell communication takes place and abiotic and biotic stresses are tackled (Flemming and Wingender, 2010).

#### *The complex role of PGN and LPS in plant immunity*

Bacterial cell wall glycans and glycoconjugates form conserved and unique structures in prokaryotes, which has driven the evolution of specialized surface-localized receptors in the hosts (Erbs and Newman, 2012; Ranf, 2016; Bacete *et al.*, 2018). In *Arabidopsis thaliana* (hereafter *Arabidopsis*), PGN is perceived by a tripartite receptor complex consisting of lysin motif (LysM) domain receptor-like proteins LYM1 and LYM3 and the LysM receptor kinase CERK1 (Willmann *et al.*, 2011). While LYM1 and LYM3 bind PGN, the transmembrane LysM receptor kinase CERK1 mediates intracellular signal transduction across the plasma membrane (Willmann *et al.*, 2011). Similarly, PGN perception in rice is mediated through the respective orthologs LYP4, LYP6, and CERK1 (B. Liu *et al.*, 2012; Ao *et al.*, 2014). PGN signaling results in initiation of canonical immune responses such as medium alkalinization, cytoplasmic calcium influx, production of nitric oxide, phosphorylation of mitogen-activated protein kinases (MAPKs), camalexin accumulation, and induction of various defense-related genes (Gust *et al.*, 2007; Erbs *et al.*, 2008; Willmann *et al.*, 2011; B. Liu *et al.*, 2012; Ao *et al.*, 2014; Liu *et al.*, 2014). In addition to defense activation by complete PGN, there is evidence that specific PGN substructures trigger immune responses in *Arabidopsis*. Muropeptides derived from *Xanthomonas campestris* pathovar (*pv.*) *campestris* (*Xcc*) and *Agrobacterium tumefaciens* PGN preparations showed immunogenic potential in *Arabidopsis* (Erbs *et al.*, 2008). Furthermore, glycan backbone structures from PGN preparations of *Staphylococcus aureus* also elicit immune responses in *Arabidopsis* (Gust *et al.*, 2007). It has recently been shown that the *Arabidopsis* chitinase LYS1 can hydrolyze the O-glycosidic  $\beta$ -1,4-bond between MurNAc and GlcNAc residues generating soluble PGN products that mediate plant recognition (Liu *et al.*, 2014). In line with PGN receptor mutants (Willmann *et al.*, 2011), knockdown of LYS1 results in super-susceptibility to the phytopathogen *Pseudomonas syringae* *pv.* *tomato* DC300 (Willmann *et al.*, 2011; Liu *et al.*, 2014). However, overexpression of LYS1 also enhances susceptibility, indicating that quantitatively regulated PGN hydrolysis is important to generate immunogenic PGN fragments of a particular DP (Liu *et al.*, 2014).

Upon recognition, LPSs can initiate classical immune responses such as cytosolic calcium influx, ROS generation, phosphorylation of MAPKs, and induction of several defense-related genes (Newman *et al.*, 1995; Zeidler *et al.*, 2004; Braun *et al.*, 2005; Silipo *et al.*, 2005; Madala

*et al.*, 2012; Desaki *et al.*, 2018; Kutschera *et al.*, 2019). Early studies promoted the notion that the Lipid A domain from LPSs triggers immune responses via the plant-specific bulb-type lectin kinase LORE in *Arabidopsis* (Ranf *et al.*, 2015). However, later studies revealed that LPS and Lipid A preparations contained co-purified medium-chain 3'-OH-fatty acids (Kutschera *et al.*, 2019). In fact, LORE mediates signal transduction upon recognition of medium-chain 3'-OH-fatty acids (fatty acid chain length: C8:0–C12:0). The LPS-bound fatty acid chains display the potential to be recognized by LORE, yet it has not been shown that they are hydrolytically released from LPS into the extracellular environment (Silipo *et al.*, 2010; Ranf, 2016; Kutschera *et al.*, 2019). Of note, two further LPS-binding proteins, LBR-1 and LBR-2, which share structural similarity with animal LPS-binding proteins (Iizasa *et al.*, 2016), were identified in *Arabidopsis* (Iizasa *et al.*, 2016, 2017). The impact on ROS generation and defense gene expression in *lbr* mutants upon LPS treatment suggests an active contribution of LBR1 and LBR2 to LPS recognition in *Arabidopsis* (Iizasa *et al.*, 2016, 2017). A different perception mechanism was observed in rice, where the LysM receptor-like kinase CERK1 is required for LPS recognition (Desaki *et al.*, 2018). Purified LPS induced ROS production and LPS-dependent transcriptional changes in wild-type-derived but not *cerk1* mutant-derived rice suspension-cultured cells (Desaki *et al.*, 2018). However, whether CERK1 induces defense signaling through direct binding of LPS remains unknown. Additionally, the core oligosaccharides and O-antigen polysaccharides of LPS were reported to trigger plant defense responses (Bedini *et al.*, 2005; Silipo *et al.*, 2005; Madala *et al.*, 2012; Kutschera *et al.*, 2019). For instance, purified core oligosaccharides from *Xcc* are immunogenic in *Arabidopsis* (Silipo *et al.*, 2005), and application of truncated LPS versions derived from *Xcc* mutants to tobacco cells suggests that the core oligosaccharide is important for LPS recognition (Braun *et al.*, 2005; Silipo *et al.*, 2005). The *P. aeruginosa* H4 strain is devoid of the O-antigen polysaccharide, lacks further sugar residues in the core oligosaccharide, and is not immunogenic, underpinning the importance of this region for immunorecognition in *Arabidopsis* (Kutschera *et al.*, 2019). Transcriptional studies with purified LPS substructures from *Burkholderia cepacia* demonstrated defense gene induction in *Arabidopsis* by the entire polysaccharide (core oligosaccharide and O-antigen polysaccharide) in addition to LPS and Lipid A (Madala *et al.*, 2012). This is supported by a study applying synthetic O-antigen polysaccharides (oligo-rhamnans) that induce defense-related gene expression in *Arabidopsis* in a DP-dependent manner, suggesting that the coiled structure is recognized by the plant (Bedini *et al.*, 2005). Besides their immunogenic activity, the core oligosaccharide from *Xcc* and the synthetic O-antigen polysaccharides harbor the potential to suppress the hypersensitive response induced by bacterial infection (Bedini, 2005; Silipo,



2005). Furthermore, purified LPSs from phytopathogenic *Xylella fastidiosa* evoke defense responses independent of the presence of the O-antigen polysaccharide, while *in vivo* studies demonstrated the importance of this polysaccharide chain in shielding immunogenic surface structures and, thereby, delaying immunorecognition (Rapicavoli et al., 2018). Additionally, the rhizobial LPS from *Sinorhizobium fredii* HH103 is unique in its structure and was recently reported to have a role in the symbiotic establishment with its host legume *Macroptilium atropurpureum* and *Cajanus cajan* (Di Lorenzo et al., 2020). *Sinorhizobium fredii* HH103 core oligosaccharide differs from previously described rhizobial core oligosaccharides by the presence of a high number of hexuronic acids and a  $\beta$ -configured pseudaminic acid derivative. LPS from the *S. fredii* HH103 *rpkM* mutant lacks the pseudaminic acid derivative residues, leading to severely impaired nodule formation and symbiosis (Di Lorenzo et al., 2020). While previous studies already reported symbiotic impairments of the *S. fredii* HH103 *rpkM* strain with different legume hosts, now the responsible structural motifs were described (Margaret et al., 2012; Acosta-Jurado et al., 2016; Di Lorenzo et al., 2020). Although these data suggest recognition of LPS sugar modules, questions regarding the components mediating their recognition and signaling remain.

#### *Bacterial extracellular polysaccharides: a way to overcome immunity*

During interaction with plants, both pathogenic and symbiotic bacteria secrete substantial amounts of extracellular polysaccharides (EPSs) into the apoplast. Several functions were attributed to bacterial EPSs such as sequestration of calcium ions, ROS scavenging, prevention of cellulose-mediated cell agglutination, tolerance to acidic pH, participation in biofilm formation, and host surface attachment (Laus et al., 2005; Aslam et al., 2008; Rinaudi and Gonzalez, 2009; Lehman and Long, 2013; Perez-Mendoza et al., 2015; Hawkins et al., 2017). The impact of EPSs on the plant host has been studied for several plant–bacterial systems. Xanthan, a polysaccharide consisting of repeating pentasaccharide units, is a key component of *Xcc* biofilms and suppresses plant immunity (Yun et al., 2006; Aslam et al., 2008). Its backbone is built by  $\beta$ -1,4-linked glucose residues and an additional trisaccharide side chain (mannose–glucuronic acid–mannose) at every second glucose unit (Yun et al., 2006). The internal mannose residues are substituted by an acetyl group, and half of the terminal mannose residues are substituted by either an acetyl- or a ketal-pyruvate residue (Yun et al., 2006). Due to its anionic nature, xanthan functions as a calcium chelator *in vitro* (Aslam et al., 2008). This capability is dramatically reduced in truncated xanthan, which is lacking the trisaccharide side chain with anionic modifications (Aslam et al., 2008). Arabidopsis pre-treatment with xanthan but not truncated xanthan prior to *Xcc* infection suppresses calcium influx-mediated defense responses such as ROS accumulation,

expression of the defense gene *PATHOGENESIS-RELATED PROTEIN 1 (PR1)*, and formation of callose depositions (Yun et al., 2006; Aslam et al., 2008). Moreover, different types of EPSs such as xanthan from *Xcc*, amylovoran from *Erwinia amylovora*, alginate from *Pseudomonas aeruginosa*, or EPS from *Ralstonia solanacearum* and the symbiotic rhizobium *Sinorhizobium meliloti* hold the potential to reduce cytosolic calcium influx and ROS generation triggered by strong bacterial peptide elicitors such as flg22 and elf18 (Aslam et al., 2008). Since most of these EPSs have been shown to exhibit strong binding to calcium ions (Aslam et al., 2008), it is assumed that the immunosuppressive effect is conferred through apoplastic calcium chelation rather than through receptor-mediated signaling. This was also supported by the fact that xanthan did not compete with flg22 receptor binding (Aslam et al., 2008). Remarkably, a study in tomato revealed that EPSs from *R. solanacearum* might also trigger defense responses depending on the host plant (Milling et al., 2011). Supported by the finding that purified EPS from *R. solanacearum* specifically elicits salicylic acid (SA)-related defense gene expression in resistant but not in the susceptible tomato cultivars, this study suggests the emergence of an as yet unknown perception mechanism for *R. solanacearum* EPS in resistant tomato varieties (Milling et al., 2011).

In rhizobia–legume symbiosis (RLS), modification of bacterial EPS is commonly associated with impaired establishment of symbiosis on the level of nodule formation, infection thread initiation and elongation, bacteroid differentiation, and/or bacterial survival inside the nodules (Downie, 2010; Kelly et al., 2013; Arnold et al., 2018; Maillet et al., 2020). The mechanism governing this EPS-mediated compatibility was intensively studied for succinoglycan. Succinoglycan consists of a repeating octasaccharide monomer composed of a galactose residue and seven glucose residues that can carry additional succinyl, acetyl, and pyruvyl modifications. In interaction with the host *Medicago truncatula* (hereafter *Medicago*), *S. meliloti* succinoglycan- (EPS-I) deficient mutants or mutants lacking the succinyl residues fail to initiate infection thread formation and to invade the plant (Jones et al., 2008; Mendis et al., 2016; Maillet et al., 2020). Further, different early transcriptional responses to wild-type *S. meliloti* and a succinoglycan-deficient mutant (*exoY*) were observed. While the presence of functional succinoglycan leads to active changes in root metabolism, the absence of succinoglycan induced a remarkably high number of plant defense genes (Jones et al., 2008). A mechanism for sensing compatible and incompatible EPSs was suggested for the *Mesorhizobium loti*–*Lotus japonicus* (hereafter *Lotus*) interaction. Screenings of different EPS-deficient *M. loti* R7A strains supported the notion that plants distinctly distinguish compatible EPSs from non-compatible EPSs in order to appropriately modulate defense responses and allow full infection thread development and bacterial release (Kelly et al., 2013). This model was supported upon identification of the *Lotus* LysM receptor kinase EPR3 that senses both native and truncated monomers of polymeric *M. loti* EPS in order

to control bacterial progression through the plant's epidermal cell layer (Kawaharada et al., 2015, 2017). The native *M. loti* EPS is *O*-acetylated and consists of an octasaccharide repeating monomer composed of glucose, galactose, glucuronic acid, and riburonic acid residues, whereas truncated EPS is a pentaglycoside lacking the terminal riburonic acid and glucuronic acid residues as well as another glucose unit (Kawaharada et al., 2015; Muszynski et al., 2016). Specificity between these two types of EPSs could be mediated by recruitment of distinct co-receptors (Kawaharada et al., 2015). Furthermore, a recent study proposes a more general role for EPR3 in surveying microbial compatibility due to its capability to bind to EPS monomers from different bacterial species (Wong et al., 2020). These findings represent a novel control mechanism for leguminous plants to differentiate between compatible and incompatible rhizobia to initiate consequent responses leading to negative or positive effects on bacterial progression (Kawaharada et al., 2017).

#### Cell surface glycans in fungi

Fungal cell walls are mesh-like structures consisting of repeatedly branched glycan polymers and proteins (Fig. 1). They are not static constructions and continuously adjust according to cell type, environmental conditions, and lifestyle phases (Geoghegan et al., 2017; Gow et al., 2017). Yet, some basic structural elements are conserved and can be considered as fundamental features. Based on recent studies, three distinct layers of glycans can be found associated with the cell surface of most fungi: a stiff inner cell wall layer, a hydrated outer layer, and a highly mobile, gel-like EPS matrix, an often overlooked fungal glycan structure loosely attached to the cell wall outer layer (Kang et al., 2018; Wawra et al., 2019). The inner cell wall layer adjacent to the plasma membrane consists of a densely packed, hydrophobic layer of chitin (Osumi, 1998; Geoghegan et al., 2017). The chitin microfibrils are linear  $\beta$ -1,4-linked GlcNAc units, highly interconnected via hydrogen bonds, resulting in a rigid skeletal layer. Additional incorporation of melanin into this chitin layer increases resistance to oxidants and mechanical resilience as observed in the penetration structures (appressoria) of *Magnaporthe oryzae* (Chumley and Valent, 1990) and *Colletotrichum graminicola* (Ludwig et al., 2014). Some chitin fibrils are covalently linked to  $\beta$ -glucan chains, the predominant component of the outer cell wall layer of many fungi (~65–90% of polysaccharide content) (Bowman and Free, 2006). The  $\beta$ -glucans in this layer are mainly connected via  $\beta$ -1,3-linkages with regularly occurring  $\beta$ -1,6-side branches every 2–25 glucose units, thought to structurally interconnect the  $\beta$ -1,3-linked fibrils (Zekovic et al., 2005). In some cases, additional  $\beta$ -1,4-linked moieties and mixed-linkage  $\beta$ -1,3/1,4-glucose polymers can be observed (Fontaine et al., 2000; Pettolino et al., 2009; Kang et al., 2018). In contrast to chitin,  $\beta$ -glucans can aggregate into helical bundles or coils and form a branched network

of non-crystalline fibrils that extends throughout the entire cell wall (Bluhm and Sarko, 1977; Bluhm et al., 1982; Osumi, 1998). On top of the  $\beta$ -glucan layer, interlinked  $\alpha$ -1,3-glucans and/or mixed-linkage mannose polymers can be found (Geoghegan et al., 2017; Gow et al., 2017). These mannans can be attached to proteins (mannoproteins), galactose, and/or rhamnose moieties (Pettolino et al., 2009; Geoghegan et al., 2017; Gow et al., 2017; Mérida et al., 2018). In general, the inner and outer cell wall layer represent the fungal cell wall in the narrower sense of the term. Cytological analyses (for more information, see Box 1) have revealed the presence of an extensive gel-like EPS matrix surrounding hyphae of different human pathogenic and plant-colonizing fungi (Gow et al., 2017; Wawra et al., 2019). This highly mobile EPS matrix is not tightly bound to the cell wall and the bulk can be removed by washing. Similar to bacterial EPSs, the fungal EPS matrix is thought to be a loose scaffold for other macromolecules such as proteins, lipids, and extracellular DNA (Martins et al., 2010; Lee and Sheppard, 2016; Wawra et al., 2019). Compositional analyses of EPS matrices from different fungal species have identified glucose, mannose, galactose, rhamnose, xylose, and/or fucose as monosaccharidic building blocks (Mahapatra and Banerjee, 2013). More specifically, the EPS matrix from the saprotrophic fungus *Trametes versicolor* (Basidiomycota) was shown to contain a linear  $\alpha$ -1,6-galactose backbone with mannose- and fucose-containing side chains (Scarpari et al., 2017). The EPS matrix of the root endophyte *Serendipita indica* (Basidiomycota) is composed of  $\beta$ -1,3/1,6-glucans (Wawra et al., 2019). Similarly, the plant pathogen *Botrytis cinerea* (Ascomycota) EPS matrix was shown to contain high molecular weight  $\beta$ -1,3/1,6-glucans (El Oirdi et al., 2011). While studies on the EPS matrix of plant-colonizing fungi are scarce, more information is available on the EPS matrix composition of human fungal pathogens. The EPS matrices from *Aspergillus fumigatus* and *Candida albicans* consist of complex galactans and mannans (Gow et al., 2017). Additionally, in *A. fumigatus*, a soluble galactosaminogalactan (GAG) made of a linear heteroglycan consisting of  $\alpha$ -1,4-linked galactose and *N*-acetylgalactosamine was described (Gravelat et al., 2013). In the human pathogen *Cryptococcus neoformans*, the capsule (highly organized EPS matrix) contains glucuronoxylomannan (GXM) and glucuronoxylomanogalactan (GalXM). GXM is an  $\alpha$ -1,3-mannose with  $\beta$ -1,2-linked xylose and glucuronic acid side chains, while GalXM consists of an  $\alpha$ -1,6-galactan chain linked to galactomannan-xylose-glucuronic acid branches (Zaragoza et al., 2008; Denham et al., 2018; Decote-Ricardo et al., 2019). The large majority of studies report data originating from the analytics of whole-cell wall preparations without detailed knowledge of whether or not a mobile EPS matrix was present and how much of this matrix was still attached to the cell wall. It is therefore often difficult to speculate on the correct compositions of the EPS matrix or outer cell wall layer. Interestingly, the cell wall layers and EPS matrix seem to be synthesized by distinct pathways in *C. albicans*,



**Box 1. Making the invisible visible: light microscopic approaches to study microbial cell walls**

Confocal laser scanning microscopy is a common tool used to assess microbial phenotypes during axenic growth and host colonization. The two major approaches for the visualization of microbes are live cell staining and staining after tissue fixation. Live cell microscopy allows the use of living samples, enabling dynamic imaging that can be used to track developments in real time and to obtain a better understanding of biological functions. This method requires easily applicable stains which do not interfere with the observed processes. Alternatively, fluorescently tagged marker proteins that localize to the region of interest can be employed. However, many organisms are not (easily) accessible to genetic engineering, especially when exhibiting an obligate biotrophic lifestyle. In these cases, exogenously applied probes are crucial tools to study the biology of these organisms. In contrast, fixation-based approaches lead to stable but inactive tissue, thus limiting the possibilities to study dynamic processes. Fixed material can be sectioned and is suitable for high-resolution light microscopy, electron microscopy, and electron microscopy tomography (Wang *et al.*, 2019; Franken *et al.*, 2020; Hansel *et al.*, 2020). Yet, sample preparation can introduce artifacts through the fixation procedure and is often labor intensive. Optimization for the respective imaging technique and specific biological sample in particular can be a bottleneck (Bell and Safiejko-Mroccka, 1997; Wisse *et al.*, 2010).

A key prerequisite for fluorescent labeling of microbes, particularly in host tissues or complex environments, is to target specific and unique microbial structures. Most of the fluorescent probes used to study microbes target cell walls or cell wall-associated components. These probes can be divided into four distinct groups: small chemical dyes; specific antibodies; fluorescent-labeled sugar-binding lectins; and engineered neolectins. The group of neolectins was reviewed in detail elsewhere and is therefore not covered here (Arnaud *et al.*, 2013). Small chemical fluorescent dyes have been used for decades, combining the advantage of having high photostability and easy application. Common stains used for the visualization of filamentous microbes are the  $\beta$ -1,3/1,4-glucan-binding fluorescent dyes Calcofluor White/Fluorescent Brightener 28 (Leigh *et al.*, 1985) and Congo Red (Darwish and Asfour, 2013). Despite the fact that both dyes target the same type of polysaccharide, they do not always localize to the same cell wall regions (Ursache *et al.*, 2018). Aniline blue, another widely used glycan stain, interacts with  $\beta$ -1,3-glucans and is also capable of detecting chitosan (Evans *et al.*, 1984; Becker *et al.*, 2016). Aniline blue stains cell walls and has been used for decades to screen for EPS-producing microorganisms (Nakanishi *et al.*, 1976). Yet, the exact nature of the interaction between these dyes and the respective glycans is still unknown. In addition, most of these small molecular fluorescent probes lack a clear specificity towards a single structure and, therefore, only function as proxies for the presence of a particular type of molecule or microbe.

In contrast to small fluorescent probes, monoclonal antibodies raised against specific glycans from microbial cell walls can display a high specificity and affinity towards the respective molecule used for immunization. However, many polysaccharides are generally far less immunogenic than proteins. While proteins generally display high internal heterogeneity and therefore carry various potential antigenic structures available for the animal immune system, large polysaccharides are often constructed of regular repeating flexible units. They often need to be conjugated to protein carriers to elicit an immune response (Cunto-Amesty *et al.*, 2001; Cobb and Kasper, 2005; Zhou *et al.*, 2009; Rydahl *et al.*, 2017). Currently, there are only a limited number of polysaccharide-directed monoclonal antibodies available. Thus, the choices for detection of cell walls of filamentous microbes and associated structures are limited. Furthermore, the use of monoclonal antibodies in confocal laser scanning microscopy is mostly confined to fixed samples, and is time consuming and expensive. A promising alternative to monoclonal antibodies are lectins, which are glycan-binding proteins. In comparison with antibodies, these proteins have lower affinities towards their selective targets but have been shaped by evolution into molecules with highly specific binding. Compared with monoclonal antibodies, lectins are small and, if fluorophore tagged, easily applicable. The binding properties of lectins to their respective glycoligand are frequently defined by the geometric arrangement of their carbohydrate recognition domains. These domains as such often display rather low affinities for monosaccharides (Gabijs, 1997). The biggest hurdle in using lectins as molecular probes lies in the determination of their glycan substrate specificity. The lack of commercially available and defined glycans for affinity screening largely limits the characterization of lectins binding to long and/or complex glycans. Therefore, most of the commercially available fluorescent lectins with defined affinities target small mono-, di-, or short oligosaccharides. A widely used lectin in the field of fungal biology is the GlcNAc-binding wheat germ

**Box 1. Continued**

agglutinin (WGA). However, GlcNAc is not only found in filamentous microbes, but also appears in the PGN layer of some bacteria or as building blocks in protein glycosylation (Quast and Lunemann, 2014; Lin *et al.*, 2017). Thus, the ability of WGA to detect a short glycoligand reduces its structural specificity. To overcome this obstacle, the use of lectins that can distinctly bind long-chain glycoligands with low affinity for short-chain ligands of the same composition would be advantageous for the field. Recently, a fungal lectin exhibiting these characteristics was identified and characterized. The WSC3 protein from *S. indica* is a lectin composed of three WSC domains that binds to long-chain  $\beta$ -1,3-glucans with no measurable affinity for shorter  $\beta$ -1,3-linked glucose oligomers (<7) (Wawra *et al.*, 2019). Optimization of the protein labeling procedure generated a very efficient probe, which is able to detect fungal EPS with very low background staining (Fig. 2). The only two described lectins able to detect fungal EPS are the  $\beta$ -1,3-glucan-binding WSC3 (Wawra *et al.*, 2019) and the  $\beta$ -1,3/1,6-glucan-binding FGB1 (Wawra *et al.*, 2016). A closer look into the microbial proteome associated with cell walls and EPSs could help to identify more lectins suitable as microscopic probes. Such probes would make a valuable contribution to the field, giving exciting insights into the structural composition of microbial cell walls and EPSs.

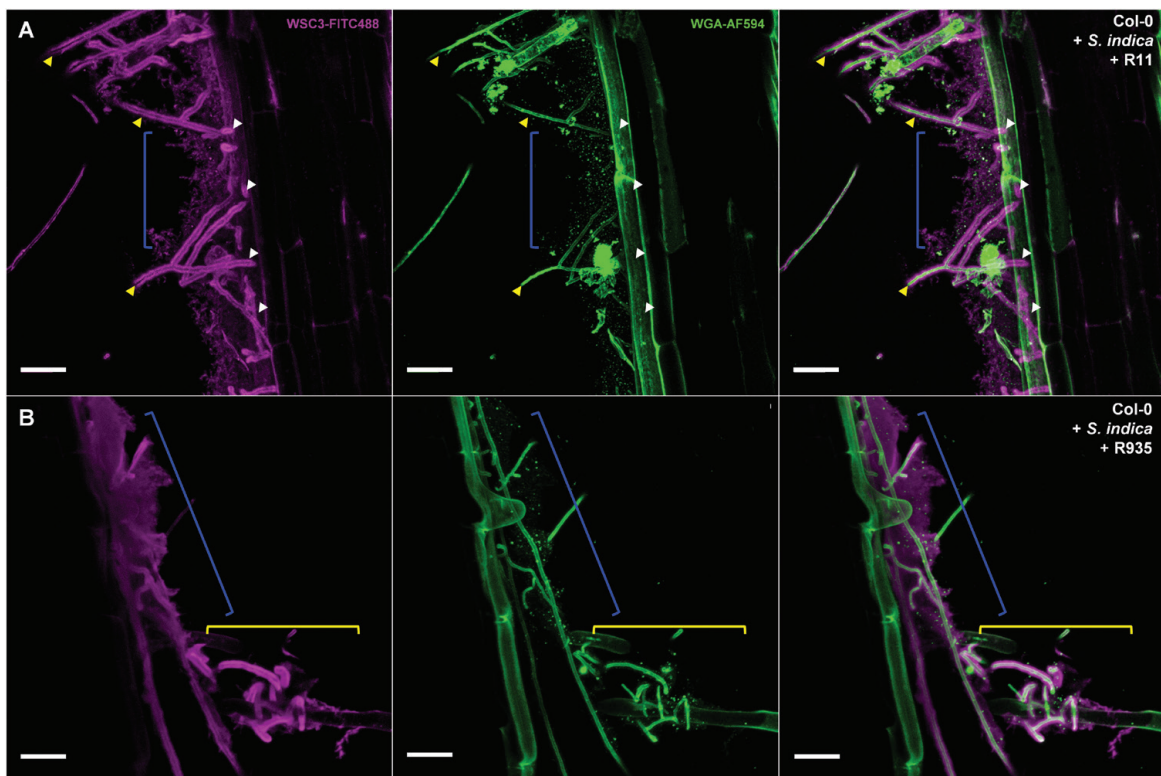


**Fig. 2.** Live cell images of root-associated bacteria embedded in the fungal  $\beta$ -glucan matrix. Confocal laser scanning microscopy live stain images of an *A. thaliana* Col-0 root segment, 12 d post-colonization with the fungus *Serendipita indica* and root-associated bacteria R11 (*Bacillus* sp.) (A) or R935 (*Flavobacterium* sp.) (B) (Bai *et al.*, 2015). The fungal cell wall and bacteria (dots) were stainable with WGA-AF594 (green pseudo-color).  $\beta$ -1,3-glucan was visualized using the FITC488-labeled lectin WSC3 (magenta pseudo-color) (Wawra *et al.*, 2019). Fungal chitin was only detected in hyphae growing in the extracellular space (yellow arrowheads), whereas the  $\beta$ -glucan matrix was also detectable after the hyphae entered the root cortical cells (white arrowheads). Interestingly, the  $\beta$ -glucan architecture was very distinct in the presence of the individual bacterial strains (structures indicated by the blue brackets). While a fine structure in the glucan network was visible for *S. indica* in combination with R11, the combination with R935 resulted in an apparently extended, more dense, and amorphous looking  $\beta$ -glucan layer. In addition, in the presence of R935, the fungal  $\beta$ -glucan matrix around the *S. indica* hyphae appeared more diffuse and less compact compared with the matrix detected around more isolated growing hyphae (B, yellow brackets). It is currently unclear whether the additionally deposited  $\beta$ -glucan is produced by the bacteria themselves or whether their presence triggers enhanced production and secretion by the fungus. Scale bars=25  $\mu$ m.

accounting for the observed structural and functional differences (Taff et al., 2012; Mitchell et al., 2015).

#### *Cell surface glycans in oomycetes—similar but different*

Despite strong morphological and lifestyle similarities to fungi, oomycetes are a phylogenetically distinct group within the Stramenopiles clade, which also includes brown algae and diatoms (Adl et al., 2012; Beakes et al., 2012). The close evolutionary relationship with algae is reflected by the presence of cellulose (linear  $\beta$ -1,4-glucan) as a major cell wall component (33.6–51%) (Mélida et al., 2013). Comparative analyses of the cell wall composition from different oomycete species have demonstrated the presence of  $\beta$ -1,3/1,4/1,6-linked homo- and heteroglucans (85.6–95%). Furthermore, chitin as well as atypical  $\beta$ -1,6-linked GlcNAc can be found in cell wall preparations of representative species from the Saprolegniales order (i.e. the legume pathogen *Aphanomyces euteiches*) (Mélida et al., 2013). Additionally, the presence of cross-linkages of  $\beta$ -1,3-glucan with cellulose or GlcNAc/chitoooligosaccharides was reported (Mélida et al., 2013; Nars et al., 2013). This association of chitin with other cell wall polymers accounts for the soluble, non-crystalline chitin fractions observed in the mycelial cell wall. In contrast to most true fungi, crystalline and non-crystalline chitin is thought to be distributed within the cell wall of oomycetes instead of being restricted to the inner layer (Badreddine et al., 2008). While chitin is reduced or absent from cell wall preparations of species from the Peronosporales order (e.g. *Phytophthora* genus), these cell walls additionally contain low amounts of mannan (6.7%) and glucuronic acid (4.7%) (Mélida et al., 2013). Few studies report on the presence of an EPS matrix secreted by encysting zoospores and germinating cysts in various oomycete species (Gubler and Hardham, 1988; Estrada-García et al., 1990; Durso et al., 1993). In the germ tubes and appressoria of *Hyaloperonospora parasitica*, the causal agent of downy mildew in many crucifers, the EPS matrix consists of  $\beta$ -1,3-glucans, mannan, galactose, GlcNAc, and *N*-acetylgalactosamine (Carzaniga et al., 2001). More work is required to further address the presence and function of the EPS matrix during later stages of plant colonization.

#### *Hide and seek: chitin perception*

In the last decades, chitin recognition in plants was intensively studied, leading to the elucidation of the main receptors and their downstream signaling pathways in several plant species (Sanchez-Vallet et al., 2015). A central player involved in chitin perception in different species is the LysM-domain receptor kinase CERK1. In Arabidopsis, recognition of chitoooligomers (COs) with at least six GlcNAc units initiates the formation of ligand-induced heteromeric complexes between CERK1 and the LysM receptor kinases LYK4 and LYK5 (Miya et al., 2007; Wan et al., 2008; Petutschnig et al., 2010; Cao et al., 2014; Xue et al., 2019). Within this complex, LYK5 exhibits the highest

affinity for COs, with a preference for oligomers having a DP of eight GlcNAc units (Cao et al., 2014). Binding to COs leads to the association of CERK1 with LYK5 and homodimerization of CERK1, which is needed for CERK1 autophosphorylation and further signal transduction (Petutschnig et al., 2010; T. Liu et al., 2012; Cao et al., 2014). LYK4 might act as a protein scaffold stabilizing the LYK5–CERK1 complex and thereby enhancing chitin-triggered responses (Xue et al., 2019). Furthermore, the weak, residual chitin response observed in *lyk5* mutants indicates that LYK4 together with CERK1 might also function as an additional receptor pair able to compensate LYK5 loss (Cao et al., 2014). In rice, chitin perception involves the CERK1 homolog and the receptor-like protein CEBiP, which is associated with the plasma membrane through a glycosylphosphatidylinositol (GPI) anchor (Kaku et al., 2006; Shimizu et al., 2010; Hayafune et al., 2014). Upon ligand binding, two CERK1 proteins associate with a pair of CEBiP receptors cooperatively binding to a single chitin molecule (Hayafune et al., 2014). Two additional rice GPI anchor receptor-like proteins, LYP4 and LYP6, also exhibit CERK1-mediated chitin binding affinity, which might function as accessory chitin perception machineries (B. Liu et al., 2012; Kouzai et al., 2014). Interestingly, CERK1-independent chitin sensing was reported within plasmodesmal membrane microdomains of Arabidopsis (Faulkner et al., 2013). Chitin-triggered plasmodesmata closure is controlled by LYM2, LYK4, and LYK5 (Faulkner et al., 2013; Cheval et al., 2020). LYM2 is a receptor-like protein with a GPI anchor which resides in plasmodesmal membranes (Faulkner et al., 2013). In response to chitin, LYM2 is suggested to oligomerize and act as a signaling platform for LYK4 and calcium-dependent protein kinases to initiate ROS production and callose synthesis (Cheval et al., 2020). These findings emphasize how a single elicitor initiates mechanistically independent responses in different membrane microdomains.

In addition to chitin-mediated activation of defense responses, several studies have shown the potential of COs (DP 4–8) to initiate nuclear calcium oscillations, a signaling hallmark during root symbiotic interactions with nitrogen-fixing rhizobia and arbuscular mycorrhizal fungi (Genre et al., 2013; Sun et al., 2015; Feng et al., 2019; He et al., 2019).

To respond to the widespread capacity of plants to detect microbial cell wall components, evolution has driven the development of a multilayered potpourri of microbial strategies to evade unintended recognition by plant receptors (Rovenich et al., 2016). Commonly observed mechanisms to avoid chitin-triggered immunity include inhibition or degradation of plant chitinases (Naumann, 2011; Jashni et al., 2015; Okmen et al., 2018) and replacement or partial conversion of chitin to chitosan, a deacetylated version of chitin with lower immunogenic potential in most plants (El Gueddari et al., 2002; Cord-Landwehr et al., 2016; Gao et al., 2019; Xu et al., 2020). Since plants lack the enzymatic toolset to degrade  $\alpha$ -1,3-glucans, decoration of exposed cell wall regions of invading hyphae with these polysaccharides acts as a protective layer

to circumvent chitin hydrolysis as was shown for *M. oryzae* (Fujikawa et al., 2012). A further layer of immunity evasion is conveyed by fungal chitin-binding effectors that are able to mask their own cell wall molecules (van den Burg et al., 2006; Marshall et al., 2011; Kombrink et al., 2017; Romero-Contreras et al., 2019; Zeng et al., 2020) or to sequester released COs (de Jonge et al., 2010; Marshall et al., 2011; Mentlak et al., 2012; Takahara et al., 2016; Romero-Contreras et al., 2019). Moreover, microbial effectors (Masachis et al., 2016; Fang et al., 2019; Irieda et al., 2019) or small RNAs (Jian and Liang, 2019) were shown to manipulate the host's chitin perception and intracellular signaling machinery.

#### *The complexity behind perception of $\beta$ -glucans from filamentous microbes*

Despite the fact that  $\beta$ -glucans are predominant components of cell walls and EPS matrices in fungi and oomycetes, comparatively little is known about their perception by plants. Early studies could show that purified  $\beta$ -glucans from plant-colonizing fungi and oomycete cell walls are potent inducers of plant defense (Ayers et al., 1976b; Anderson, 1978). Pioneering work was performed on *Phytophthora sojae* culture filtrates and cell wall hydrolysates which identified  $\beta$ -1,3/1,6-glucans as potent elicitors of plant immunity resulting in phytoalexin accumulation (Ayers et al., 1976a, b; Keen and Yoshikawa, 1983; Okinaka et al., 1995). The smallest fragment with immunogenic capability was shown to be a purified  $\beta$ -glucan heptagluco-side composed of a  $\beta$ -1,6-linked backbone with two  $\beta$ -1,3-linked glucose side branches (Cheong et al., 1991; Sharp et al., 1984a, b). Later, a high-affinity  $\beta$ -glucan-binding protein (GBP) isolated from soybean root membrane fractions was proposed to act as part of a multimeric  $\beta$ -glucan receptor complex (Umemoto et al., 1997; Cheong et al., 1993; Fliegmann et al., 2004). GBP has a glucan-binding domain and  $\beta$ -1,3-glucanase activity (Umemoto et al., 1997; Fliegmann et al., 2004). Despite the lack of membrane targeting and secretion signals, GBP localizes to both the plasma membrane and apoplast (Umemoto et al., 1997). GBP inhibition via a specific antibody diminished  $\beta$ -glucan-elicited phytoalexin synthesis in soybean, indirectly validating its role in glucan perception (Umemoto et al., 1997). Although most plant species encode GBP homologs in their genomes, only legumes mount defense responses upon elicitation with the oomycete-derived  $\beta$ -glucan (Fliegmann et al., 2004). Whether this specificity is due to missing components of the receptor complex in other plant species or whether GBPs from non-leguminous plants bind to distinct  $\beta$ -glucan structures remains open. Alternatively, GBP activity could produce tailored  $\beta$ -glucan structures subsequently recognized by plant species-specific receptor systems. Other glucans such as short and unbranched  $\beta$ -1,3-linked glucose pentamers (laminaripentaose), hexamers (laminarihexaose), and laminarin, a  $\beta$ -1,3-glucan (DP 20–30) with  $\beta$ -1,6-linked side branches, can elicit immune responses in a wide range of plant species (Fesel and Zuccaro, 2016). Laminarin is a storage

carbohydrate derived from marine brown algae which bears a remarkable resemblance to  $\beta$ -glucan structures present in many cell walls of filamentous microbes and, therefore, has often been used to investigate  $\beta$ -glucan-triggered immunity in plants and animals. Studies in monocot and dicot species have demonstrated that laminaripentaose (Klarzynski et al., 2000) and laminarihexaose (Mélida et al., 2018; Wanke et al., 2020) as well as laminarin (Klarzynski et al., 2000; Aziz et al., 2003; Ménard et al., 2004; Gauthier et al., 2014; Wawra et al., 2016; Wanke et al., 2020) activate immune responses such as calcium influx, ROS production, MAPK activation, medium alkalinization, expression of pathogenesis-related genes, phytoalexin synthesis, and phytohormone signaling. Moreover, laminarin is able to prime plant immunity and induces resistance to fungal plant pathogens and viruses in *Nicotiana tabacum* and *Vitis vinifera* (Aziz et al., 2003; Ménard et al., 2004; Gauthier et al., 2014). While the perception of laminarihexaose was shown to be mediated by CERK1 and an as yet unknown co-receptor in Arabidopsis (Mélida et al., 2018), long branched and unbranched  $\beta$ -glucans are recognized via a CERK1-independent pathway in *N. benthamiana* and rice (Wanke et al., 2020). Despite the fact that most plants are able to respond to  $\beta$ -glucans, it is striking that there are species-specific differences regarding the length, branching pattern, and presence of chemical modification (e.g. sulfation) of the perceived structures (Yamaguchi et al., 2000; Ménard et al., 2004; Wanke et al., 2020). The degree of variation in  $\beta$ -glucan recognition reflects the high structural diversity of microbial cell wall architectures between species. This implies that while chitin acts as a more general elicitor of plant immunity,  $\beta$ -glucan cues could allow for a rather specialized discrimination between different microbial groups.

A novel, chimeric type of elicitor was identified in glucanase- and chitinase-treated cell wall preparations of *A. euteiches* (Nars et al., 2013). This group of chito-glucans consists of a  $\beta$ -1,3/1,4-mixed-linkage glucan backbone with  $\beta$ -1,6-linked GlcNAc branches and is able to induce defense gene expression and nuclear calcium oscillation in *Medicago*. In contrast to lipochitooligosaccharides, chito-glucan-mediated nuclear calcium oscillations are not dependent either on the receptor kinase NFP or on the common symbiosis signaling pathway (Nars et al., 2013).

Cell wall  $\beta$ -glucans are crucial for microbial development and the formation of infection structures, but at the same time they pose the risk of disclosing the microbe's presence to the plant. To successfully manage this trade-off, cell wall synthesis is highly synchronized to microbial development in a spatial and temporal manner. Investigations of glucan synthesis in the hemibiotrophic maize pathogen *C. graminicola* demonstrated that the glucan synthases GLS1, KRE5, and KRE6 participate in the production of  $\beta$ -1,3- and  $\beta$ -1,6-glucans. Invading biotrophic hyphae of this fungus coordinately down-regulate *GLS1*, *KRE5*, and *KRE6* expression, resulting in the formation of hyphae with little or no exposed  $\beta$ -1,3/1,6-glucans (Oliveira-Garcia and Deising, 2013, 2016). Overexpression of these glucan



synthesis genes in biotrophic hyphae provokes callose production and defense gene expression. This highlights that dynamic remodeling of the cell wall architecture is an important strategy to subvert plant immunity (Oliveira-Garcia and Deising, 2013, 2016). Since plants have not been reported to possess  $\beta$ -1,6-glucanases, frequent branching patterns might spatially hinder host  $\beta$ -1,3-glucanases binding to their respective substrates and thus protect the microbe against cell wall hydrolysis (Nars *et al.*, 2013). A further microbial strategy to safeguard its cell wall integrity is mediated via glucanase inhibitor proteins (Ham *et al.*, 1997; Rose *et al.*, 2002). These secreted proteins identified in the culture filtrate of *P. sojae* prevent cleavage of cell wall glucans by binding to host  $\beta$ -glucanases. The high-affinity complex formation is driven by a serine protease domain without a functional catalytic triad necessary for protein cleavage (Rose *et al.*, 2002). More recently, the dual-function effector FGB1 from the beneficial root endophyte *Serendipita indica* was reported to mediate cell wall resistance to stress and to suppress  $\beta$ -glucan-triggered immunity in Arabidopsis and *N. benthamiana* (Wawra *et al.*, 2016). FGB1 is a fungal lectin with a strong binding affinity for  $\beta$ -1,6-linked glucose residues (Wawra *et al.*, 2016). This study draws attention to the fact that not only phytopathogenic but also beneficial fungi evolved mechanisms to circumvent recognition of their own cell wall components.

#### *The EPS of filamentous microbes: an emerging player in plant microbe-interaction?*

Although several reports document the presence of highly mobile, gel-like EPS matrices surrounding the hyphae of plant-colonizing microbes, their function is largely unknown (Carzaniga *et al.*, 2001; Wawra *et al.*, 2019). Different types of EPS matrices were shown to contribute to host adhesion (Deising *et al.*, 1992; Moloshok *et al.*, 1993; Epstein and Nicholson, 1997; Doss, 1999; Carzaniga *et al.*, 2001), act as an enzymatic scaffold (Nicholson and Moraes, 1980; Moloshok *et al.*, 1993; Doss, 1999), or confer resistance to environmental stresses (Nicholson and Moraes, 1980) in different fungi and oomycetes. Still, little is known about their direct implications in interactions with plants. Analyses of  $\beta$ -glucan-containing EPS purified from culture supernatants of an endophytic *Fusarium* species (Li *et al.*, 2014) and *B. cinerea* (El Oirdi *et al.*, 2011) revealed activation of defense-related responses in their respective hosts. In *B. cinerea*, the EPS matrix induces accumulation of SA, an important player in the complex phytohormone signaling network regulating different defense pathways (El Oirdi *et al.*, 2011). Whereas SA signaling often leads to host cell death and thereby restricts growth of biotrophic invaders, jasmonic acid (JA)-related defense generally accounts for resistance against necrotrophic pathogens (Glazebrook, 2005). Antagonistic crosstalk between these two phytohormones presents a fine-tuning mechanism to adapt immune responses according to different pathogenic lifestyles (Koornneef and Pieterse, 2008). This counteractive relationship between SA and JA is utilized by *B. cinerea* to increase disease progression in tomato

through EPS-triggered SA accumulation and consequent suppression of JA-mediated pathways (El Oirdi *et al.*, 2011).

A look into the body of literature on EPS matrices from *A. fumigatus* and *C. albicans* reveals that their EPSs can contribute to evasion of host immunity. In *A. fumigatus*, GAG polymers in the EPS matrix conceal immunogenic cell wall structures from recognition by host immune receptors (Gravelat *et al.*, 2013). Furthermore, charges within the GAG polymers can protect the hyphae from antifungal peptides via electrostatic repulsion (Lee *et al.*, 2015). Comparative genomic analyses identified the presence of a GAG biosynthetic gene cluster in plant-pathogenic fungi, indicating that GAG-like structures could play a role in plant pathogenesis (Lee *et al.*, 2016). In *C. neoformans*, the GXM of its capsule was shown to confer resistance due to its function as a ROS scavenger (Zaragoza *et al.*, 2008; Denham *et al.*, 2018). Furthermore, capsular GXM and GalXM harbor immunomodulatory properties and contribute to host immune evasion (Decote-Ricardo *et al.*, 2019). Similarly, the heterogalactan EPS from *Trametes versicolor* functions as a pro-antioxidant agent in mammalian cell lines, plants, and fungi (Scarpari *et al.*, 2017). To what extent EPS matrices from plant-colonizing fungi or oomycetes can be considered fundamental virulence and symbiosis factors needs to be further addressed.

#### **Secreted microbial glycans: messengers of peace?**

In addition to cell surface-attached glycans, microbes can secrete small and diffusible sugar oligomers and glycoconjugates that directly impact the outcome of plant–microbe interaction. While some function as signaling molecules to activate signaling cascades needed for the establishment of symbioses, others hold the potential to suppress immune responses in order to support successful plant colonization (Supplementary Table S1).

#### *The symbiont's sweet words: small secreted glycoconjugates involved in the establishment of symbiotic interactions*

Many plants form intimate associations with beneficial microbes. Among different forms of symbiotic interactions, arbuscular mycorrhiza (AM) and the RLS are two widespread representatives whose signaling pathways have been intensively studied for decades. While AM fungi improve the uptake of water and soil minerals in exchange for photoassimilates and lipids, rhizobia fix inert atmospheric nitrogen in specialized organs (nodules) functioning as an environmental niche for these bacteria. AM is genetically controlled by an ancient and highly conserved signaling pathway—the so-called common symbiosis signaling pathway—for recognition and initiation of symbiotic interactions (Oldroyd, 2013). In legumes, this

pathway is required for the establishment of both AM and RLS. Several plant genes required for symbiosis have therefore been conserved throughout evolution in monocot and dicot plants (Genre and Russo, 2016). Since these bacterial and fungal symbionts share many structural patterns with pathogens, successful establishment of mutual interactions is dependent on the integration of stimuli obtained from both immunogenic and symbiotic signals. The main glycoconjugate messengers involved in the establishment of symbiosis are chitooligosaccharides and lipochitooligosaccharides (LCOs), the latter also referred to as myc-LCOs (in AM) or nod-LCOs (in RLS) (Liang *et al.*, 2014). Their perception activates pre-symbiotic signaling, gene expression changes, and developmental programs facilitating infection and the formation of symbiotic structures such as arbuscules and root nodules (Liang *et al.*, 2014; Schmitz and Harrison, 2014). In general, LCOs are short, acylated COs (DP 3–5) with a variety of chemical modifications at their reducing and non-reducing termini. They are associated with a fatty acid at their non-reducing end and often carry further chemical modifications. The high diversity in chemical structure (backbone chain length, acetylation, sulfation, etc.) is assumed to mediate compatibility between host and microbe for specific establishment of symbiosis. Analogous to the perception of microbial cell wall components, the class of LysM motif receptor kinases is also involved in LCO signal recognition. In *Medicago*, nod-LCO perception is mediated via a heteromeric complex of the receptor-like kinases LYK3 and NFP (in *Lotus* NFR1 and NFR5) (Amor *et al.*, 2003; Limpens *et al.*, 2003; Madsen *et al.*, 2003; Radutoiu *et al.*, 2003; Arrighi *et al.*, 2006). A previous study in *Lotus* suggested a two-step mechanism for establishment of nodulation in which nod-LCOs initiate symbiotic signaling and EPR3-driven EPS sensing acts as a subsequent quality control mechanism. Nod-LCO perception triggers the first step of symbiotic signal transduction, including intranuclear oscillatory calcium spiking at the root hair tip (Ehrhardt *et al.*, 1996; Sieberer *et al.*, 2009). Further, this induces EPR3 expression and initiates nodule organogenesis within the root cortex and bacterial infection through infection threads towards the nodule primordia (Gage, 2004). During these stages, iterative EPS recognition ensures colonization with compatible bacteria and promotes the progressing infection (Kawaharada *et al.*, 2017). This collaborative recognition of nod-LCOs and rhizobial EPS presents a sophisticated way to repetitively control the advancing endosymbiosis without risking contamination with non-compatible bacteria. Of note, endophytic colonization of non-symbiotic bacteria (e.g. in mixed-colonized nodules) is also based on host-determined compatibility of their EPS (Zgadaj *et al.*, 2015). In addition to this well-established role of nod-LCOs, it was shown that nod-LCOs actively suppress defense signaling in different nodulating and non-nodulating species (Liang *et al.*, 2013).

Initiation of AM is based on perception of myc-LCOs and COs, the two major classes of diffusible symbiotic signals

found within fungal exudates. In *Medicago*, fungal myc-LCOs have been shown to trigger nuclear calcium spiking, alter gene expression patterns, and promote lateral root formation in an NFP-dependent manner (Maillet *et al.*, 2011; Czaja *et al.*, 2012; Sun *et al.*, 2015). Unexpectedly, studies in *nfp* mutants in *Medicago* revealed that overall mycorrhization was not dependent on this receptor (Amor *et al.*, 2003; Maillet *et al.*, 2011). Notably, a recent study revealed that the LysM receptor-like kinase LYK10 confers binding to myc-LCO in non-leguminous plants. In contrast to the lacking phenotype in the *Medicago nfp* mutant, *lyk10* mutation impairs AM formation in tomato and petunia (Girardin *et al.*, 2019). Since the family of LysM domain proteins is massively expanded in many plant species, it cannot be excluded that redundancy in the perception of myc-LCOs may cause the observed discrepancies.

Since perception of fungal COs also leads to oscillatory calcium fluxes, this glycoconjugate is assumed to play an important role in establishment of AM symbiosis (Genre *et al.*, 2013). While short COs (DP 3–4) are often considered as symbiotic signals and long COs (DP 6–8) as defense patterns, recent work from Feng *et al.* (2019) demonstrates that COs independent of their length activate both defense and symbiotic signaling at the same time in *Medicago*. CO sensing involves the receptor kinases LYK9 (also CERK1) and LYR4 (Bozsoki *et al.*, 2017). Combinatory application of both COs and LCOs was able to suppress immunity signaling in *Medicago*, leading to an overall symbiotic outcome (Feng *et al.*, 2019). The integration of signaling cascades from different simultaneously perceived molecules forms an elegant mechanism supporting the plant to discriminate between detrimental or symbiotic microbes in order to respond with an adequate molecular program. Moreover, CO perception demonstrates that signaling mechanisms are entangled, often making it hard to classify signaling molecules within a dichotomous conception of immunity and symbiosis.

#### *Cellooligomers and cyclic $\beta$ -glucans: secreted glycans in the extracellular space*

Cellooligomers,  $\beta$ -1,4-linked glucose oligomers, can induce mild defense-like responses in plants. The strength of these responses in Arabidopsis and grapevine is strictly coupled to the DP (Aziz *et al.*, 2007; Johnson *et al.*, 2018). So far, these molecules were mainly considered as plant cell wall-derived molecules that are perceived by membrane-bound PRRs upon activity of pathogenic cell wall-degrading enzymes or during cell wall remodeling (Aziz *et al.*, 2007; Souza *et al.*, 2017). Only recently, cellotriase was discovered to be produced by the root endophyte *S. indica*. This trisaccharide triggers cytosolic calcium elevation, weak ROS induction, and membrane depolarization in Arabidopsis and induces the up-regulation of genes involved in plant defense (Johnson *et al.*, 2018). Interestingly, a previous report on cellobiose-induced signaling

in *Arabidopsis* demonstrated a ROS-independent host response including the activation of MAPKs and up-regulation of defense-related WRKY transcription factors (Souza *et al.*, 2017). Cellotriose and cellobiose harbor the potential to synergistically increase host responses to chitin (Johnson *et al.*, 2018) and flg22 when co-applied in *Arabidopsis* (Souza *et al.*, 2017; Johnson *et al.*, 2018). Additionally, pre-treatment of grapevine with cellooligomers of different DPs (DP 7–9) was shown to promote resistance against *B. cinerea* (Aziz *et al.*, 2007), and cellobiose pre-treatment of *Arabidopsis* conferred enhanced resistance against the hemibiotrophic pathogen *P. syringae* pv. *tomato* DC3000 (Aziz *et al.*, 2007; Souza *et al.*, 2017). Yet, the components that mediate cellooligomer signaling remain unknown. In *Arabidopsis*, CERK1 and BAK1 receptor mutants remain sensitive to cellooligomers (Souza *et al.*, 2017). Furthermore, cellooligomer-pre-treated grapevine plants do not present refractory behavior in their defense response to plant cell wall-derived oligogalacturonides, indicating a separate recognition mechanism (Aziz *et al.*, 2007).

The fact that *S. indica* colonization of *Arabidopsis* (Vadassery *et al.*, 2009) and cellotriose application (Johnson *et al.*, 2018) both result in growth benefit for the plant suggests that cellotriose signaling might be involved in growth-promoting effects. Indeed, cellotriose treatment induced *Arabidopsis* genes involved in cell growth and root development, suggesting a genetically regulated mechanism for growth promotion (Vadassery *et al.*, 2009; Johnson *et al.*, 2018).

Cyclic  $\beta$ -glucans (CbGs) are produced by both pathogenic and symbiotic plant-colonizing bacteria and accumulate in the periplasmic and extracellular space (Breedveld and Miller, 1994). CbGs are involved in hypoosmotic adaption (Crespo-Rivas *et al.*, 2009), motility (Breedveld and Miller, 1994; Bhagwat *et al.*, 1996; Gay-Fraret *et al.*, 2012), and stress protection (Javvadi *et al.*, 2018). Bacterial mutants affected in CbG synthesis or periplasmic secretion form no or inefficient symbiosis or have reduced virulence, which emphasizes their relevance for plant–microbe interactions (Breedveld and Miller, 1994). CbGs can be separated into two groups based on the type of glycosidic linkage and DP. Bradyrhizobial  $\beta$ -1,3/1,6-linked cyclic glucans are built of 10–13 glucose molecules where the majority form a  $\beta$ -1,3-linked ring carrying branches of  $\beta$ -1,6-linked glucoses (Breedveld and Miller, 1994). In contrast, rhizobial cyclic glucans consist of 17–40  $\beta$ -1,2-linked glucose moieties (Breedveld and Miller, 1994). Early evidence that CbGs can act as signaling molecules was derived from studies where the  $\beta$ -1,3/1,6-linked cyclic glucans from *Bradyrhizobium japonicum* were able to suppress the immuno-eliciting activity of  $\beta$ -1,3/1,6-glucans from the soybean pathogen *P. sojae* in a concentration-dependent manner (Mithöfer *et al.*, 1996). The observation that both  $\beta$ -glucans bind to the same  $\beta$ -glucan-binding site in soybean roots suggests that the suppressive activity is mediated by competition. Bradyrhizobial CbGs were also shown to weakly

induce production of the isoflavone daidzein, a known *Nod* gene inducer in *B. japonicum* which stimulates the production of bacterial LCOs (Mithöfer *et al.*, 1996). Their impact on symbiotic interaction with soybean is dependent on the  $\beta$ -1,6-linked glucoses (Bhagwat *et al.*, 1999). In contrast to bradyrhizobial CbGs, rhizobial CbGs ( $\beta$ -1,2-linked) from symbiotic *Rhizobium leguminosarium* and the phytopathogen *Agrobacterium tumefaciens* did not lead to the production of isoflavonoids (Miller *et al.*, 1994). Furthermore, *S. meliloti* CbGs did not compete for the same receptor-binding site with the oomycete-derived  $\beta$ -1,3/1,6-glucans (Mithöfer *et al.*, 1996).

CbGs from the leaf-colonizing phytopathogenic bacterium *Xcc* were shown to actively suppress local and systemic host defense responses. This type of CbG is structurally unique due to the presence of a single  $\alpha$ -1,6-linked glycosyl residue among 15  $\beta$ -1,2-linked glycosyl-residues (York, 1995). In *N. benthamiana*, CbGs from *Xcc* suppress *PR1* induction and, locally as well as systemically, callose deposition. Accordingly, pre-treatment of *Arabidopsis* and *N. benthamiana* with physiologically relevant concentrations of bacterial CbGs increased the susceptibility to *Xcc* in a systemic manner (Rigano *et al.*, 2007). The *Xcc ndvB* mutant strain deficient in CbG production shows earlier and longer lasting *PR1* gene expression and enhanced callose deposition, resulting in lower virulence in *Arabidopsis* and *N. benthamiana* that could be restored by external application of CbGs (Rigano *et al.*, 2007). Intriguingly, restoration of the symbiotic relationship between a CbG-deficient rhizobia strain and the legume host was not observed after external application of the respective CbGs, indicating a more complex role for rhizobial CbGs during plant–bacteria interaction (Dylan *et al.*, 1990).

### Learning from the inconspicuous—a case study: the role of extracellular polysaccharides in the lichen symbiosis

An excellent example of the important role played by extracellular polysaccharides is given by the multipartite interactions occurring in lichens. Lichens are stable, long-term interactions between one or more multicellular fungi (mycobionts) and photosynthesizing single-celled algae or cyanobacteria (photobionts). These symbioses have repeatedly evolved complex three-dimensional architectures held together by hyphal cells (which represents up to 90% of the total biomass) and hydrophilic extracellular polymeric substances in the outermost layer. Below this hydrophilic layer, typically a water-repellent, gas-filled internal space is present where the photobiont is located, a prerequisite for efficient photosynthesis. Nutrients and water are diffusing from the EPS matrix into the fungal cell wall, and through the apoplast they reach the photobiont partners. Lichens and their photobionts are tolerant to desiccation

and exhibit complete physiological recovery upon rehydration. Their water content is determined by environmental water availability and they are often subjected to alternating desiccation–rehydration cycles. When hydrated, the lichen thallus expands to many times its desiccated volume. The hydrophilic properties of the EPS matrix in the outmost layer account for this effect and determine the point at which surface tension is broken and water is taken up from the environment and retained (Spribille *et al.*, 2020). Biochemical remodeling of the EPS matrix in desiccation-tolerant lichens is species-specific and seems to play a role in the response to changes in environmental water availability. Additionally, the EPS matrix serves as a surface-maximized depot for mineral nutrients and microbial-derived secondary metabolites. Because of its affinity for positively charged molecules, the EPS matrix plays an important role in heavy metal sequestration, preventing the uptake of toxic compounds into cells. This may explain the ability of certain pioneer lichens to colonize extremely polluted sites (Backor and Loppi, 2009). The EPS matrix also acts as substrate for colonization by bacteria and basidiomycetous yeasts commonly found in lichens. As in biofilms, the lichen EPS matrix functions as the main medium by which cell–cell communication between different microbial partners takes place (Spribille *et al.*, 2020).

The EPS matrix in lichens can be considered as a multipartite structure. Its composition is not determined by a single organism but instead depends on the participating symbionts. Fungi are considered to be the major inhabitant contributing the bulk of secreted polysaccharides. Using histological stains, strongly acidic polysaccharides were visualized with distinguishable differences in anionic density between the fungal cell walls and the EPS matrix, suggesting that fungal sulfated polysaccharides and polyuronic acids are present in the matrix. Most of the reports have identified neutral  $\beta$ - and  $\alpha$ -glucans and  $\alpha$ -mannans with varying ratios of glucose, galactose, and mannan as the major components in whole lichens (Olafsdottir and Ingolfsson, 2001; Carbonero *et al.*, 2002; Reis *et al.*, 2002). The  $\beta$ -glucans are mainly represented by  $\beta$ -1,3- or  $\beta$ -1,3/1,4-glucans (lichenan), while the  $\alpha$ -glucans are represented by the  $\alpha$ -1,3/1,4-glucans isolichenan and nigeran, and less commonly by mixed-linkage  $\alpha$ -1,4/1,6-glucan. Branched  $\beta$ -1,3/1,6-glucans and the  $\beta$ -1,6-glucan pustulan have also been reported in Lecanoromycetidae and Umbilicariomycetidae. These glucans are structurally similar to the core cell wall polysaccharides of fungi (Gow *et al.*, 2017). In the few basidiomycete-based lichen symbioses, different cell wall components have been found with linear  $\alpha$ -1,3-glucan (pseudonigeran). A comprehensive review of lichen EPSs is provided by Spribille *et al.* (2020). Despite the large amount of fungal biomass in lichens, other microbial partners may participate in the production of the extracellular polysaccharide matrix. Green algal symbionts are often found in the hydrophobin-lined internal chambers, generally not in direct contact with the matrix. However, recent reports have shown that algal partners can also excrete

EPS, including medium to small sized uronic acid-containing polysaccharides and sulfated polysaccharides. The composition and amount of the secreted polysaccharides were shown to depend, at least in part, on abiotic stresses such as nitrogen, light and water availability, and presence of heavy metals (Gonzalez-Hourcade *et al.*, 2020). Cyanobacterial symbionts, on the other hand, are typically embedded in a self-produced matrix. Bacterial and basidiomycetous yeast-derived EPSs in lichens are less studied but their potential functions should not be underestimated. Indeed the presence of the *nifH* gene involved in nitrogen fixation was demonstrated in several lichen-associated  $\alpha$ -proteobacteria,  $\gamma$ -proteobacteria, actinobacteria, and firmicutes (Grube *et al.*, 2009; Almendras *et al.*, 2018). Prominent among the  $\alpha$ -proteobacteria are the Rhizobiales with LAR1, a lichen-associated bacterial clade (Hodkinson and Lutzoni, 2009). It is therefore plausible to think that nitrogen-fixing bacteria represent a third important partner in the lichen symbiosis.

Understanding the structure and function of this highly organized EPS matrix in the extreme examples of lichen symbioses will help to shed light on the function of EPS matrices formed during multipartite interactions in the rhizoplane (Fig. 2) and their potential function in water, secondary metabolite, and mineral nutrient storage/utilization and immunity.

## Concluding remarks and perspective

The outcome of plant–microbe interactions is strictly governed by persistent communication processes between the involved partners. Due to the inherent structural and functional complexity of glycans and glycoconjugates, they represent an important group of messengers involved in this ongoing crosstalk. The high degree of specificity within this molecular dialog is influenced by various factors. Microbial cell walls, which are diverse networks of crystalline and soluble exopolysaccharides, often represent the starting point for recognition. While many of those structural motifs are highly conserved and can be recognized by a wide range of plants, perception of other unique structural motifs is limited to a few plant species. On the other hand, microbes secrete a fleet of molecules such as enzymes, effector proteins, and soluble glycans, in order to interfere with host recognition and the activation of defense responses. Collectively, the apoplastic encounter of plant and microbes gives rise to a multitude of signaling molecules, which need to be processed by both partners. Ancient endosymbioses such as AM and RLS highlight that collaborative receptor perception, continuous scrutiny, and integration of multiple signals is required to assess microbial compatibility and guide developmental reprogramming (Kawaharada *et al.*, 2017). While our understanding of these signaling networks and their components is constantly increasing, many questions remain unanswered. The widespread use of heterogeneous substrates



instead of pure and defined glycan structures is prompting the knowledge gap regarding receptors and downstream components for several glycan-based ligands (e.g.  $\beta$ -glucans and LPSs). Recent technological advances made in glycoscience, glycan synthesis, and structural biology will improve the quality of glycan substrates and help to revisit our understanding of how carbohydrate signatures contribute to host–microbe interactions (Weishaupt *et al.*, 2017; Kang *et al.*, 2018; Guberman and Seeberger, 2019; Reichhardt *et al.*, 2019). Furthermore, not much attention has been paid to the impact of microbial EPS matrices surrounding plant organs. Although the composition and structural organization of EPS matrices differ between different microbial classes, functional convergence can be observed. Since EPS matrices of plant-colonizing bacteria and human-pathogenic fungi have been shown to be crucial determinants of host–microbe interactions, a similarly important function can be assumed for EPS matrices of filamentous microbes interacting with plants. Interestingly, bacteria and fungi commonly form mixed, interkingdom biofilms on plant tissues and in lichens (van Overbeek and Saikkonen, 2016; Guennoc *et al.*, 2018). As observed in the latter, the EPS architecture within such multipartite consortia is jointly shaped and highly adapted to the demands of its inhabitants. Taking into account that each partner within collaborative microbial biofilms contributes its own set of enzymes involved in glycan synthesis and hydrolysis (Bamford *et al.*, 2019), this could fuel the generation of unique community patterns. Therefore, it would be of great interest to understand whether such community-derived glycan signatures are relevant for microbiota assembly and plant recognition. The recent technological advances made in glycoscience, glycan synthesis, and structural biology will surely help to increase our understanding of these glycan structures and shed light on their contribution to host–microbe interactions.

## Supplementary data

The following supplementary data are available at *JXB* online.

Table S1. Overview of microbial glycans and glycoconjugate structures and their relevance for host–microbe interactions.

## Acknowledgements

We apologize to all our colleagues in this field whose work could not be cited due to word count limitation. We thank Ruben Garrido-Oter, Paul Schulze-Lefert and the DECRYPT community (SPP 2125) for providing the bacterial strains used for microscopy. AW was supported by the Max-Planck-Gesellschaft through the International Max Planck Research School (IMPRS) on ‘Understanding Complex Plant Traits using Computational and Evolutionary Approaches’ and the University of Cologne. AZ, MM, and SW acknowledge support from the Cluster of Excellence on Plant Sciences (CEPLAS) funded by the Deutsche Forschungsgemeinschaft (DFG, German Research Foundation) under Germany’s Excellence Strategy – EXC 2048/1 – Project ID: 390686111

## Extracellular glycans in plant–microbe interactions | 29

and ZU 263/11-1 (SPP DECRYPT). Graphical illustrations were designed with the BioRender online tool.

## Author contributions

AW, MM, and AZ developed the concept of this review. All authors wrote the manuscript, AW coordinated the writing process. AW and SW prepared the figures; SW performed the microscopy. AZ supervised the project and acquired the funding.

## Conflict of interest

The authors declare no competing interests.

## Data availability

All data supporting the content of this study are available within the review and within its supplementary data published online.

## References

- Acosta-Jurado S, Rodriguez-Navarro DN, Kawaharada Y, *et al.* 2016. *Sinorhizobium fredii* HH103 invades *Lotus burtii* by crack entry in a nod factor- and surface polysaccharide-dependent manner. *Molecular Plant-Microbe Interactions* **29**, 925–937.
- Adl SM, Simpson AG, Lane CE, *et al.* 2012. The revised classification of eukaryotes. *Journal of Eukaryotic Microbiology* **59**, 429–493.
- Albert I, Hua C, Nürnberger T, Pruitt RN, Zhang L. 2020. Surface sensor systems in plant immunity. *Plant Physiology* **182**, 1582–1596.
- Almendras K, Garcia J, Caru M, Orlando J. 2018. Nitrogen-fixing bacteria associated with *Peltigera cyanolichens* and *Cladonia chlorolichens*. *Molecules* **23**.
- Amor BB, Shaw SL, Oldroyd GE, Maillet F, Penmetsa RV, Cook D, Long SR, Denarie J, Gough C. 2003. The NFP locus of *Medicago truncatula* controls an early step of Nod factor signal transduction upstream of a rapid calcium flux and root hair deformation. *The Plant Journal* **34**, 495–506.
- Anderson JA. 1978. The isolation from three species of *Colletotrichum* of glucan containing polysaccharides that elicit a defense response in bean (*Phaseolus vulgaris*). *Phytopathology* **68**, 189–194.
- Ao Y, Li Z, Feng D, Xiong F, Liu J, Li JF, Wang M, Wang J, Liu B, Wang HB. 2014. OsCERK1 and OsRLCK176 play important roles in peptidoglycan and chitin signaling in rice innate immunity. *The Plant Journal* **80**, 1072–1084.
- Arnaud J, Audfray A, Imbert A. 2013. Binding sugars: from natural lectins to synthetic receptors and engineered neolectins. *Chemical Society Reviews* **42**, 4798–4813.
- Arnold MFF, Penterman J, Shabab M, Chen EJ, Walker GC. 2018. Important late-stage symbiotic role of the *Sinorhizobium mellotti* exopolysaccharide succinoglycan. *Journal of Bacteriology* **200**, e00665-17.
- Arrighi JF, Barre A, Ben Amor B, *et al.* 2006. The *Medicago truncatula* lysin [corrected] motif-receptor-like kinase gene family includes NFP and new nodule-expressed genes. *Plant Physiology* **142**, 265–279.
- Aslam SN, Newman MA, Erbs G, *et al.* 2008. Bacterial polysaccharides suppress induced innate immunity by calcium chelation. *Current Biology* **18**, 1078–1083.
- Ayers AR, Ebel J, Finelli F, Berger N, Albersheim P. 1976a. Host–pathogen interactions: IX. Quantitative assays of elicitor activity and

- characterization of the elicitor present in the extracellular medium of cultures of *Phytophthora megasperma* var. *sojiae*. *Plant Physiology* **57**, 751–759.
- Ayers AR, Ebel J, Valent B, Albersheim P.** 1976b. Host–pathogen interactions: X. Fractionation and biological activity of an elicitor isolated from the mycelial walls of *Phytophthora megasperma* var. *sojiae*. *Plant Physiology* **57**, 760–765.
- Aziz A, Gauthier A, Bézier A, Poinssot B, Joubert JM, Pugin A, Heyraud A, Baillieu F.** 2007. Elicitor and resistance-inducing activities of beta-1,4 cellodextrins in grapevine, comparison with beta-1,3 glucans and alpha-1,4 oligogalacturonides. *Journal of Experimental Botany* **58**, 1463–1472.
- Aziz A, Poinssot B, Daire X, Adrian M, Bézier A, Lambert B, Joubert JM, Pugin A.** 2003. Laminarin elicits defense responses in grapevine and induces protection against *Botrytis cinerea* and *Plasmopara viticola*. *Molecular Plant-Microbe Interactions* **16**, 1118–1128.
- Bacete L, Mélida H, Miedes E, Molina A.** 2018. Plant cell wall-mediated immunity: cell wall changes trigger disease resistance responses. *The Plant Journal* **93**, 614–636.
- Backor M, Loppi S.** 2009. Interactions of lichens with heavy metals. *Biologia Plantarum* **53**, 214–222.
- Badreddine I, Lafitte C, Heux L, Skandalis N, Spanou Z, Martinez Y, Esquerré-Tugayé MT, Bulone V, Dumas B, Bottin A.** 2008. Cell wall chitosaccharides are essential components and exposed patterns of the phytopathogenic oomycete *Aphanomyces euteiches*. *Eukaryotic Cell* **7**, 1980–1993.
- Bai Y, Müller DB, Srinivas G, et al.** 2015. Functional overlap of the *Arabidopsis* leaf and root microbiota. *Nature* **528**, 364–369.
- Bamford NC, Le Mauff F, Subramanian AS, et al.** 2019. Ega3 from the fungal pathogen *Aspergillus fumigatus* is an endo-alpha-1,4-galactosaminidase that disrupts microbial biofilms. *Journal of Biological Chemistry* **294**, 13833–13849.
- Beakes GW, Glockling SL, Sekimoto S.** 2012. The evolutionary phylogeny of the oomycete ‘fungi’. *Protoplasma* **249**, 3–19.
- Becker M, Becker Y, Green K, Scott B.** 2016. The endophytic symbiont *Epichloë festucae* establishes an epiphyllous net on the surface of *Lolium perenne* leaves by development of an expressorium, an appressorium-like leaf exit structure. *New Phytologist* **211**, 240–254.
- Bedini E, De Castro C, Erbs G, Mangoni L, Dow JM, Newman MA, Parrilli M, Unverzagt C.** 2005. Structure-dependent modulation of a pathogen response in plants by synthetic O-antigen polysaccharides. *Journal of the American Chemical Society* **127**, 2414–2416.
- Bell PBJ, Safiejko-Mroccka B.** 1997. Preparing whole mounts of biological specimens for imaging macromolecular structures by light and electron microscopy. *International Journal of Imaging Systems and Technology* **8**, 225–239.
- Bhagwat AA, Gross KC, Tully RE, Keister DL.** 1996. Beta-glucan synthesis in *Bradyrhizobium japonicum*: characterization of a new locus (*ndvC*) influencing beta-(1→6) linkages. *Journal of Bacteriology* **178**, 4635–4642.
- Bhagwat AA, Mithöfer A, Pfeffer PE, Kraus C, Spickers N, Hotchkiss A, Ebel J, Keister DL.** 1999. Further studies of the role of cyclic beta-glucans in symbiosis. An *NdvC* mutant of *Bradyrhizobium japonicum* synthesizes cyclodecakis-(1→3)-beta-glucosyl. *Plant Physiology* **119**, 1057–1064.
- Bluhm TL, Deslandes Y, Marchessault RH, Perez S, Rinaudo M.** 1982. Solid-state and solution conformation of scleroglucan. *Carbohydrate Research* **100**, 117–130.
- Bluhm TL, Sarko A.** 1977. The triple helical structure of lentinan, a linear  $\beta$ -(1→3)-D-glucan. *Canadian Journal of Chemistry* **55**, 293–299.
- Bolouri Moghaddam MR, Van den Ende W.** 2013. Sweet immunity in the plant circadian regulatory network. *Journal of Experimental Botany* **64**, 1439–1449.
- Bowman SM, Free SJ.** 2006. The structure and synthesis of the fungal cell wall. *Bioessays* **28**, 799–808.
- Bozsoki Z, Cheng J, Feng F, Gysel K, Vinther M, Andersen KR, Oldroyd G, Blaise M, Radutoiu S, Stougaard J.** 2017. Receptor-mediated chitin perception in legume roots is functionally separable from Nod factor perception. *Proceedings of the National Academy of Sciences, USA* **114**, E8118–E8127.
- Braun SG, Meyer A, Holst O, Pühler A, Niehaus K.** 2005. Characterization of the *Xanthomonas campestris* pv. *campestris* lipopolysaccharide substructures essential for elicitation of an oxidative burst in tobacco cells. *Molecular Plant-Microbe Interactions* **18**, 674–681.
- Breedveld MW, Miller KJ.** 1994. Cyclic beta-glucans of members of the family Rhizobiaceae. *Microbiological Reviews* **58**, 145–161.
- Cao Y, Liang Y, Tanaka K, Nguyen CT, Jedrzejczak RP, Joachimiak A, Stacey G.** 2014. The kinase LYK5 is a major chitin receptor in *Arabidopsis* and forms a chitin-induced complex with related kinase CERK1. *eLife* **3**, e03766.
- Carbonero ER, Sasaki GL, Gorin PA, Iacomini M.** 2002. A (1→6)-linked beta-mannopyranan, pseudonigeran, and a (1→4)-linked beta-xylan, isolated from the lichenised basidiomycete *Dictyonema glabratum*. *FEMS Microbiology Letters* **206**, 175–178.
- Carzaniga R, Bowyer P, O’Connell RJ.** 2001. Production of extracellular matrices during development of infection structures by the downy mildew *Peronospora parasitica*. *New Phytologist* **149**, 83–93.
- Chen T, Nomura K, Wang X, et al.** 2020. A plant genetic network for preventing dysbiosis of the phyllosphere. *Nature* **580**, 653–657.
- Cheong JJ, Alba R, Côté F, Enkerli J, Hahn MG.** 1993. Solubilization of functional plasma membrane-localized hepta-beta-glucoside elicitor-binding proteins from soybean. *Plant Physiology* **103**, 1173–1182.
- Cheong JJ, Birberg W, Fügedi P, Pilotti A, Garegg PJ, Hong N, Ogawa T, Hahn MG.** 1991. Structure–activity relationships of oligo-beta-glucoside elicitors of phytoalexin accumulation in soybean. *The Plant Cell* **3**, 127–136.
- Cheval C, Samwald S, Johnston MG, de Keijzer J, Breakspear A, Liu X, Bellandi A, Kadota Y, Zipfel C, Faulkner C.** 2020. Chitin perception in plasmodesmata characterizes submembrane immune-signaling specificity in plants. *Proceedings of the National Academy of Sciences, USA* **117**, 9621–9629.
- Chumley FG, Valent B.** 1990. Genetic analysis of melanin-deficient, nonpathogenic mutants of *Magnaporthe grisea*. *Molecular Plant-Microbe Interactions* **3**, 135–143.
- Cobb BA, Kasper DL.** 2005. Coming of age: carbohydrates and immunity. *European Journal of Immunology* **35**, 352–356.
- Cook DE, Mesarich CH, Thomma BP.** 2015. Understanding plant immunity as a surveillance system to detect invasion. *Annual Review of Phytopathology* **53**, 541–563.
- Cord-Landwehr S, Melcher RL, Kolkenbrock S, Moerschbacher BM.** 2016. A chitin deacetylase from the endophytic fungus *Pestalotiopsis* sp. efficiently inactivates the elicitor activity of chitin oligomers in rice cells. *Scientific Reports* **6**, 38018.
- Coronado JE, Mneimneh S, Epstein SL, Qiu WG, Lipke PN.** 2007. Conserved processes and lineage-specific proteins in fungal cell wall evolution. *Eukaryotic Cell* **6**, 2269–2277.
- Couto D, Zipfel C.** 2016. Regulation of pattern recognition receptor signalling in plants. *Nature Reviews. Immunology* **16**, 537–552.
- Crespo-Rivas JC, Margaret I, Hidalgo A, et al.** 2009. *Sinorhizobium fredii* HH103 cgs mutants are unable to nodulate determinate- and indeterminate nodule-forming legumes and overproduce an altered EPS. *Molecular Plant-Microbe Interactions* **22**, 575–588.
- Cunto-Amesty G, Dam TK, Luo P, Monzavi-Karbassi B, Brewer CF, Van Cott TC, Kieber-Emmons T.** 2001. Directing the immune response to carbohydrate antigens. *Journal of Biological Chemistry* **276**, 30490–30498.
- Czaja LF, Hogeckamp C, Lamm P, Maillat F, Martinez EA, Samain E, Dénarié J, Küster H, Hohnjec N.** 2012. Transcriptional responses toward diffusible signals from symbiotic microbes reveal MtNFP- and MtDMI3-dependent reprogramming of host gene expression by arbuscular mycorrhizal fungal lipochitooligosaccharides. *Plant Physiology* **159**, 1671–1685.
- Darwish SF, Asfour HA.** 2013. Investigation of biofilm forming ability in *Staphylococci* causing bovine mastitis using phenotypic and genotypic assays. *TheScientificWorldJournal* **2013**, 378492.

- Decote-Ricardo D, LaRocque-de-Freitas IF, Rocha JDB, Nascimento DO, Nunes MP, Morrot A, Freire-de-Lima L, Previato JO, Mendonça-Previato L, Freire-de-Lima CG.** 2019. Immunomodulatory role of capsular polysaccharides constituents of *Cryptococcus neoformans*. *Frontiers in Medicine* **6**, 129.
- Deising H, Nicholson RL, Haug M, Howard RJ, Mendgen K.** 1992. Adhesion pad formation and the involvement of cutinase and esterases in the attachment of uredospores to the host cuticle. *The Plant Cell* **4**, 1101–1111.
- de Jonge R, van Esse HP, Kombrink A, Shinya T, Desaki Y, Bours R, van der Krol S, Shibuya N, Joosten MH, Thomma BP.** 2010. Conserved fungal LysM effector Ecp6 prevents chitin-triggered immunity in plants. *Science* **329**, 953–955.
- Denham ST, Verma S, Reynolds RC, Worne CL, Daugherty JM, Lane TE, Brown JCS.** 2018. Regulated release of cryptococcal polysaccharide drives virulence and suppresses immune cell infiltration into the central nervous system. *Infection and Immunity* **86**.
- Desaki Y, Kouzai Y, Ninomiya Y, et al.** 2018. OsCERK1 plays a crucial role in the lipopolysaccharide-induced immune response of rice. *New Phytologist* **217**, 1042–1049.
- D’Haeze W, Holsters M.** 2004. Surface polysaccharides enable bacteria to evade plant immunity. *Trends in Microbiology* **12**, 555–561.
- Di Lorenzo F, Speciale I, Silipo A, et al.** 2020. Structure of the unusual *Sinorhizobium fredii* HH103 lipopolysaccharide and its role in symbiosis. *Journal of Biological Chemistry* **295**, 10969–10987.
- Dodds PN, Rathjen JP.** 2010. Plant immunity: towards an integrated view of plant–pathogen interactions. *Nature Reviews. Genetics* **11**, 539–548.
- Doss RP.** 1999. Composition and enzymatic activity of the extracellular matrix secreted by germlings of *Botrytis cinerea*. *Applied and Environmental Microbiology* **65**, 404–408.
- Downie JA.** 2010. The roles of extracellular proteins, polysaccharides and signals in the interactions of rhizobia with legume roots. *FEMS Microbiology Reviews* **34**, 150–170.
- Durso L, Lehnen LP, Powell MJ.** 1993. Characteristics of extracellular adhesions produced during *Saprolegnia ferax* secondary zoospore encystment and cystospore germination. *Mycologia* **85**, 744–755.
- Dylan T, Nagpal P, Helinski DR, Ditta GS.** 1990. Symbiotic pseudorevertants of *Rhizobium melloti* *ndv* mutants. *Journal of Bacteriology* **172**, 1409–1417.
- Ehrhardt DW, Wais R, Long SR.** 1996. Calcium spiking in plant root hairs responding to *Rhizobium* nodulation signals. *Cell* **85**, 673–681.
- El Gueddari NE, Rauchhaus U, Moerschbacher BM, Deising HB.** 2002. Developmentally regulated conversion of surface-exposed chitin to chitosan in cell walls of plant pathogenic fungi. *New Phytologist* **156**, 103–112.
- El Oirdi M, El Rahman TA, Rigano L, El Hadrami A, Rodriguez MC, Daayf F, Vojnov A, Bouarab K.** 2011. *Botrytis cinerea* manipulates the antagonistic effects between immune pathways to promote disease development in tomato. *The Plant cell* **23**, 2405–2421.
- Epstein L, Nicholson RL.** 1997. Adhesion of spores and hyphae to plant surfaces. In: Carroll GC, Tudzynski P, eds. *Plant relationships: Part A*. Berlin, Heidelberg: Springer Berlin Heidelberg, 11–25.
- Erbs G, Newman MA.** 2012. The role of lipopolysaccharide and peptidoglycan, two glycosylated bacterial microbe-associated molecular patterns (MAMPs), in plant innate immunity. *Molecular Plant Pathology* **13**, 95–104.
- Erbs G, Silipo A, Aslam S, et al.** 2008. Peptidoglycan and muropeptides from pathogens *Agrobacterium* and *Xanthomonas* elicit plant innate immunity: structure and activity. *Chemistry & Biology* **15**, 438–448.
- Estrada-Garcia MT, Callow JA, Green JR.** 1990. Monoclonal antibodies to the adhesive cell coat secreted by *Pythium aphanidermatum* zoospores recognise 200×10<sup>3</sup> M, glycoproteins stored within large peripheral vesicles. *Journal of Cell Science* **95**, 199–206.
- Evans NA, Hoynes PA, Stone BA.** 1984. Characteristics and specificity of the interaction of a fluorochrome from aniline blue (siflofluor) with polysaccharides. *Carbohydrate Polymers* **4**, 215–230.
- Fang A, Gao H, Zhang N, Zheng X, Qiu S, Li Y, Zhou S, Cui F, Sun W.** 2019. A novel effector gene SCRE2 contributes to full virulence of *Ustilagoideae virens* to rice. *Frontiers in Microbiology* **10**, 845.
- Faulkner C, Petutschnig E, Benitez-Alfonso Y, Beck M, Robatzek S, Lipka V, Maule AJ.** 2013. LYM2-dependent chitin perception limits molecular flux via plasmodesmata. *Proceedings of the National Academy of Sciences, USA* **110**, 9166–9170.
- Feng F, Sun J, Radhakrishnan GV, et al.** 2019. A combination of chitooligosaccharide and lipochitooligosaccharide recognition promotes arbuscular mycorrhizal associations in *Medicago truncatula*. *Nature Communications* **10**, 5047.
- Fesel PH, Zuccaro A.** 2016. Beta-glucan: crucial component of the fungal cell wall and elusive MAMP in plants. *Fungal Genetics and Biology* **90**, 53–60.
- Flemming HC, Wingender J.** 2010. The biofilm matrix. *Nature Reviews. Microbiology* **8**, 623–633.
- Fliegmann J, Mithofer A, Wanner G, Ebel J.** 2004. An ancient enzyme domain hidden in the putative beta-glucan elicitor receptor of soybean may play an active part in the perception of pathogen-associated molecular patterns during broad host resistance. *Journal of Biological Chemistry* **279**, 1132–1140.
- Fontaine T, Simenel C, Dubreucq G, Adam O, Delepierre M, Lemoine J, Vorgias CE, Diaquin M, Latge JP.** 2000. Molecular organization of the alkali-insoluble fraction of *Aspergillus fumigatus* cell wall. *Journal of Biological Chemistry* **275**, 41528.
- Franken LE, Grünwald K, Boekema EJ, Stuart MCA.** 2020. A technical introduction to transmission electron microscopy for soft-matter: imaging, possibilities, choices, and technical developments. *Small* **16**, e1906198.
- Fujikawa T, Sakaguchi A, Nishizawa Y, Kouzai Y, Minami E, Yano S, Koga H, Meshi T, Nishimura M.** 2012. Surface  $\alpha$ -1,3-glucan facilitates fungal stealth infection by interfering with innate immunity in plants. *PLoS Pathogens* **8**, e1002882.
- Gabius HJ.** 1997. Animal lectins. *European Journal of Biochemistry* **243**, 543–576.
- Gage DJ.** 2004. Infection and invasion of roots by symbiotic, nitrogen-fixing rhizobia during nodulation of temperate legumes. *Microbiology and Molecular Biology Reviews* **68**, 280–300.
- Gallucci S, Maffei ME.** 2017. DNA sensing across the tree of life. *Trends in Immunology* **38**, 719–732.
- Gao F, Zhang BS, Zhao JH, Huang JF, Jia PS, Wang S, Zhang J, Zhou JM, Guo HS.** 2019. Deacetylation of chitin oligomers increases virulence in soil-borne fungal pathogens. *Nature Plants* **5**, 1167–1176.
- Gauthier A, Trouvelot S, Kelloniemi J, et al.** 2014. The sulfated laminarin triggers a stress transcriptome before priming the SA- and ROS-dependent defenses during grapevine’s induced resistance against *Plasmopara viticola*. *PLoS One* **9**, e88145.
- Gay-Fraret J, Ardisson S, Kambara K, Broughton WJ, Deakin WJ, Le Quéré A.** 2012. Cyclic- $\beta$ -glucans of *Rhizobium* (*Sinorhizobium*) sp. strain NGR234 are required for hypo-osmotic adaptation, motility, and efficient symbiosis with host plants. *FEMS Microbiology Letters* **333**, 28–36.
- Genre A, Chabaud M, Balzergue C, et al.** 2013. Short-chain chitin oligomers from arbuscular mycorrhizal fungi trigger nuclear Ca<sup>2+</sup> spiking in *Medicago truncatula* roots and their production is enhanced by strigolactone. *New Phytologist* **198**, 190–202.
- Genre A, Russo G.** 2016. Does a common pathway transduce symbiotic signals in plant–microbe interactions? *Frontiers in Plant Science* **7**, 96.
- Geoghegan I, Steinberg G, Gurr S.** 2017. The role of the fungal cell wall in the infection of plants. *Trends in Microbiology* **25**, 957–967.
- Girardin A, Wang T, Ding Y, et al.** 2019. LCO receptors involved in arbuscular mycorrhiza are functional for rhizobia perception in legumes. *Current Biology* **29**, 4249–4259.
- Glazebrook J.** 2005. Contrasting mechanisms of defense against biotrophic and necrotrophic pathogens. *Annual Review of Phytopathology* **43**, 205–227.



- González-Hourcade M, Del Campo EM, Braga MR, Salgado A, Casano LM.** 2020. Disentangling the role of extracellular polysaccharides in desiccation tolerance in lichen-forming microalgae. First evidence of sulfated polysaccharides and ancient sulfotransferase genes. *Environmental Microbiology* **22**, 3096–3111.
- Gow NAR, Latge JP, Munro CA.** 2017. The fungal cell wall: structure, biosynthesis, and function. *Microbiology Spectrum* **5**, doi:10.1128/microbiolspec.FUNK-0035-2016.
- Gravelat FN, Beauvais A, Liu H, et al.** 2013. *Aspergillus galactosaminogalactan* mediates adherence to host constituents and conceals hyphal  $\beta$ -glucan from the immune system. *PLoS Pathogens* **9**, e1003575.
- Grube M, Cardinale M, de Castro JV Jr, Müller H, Berg G.** 2009. Species-specific structural and functional diversity of bacterial communities in lichen symbioses. *The ISME Journal* **3**, 1105–1115.
- Guberman M, Seeberger PH.** 2019. Automated glycan assembly: a perspective. *Journal of the American Chemical Society* **141**, 5581–5592.
- Gubler F, Hardham AR.** 1988. Secretion of adhesive material during encystment of *Phytophthora cinnamomi* zoospores, characterized by immunogold labelling with monoclonal antibodies to components of peripheral vesicles. *Journal of Cell Science* **90**, 225–235.
- Guenoc CM, Rose C, Labbe J, Deveau A.** 2018. Bacterial biofilm formation on the hyphae of ectomycorrhizal fungi: a widespread ability under controls? *FEMS Microbiology Ecology* **94**, fty093.
- Gust AA, Biswas R, Lenz HD, et al.** 2007. Bacteria-derived peptidoglycans constitute pathogen-associated molecular patterns triggering innate immunity in Arabidopsis. *Journal of Biological Chemistry* **282**, 32338–32348.
- Hacquard S, Spaepen S, Garrido-Oter R, Schulze-Lefert P.** 2017. Interplay between innate immunity and the plant microbiota. *Annual Review of Phytopathology* **55**, 565–589.
- Ham K-S, Wu S-C, Darvill AG, Albersheim P.** 1997. Fungal pathogens secrete an inhibitor protein that distinguishes isoforms of plant pathogenesis-related endo- $\beta$ -1,3-glucanases. *The Plant Journal* **11**, 169–179.
- Hansel CS, Holme MN, Gopal S, Stevens MM.** 2020. Advances in high-resolution microscopy for the study of intracellular interactions with biomaterials. *Biomaterials* **226**, 119406.
- Hawkins JP, Geddes BA, Oresnik IJ.** 2017. Succinoglycan production contributes to acidic pH tolerance in *Sinorhizobium meliloti* Rm1021. *Molecular Plant-Microbe Interactions* **30**, 1009–1019.
- Hayafune M, Berisio R, Marchetti R, et al.** 2014. Chitin-induced activation of immune signaling by the rice receptor CEBiP relies on a unique sandwich-type dimerization. *Proceedings of the National Academy of Sciences, USA* **111**, E404–E413.
- He J, Zhang C, Dai H, et al.** 2019. A LysM receptor heteromer mediates perception of arbuscular mycorrhizal symbiotic signal in rice. *Molecular Plant* **12**, 1561–1576.
- Hodkinson BP, Lutzoni F.** 2009. A microbiotic survey of lichen-associated bacteria reveals a new lineage from the Rhizobiales. *Symbiosis* **49**, 163–180.
- Iizasa S, Iizasa E, Matsuzaki S, Tanaka H, Kodama Y, Watanabe K, Nagano Y.** 2016. Arabidopsis LBP/BPI related-1 and -2 bind to LPS directly and regulate PR1 expression. *Scientific Reports* **6**, 27527.
- Iizasa S, Iizasa E, Watanabe K, Nagano Y.** 2017. Transcriptome analysis reveals key roles of AtLBR-2 in LPS-induced defense responses in plants. *BMC Genomics* **18**, 995.
- Irieda H, Inoue Y, Mori M, et al.** 2019. Conserved fungal effector suppresses PAMP-triggered immunity by targeting plant immune kinases. *Proceedings of the National Academy of Sciences, USA* **116**, 496–505.
- Jashni MK, Dols IH, Iida Y, Boeren S, Beenen HG, Mehrabi R, Collemare J, de Wit PJ.** 2015. Synergistic action of a metalloprotease and a serine protease from *Fusarium oxysporum* f. sp. *lycopersici* cleaves chitin-binding tomato chitinases, reduces their antifungal activity, and enhances fungal virulence. *Molecular Plant-Microbe Interactions* **28**, 996–1008.
- Javvadi S, Pandey SS, Mishra A, Pradhan BB, Chatterjee S.** 2018. Bacterial cyclic  $\beta$ -(1,2)-glucans sequester iron to protect against iron-induced toxicity. *EMBO Reports* **19**, 172–186.
- Jian J, Liang X.** 2019. One small RNA of *Fusarium graminearum* targets and silences CEBiP gene in common wheat. *Microorganisms* **7**, 425.
- Johnson JM, Thürich J, Petutschnig EK, et al.** 2018. A poly(A) ribonuclease controls the cellobiose-based interaction between *Piriformospora indica* and its host Arabidopsis. *Plant Physiology* **176**, 2496–2514.
- Jones KM, Sharopova N, Lohar DP, Zhang JQ, VandenBosch KA, Walker GC.** 2008. Differential response of the plant *Medicago truncatula* to its symbiont *Sinorhizobium meliloti* or an exopolysaccharide-deficient mutant. *Proceedings of the National Academy of Sciences, USA* **105**, 704–709.
- Kaku H, Nishizawa Y, Ishii-Minami N, Akimoto-Tomiyama C, Dohmae N, Takio K, Minami E, Shibuya N.** 2006. Plant cells recognize chitin fragments for defense signaling through a plasma membrane receptor. *Proceedings of the National Academy of Sciences, USA* **103**, 11086–11091.
- Kanagawa M, Satoh T, Ikeda A, Adachi Y, Ohno N, Yamaguchi Y.** 2011. Structural insights into recognition of triple-helical beta-glucans by an insect fungal receptor. *Journal of Biological Chemistry* **286**, 29158–29165.
- Kang X, Kirui A, Muszyński A, Widanage MCD, Chen A, Azadi P, Wang P, Mentink-Vigier F, Wang T.** 2018. Molecular architecture of fungal cell walls revealed by solid-state NMR. *Nature Communications* **9**, 2747.
- Kawaharada Y, Kelly S, Nielsen MW, et al.** 2015. Receptor-mediated exopolysaccharide perception controls bacterial infection. *Nature* **523**, 308–312.
- Kawaharada Y, Nielsen MW, Kelly S, et al.** 2017. Differential regulation of the Epr3 receptor coordinates membrane-restricted rhizobial colonization of root nodule primordia. *Nature Communications* **8**, 14534.
- Keen NT, Yoshikawa M.** 1983. beta-1,3-Endoglucanase from soybean releases elicitor-active carbohydrates from fungus cell walls. *Plant Physiology* **71**, 460–465.
- Kelly SJ, Muszyński A, Kawaharada Y, Hubber AM, Sullivan JT, Sandal N, Carlson RW, Stougaard J, Ronson CW.** 2013. Conditional requirement for exopolysaccharide in the *Mesorhizobium-Lotus* symbiosis. *Molecular Plant-Microbe Interactions* **26**, 319–329.
- Klarzynski O, Plesse B, Joubert JM, Yvin JC, Kopp M, Kloareg B, Fritig B.** 2000. Linear beta-1,3 glucans are elicitors of defense responses in tobacco. *Plant Physiology* **124**, 1027–1038.
- Kombrink A, Rovenich H, Shi-Kunne X, et al.** 2017. *Verticillium dahliae* LysM effectors differentially contribute to virulence on plant hosts. *Molecular Plant Pathology* **18**, 596–608.
- Koornneef A, Pieterse CM.** 2008. Cross talk in defense signaling. *Plant Physiology* **146**, 839–844.
- Kouzai Y, Mochizuki S, Nakajima K, et al.** 2014. Targeted gene disruption of OsCERK1 reveals its indispensable role in chitin perception and involvement in the peptidoglycan response and immunity in rice. *Molecular Plant-Microbe Interactions* **27**, 975–982.
- Kutschera A, Dawid C, Gisch N, et al.** 2019. Bacterial medium-chain 3-hydroxy fatty acid metabolites trigger immunity in Arabidopsis plants. *Science* **364**, 178–181.
- Laus MC, van Brussel AA, Kijne JW.** 2005. Role of cellulose fibrils and exopolysaccharides of *Rhizobium leguminosarum* in attachment to and infection of *Vicia sativa* root hairs. *Molecular Plant-Microbe Interactions* **18**, 533–538.
- Lee MJ, Geller AM, Bamford NC, et al.** 2016. Deacetylation of fungal exopolysaccharide mediates adhesion and biofilm formation. *mBio* **7**, e00252–e00216.
- Lee MJ, Liu H, Barker BM, et al.** 2015. The fungal exopolysaccharide galactosaminogalactan mediates virulence by enhancing resistance to neutrophil extracellular traps. *PLoS Pathogens* **11**, e1005187.
- Lee MJ, Sheppard DC.** 2016. Recent advances in the understanding of the *Aspergillus fumigatus* cell wall. *Journal of Microbiology* **54**, 232–242.
- Lehman AP, Long SR.** 2013. Exopolysaccharides from *Sinorhizobium meliloti* can protect against H<sub>2</sub>O<sub>2</sub>-dependent damage. *Journal of Bacteriology* **195**, 5362–5369.
- Leigh JA, Signer ER, Walker GC.** 1985. Exopolysaccharide-deficient mutants of *Rhizobium meliloti* that form ineffective nodules. *Proceedings of the National Academy of Sciences, USA* **82**, 6231–6235.

- Li P, Luo H, Meng J, Sun W, Wang X, Lu S, Peng Y, Zhou L. 2014. Effects of oligosaccharides from endophytic *Fusarium oxysporum* Dzf17 on activities of defense-related enzymes in *Dioscorea zingiberensis* suspension cell and seedling cultures. *Electronic Journal of Biotechnology* **17**, 156–161.
- Liang Y, Cao Y, Tanaka K, Thibivilliers S, Wan J, Choi J, Kang Ch, Qiu J, Stacey G. 2013. Nonlegumes respond to rhizobial Nod factors by suppressing the innate immune response. *Science* **341**, 1384–1387.
- Liang Y, Tóth K, Cao Y, Tanaka K, Espinoza C, Stacey G. 2014. Lipochitooligosaccharide recognition: an ancient story. *New Phytologist* **204**, 289–296.
- Limpens E, Franken C, Smit P, Willemsse J, Bisseling T, Geurts R. 2003. LysM domain receptor kinases regulating rhizobial Nod factor-induced infection. *Science* **302**, 630–633.
- Limpens E, van Zeijl A, Geurts R. 2015. Lipochitooligosaccharides modulate plant host immunity to enable endosymbioses. *Annual Review of Phytopathology* **53**, 311–334.
- Lin S, Yang L, Chen G, Li B, Chen D, Li L, Xu Z. 2017. Pathogenic features and characteristics of food borne pathogens biofilm: biomass, viability and matrix. *Microbial Pathogenesis* **111**, 285–291.
- Liu B, Li JF, Ao Y, et al. 2012. Lysin motif-containing proteins LYP4 and LYP6 play dual roles in peptidoglycan and chitin perception in rice innate immunity. *The Plant Cell* **24**, 3406–3419.
- Liu T, Liu Z, Song C, et al. 2012. Chitin-induced dimerization activates a plant immune receptor. *Science* **336**, 1160–1164.
- Liu X, Grabherr HM, Willmann R, et al. 2014. Host-induced bacterial cell wall decomposition mediates pattern-triggered immunity in Arabidopsis. *eLife* **3**, e01990.
- Lopez-Baena FJ, Ruiz-Sainz JE, Rodriguez-Carvajal MA, Vinardell JM. 2016. Bacterial molecular signals in the *Sinorhizobium fredii*–soybean symbiosis. *International Journal of Molecular Sciences* **17**, 755.
- Ludwig N, Löhner M, Hempel M, Mathea S, Schliebner I, Menzel M, Kiesow A, Schaffrath U, Deising HB, Horbach R. 2014. Melanin is not required for turgor generation but enhances cell-wall rigidity in appressoria of the corn pathogen *Colletotrichum graminicola*. *Molecular Plant-Microbe Interactions* **27**, 315–327.
- Madala NE, Molinaro A, Dubery IA. 2012. Distinct carbohydrate and lipid-based molecular patterns within lipopolysaccharides from *Burkholderia cepacia* contribute to defense-associated differential gene expression in *Arabidopsis thaliana*. *Innate Immunity* **18**, 140–154.
- Madsen EB, Madsen LH, Radutoiu S, et al. 2003. A receptor kinase gene of the LysM type is involved in legume perception of rhizobial signals. *Nature* **425**, 637–640.
- Mahapatra S, Banerjee D. 2013. Fungal exopolysaccharide: production, composition and applications. *Microbiology Insights* **6**, 1–16.
- Maillet F, Fournier J, Mendis HC, Tadege M, Wen J, Ratet P, Mysore KS, Gough C, Jones KM. 2020. *Sinorhizobium melliloti* succinylated high-molecular-weight succinoglycan and the *Medicago truncatula* LysM receptor-like kinase MtLYK10 participate independently in symbiotic infection. *The Plant Journal* **102**, 311–326.
- Maillet F, Poinsoit V, André O, et al. 2011. Fungal lipochitooligosaccharide symbiotic signals in arbuscular mycorrhiza. *Nature* **469**, 58–63.
- Margaret I, Crespo-Rivas JC, Acosta-Jurado S, et al. 2012. *Sinorhizobium fredii* HH103 rkp-3 genes are required for K-antigen polysaccharide biosynthesis, affect lipopolysaccharide structure and are essential for infection of legumes forming determinate nodules. *Molecular Plant-Microbe Interactions* **25**, 825–838.
- Marshall R, Kombrink A, Motteram J, Loza-Reyes E, Lucas J, Hammond-Kosack KE, Thomma BP, Rudd JJ. 2011. Analysis of two in planta expressed LysM effector homologs from the fungus *Mycosphaerella graminicola* reveals novel functional properties and varying contributions to virulence on wheat. *Plant Physiology* **156**, 756–769.
- Martins M, Uppuluri P, Thomas DP, Cleary IA, Henriques M, Lopez-Ribot JL, Oliveira R. 2010. Presence of extracellular DNA in the *Candida albicans* biofilm matrix and its contribution to biofilms. *Mycopathologia* **169**, 323–331.
- Masachis S, Segorbe D, Turrà D, et al. 2016. A fungal pathogen secretes plant alkalizing peptides to increase infection. *Nature Microbiology* **1**, 16043.
- Mélida H, Sandoval-Sierra JV, Diéguez-Urbeondo J, Bulone V. 2013. Analyses of extracellular carbohydrates in oomycetes unveil the existence of three different cell wall types. *Eukaryotic Cell* **12**, 194–203.
- Mélida H, Sopena-Torres S, Bacete L, Garrido-Arandia M, Jordá L, López G, Muñoz-Barrios A, Pacios LF, Molina A. 2018. Non-branched  $\beta$ -1,3-glucan oligosaccharides trigger immune responses in Arabidopsis. *The Plant Journal* **93**, 34–49.
- Ménard R, Alban S, de Ruffray P, Jamois F, Franz G, Fritig B, Yvin JC, Kauffmann S. 2004. Beta-1,3 glucan sulfate, but not beta-1,3 glucan, induces the salicylic acid signaling pathway in tobacco and Arabidopsis. *The Plant Cell* **16**, 3020–3032.
- Mendis HC, Madzima TF, Queiroux C, Jones KM. 2016. Function of succinoglycan polysaccharide in *Sinorhizobium melliloti* host plant invasion depends on succinylation, not molecular weight. *mBio* **7**, e00606-16.
- Mentlak TA, Kombrink A, Shinya T, et al. 2012. Effector-mediated suppression of chitin-triggered immunity by *Magnaporthe oryzae* is necessary for rice blast disease. *The Plant Cell* **24**, 322–335.
- Miller KJ, Hadley JA, Gustine DL. 1994. Cyclic [beta]-1,6-1,3-glucans of *Bradyrhizobium japonicum* USDA 110 elicit isoflavonoid production in the soybean (*Glycine max*) host. *Plant Physiology* **104**, 917–923.
- Milling A, Babujee L, Allen C. 2011. *Ralstonia solanacearum* extracellular polysaccharide is a specific elicitor of defense responses in wilt-resistant tomato plants. *PLoS One* **6**, e15853.
- Mitchell KF, Zarnowski R, Sanchez H, Edward JA, Reinicke EL, Nett JE, Mitchell AP, Andes DR. 2015. Community participation in biofilm matrix assembly and function. *Proceedings of the National Academy of Sciences, USA* **112**, 4092–4097.
- Mithöfer A, Bhagwat AA, Feger M, Ebel J. 1996. Suppression of fungal  $\beta$ -glucan-induced plant defence in soybean (*Glycine max* L) by cyclic 1,3-1,6- $\beta$ -glucans from the symbiont *Bradyrhizobium japonicum*. *Planta* **199**, 270–275.
- Miya A, Albert P, Shinya T, Desaki Y, Ichimura K, Shirasu K, Narusaka Y, Kawakami N, Kaku H, Shibuya N. 2007. CERK1, a LysM receptor kinase, is essential for chitin elicitor signaling in Arabidopsis. *Proceedings of the National Academy of Sciences, USA* **104**, 19613–19618.
- Moloshok TD, Leinhos GME, Staples RC, Hoch HC. 1993. The autogenic extracellular environment of *Uromyces appendiculatus* urediospore germlings. *Mycologia* **85**, 392–400.
- Money PN. 2008. Insights on the mechanics of hyphal growth. *Fungal Biology Reviews* **22**, 71–76.
- Muszyński A, Heiss C, Hjuler CT, Sullivan JT, Kelly SJ, Thygesen MB, Stougaard J, Azadi P, Carlson RW, Ronson CW. 2016. Structures of exopolysaccharides involved in receptor-mediated perception of *Mesorhizobium loti* by *Lotus japonicus*. *Journal of Biological Chemistry* **291**, 20946–20961.
- Nakanishi I, Kimura K, Suzuki T, Ishikawa M, Banno I, Sakane T, Harada T. 1976. Demonstration of curdlan-type polysaccharide and some other beta-1,3-glucan in microorganisms with aniline blue. *Journal of General and Applied Microbiology* **22**, 1–11.
- Nars A, Lafitte C, Chabaud M, et al. 2013. *Aphanomyces euteiches* cell wall fractions containing novel glucan-chitosaccharides induce defense genes and nuclear calcium oscillations in the plant host *Medicago truncatula*. *PLoS One* **8**, e75039.
- Naumann TA. 2011. Modification of recombinant maize ChitA chitinase by fungal chitinase-modifying proteins. *Molecular Plant Pathology* **12**, 365–372.
- Newman MA, Daniels MJ, Dow JM. 1995. Lipopolysaccharide from *Xanthomonas campestris* induces defense-related gene expression in *Brassica campestris*. *Molecular Plant-Microbe Interactions* **8**, 778–780.
- Nicholson RL, Moraes WBC. 1980. Survival of *Colletotrichum graminicola*: importance of the spore matrix. *Phytopathology* **70**, 225–261.

- Souza CA, Li S, Lin AZ, Boutrot F, Grossmann G, Zipfel C, Somerville SC.** 2017. Cellulose-derived oligomers act as damage-associated molecular patterns and trigger defense-like responses. *Plant Physiology* **173**, 2383–2398.
- Spribille T, Tagirdzhanova G, Goyette S, Tuovinen V, Case R, Zandberg WF.** 2020. 3D biofilms: in search of the polysaccharides holding together lichen symbioses. *FEMS Microbiology Letters* **367**, fnaa023
- Sun J, Miller JB, Granqvist E, et al.** 2015. Activation of symbiosis signaling by arbuscular mycorrhizal fungi in legumes and rice. *The Plant Cell* **27**, 823–838.
- Taff HT, Nett JE, Zarnowski R, Ross KM, Sanchez H, Cain MT, Hamaker J, Mitchell AP, Andes DR.** 2012. A *Candida* biofilm-induced pathway for matrix glucan delivery: implications for drug resistance. *PLoS Pathogens* **8**, e1002848.
- Takahara H, Hacquard S, Kombrink A, et al.** 2016. *Colletotrichum higginsianum* extracellular LysM proteins play dual roles in appressorial function and suppression of chitin-triggered plant immunity. *New Phytologist* **211**, 1323–1337.
- Takahasi K, Ochiai M, Horiuchi M, Kumeta H, Ogura K, Ashida M, Inagaki F.** 2009. Solution structure of the silkworm betaGRP/GNBP3 N-terminal domain reveals the mechanism for beta-1,3-glucan-specific recognition. *Proceedings of the National Academy of Sciences, USA* **106**, 11679–11684.
- Teixeira PJP, Colaiani NR, Fitzpatrick CR, Dangl JL.** 2019. Beyond pathogens: microbiota interactions with the plant immune system. *Current Opinion in Microbiology* **49**, 7–17.
- Umemoto N, Kakitani M, Iwamatsu A, Yoshikawa M, Yamaoka N, Ishida I.** 1997. The structure and function of a soybean beta-glucan-elicitor-binding protein. *Proceedings of the National Academy of Sciences, USA* **94**, 1029–1034.
- Ursache R, Andersen TG, Marhavý P, Geldner N.** 2018. A protocol for combining fluorescent proteins with histological stains for diverse cell wall components. *The Plant Journal* **93**, 399–412.
- Vadassery J, Ranf S, Drzewiecki C, Mithöfer A, Mazars C, Scheel D, Lee J, Oelmüller R.** 2009. A cell wall extract from the endophytic fungus *Piriformospora indica* promotes growth of *Arabidopsis* seedlings and induces intracellular calcium elevation in roots. *The Plant Journal* **59**, 193–206.
- van den Burg HA, Harrison SJ, Joosten MH, Vervoort J, de Wit PJ.** 2006. *Cladosporium fulvum* Avr4 protects fungal cell walls against hydrolysis by plant chitinases accumulating during infection. *Molecular Plant-Microbe Interactions* **19**, 1420–1430.
- van Overbeek LS, Saikkonen K.** 2016. Impact of bacterial–fungal interactions on the colonization of the endosphere. *Trends in Plant Science* **21**, 230–242.
- Vollmer W, Blanot D, de Pedro MA.** 2008. Peptidoglycan structure and architecture. *FEMS Microbiology Reviews* **32**, 149–167.
- Wan J, Zhang XC, Neece D, Ramonell KM, Clough S, Kim SY, Stacey MG, Stacey G.** 2008. A LysM receptor-like kinase plays a critical role in chitin signaling and fungal resistance in *Arabidopsis*. *The Plant Cell* **20**, 471–481.
- Wang P, Liang Z, Kang BH.** 2019. Electron tomography of plant organelles and the outlook for correlative microscopic approaches. *New Phytologist* **223**, 1756–1761.
- Wanke A, Rovenich H, Schwanke F, Velte S, Becker S, Hehemann JH, Wawra S, Zuccaro A.** 2020. Plant species-specific recognition of long and short  $\beta$ -1,3-linked glucans is mediated by different receptor systems. *The Plant Journal* **102**, 1142–1156.
- Wawra S, Fesel P, Widmer H, et al.** 2016. The fungal-specific  $\beta$ -glucan-binding lectin FGB1 alters cell-wall composition and suppresses glucan-triggered immunity in plants. *Nature Communications* **7**, 13188.
- Wawra S, Fesel P, Widmer H, Neumann U, Lahrman U, Becker S, Hehemann JH, Langen G, Zuccaro A.** 2019. FGB1 and WSC3 are in planta-induced  $\beta$ -glucan-binding fungal lectins with different functions. *New Phytologist* **222**, 1493–1506.
- Weishaupt MW, Hahn HS, Geissner A, Seeberger PH.** 2017. Automated glycan assembly of branched beta-(1,3)-glucans to identify antibody epitopes. *Chemical Communications* **53**, 3591–3594.
- Whitfield C, Trent MS.** 2014. Biosynthesis and export of bacterial lipopolysaccharides. *Annual Review of Biochemistry* **83**, 99–128.
- Willmann R, Lajunen HM, Erbs G, et al.** 2011. *Arabidopsis* lysin-motif proteins LYM1 LYM3 CERK1 mediate bacterial peptidoglycan sensing and immunity to bacterial infection. *Proceedings of the National Academy of Sciences, USA* **108**, 19824–19829.
- Wisse E, Braet F, Duimel H, et al.** 2010. Fixation methods for electron microscopy of human and other liver. *World Journal of Gastroenterology* **16**, 2851–2866.
- Wong JEMM, Gysel K, Birkefeldt TG, et al.** 2020. Structural signatures in EPR3 form a unique class of plant carbohydrate receptors. *Nature Communications* **11**, 3797.
- Xin XF, Nomura K, Aung K, Velásquez AC, Yao J, Boutrot F, Chang JH, Zipfel C, He SY.** 2016. Bacteria establish an aqueous living space in plants crucial for virulence. *Nature* **539**, 524–529.
- Xu Q, Wang J, Zhao J, Xu J, Sun S, Zhang H, Wu J, Tang C, Kang Z, Wang X.** 2020. A polysaccharide deacetylase from *Puccinia striiformis* f. sp. *tritici* is an important pathogenicity gene that suppresses plant immunity. *Plant Biotechnology Journal* **18**, 1830–1842.
- Xue DX, Li CL, Xie ZP, Staehelin C.** 2019. LYK4 is a component of a tripartite chitin receptor complex in *Arabidopsis thaliana*. *Journal of Experimental Botany* **70**, 5507–5516.
- Yamaguchi T, Yamada A, Hong N, Ogawa T, Ishii T, Shibuya N.** 2000. Differences in the recognition of glucan elicitor signals between rice and soybean: beta-glucan fragments from the rice blast disease fungus *Piricularia oryzae* that elicit phytoalexin biosynthesis in suspension-cultured rice cells. *The Plant Cell* **12**, 817–826.
- York WS.** 1995. A conformational model for cyclic beta-(1→2)-linked glucans based on NMR analysis of the beta-glucans produced by *Xanthomonas campestris*. *Carbohydrate Research* **278**, 205–225.
- Yun MH, Torres PS, El Oirdi M, Rigano LA, Gonzalez-Lamothe R, Marano MR, Castagnaro AP, Dankert MA, Bouarab K, Vojnov AA.** 2006. Xanthan induces plant susceptibility by suppressing callose deposition. *Plant Physiology* **141**, 178–187.
- Zaragoza O, Chrisman CJ, Castelli MV, Frases S, Cuenca-Estrella M, Rodriguez-Tudela JL, Casadevall A.** 2008. Capsule enlargement in *Cryptococcus neoformans* confers resistance to oxidative stress suggesting a mechanism for intracellular survival. *Cellular Microbiology* **10**, 2043–2057.
- Zeidler D, Zähringer U, Gerber I, Dubery I, Hartung T, Bors W, Hutzler P, Durner J.** 2004. Innate immunity in *Arabidopsis thaliana*: lipopolysaccharides activate nitric oxide synthase (NOS) and induce defense genes. *Proceedings of the National Academy of Sciences, USA* **101**, 15811–15816.
- Zeković DB, Kwiatkowski S, Vrvic MM, Jakovljević D, Moran CA.** 2005. Natural and modified (1→3)-beta-D-glucans in health promotion and disease alleviation. *Critical Reviews in Biotechnology* **25**, 205–230.
- Zeng T, Rodriguez-Moreno L, Mansurkhodzhev A, et al.** 2020. A lysin motif effector subverts chitin-triggered immunity to facilitate arbuscular mycorrhizal symbiosis. *New Phytologist* **225**, 448–460.
- Zgad Zaj R, James EK, Kelly S, Kawaharada Y, de Jonge N, Jensen DB, Madsen LH, Radutoiu S.** 2015. A legume genetic framework controls infection of nodules by symbiotic and endophytic bacteria. *PLoS Genetics* **11**, e1005280.
- Zhou H, Wang Y, Wang W, Jia J, Li Y, Wang Q, Wu Y, Tang J.** 2009. Generation of monoclonal antibodies against highly conserved antigens. *PLoS One* **4**, e6087.
- Zipfel C, Oldroyd GE.** 2017. Plant signalling in symbiosis and immunity. *Nature* **543**, 328–336.



- Nizam S, Qiang X, Wawra S, Nostadt R, Getzke F, Schwanke F, Dreyer I, Langen G, Zuccaro A.** 2019. *Serendipita indica* E5'NT modulates extracellular nucleotide levels in the plant apoplast and affects fungal colonization. *EMBO Reports* **20**, e47430.
- Okinaka Y, Mimori K, Takeo K, Kitamura S, Takeuchi Y, Yamaoka N, Yoshikawa M.** 1995. A structural model for the mechanisms of elicitor release from fungal cell walls by plant beta-1,3-endoglucanase. *Plant Physiology* **109**, 839–845.
- Ökmen B, Kemmerich B, Hilbig D, Wemhöner R, Aschenbroich J, Perrar A, Huesgen PF, Schipper K, Doehlemann G.** 2018. Dual function of a secreted fungalysin metalloprotease in *Ustilago maydis*. *New Phytologist* **220**, 249–261.
- Olafsdottir ES, Ingólfssdóttir K.** 2001. Polysaccharides from lichens: structural characteristics and biological activity. *Planta Medica* **67**, 199–208.
- Oldroyd GE.** 2013. Speak, friend, and enter: signalling systems that promote beneficial symbiotic associations in plants. *Nature Reviews. Microbiology* **11**, 252–263.
- Oliveira-Garcia E, Deising HB.** 2013. Infection structure-specific expression of beta-1,3-glucan synthase is essential for pathogenicity of *Colletotrichum graminicola* and evasion of beta-glucan-triggered immunity in maize. *The Plant Cell* **25**, 2356–2378.
- Oliveira-Garcia E, Deising HB.** 2016. Attenuation of PAMP-triggered immunity in maize requires down-regulation of the key beta-1,6-glucan synthesis genes KRE5 and KRE6 in biotrophic hyphae of *Colletotrichum graminicola*. *The Plant Journal* **87**, 355–375.
- Osumi M.** 1998. The ultrastructure of yeast: cell wall structure and formation. *Micron* **29**, 207–233.
- Pérez-Mendoza D, Rodríguez-Carvajal MÁ, Romero-Jiménez L, Fariás Gde A, Lloret J, Gallegos MT, Sanjuán J.** 2015. Novel mixed-linkage beta-glucan activated by c-di-GMP in *Sinorhizobium meliloti*. *Proceedings of the National Academy of Sciences, USA* **112**, E757–E765.
- Pettolino F, Sasaki I, Turbic A, Wilson SM, Bacic A, Hrmova M, Fincher GB.** 2009. Hyphal cell walls from the plant pathogen *Rhynchosporium secalis* contain (1,3/1,6)-beta-D-glucans, galacto- and rhamnmannans, (1,3;1,4)-beta-D-glucans and chitin. *The FEBS Journal* **276**, 3698–3709.
- Petutschnig EK, Jones AM, Serazetdinova L, Lipka U, Lipka V.** 2010. The lysin motif receptor-like kinase (LysM-RLK) CERK1 is a major chitin-binding protein in *Arabidopsis thaliana* and subject to chitin-induced phosphorylation. *Journal of Biological Chemistry* **285**, 28902–28911.
- Quast I, Lünemann JD.** 2014. Fc glycan-modulated immunoglobulin G effector functions. *Journal of Clinical Immunology* **34** Suppl 1, S51–S55.
- Radutoiu S, Madsen LH, Madsen EB, et al.** 2003. Plant recognition of symbiotic bacteria requires two LysM receptor-like kinases. *Nature* **425**, 585–592.
- Ranf S.** 2016. Immune sensing of lipopolysaccharide in plants and animals: same but different. *PLoS Pathogens* **12**, e1005596.
- Ranf S, Gisch N, Schäffer M, et al.** 2015. A lectin S-domain receptor kinase mediates lipopolysaccharide sensing in *Arabidopsis thaliana*. *Nature Immunology* **16**, 426–433.
- Rapicavoli JN, Blanco-Ulate B, Muszyński A, Figueroa-Balderas R, Morales-Cruz A, Azadi P, Dobruchowska JM, Castro C, Cantu D, Roper MC.** 2018. Lipopolysaccharide O-antigen delays plant innate immune recognition of *Xylella fastidiosa*. *Nature Communications* **9**, 390.
- Reichhardt C, Joubert LM, Clemons KV, Stevens DA, Cegelski L.** 2019. Integration of electron microscopy and solid-state NMR analysis for new views and compositional parameters of *Aspergillus fumigatus* biofilms. *Medical Mycology* **57**, S239–S244.
- Reis RA, Tischer CA, Gorin PA, Iacomini M.** 2002. A new pullulan and a branched (1→3)-, (1→6)-linked beta-glucan from the lichenised ascomycete *Teloschistes flavicans*. *FEMS Microbiology Letters* **210**, 1–5.
- Rigano LA, Payette C, Brouillard G, et al.** 2007. Bacterial cyclic beta-(1,2)-glucan acts in systemic suppression of plant immune responses. *The Plant Cell* **19**, 2077–2089.
- Rinaudi LV, González JE.** 2009. The low-molecular-weight fraction of exopolysaccharide II from *Sinorhizobium meliloti* is a crucial determinant of biofilm formation. *Journal of Bacteriology* **191**, 7216–7224.
- Rocafort M, Fudal I, Mesarich CH.** 2020. Apoplastic effector proteins of plant-associated fungi and oomycetes. *Current Opinion in Plant Biology* **56**, 9–19.
- Romero-Contreras YJ, Ramírez-Valdespino CA, Guzmán-Guzmán P, Macías-Segoviano JI, Villagómez-Castro JC, Olmedo-Monfil V.** 2019. Tal6 from *Trichoderma atroviride* is a LysM effector involved in mycoparasitism and plant association. *Frontiers in Microbiology* **10**, 2231.
- Rose JK, Ham KS, Darvill AG, Albersheim P.** 2002. Molecular cloning and characterization of glucanase inhibitor proteins: coevolution of a counterdefense mechanism by plant pathogens. *The Plant Cell* **14**, 1329–1345.
- Rovenich H, Zuccaro A, Thomma BP.** 2016. Convergent evolution of filamentous microbes towards evasion of glycan-triggered immunity. *New Phytologist* **212**, 896–901.
- Rydahl MG, Krac Un SK, Fangel JU, et al.** 2017. Development of novel monoclonal antibodies against starch and ulvan—implications for antibody production against polysaccharides with limited immunogenicity. *Scientific Reports* **7**, 9326.
- Saijo Y, Loo EP, Yasuda S.** 2018. Pattern recognition receptors and signaling in plant–microbe interactions. *The Plant Journal* **93**, 592–613.
- Samalova M, Mérida H, Vilaplana F, Bulone V, Soanes DM, Talbot NJ, Gurr SJ.** 2017. The beta-1,3-glucanase transferases (Gels) affect the structure of the rice blast fungal cell wall during appressorium-mediated plant infection. *Cell Microbiology* **19**, e12659.
- Sánchez-Vallet A, Mesters JR, Thomma BP.** 2015. The battle for chitin recognition in plant–microbe interactions. *FEMS Microbiology Reviews* **39**, 171–183.
- Scarpari M, Reverberi M, Parroni A, et al.** 2017. Tramesan, a novel polysaccharide from *Trametes versicolor*. Structural characterization and biological effects. *PLoS One* **12**, e0171412.
- Schmitz AM, Harrison MJ.** 2014. Signaling events during initiation of arbuscular mycorrhizal symbiosis. *Journal of Integrative Plant Biology* **56**, 250–261.
- Sharp JK, Albersheim P, Ossowski P, Pilotti A, Garegg P, Lindberg B.** 1984a. Comparison of the structures and elicitor activities of a synthetic and a mycelial-wall-derived hexa(beta-D-glucopyranosyl)-D-glucitol. *Journal of Biological Chemistry* **259**, 11341–11345.
- Sharp JK, Valent B, Albersheim P.** 1984b. Purification and partial characterization of a beta-glucan fragment that elicits phytoalexin accumulation in soybean. *Journal of Biological Chemistry* **259**, 11312–11320.
- Shimizu T, Nakano T, Takamizawa D, et al.** 2010. Two LysM receptor molecules, CEBIP and OsCERK1, cooperatively regulate chitin elicitor signaling in rice. *The Plant Journal* **64**, 204–214.
- Shockman GD, Barrett JF.** 1983. Structure, function, and assembly of cell walls of gram-positive bacteria. *Annual Review of Microbiology* **37**, 501–527.
- Sieberer BJ, Chabaud M, Timmers AC, Monin A, Fournier J, Barker DG.** 2009. A nuclear-targetedameleon demonstrates intranuclear Ca<sup>2+</sup> spiking in *Medicago truncatula* root hairs in response to rhizobial nodulation factors. *Plant Physiology* **151**, 1197–1206.
- Silhavy TJ, Kahne D, Walker S.** 2010. The bacterial cell envelope. *Cold Spring Harbor Perspectives in Biology* **2**, a000414.
- Silipo A, Erbs G, Shinya T, Dow JM, Parrilli M, Lanzetta R, Shibuya N, Newman MA, Molinaro A.** 2010. Glyco-conjugates as elicitors or suppressors of plant innate immunity. *Glycobiology* **20**, 406–419.
- Silipo A, Molinaro A, Sturiale L, Dow JM, Erbs G, Lanzetta R, Newman MA, Parrilli M.** 2005. The elicitation of plant innate immunity by lipooligosaccharide of *Xanthomonas campestris*. *Journal of Biological Chemistry* **280**, 33660–33668.

- Souza CA, Li S, Lin AZ, Boutrot F, Grossmann G, Zipfel C, Somerville SC.** 2017. Cellulose-derived oligomers act as damage-associated molecular patterns and trigger defense-like responses. *Plant Physiology* **173**, 2383–2398.
- Spribille T, Tagirdzhanova G, Goyette S, Tuovinen V, Case R, Zandberg WF.** 2020. 3D biofilms: in search of the polysaccharides holding together lichen symbioses. *FEMS Microbiology Letters* **367**, fnaa023
- Sun J, Miller JB, Granqvist E, et al.** 2015. Activation of symbiosis signaling by arbuscular mycorrhizal fungi in legumes and rice. *The Plant Cell* **27**, 823–838.
- Taff HT, Nett JE, Zarnowski R, Ross KM, Sanchez H, Cain MT, Hamaker J, Mitchell AP, Andes DR.** 2012. A *Candida* biofilm-induced pathway for matrix glucan delivery: implications for drug resistance. *PLoS Pathogens* **8**, e1002848.
- Takahara H, Hacquard S, Kombrink A, et al.** 2016. *Colletotrichum higginsianum* extracellular LysM proteins play dual roles in appressorial function and suppression of chitin-triggered plant immunity. *New Phytologist* **211**, 1323–1337.
- Takahasi K, Ochiai M, Horiuchi M, Kumeta H, Ogura K, Ashida M, Inagaki F.** 2009. Solution structure of the silkworm betaGRP/GNBP3 N-terminal domain reveals the mechanism for beta-1,3-glucan-specific recognition. *Proceedings of the National Academy of Sciences, USA* **106**, 11679–11684.
- Teixeira PJP, Colaianni NR, Fitzpatrick CR, Dangl JL.** 2019. Beyond pathogens: microbiota interactions with the plant immune system. *Current Opinion in Microbiology* **49**, 7–17.
- Umemoto N, Kakitani M, Iwamatsu A, Yoshikawa M, Yamaoka N, Ishida I.** 1997. The structure and function of a soybean beta-glucan-elicitor-binding protein. *Proceedings of the National Academy of Sciences, USA* **94**, 1029–1034.
- Ursache R, Andersen TG, Marhavý P, Geldner N.** 2018. A protocol for combining fluorescent proteins with histological stains for diverse cell wall components. *The Plant Journal* **93**, 399–412.
- Vadassery J, Ranf S, Drzewiecki C, Mithöfer A, Mazars C, Scheel D, Lee J, Oelmüller R.** 2009. A cell wall extract from the endophytic fungus *Piriformospora indica* promotes growth of *Arabidopsis* seedlings and induces intracellular calcium elevation in roots. *The Plant Journal* **59**, 193–206.
- van den Burg HA, Harrison SJ, Joosten MH, Vervoort J, de Wit PJ.** 2006. *Cladosporium fulvum* Avr4 protects fungal cell walls against hydrolysis by plant chitinases accumulating during infection. *Molecular Plant-Microbe Interactions* **19**, 1420–1430.
- van Overbeek LS, Saikkonen K.** 2016. Impact of bacterial–fungal interactions on the colonization of the endosphere. *Trends in Plant Science* **21**, 230–242.
- Vollmer W, Blanot D, de Pedro MA.** 2008. Peptidoglycan structure and architecture. *FEMS Microbiology Reviews* **32**, 149–167.
- Wan J, Zhang XC, Neece D, Ramonell KM, Clough S, Kim SY, Stacey MG, Stacey G.** 2008. A LysM receptor-like kinase plays a critical role in chitin signaling and fungal resistance in *Arabidopsis*. *The Plant Cell* **20**, 471–481.
- Wang P, Liang Z, Kang BH.** 2019. Electron tomography of plant organelles and the outlook for correlative microscopic approaches. *New Phytologist* **223**, 1756–1761.
- Wanke A, Rovenich H, Schwanke F, Velte S, Becker S, Hehemann JH, Wawra S, Zuccaro A.** 2020. Plant species-specific recognition of long and short  $\beta$ -1,3-linked glucans is mediated by different receptor systems. *The Plant Journal* **102**, 1142–1156.
- Wawra S, Fesel P, Widmer H, et al.** 2016. The fungal-specific  $\beta$ -glucan-binding lectin FGB1 alters cell-wall composition and suppresses glucan-triggered immunity in plants. *Nature Communications* **7**, 13188.
- Wawra S, Fesel P, Widmer H, Neumann U, Lahrmann U, Becker S, Hehemann JH, Langen G, Zuccaro A.** 2019. FGB1 and WSC3 are in planta-induced  $\beta$ -glucan-binding fungal lectins with different functions. *New Phytologist* **222**, 1493–1506.
- Weishaupt MW, Hahn HS, Geissner A, Seeberger PH.** 2017. Automated glycan assembly of branched beta-(1,3)-glucans to identify antibody epitopes. *Chemical Communications* **53**, 3591–3594.
- Whitfield C, Trent MS.** 2014. Biosynthesis and export of bacterial lipopolysaccharides. *Annual Review of Biochemistry* **83**, 99–128.
- Willmann R, Lajunen HM, Erbs G, et al.** 2011. *Arabidopsis* lysin-motif proteins LYM1 LYM3 CERK1 mediate bacterial peptidoglycan sensing and immunity to bacterial infection. *Proceedings of the National Academy of Sciences, USA* **108**, 19824–19829.
- Wisse E, Braet F, Duimel H, et al.** 2010. Fixation methods for electron microscopy of human and other liver. *World Journal of Gastroenterology* **16**, 2851–2866.
- Wong JEMM, Gysel K, Birkefeldt TG, et al.** 2020. Structural signatures in EPR3 define a unique class of plant carbohydrate receptors. *Nature Communications* **11**, 3797.
- Xin XF, Nomura K, Aung K, Velásquez AC, Yao J, Boutrot F, Chang JH, Zipfel C, He SY.** 2016. Bacteria establish an aqueous living space in plants crucial for virulence. *Nature* **539**, 524–529.
- Xu Q, Wang J, Zhao J, Xu J, Sun S, Zhang H, Wu J, Tang C, Kang Z, Wang X.** 2020. A polysaccharide deacetylase from *Puccinia striiformis* f. sp. *tritici* is an important pathogenicity gene that suppresses plant immunity. *Plant Biotechnology Journal* **18**, 1830–1842.
- Xue DX, Li CL, Xie ZP, Staehelin C.** 2019. LYK4 is a component of a tripartite chitin receptor complex in *Arabidopsis thaliana*. *Journal of Experimental Botany* **70**, 5507–5516.
- Yamaguchi T, Yamada A, Hong N, Ogawa T, Ishii T, Shibuya N.** 2000. Differences in the recognition of glucan elicitor signals between rice and soybean: beta-glucan fragments from the rice blast disease fungus *Piricularia oryzae* that elicit phytoalexin biosynthesis in suspension-cultured rice cells. *The Plant Cell* **12**, 817–826.
- York WS.** 1995. A conformational model for cyclic beta-(1→2)-linked glucans based on NMR analysis of the beta-glucans produced by *Xanthomonas campestris*. *Carbohydrate Research* **278**, 205–225.
- Yun MH, Torres PS, El Oirdi M, Rigano LA, Gonzalez-Lamothe R, Marano MR, Castagnaro AP, Dankert MA, Bouarab K, Vojnov AA.** 2006. Xanthan induces plant susceptibility by suppressing callose deposition. *Plant Physiology* **141**, 178–187.
- Zaragoza O, Chrisman CJ, Castelli MV, Frases S, Cuenca-Estrella M, Rodríguez-Tudela JL, Casadevall A.** 2008. Capsule enlargement in *Cryptococcus neoformans* confers resistance to oxidative stress suggesting a mechanism for intracellular survival. *Cellular Microbiology* **10**, 2043–2057.
- Zeidler D, Zähringer U, Gerber I, Dubery I, Hartung T, Bors W, Hutzler P, Durner J.** 2004. Innate immunity in *Arabidopsis thaliana*: lipopolysaccharides activate nitric oxide synthase (NOS) and induce defense genes. *Proceedings of the National Academy of Sciences, USA* **101**, 15811–15816.
- Zeković DB, Kwiatkowski S, Vrvčić MM, Jakovljević D, Moran CA.** 2005. Natural and modified (1→3)-beta-D-glucans in health promotion and disease alleviation. *Critical Reviews in Biotechnology* **25**, 205–230.
- Zeng T, Rodríguez-Moreno L, Mansurkhodzaev A, et al.** 2020. A lysin motif effector subverts chitin-triggered immunity to facilitate arbuscular mycorrhizal symbiosis. *New Phytologist* **225**, 448–460.
- Zgadaj R, James EK, Kelly S, Kawaharada Y, de Jonge N, Jensen DB, Madsen LH, Radutoiu S.** 2015. A legume genetic framework controls infection of nodules by symbiotic and endophytic bacteria. *PLoS Genetics* **11**, e1005280.
- Zhou H, Wang Y, Wang W, Jia J, Li Y, Wang Q, Wu Y, Tang J.** 2009. Generation of monoclonal antibodies against highly conserved antigens. *PLoS One* **4**, e6087.
- Zipfel C, Oldroyd GE.** 2017. Plant signalling in symbiosis and immunity. *Nature* **543**, 328–336.

The following supplementary data is available at *JXB* online.

Table S1. Overview of microbial glycans and glycoconjugate structures and their relevance for host–microbe interactions.



# Chapter 3

## Plant species-specific recognition of long and short $\beta$ -1,3-linked glucans is mediated by different receptor systems

Alan Wanke<sup>1,2,#</sup>, Hanna Rovenich<sup>1,3,#</sup>, Florian Schwanke<sup>1</sup>, Stefanie Velte<sup>1</sup>, Stefan Becker<sup>4,5</sup>, Jan-Hendrik Hehemann<sup>4,5</sup>, Stephan Wawra<sup>1,3</sup>, Alga Zuccaro<sup>1,3</sup>

<sup>1</sup> University of Cologne, Institute for Plant Sciences, 60679 Cologne, Germany

<sup>2</sup> Max Planck Institute for Plant Breeding Research, 50829 Cologne, Germany

<sup>3</sup> University of Cologne, Cluster of Excellence on Plant Sciences (CEPLAS), 50679 Cologne, Germany

<sup>4</sup> Center for Marine Environmental Sciences, University of Bremen, MARUM, 28359 Bremen, Germany

<sup>5</sup> Max Planck Institute for Marine Microbiology, 28359 Bremen, Germany

# equal contribution

This article was published in *The Plant Journal*, **102**: 1142-156 (2020).

DOI: <https://doi.org/10.1111/tpj.1468>

## Plant species-specific recognition of long and short $\beta$ -1,3-linked glucans is mediated by different receptor systems

Alan Wanke<sup>1,2,†</sup>, Hanna Rovenich<sup>1,3,†</sup>, Florian Schwanke<sup>1</sup>, Stefanie Velte<sup>1</sup>, Stefan Becker<sup>4,5</sup>, Jan-Hendrik Hehemann<sup>4,5</sup>, Stephan Wawra<sup>1,3</sup> and Alga Zuccaro<sup>1,3,\*</sup> 

<sup>1</sup>University of Cologne, Institute for Plant Sciences, 50679 Cologne, Germany,

<sup>2</sup>Max Planck Institute for Plant Breeding Research, 50829 Cologne, Germany,

<sup>3</sup>University of Cologne, Cluster of Excellence on Plant Sciences (CEPLAS), 50679 Cologne, Germany,

<sup>4</sup>Center for Marine Environmental Sciences, University of Bremen, MARUM, 28359 Bremen, Germany, and

<sup>5</sup>Max Planck Institute for Marine Microbiology, 28359 Bremen, Germany

Received 10 May 2019; revised 26 December 2019; accepted 6 January 2020; published online 11 January 2020.

\*For correspondence (e-mail azuccaro@uni-koeln.de).

<sup>†</sup>These authors contributed equally to this study.

### SUMMARY

Plants survey their environment for the presence of potentially harmful or beneficial microbes. During colonization, cell surface receptors perceive microbe-derived or modified-self ligands and initiate appropriate responses. The recognition of fungal chitin oligomers and the subsequent activation of plant immunity are well described. In contrast, the mechanisms underlying  $\beta$ -glucan recognition and signaling activation remain largely unexplored. Here, we systematically tested immune responses towards different  $\beta$ -glucan structures and show that responses vary between plant species. While leaves of the monocots *Hordeum vulgare* and *Brachypodium distachyon* can recognize longer (laminarin) and shorter (laminarihexaose)  $\beta$ -1,3-glucans with responses of varying intensity, duration and timing, leaves of the dicot *Nicotiana benthamiana* activate immunity in response to long  $\beta$ -1,3-glucans, whereas *Arabidopsis thaliana* and *Capsella rubella* perceive short  $\beta$ -1,3-glucans. Hydrolysis of the  $\beta$ -1,6 side-branches of laminarin demonstrated that not the glycosidic decoration but rather the degree of polymerization plays a pivotal role in the recognition of long-chain  $\beta$ -glucans. Moreover, in contrast to the recognition of short  $\beta$ -1,3-glucans in *A. thaliana*, perception of long  $\beta$ -1,3-glucans in *N. benthamiana* and rice is independent of CERK1, indicating that  $\beta$ -glucan recognition may be mediated by multiple  $\beta$ -glucan receptor systems.

**Keywords:** glycan ligand, fungal cell wall, plant immunity, cell surface receptors, reactive oxygen species, calcium influx, mitogen-activated protein kinase, CERK1, BAK1.

### INTRODUCTION

Plants establish intimate relationships with a broad range of microorganisms, most of which do not affect or are beneficial to their health. Some microbial invaders, however, are pathogens that pose a serious threat to plant survival. In order to identify beneficial and potentially harmful microbes, plants employ surface-localized receptor proteins. Such receptors recognize either modified-self or microbe-derived molecules (Cook *et al.*, 2015). Depending on the type of molecule, ligand recognition by corresponding receptors leads to a series of cellular events that either promote or restrict microbial colonization (Zipfel and Oldroyd, 2017).

The microbial cell wall plays an important role in the interaction with plants as it represents the site of first

physical contact with plant host cells. One structural building block of fungal cell walls is chitin, a polymer consisting of  $\beta$ -1,4-linked *N*-acetylglucosamine monosaccharides (Latgé, 2007). In plants, recognition of chitin oligosaccharides results in the activation of immunity (Antolín-Llovera *et al.*, 2014; Sánchez-Vallet *et al.*, 2015). The first responses include an increase in cytosolic calcium ( $\text{Ca}^{2+}$ ) concentrations, the generation of extracellular reactive oxygen species (ROS), and the phosphorylation of intracellular receptor-like cytoplasmic kinases (Boller and Felix, 2009; Couto and Zipfel, 2016). The subsequent activation of calcium-dependent protein kinase and mitogen-activated protein kinase (MAPK) cascades ultimately result in gene expression changes to protect the plant from invasion by potential pathogens (Boller and Felix, 2009; Seybold *et al.*,

2014; Lee *et al.*, 2015). Several lysin motif (LysM)-containing receptors involved in chitin recognition have been identified and functionally characterized (Antolín-Llovera *et al.*, 2014; Sánchez-Vallet *et al.*, 2015). Both in rice (*Oryza sativa*) and *Arabidopsis thaliana*, the LysM receptor kinase CHITIN ELICITOR RECEPTOR KINASE 1 (CERK1) plays a central role in the activation of immune signaling upon chitin recognition (Miya *et al.*, 2007; Petutschnig *et al.*, 2010; Shimizu *et al.*, 2010; Liu *et al.*, 2012b; Cao *et al.*, 2014; Hayafune *et al.*, 2014; Erwig *et al.*, 2017). Additionally, CERK1 is required for the activation of immune signaling following the perception of bacterial peptidoglycan (Willmann *et al.*, 2011; Liu *et al.*, 2012a; Ao *et al.*, 2014; Gust, 2015). Chitin derivatives such as lipochitooligosaccharides produced by rhizobacteria and arbuscular mycorrhizal fungi are similarly perceived by LysM receptors, and require close homologs of CERK1 to initiate signaling events leading to the establishment of beneficial symbiotic relationships (Oldroyd, 2013; Limpens *et al.*, 2015). Interestingly, chitooligosaccharides and lipochitooligosaccharides together enhance symbiosis signaling while suppressing plant immunity, which is mediated by host receptors involved in the perception of both types of ligands during mycorrhizal colonization (Feng *et al.*, 2019). In contrast to chitin and its derivatives, proteinaceous ligands are recognized by receptors with extracellular leucine-rich repeat (LRR) domains. Equivalent to LysM receptor proteins, LRR receptors form complexes with the co-receptor BRASSINOSTEROID INSENSITIVE 1 (BAK1/SERK3) to activate immune signaling (Monaghan and Zipfel, 2012; Macho and Zipfel, 2015; Couto and Zipfel, 2016). Thus, the recruitment of co-receptor kinases seems to be determined by the type of ligand–receptor pairs.

Despite the strong immune responses triggered by chitin, it only accounts for a small fraction of cell wall glycans in fungi and several oomycete genera including *Saprolegnia* and *Aphanomyces* (Mélida *et al.*, 2013). Depending on the species of filamentous microbes, 50–60% of the cell wall's dry weight consists of glucan (Bowman and Free, 2006). Glucans are composed of glucose subunits that are assembled into polymers through various chemical linkages. By far the most abundant polymer is  $\beta$ -1,3-linked glucan (Fesel and Zuccaro, 2016). The linear  $\beta$ -1,3-glucan backbones are frequently modified with  $\beta$ -1,6-linked glucose, forming branched polysaccharides that are unique to filamentous microbes. These polymers can be tightly associated to the cell wall or form a gelatinous and diffuse  $\beta$ -glucan matrix, as has recently been shown for the hyphae of some root associated-fungi during root colonization (Wawra *et al.*, 2019). The most widely studied oomycete-derived heptagluco-side (a  $\beta$ -1,6-linked and  $\beta$ -1,3-branched glucan) was shown to induce phytoalexin biosynthesis after partial purification in several legumes and in potato (Cline *et al.*, 1978; Sharp *et al.*, 1984b; Cosio

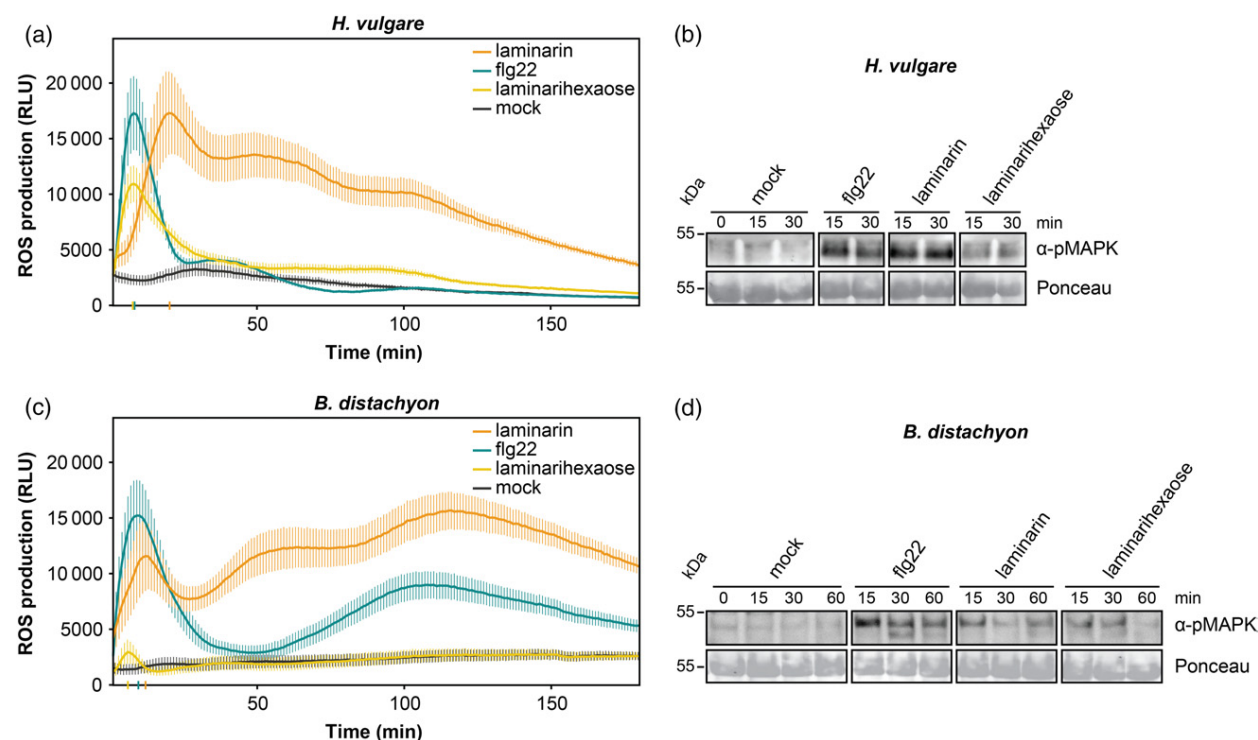
*et al.*, 1996; Côté *et al.*, 2000). Laminarin, a long-chain  $\beta$ -1,3-glucan backbone with side-branches of one or more glucose units linked via  $\beta$ -1,6 linkage from the marine brown algae *Laminaria digitata*, triggers defense responses *in planta* (Klarzynski *et al.*, 2000; Aziz *et al.*, 2003; Wawra *et al.*, 2016). Similarly, the short linear  $\beta$ -1,3-glucan laminarihexaose induces changes in cytosolic  $\text{Ca}^{2+}$  levels, MAPK activation and defense-related gene expression in *A. thaliana* (Mélida *et al.*, 2018). So far, only a single putative  $\beta$ -glucan receptor (GBP) with high affinity for the oomycete-derived heptagluco-side was identified from soybean (*Glycine max*) (Mithöfer *et al.*, 1996, 2000; Umemoto *et al.*, 1997; Fliegmann *et al.*, 2004). Its role in  $\beta$ -glucan-triggered defense signaling remains unclear, and it has been proposed that GBP alone is not sufficient for the activation of  $\beta$ -glucan immunity (Fliegmann *et al.*, 2004). This hypothesis is in line with the recent finding that laminarihexaose-induced immune responses in *A. thaliana* are dependent on CERK1 (Mélida *et al.*, 2018), indicating that CERK1 may additionally act as co-receptor of  $\beta$ -glucan receptor(s) in this plant.

To clarify the commonalities and differences in  $\beta$ -glucan perception between plant species, we systematically analyzed immune responses in monocot (*Hordeum vulgare* and *Brachypodium distachyon*) and dicot species (*Nicotiana benthamiana* and *A. thaliana*) upon treatment with short (laminarihexaose consisting of six glucose subunits) and long (laminarin with a backbone of 20–25 glucose subunits; Nelson and Lewis, 1974; Alderkamp *et al.*, 2007)  $\beta$ -1,3-glucans. We show that the perception of the short and the long  $\beta$ -1,3-glucans differs between plant species, and that recognition of the long  $\beta$ -1,3-glucan is not determined by the presence of the  $\beta$ -1,6-glycosidic side-branches but rather depends on the length of the  $\beta$ -1,3-linked polymer in *N. benthamiana*. Moreover, in contrast to short non-branched  $\beta$ -1,3-glucan, immune responses triggered by long-chained  $\beta$ -1,3-glucan do not depend on CERK1 in *N. benthamiana* and rice. Our findings emphasize the diversity of  $\beta$ -glucan perception systems among plant species and their specialized role in glycan-triggered immunity.

## RESULTS

### Recognition of $\beta$ -glucan structures is plant species-specific

In order to test whether different  $\beta$ -1,3-glucans activate early immune reactions in monocots, ROS production was measured upon addition of laminarihexaose and laminarin to leaf discs of 2- to 3-week-old barley (*H. vulgare*) or 4- to 5-week-old *B. distachyon*, when plants were at comparable developmental stages under our growth conditions. In these grasses both sugars triggered ROS production (Figure 1a,c). While laminarihexaose evoked a distinct ROS peak within the first 10 min, laminarin generally led to a

1144 Alan Wanke *et al.*

**Figure 1.**  $\beta$ -Glucan-triggered immune responses in *Hordeum vulgare* and *Brachypodium distachyon*.

Leaf discs were collected from 2- to 3-week-old barley (*H. vulgare*) and 4- to 5-week-old *B. distachyon* plants. Production of reactive oxygen species (ROS) was measured using luminol-based chemiluminescence for 180 min after treatment of (a) barley and (c) *B. distachyon* leaf discs with 100 nM flg22, 4 mg ml<sup>-1</sup> (1 mM) laminarin and 250  $\mu$ M laminarihexaose. Water (mock) served as negative control. ROS response intensity was measured in relative luminescence units (RLU). The order of the graph legend is organized according to total ROS production (integral). Colored ticks on the x-axis indicate the timing of the first ROS peak for each treatment. Values represent means  $\pm$  SE of 16–24 leaf discs from four different plants. Experiments were performed at least three times with similar results. MAPK activation in (b) barley and (d) *B. distachyon* leaf discs was detected using phospho-p44/42 MAPK (ERK1/2) antibody following elicitor treatment at the indicated time points. Membranes were stained with PonceauS to confirm equal loading.

later but long-lasting phase of ROS production with up to three peaks. To further corroborate the activation of immune signaling by these glucans, we tested the activation of MAPKs, which represents a prominent molecular link between ligand perception and immune reprogramming (Meng and Zhang, 2013). In barley, treatment with the bacterial flagellin derivate flg22 and laminarin prompted stronger phosphorylation of MAPKs after 15 and 30 min (Figure 1b), compared with MAPK activation after the addition of laminarihexaose. Treatment with flg22 resulted in strong MAPK phosphorylation after 15 min in *B. distachyon*, whereas weaker but distinct MAPK signals were detected in response to both  $\beta$ -glucans (Figure 1d). To confirm the activation of downstream defense responses, we tested whether the expression of the defense-regulatory transcription factor genes *HvWRKY1* and *HvWRKY2* would be activated by the different  $\beta$ -glucans in barley (Shen *et al.*, 2007; Method S1; Table S1). Confirming previously published work, flg22 treatment resulted in a significant upregulation of the expression of both *transcription factor* genes at 1 h (Figure S1a). Similarly, *HvWRKY1* and *HvWRKY2* were strongly induced 1 h

after laminarin and laminarihexaose addition (Figure S1a). Together with the generation of ROS and the activation of MAPKs, the changes in barley defense-related gene expression show that both  $\beta$ -glucans display immunomodulatory activities in the tested monocots.

To monitor the activation of common  $\beta$ -glucan-triggered responses among dicots, a similar set of experiments was performed using leaf discs of 3- to 4-week-old *A. thaliana* and *N. benthamiana*. All assays were carried out in lines expressing the Ca<sup>2+</sup> reporter aequorin to test cytosolic Ca<sup>2+</sup> influx upon  $\beta$ -glucan treatment in addition to ROS production and MAPK activation (Segonzac *et al.*, 2011; Choi *et al.*, 2014). In contrast to the tested monocots, *N. benthamiana* SLJR15 and *A. thaliana* Col-0<sup>AEO</sup> displayed substrate-specific perception of  $\beta$ -glucans (Figure 2). In *N. benthamiana* SLJR15 plants, treatment with the long-chained, branched  $\beta$ -glucan laminarin resulted in the generation of extracellular ROS, an increase in cytosolic Ca<sup>2+</sup>, and MAPK activation (Figure 2a–c). Similarly, expression of the two defense-related genes *NbACRE31* and *NbWRKY4* (Kanzaki *et al.*, 2003; Heese *et al.*, 2007; Segonzac *et al.*, 2011) was significantly induced 1 and 3 h after laminarin

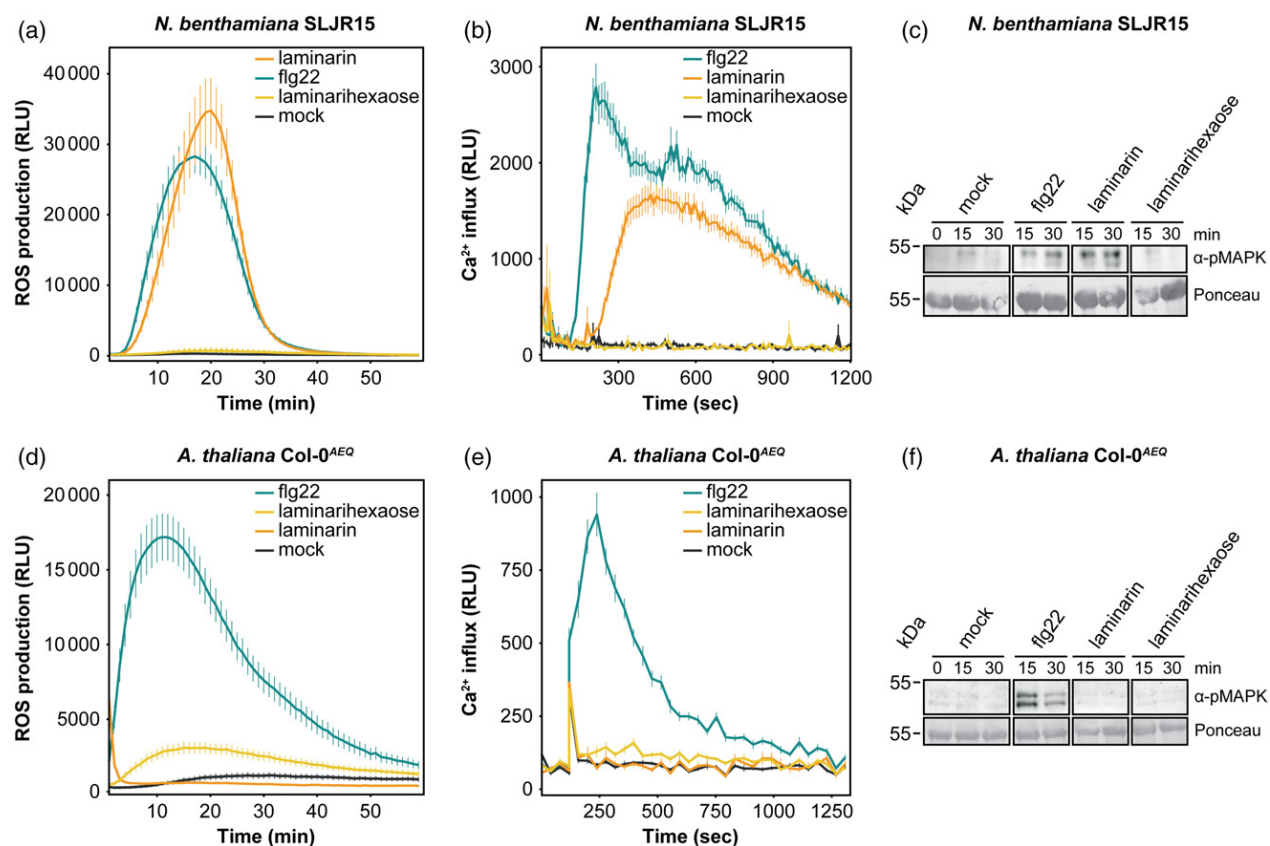


**Figure 2.**  $\beta$ -Glucan-triggered immune responses in *Arabidopsis thaliana* and *Nicotiana benthamiana*.

Leaf discs were collected from 3- to 4-week-old *A. thaliana* Col-0<sup>AEQ</sup> and *N. benthamiana* SLJR15 plants. Production of reactive oxygen species (ROS) was measured using luminol-based chemiluminescence for 60 min after treatment of (a) *N. benthamiana* SLJR15 and (d) *A. thaliana* Col-0<sup>AEQ</sup> leaf discs with 100 nM flg22, 2–4 mg ml<sup>-1</sup> (0.5–1 mM) laminarin and 250  $\mu$ M laminarihexaose. Water (mock) served as negative control. ROS response intensity was measured in relative luminescence units (RLU). Values represent means  $\pm$  SE of 24 leaf discs from four different plants. Experiments were performed three times with similar results. Elevations of cytosolic calcium concentrations (Ca<sup>2+</sup> influx) were measured as RLU following elicitor treatment in (b) *N. benthamiana* SLJR15 and (e) *A. thaliana* Col-0<sup>AEQ</sup>. The remaining aequorin was discharged by adding CaCl<sub>2</sub>. Discharge kinetics were integrated and normalized to the maximum Ca<sup>2+</sup> level. The discharge integral was then used to normalize Ca<sup>2+</sup> kinetics in response to elicitor treatment. Values represent means  $\pm$  SE of 24 leaf discs from six different plants. The order of the graph legend for ROS and calcium influx measurements was organized according to total ROS production or total calcium influx (integral). MAPK activation in (c) *N. benthamiana* SLJR15 and (f) *A. thaliana* Col-0<sup>AEQ</sup> leaf discs was detected using phospho-p44/42 MAPK (ERK1/2) antibody following elicitor treatment at the indicated time points. Membranes were stained with PonceauS to confirm equal loading. All experiments were performed at least three times with similar results.

treatment (Figure S1b). In contrast, the addition of short-chain laminarihexaose did not elicit early immune responses, and only had a weak and transient effect on defense gene expression (Figures 2a–c and S1b). In the aequorin-expressing *A. thaliana* accession Col-0, laminarihexaose but not laminarin triggered a weak but consistent cytosolic Ca<sup>2+</sup> influx and production of ROS (Figure 2d,e). Despite these responses, no activation of MAPKs was observed under the conditions tested (Figure 2f). This is in contrast to previously published work where the perception of laminarihexaose prompted Ca<sup>2+</sup> influx and MAPK phosphorylation in *A. thaliana* Col-0 seedlings (Mélida *et al.*, 2018). To test whether these apparently contradicting observations were due to the different plant tissues tested, we repeated our experiments using *A. thaliana* Col-0<sup>AEQ</sup> seedlings. Indeed, addition of laminarihexaose to

seedlings resulted in MAPK phosphorylation after 15 min (Figure S2), indicating that the different immune responses of *A. thaliana* to laminarihexaose could be age- and/or tissue-dependent. As for leaf discs from 3- to 4-week-old plants, we did not observe ROS production or elevations of cytosolic Ca<sup>2+</sup> in *A. thaliana* Col-0<sup>AEQ</sup> seedlings upon laminarin treatment despite the high elicitor concentrations used. This is in contrast to the laminarin-responsive species barley and *N. benthamiana* where ROS generation was concentration dependent (Figure S3). It has previously been reported that different batches of laminarin exhibit considerable variability in activity (Smith *et al.*, 2018). Therefore, we have tested various batches of laminarin, but have not observed differences in responsiveness. Additionally, the characterization of two laminarin batches used in this study by high-performance liquid chromatography



1146 Alan Wanke *et al.*

did not show differences in glucan composition (Figure S4; Method S2), suggesting that laminarin is, if at all, only weakly immunogenic in *A. thaliana* Col-0. To further investigate whether the lack of laminarin-triggered immune response activation in *A. thaliana* Col-0 is a conserved trait in *Brassicaceae*, we additionally tested ROS production in leaf discs of *Capsella rubella*, a phylogenetically close relative of *A. thaliana* (Koch *et al.*, 1999). Similar to *A. thaliana* Col-0<sup>AEQ</sup>, *C. rubella* responded with a ROS burst to laminarihexaose but not to laminarin (Figure S5), suggesting that the inability to mount a ROS response after addition of long-chain  $\beta$ -1,3-glucan may represent a common feature among *Brassicaceae*.

#### Presence of $\beta$ -1,6-linkages does not contribute to recognition of laminarin

Laminarihexaose and laminarin consist of glucose monomers, but display different degrees of polymerization (DP) and branching (DB). While laminarihexaose is a defined linear hexamer of glucose subunits solely linked by  $\beta$ -1,3-linkages, laminarin is composed of a mix of  $\beta$ -1,3-linked glucose polymers of varying length that additionally contain  $\beta$ -1,6-glycosidic side-branches. To clarify if the  $\beta$ -1,6 side-chains of laminarin are required for recognition, we produced a laminarin substrate that was debranched with the enzyme *FbGH30* from the bacterium *Formosa* sp. strain B and purified by size exclusion chromatography (SEC; Becker *et al.*, 2017; Unfried *et al.*, 2018; Wawra *et al.*, 2019). *FbGH30* specifically removes the  $\beta$ -1,6-linked glucose side-chains of laminarin producing long, linear  $\beta$ -1,3-glucan polymers. The specific release of  $\beta$ -1,6-linked glucose from laminarin following hydrolysis with *FbGH30* could be visualized on thin-layer chromatography (TLC; Figure S6a). Additionally, the absence of  $\beta$ -1,6 side-chains after hydrolysis was confirmed by microscale thermophoresis showing the lack of binding between debranched laminarin and the lectin FGB1 (Wawra *et al.*, 2019). This lectin specifically and efficiently binds to  $\beta$ -1,6-linked glucose attached to linear  $\beta$ -1,3-glucan (Wawra *et al.*, 2016). We then tested the immunogenic activity of laminarin and debranched laminarin in ROS production assays. In *N. benthamiana* SLJR15, both substrates elicited similar ROS responses (Figure 3a). Comparable results were obtained in *N. benthamiana* SLJR15 (Figure 3b) and *H. vulgare* (Figure S6b) using debranched laminarin that was not purified by SEC, indicating that not the  $\beta$ -1,6-glycosidic side-branches but rather the polymer length is essential for  $\beta$ -glucan recognition in these plant species. To test this hypothesis, we treated laminarin with a mixture of commercially available  $\beta$ -1,3 exo- and endoglucanases, which resulted in the complete hydrolysis of long  $\beta$ -glucan chains yielding mainly laminaribiose and glucose (Figures 3c and S4). This hydrolyzed laminarin was then tested for its activity in *N. benthamiana* SLJR15 plants. Unlike debranched

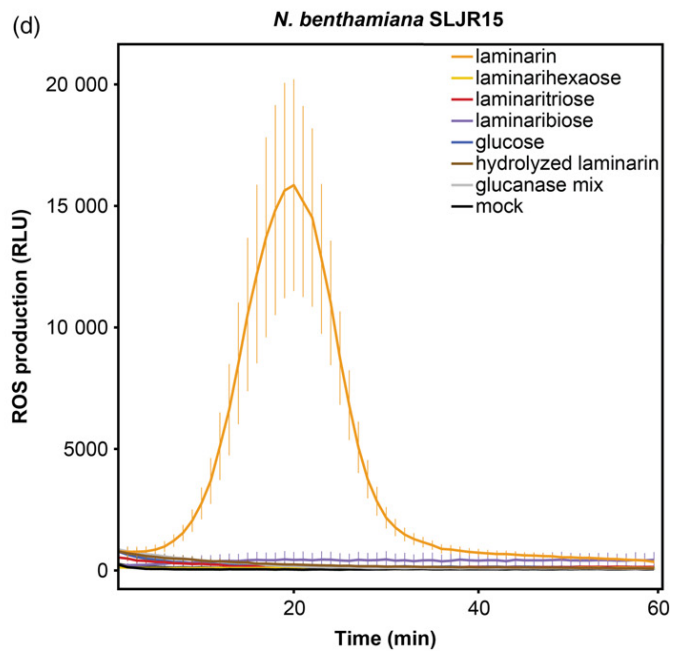
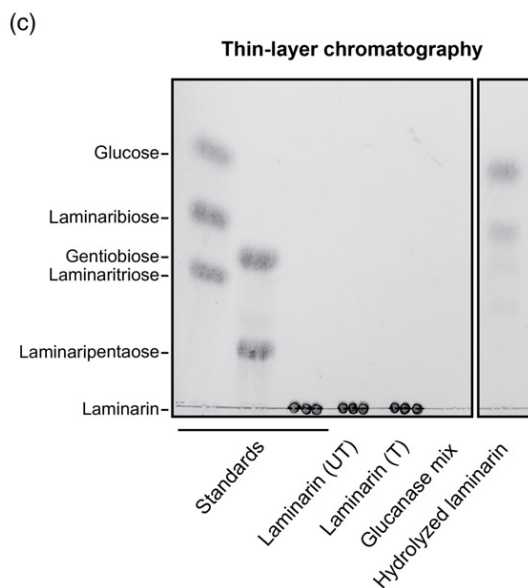
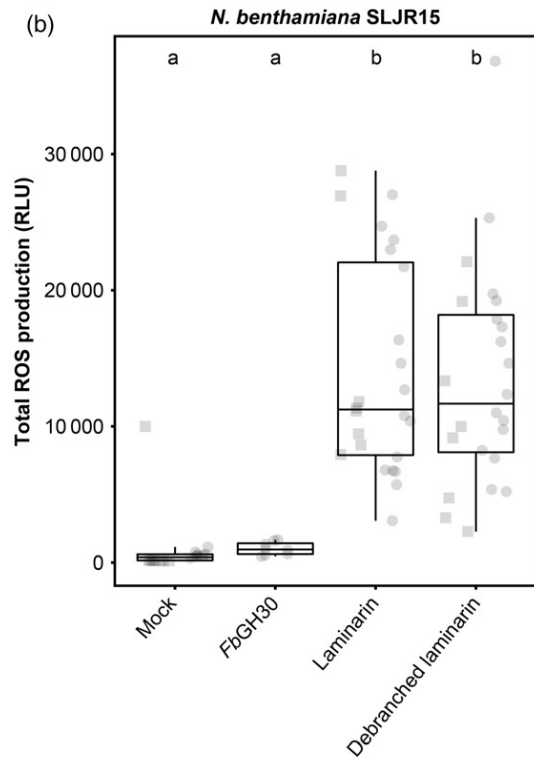
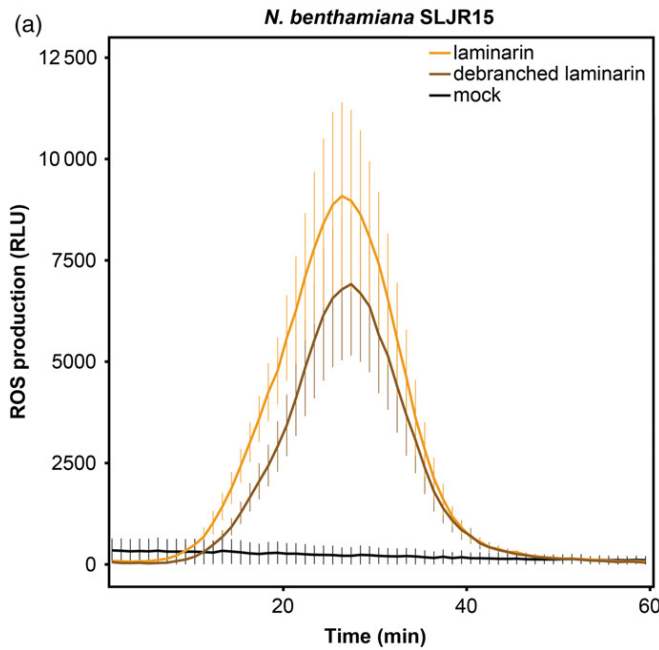
laminarin, hydrolyzed laminarin did not elicit ROS production in *N. benthamiana* SLJR15 (Figure 3d). This demonstrates that *N. benthamiana* is not able to mount early immune responses upon treatment with short  $\beta$ -glucan fragments with a DP smaller than six, but requires longer  $\beta$ -1,3-linked glucan chains for recognition (Figure 3). In contrast, the ability of *H. vulgare* to respond to laminarihexaose led us to speculate that hydrolyzed laminarin would still be able to elicit ROS responses in this plant species. We therefore incubated *H. vulgare* leaf discs with laminarin, hydrolyzed laminarin and various short  $\beta$ -glucan fragments with a DP smaller than six (Figure S6c,d). While *H. vulgare* could respond to the shorter fragments as well as the hydrolyzed laminarin, the level of ROS production was clearly decreased compared with untreated laminarin.

#### Long-chain $\beta$ -glucan recognition is not dependent on CERK1 or BAK1

It was recently shown that CERK1 plays a crucial role in the recognition of laminarihexaose in *A. thaliana* Col-0. In contrast, mutation of *AtBAK1* did not alter laminarihexaose perception (Mélida *et al.*, 2018). However, whether CERK1 is a general component involved in the recognition of different  $\beta$ -glucans and  $\beta$ -glucan-triggered immunity across plant species remains unanswered. To address this question, we silenced the homologs of *AtCERK1* and *AtBAK1* in *N. benthamiana* by tobacco rattle virus (TRV)-based virus-induced gene silencing (VIGS; Figure 4a; Liu *et al.*, 2002; Senthil-Kumar and Mysore, 2014). Plants treated with TRV:*NbCERK1* displayed significantly reduced *NbCERK1* mRNA levels, whereas those of *NbBAK1* were not affected (Figure S7; Gimenez-Ibanez *et al.*, 2009). Similarly, by using primers targeting the two homologs of *NbBAK1* (*NbSERK3a* and *NbSERK3b*) present in the *N. benthamiana* genome, we confirmed that the TRV construct for *NbBAK1* efficiently silenced both homologs but not *NbCERK1* (Figure S7). The same construct was previously shown to not target the closely related *NbSERK2* highlighting construct specificity (Heese *et al.*, 2007; Chaparro-Garcia *et al.*, 2011). Plants treated with silencing constructs against the green fluorescent protein gene (*GFP*) from *Aequorea victoria* (TRV:*GFP*) were used as negative controls (Saur *et al.*, 2016). As shown previously, plants silenced for *NbCERK1* and *NbBAK1* but not those silenced for *GFP* showed reduced ROS production and  $\text{Ca}^{2+}$  influx upon addition of chitohexaose and flg22 in *N. benthamiana* SLJR15, respectively (Figures 4 and 5; Heese *et al.*, 2007; Gimenez-Ibanez *et al.*, 2009; Segonzac *et al.*, 2011). However, *NbBAK1* silencing did not affect immune activation following laminarin treatment, confirming that BAK1 is not required for  $\beta$ -glucan-triggered immunity (Figures 4c,g and 5b,f). Similarly, silencing of *NbCERK1* did not result in altered laminarin-triggered immunity (Figures 4b,g and 5a,f), suggesting the presence of a CERK1-independent perception pathway for long-chain  $\beta$ -glucans in *N. benthamiana*.

To test whether the perception of long-chain  $\beta$ -glucans is similarly independent of CERK1 in monocots, we made use of two independent rice lines in which the first exon of *OsCERK1* was replaced with a hygromycin resistance cassette resulting in the disruption of the *OsCERK1* gene (#53-KO and #117-KO; Kouzai *et al.*, 2014). These mutants were previously shown to have lost their ability to perceive

chitoooligomers and to display reduced responsiveness to peptidoglycan. Segregated wild-type plants (#53-Rev and #117-Rev) were used as respective controls. As expected, *oscerk1* lines were still responsive to flg22, while ROS production following chitohexaose treatment was completely abolished in the KO mutant lines (Figure S8). In contrast, laminarin-triggered ROS production was not affected in



1148 Alan Wanke *et al.*

**Figure 3.** Reactive oxygen species (ROS) production is dependent on the length of the  $\beta$ -glucan backbone but not on the  $\beta$ -1,6 side-branches of laminarin in *Nicotiana benthamiana*.

Leaf discs were collected from 3- to 4-week-old *N. benthamiana* SLJR15.

(a) Laminarin was debranched using the  $\beta$ -1,6-exoglucanase *FbGH30* (Becker *et al.*, 2017) and purified via size exclusion chromatography (SEC; debranched laminarin). Laminarin without glucanase treatment was used as positive control. Production of ROS was measured using luminol-based chemiluminescence for 60 min after treatment with 4 mg ml<sup>-1</sup> laminarin or 4 mg ml<sup>-1</sup> debranched laminarin. Water (mock) served as negative control. ROS response intensity was measured in relative luminescence units (RLU).

(b) Integration of ROS kinetics (total ROS production) following elicitor treatment. Significant differences between treatments were determined with a non-parametric Kruskal–Wallis analysis ( $P < 0.05$ ) followed by Dunn's *post hoc* test. The values shown are from two independent experiments, in which either purified debranched laminarin (squares) or crude debranched laminarin (circles) was used. As positive control treatments, laminarin solutions were treated like their respective debranched counterparts.

(c, d) Laminarin was completely hydrolyzed using an enzyme mix consisting of 0.1 mg ml<sup>-1</sup> endo- $\beta$ -1,3-glucanase from *Helix pomatia* (Sigma), 0.1 mg ml<sup>-1</sup> exo- $\beta$ -1,3-glucanase from *Trichoderma virens* (Megazyme) and 0.1 mg ml<sup>-1</sup> endo- $\beta$ -1,3-glucanase from *Hordeum vulgare* (Megazyme). The complete digest (hydrolyzed laminarin) was analysed by thin-layer chromatography (TLC) (c) using glucose, laminaribiose, gentiobiose, laminaritriose, laminaripentose and laminarin (each 2 mg ml<sup>-1</sup>) as standards. ROS assays (d) were performed on leaf discs of *N. benthamiana* SLJR15 with treated (T) and untreated (UT) laminarin (2 mg ml<sup>-1</sup>, 0.5 mm) as well as glucose, laminaribiose, laminaritriose and laminarihexaose (each 250  $\mu$ M). Water and the enzyme mix alone were used as controls. Values represent means  $\pm$  SE of 8–16 leaf discs from four different plants. Experiments were performed three times with similar results.

*oscerk1* lines, confirming that the activation of immune responses upon laminarin perception does not require CERK1.

## DISCUSSION

Cell walls of filamentous microbes mainly consist of chitin and  $\beta$ -glucans (Lalgé, 2007). During plant host colonization these polysaccharides are targeted by plant hydrolases that release soluble fragments and interfere with cell wall integrity (Kombrink *et al.*, 2011; Sánchez-Vallet *et al.*, 2015; Fesel and Zuccaro, 2016). Recognition of chito oligomers results in the activation of plant immune responses, including ROS production, accumulation of cytosolic Ca<sup>2+</sup>, MAPK activation and changes in gene expression (Antolín-Llovera *et al.*, 2014; Sánchez-Vallet *et al.*, 2015; Rovenich *et al.*, 2016). Similarly,  $\beta$ -glucans are well-characterized elicitors of immunity in animals (Romani, 2011). Moreover, recent evidence indicates that  $\beta$ -glucans also play an important role during interactions between plants and filamentous microbes (Wawra *et al.*, 2016; Mérida *et al.*, 2018).

Using mycelial cell wall fractions of the fungal phytopathogen *Plectosphaerella cucumerina*, Mérida *et al.* (2018) have recently identified the linear  $\beta$ -1,3-glucan hexamer laminarihexaose as major *P. cucumerina* cell wall component and elicitor of immunity in seedlings of *A. thaliana* Col-0. Here we show that laminarihexaose also activates immunity in the form of ROS production and MAPK activation in leaf tissue of the monocots barley and *B. distachyon* (Figure 1). However, the leaves of *N. benthamiana* did not mount immune responses upon treatment with laminarihexaose (Figure 2a–c), suggesting that this short  $\beta$ -1,3-glucan hexamer is not a universal elicitor of immunity in plants. Depending on the species, plant cell walls may also contain  $\beta$ -1,3-linked glucan. Grasses, including barley, rice, sorghum (*Sorghum bicolor*) and wheat (*Triticum aestivum*), as well as the herbaceous perennial *Equisetum arvense*, harbor unbranched glucose polysaccharides with alternating  $\beta$ -1,3 and  $\beta$ -1,4 linkages

that are absent from dicots (Trethewey *et al.*, 2005; Burton *et al.*, 2006; Sørensen *et al.*, 2008). In contrast, *N. alata* cell walls were found to contain large amounts of  $\beta$ -1,3-linked glucan polysaccharides (Rae *et al.*, 1985). Moreover, plants may form papillae that consist of  $\beta$ -1,3-glucan-rich callose to reinforce their cell walls at sites of filamentous microbe penetrations (Hückelhoven, 2007; Albersheim *et al.*, 2011; Chowdhury *et al.*, 2014; Hückelhoven, 2014). Thus, like fungal-derived  $\beta$ -1,3-glucan structures, short  $\beta$ -1,3-glucans could be released from plant cell walls during growth, physical injury, and through the activity of plant or microbial hydrolytic enzymes during colonization by filamentous microbes. It has previously been shown that genomes of plant-associated fungal endophytes, as well as hemibiotrophic and necrotrophic pathogens, are enriched for genes encoding cell-wall-degrading enzymes required for host cell invasion (Lahrmann *et al.*, 2015). Because plant-derived  $\beta$ -1,3-glucan fragments would be virtually indistinguishable from  $\beta$ -1,3-glucans of microbial origin, these molecules defy the classical categorization into self and non-self. This is in contrast to oligogalacturonides and cellobiose, which are almost solely derived from plant-specific pectin and cellulose carbohydrates, respectively, and activate plant immune responses (Kohorn *et al.*, 2009; Brutus *et al.*, 2010; de Azevedo Souza *et al.*, 2017).

In contrast to  $\beta$ -1,3-linked glucans,  $\beta$ -1,6-glucosidic linkages do not occur in plants but are present in cell walls of filamentous microbes (Bowman and Free, 2006; Lalgé, 2007). To date,  $\beta$ -1,6-glucan backbones have been reported in cell walls of several yeasts, lichenized fungi, and are common among oomycetes (Pereyra *et al.*, 2003; Carbonero *et al.*, 2006; Lalgé and Calderone, 2006). Oomycetes, like diatoms and brown algae, from which laminarin is isolated, belong to the phylum Heterokonta. This evolutionary relatedness explains the similarity in  $\beta$ -1,6-linkage-containing glucan structures between these classes. More recently,  $\beta$ -1,6-glucosidic linkages were shown to frequently occur in the extrahyphal matrix surrounding the



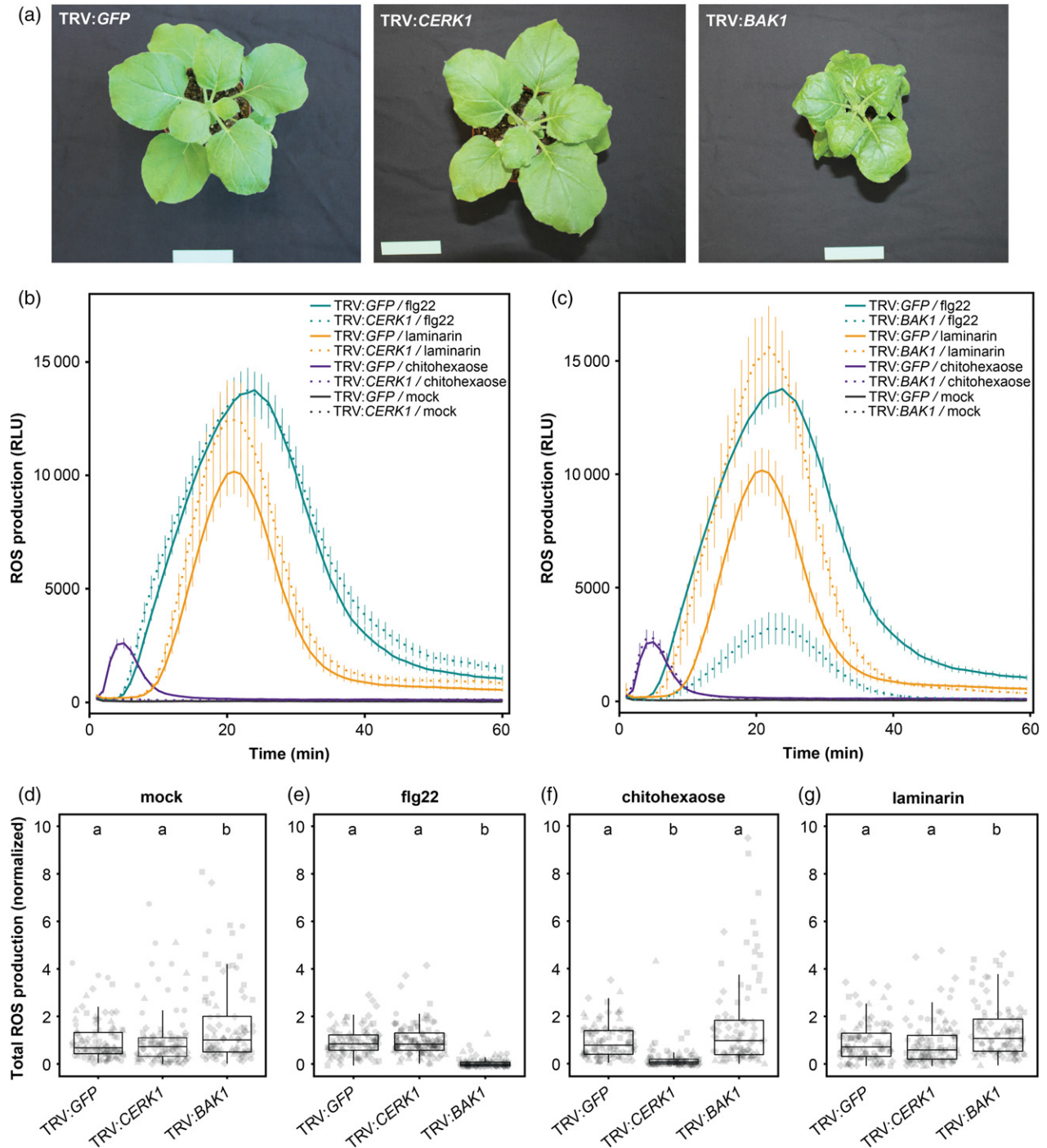


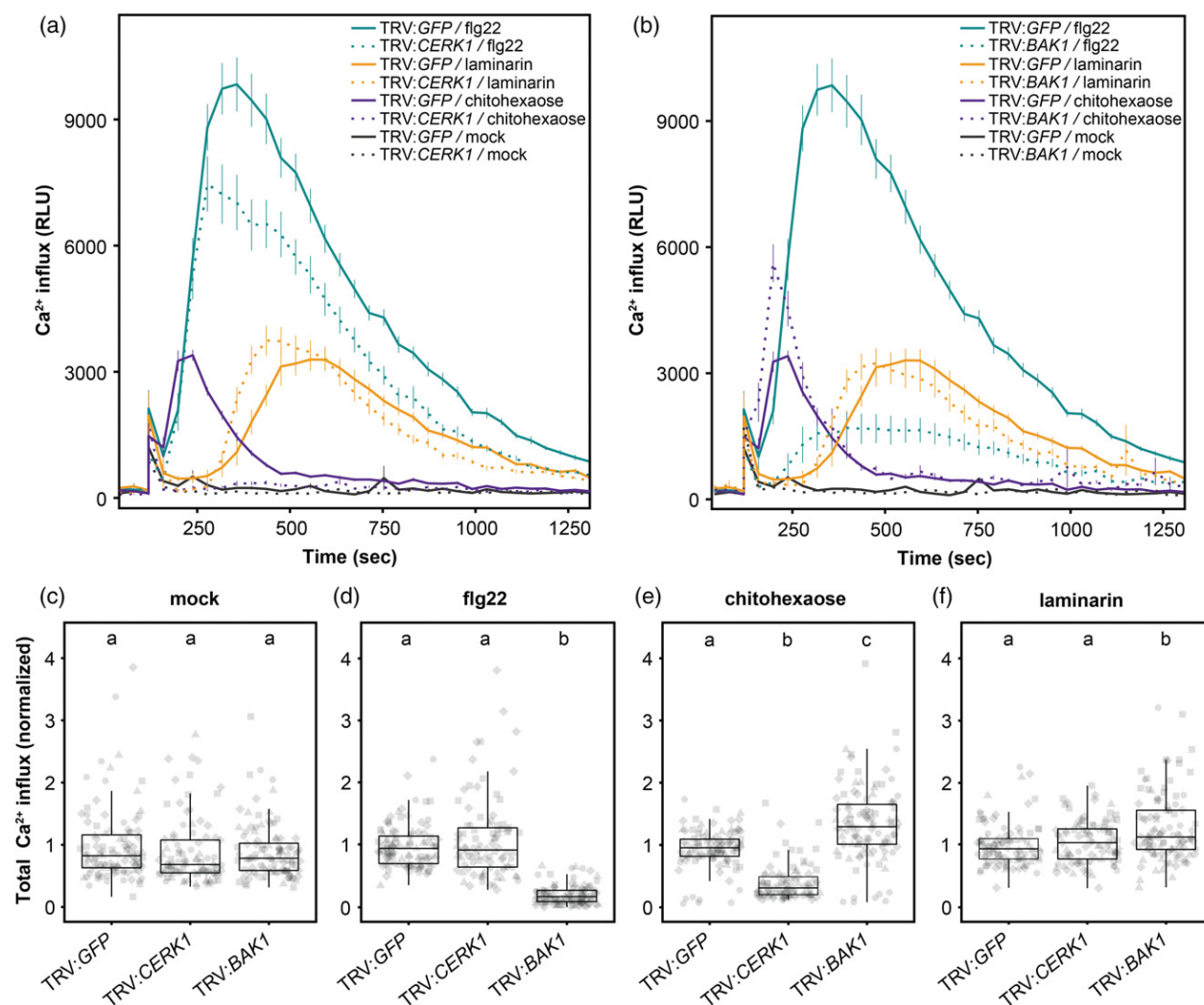
**Figure 4.** Virus-induced gene silencing (VIGS) of *NbCERK1* and *NbBAK1* in *Nicotiana benthamiana* does not reduce  $\beta$ -glucan-triggered reactive oxygen species (ROS) accumulation.

Young, fully-developed leaves of 2-week-old *N. benthamiana* SLJR15 ( $n = 5-8$ ) were infiltrated with *Agrobacterium tumefaciens* suspensions for tobacco rattle virus (TRV)-based silencing of *NbCERK1* or *NbBAK1*. TRV constructs targeting *GFP* were used as negative control.

(a) Phenotypes of TRV-treated plants ~3.5 weeks following infiltration. Green marker: 6 cm.

(b, c) Generation of ROS was measured using luminol-based chemiluminescence for 60 min after treatment with 100 nM flg22, 10  $\mu$ M chitohexaose or 2 mg ml<sup>-1</sup> (0.5 mM) laminarin of TRV:*NbCERK1*- (TRV:*CERK1*) (b) or TRV:*NbBAK1*-treated (TRV:*BAK1*) (c) plants. Water (mock) served as negative control. Values represent means  $\pm$  SE of 24–32 leaf discs. Results are representative of four biological replicate experiments. ROS response intensity was measured in relative luminescence units (RLU).

(d–g) Integrals of ROS kinetics following elicitor treatment were normalized to TRV:*GFP* control (total ROS production). Significant differences in ROS production between *GFP*-, *NbCERK1*- and *NbBAK1*-silenced plants are depicted with letters ( $P < 0.05$ , Kruskal–Wallis analysis with Dunn's *post hoc* test). Each independent experiment is represented by a different shape.

1150 Alan Wanke *et al.*

**Figure 5.** Glucan-triggered cytosolic Ca<sup>2+</sup> fluxes are not affected by virus-induced gene silencing (VIGS) of *NbCERK1* and *NbBAK1*.

Young, fully-developed leaves of 2-week-old *Nicotiana benthamiana* SLJR15 ( $n = 5-8$ ) were infiltrated with *Agrobacterium tumefaciens* suspensions for tobacco rattle virus (TRV)-based silencing of *NbCERK1* or *NbBAK1*.

(a, b) TRV constructs targeting *GFP* were used as negative control. Elevations of cytosolic calcium concentrations (Ca<sup>2+</sup> influx) were measured as relative luminescence units (RLU) following treatment with 100 nM flg22, 10  $\mu$ M chitohexaose or 2 mg ml<sup>-1</sup> (0.5 mM) laminarin of TRV:*NbCERK1*- (TRV:*CERK1*) (a) or TRV:*NbBAK1*-treated (TRV:*BAK1*) (b) plants. Water (mock) served as negative control. Remaining aequorin was discharged by adding CaCl<sub>2</sub>. Discharge kinetics were integrated and normalized to the maximum Ca<sup>2+</sup> level. The discharge integral was then used to normalize Ca<sup>2+</sup> kinetics in response to elicitor treatment. Values represent means  $\pm$  SE of 24–32 leaf discs.

(c–f) Integrals of Ca<sup>2+</sup> kinetics following elicitor treatment (total Ca<sup>2+</sup> influx) were normalized to TRV:*GFP* control. Significant differences in Ca<sup>2+</sup> influx between *GFP*-, *NbCERK1*- and *NbBAK1*-silenced plants are depicted with letters ( $P < 0.05$ , Kruskal–Wallis analysis with Dunn’s *post hoc* test). Each independent experiment is represented by a different shape.

cells of plant-associated fungi during host colonization (Wawra *et al.*, 2019). The best-studied  $\beta$ -1,6-glucan in this context is a heptaglycoside from cell walls of pathogenic oomycetes (Ayers *et al.*, 1976; Ebel *et al.*, 1976; Albersheim and Valent, 1978; Sharp *et al.*, 1984b). This oomycete-derived heptaglycoside consists of a  $\beta$ -1,6-linked glucose pentamer backbone with two  $\beta$ -1,3-linked glucosyl branches (Sharp *et al.*, 1984a). It triggers phytoalexin production in several leguminous plant species and in potato (Cline *et al.*, 1978; Sharp *et al.*, 1984b; Cosio *et al.*, 1996;

Côté *et al.*, 2000), but is not active in tobacco and rice cell suspensions (Klarzynski *et al.*, 2000; Yamaguchi *et al.*, 2000). Instead, tobacco cells respond to the long linear  $\beta$ -1,3-glucan laminarin with  $\beta$ -1,6 side-branches, which elicits a wide range of defense responses, including medium alkalization, ROS production, salicylic acid accumulation and defense gene expression (Klarzynski *et al.*, 2000; Ménard *et al.*, 2004). Similar responses to laminarin were reported for grapevine (Aziz *et al.*, 2003). In addition to ROS production, we could show that laminarin triggers

MAPK activation in barley and *B. distachyon* leaf tissue (Figure 1). Interestingly, the kinetics of laminarin-triggered ROS production in *B. distachyon* and barley differed greatly from the fast and short immune responses to chitin and laminarihexaose. As has been observed upon activation of the LRR receptor kinase flagellin sensing 2 (FLS2) and the LRR receptor protein Cf4 (Robatzek *et al.*, 2006; Salomon and Robatzek, 2006; Beck *et al.*, 2012; Spallek *et al.*, 2013; Postma *et al.*, 2016), laminarin binding could result in the internalization and degradation of its corresponding receptor (complex). The resulting depletion of such a receptor at the cell surface would then cause a temporary inability of that plant to respond to laminarin causing a drop in ROS production. The replenishment of the relevant receptor at the plasma membrane would then allow the renewed recognition of remaining elicitor molecules. Conversely, considering the constitutive presence of extracellular plant glucanases (Wawra *et al.*, 2016), the long-lasting accumulation of peaks could be caused by the gradual hydrolysis of  $\beta$ -glucans resulting in the production of a laminarin-derived  $\beta$ -glucan elicitor structure. This hypothesis should be tested following the identification of glucanases responsible for laminarin hydrolysis in barley or *B. distachyon*.

In *N. benthamiana*, laminarin treatment triggered ROS production, MAPK activation, increased intracellular  $\text{Ca}^{2+}$  concentrations and defense gene expression (Figures 2a–c and S1b). The consistent activation of immune responses following laminarin but not laminarihexaose treatment in *N. benthamiana* led us to investigate whether the  $\beta$ -1,6-glucosidic branches in laminarin were required for its immunoactivity. Leaf discs treated with enzymatically debranched laminarin produced ROS similar to laminarin-treated controls (Figure 3a,b), suggesting that, similar to *Nicotiana tabacum* (Klarzynski *et al.*, 2000),  $\beta$ -1,6-glucan linkages are dispensable for the recognition of long  $\beta$ -1,3-glucan in *N. benthamiana*. Similar results were obtained after the addition of debranched laminarin to barley leaf discs (Figure S6). In contrast to *N. tabacum* and barley, however, the recognition of  $\beta$ -1,3-glucan appears to be determined by the DP in *N. benthamiana* as treatment with  $\beta$ -1,3-glucan fragments with a DP smaller than six did not result in the activation of early immune responses (Figure 2a–c), and laminarihexaose elicited only a weak and transient upregulation of defense-related genes (Figure S1b). Additionally, laminarin hydrolysis by  $\beta$ -1,3-glucanases yielded short  $\beta$ -glucan fragments and glucose, and abolished ROS production (Figure 3c,d). Moreover, long linear  $\beta$ -1,3-glucan was shown to assume a triple helical structure (Chuah *et al.*, 1983; Kulicke *et al.*, 1997; Young *et al.*, 2000; Okobira *et al.*, 2008), which is required for  $\beta$ -1,3-glucan recognition in insects (Mishima *et al.*, 2009; Takahashi *et al.*, 2009; Kanagawa *et al.*, 2011). This triple helical quaternary structure is also crucial for effective

binding by laminarin-degrading enzymes (GH81) from bacteria (Pluvinage *et al.*, 2017). Whether the assembly of long  $\beta$ -1,3-glucans into a triple helix plays a similar role in the activation of plant immunity remains to be investigated.

Unlike other plant species tested here, *A. thaliana* Col-0 leaves and seedlings did not respond to laminarin (Figures 2d–f and S2). In contrast, previous work by Mérida *et al.* (2018) showed that seedlings of *A. thaliana* Col-0 respond with a weak increase in cytosolic  $\text{Ca}^{2+}$  upon laminarin treatment. In general, the activity of laminarin, if any, appears to be weak and inconsistent in *A. thaliana* Col-0. It is likely that variations in growth conditions, elicitor purity, DP and resulting quaternary structures in the different laminarin batches contributed to these observations. This is in accordance with a previous report that laminarin batches from various commercial sources contained ‘impurities’, resulting in variations of their immunomodulatory activity in animal systems (Smith *et al.*, 2018). These variations may also explain our finding that *C. rubella* does not produce ROS upon laminarin treatment (Figure S5). However, we have tested several laminarin batches in *A. thaliana* Col-0 and did not observe differences in responsiveness. Additionally, high-performance anion exchange chromatography-based analysis of two of these batches showed no variations in  $\beta$ -glucan composition (Figure S4), supporting the conclusion that laminarin is a poor elicitor of immunity in *Brassicaceae* at least for those batches. In contrast, laminarihexaose triggered weak but consistent ROS production and cytosolic  $\text{Ca}^{2+}$  influx in *A. thaliana* Col-0 leaves (Figure 2d,e), while no MAPK activation was detectable. MAPK activation and ROS production have been shown to be two independent signaling events in plant immunity (Ranf *et al.*, 2011; Segonzac *et al.*, 2011; Xu *et al.*, 2014; de Azevedo Souza *et al.*, 2017), which is in agreement with our findings. Interestingly, laminarihexaose-triggered MAPK activation was visible in seedlings (Figure S2c; Mérida *et al.*, 2018), suggesting that the different immune responses of *A. thaliana* Col-0 to laminarihexaose may be age- and/or tissue-dependent.

These findings show that the structural complexity of  $\beta$ -glucans contributes to their differential recognition by plant species. In addition to the large number of variants in side-chain decorations and linkage patterns within  $\beta$ -glucan backbones, chemical modifications can influence  $\beta$ -glucan recognition in plants (Ménard *et al.*, 2004; Gauthier *et al.*, 2014). To solve the question whether these specific responses are the result of adaptation processes to particular microbial partners or microbe-dependent plant cell wall modifications, chemical synthesis of defined  $\beta$ -glucan structures as test substrates would be of high interest (Weishaupt *et al.*, 2017).

In conclusion, the differential recognition of  $\beta$ -glucan structures suggests the existence of multiple receptor molecules with varying ligand specificities. To date, the



1152 Alan Wanke *et al.*

only known putative  $\beta$ -glucan receptor is the  $\beta$ -glucan binding protein GBP of soybean, which displays high affinity for the oomycete-derived heptagluco-side (Yoshikawa *et al.*, 1983; Mithöfer *et al.*, 1996; Umemoto *et al.*, 1997; Mithöfer *et al.*, 2000; Fliegmann *et al.*, 2004). Unlike other receptor proteins, GBP contains an enzymatically active endo- $\beta$ -1,3-glucanase domain in addition to a carbohydrate-binding site (Fliegmann *et al.*, 2004). Despite the lack of a canonical signal peptide sequence, GBP was found to localize to the apoplast as well as to the cell surface. It was, therefore, suggested that GBP represents a multi-component receptor molecule that retains the ability to hydrolyze complex  $\beta$ -glucan in microbial cell walls. If and how GBP interacts with co-receptor proteins and activates immune signaling remains to be answered. In most cases, ligand binding to a receptor results in the formation of large receptor complexes that are required for the activation of downstream signaling (Couto and Zipfel, 2016). BAK1 and other members of the SERK protein family generally associate with LRR-type receptor proteins upon recognition of proteinaceous ligands, thereby mediating important processes in growth, development and immunity (Ma *et al.*, 2016). There is currently no evidence that BAK1 is involved in the perception of carbohydrate-based ligands, which is in line with our data (Figures 4 and 5). However, based on the experiments conducted here, we cannot exclude that other SERK proteins may be required for  $\beta$ -glucan-triggered signaling. Recognition of chitin and chitin-derived molecules is mediated by CERK1 in *A. thaliana* and rice (Sánchez-Vallet *et al.*, 2015). Similarly, laminarihexaose-triggered immune responses are mediated by CERK1 in *A. thaliana* Col-0 (Mélida *et al.*, 2018). In contrast, our findings demonstrate that the recognition of long  $\beta$ -1,3-glucan leads to the activation of immunity via a CERK1-independent pathway in *N. benthamiana* and rice (Figures 4, 5 and S8), suggesting that there may be different receptor systems that mediate  $\beta$ -1,3-glucan recognition in plants.

## EXPERIMENTAL PROCEDURES

### Plant material and growth conditions

*Arabidopsis thaliana* and *Capsella rubella*. All assays were performed with seeds of aequorin-expressing *A. thaliana* accessions Col-0 (Choi *et al.*, 2014) or wild-type *C. rubella* Monte Gargano. For seedling assays, seeds were surface sterilized as described previously (Nizam *et al.*, 2019). Sterile seeds were sown on ½ Murashige & Skoog (MS) medium (pH 5.7) supplemented with 0.5% sucrose and 0.4% Gelrite (Duchefa, Haarlem, the Netherlands) and stratified for 3 days. Plates were transferred to climate chambers with an 8/16 h light/dark regime (light intensity of  $110 \mu\text{mol m}^{-2} \text{sec}^{-1}$ ) at 22/18°C. Five-day-old seedlings were transferred to fresh ½ MS agar plates or liquid medium and grown for seven additional days under the same conditions. For leaf disc assays, seeds were sterilized as before and sown on soil. Pots

were kept at 4°C for 3 days. Plants were then grown in climate chambers under the conditions described above for 3–4 weeks.

*Nicotiana benthamiana*. Seeds of *N. benthamiana* aequorin-expressing SLJR15 (Segonzac *et al.*, 2011) lines were sown on soil and grown in the greenhouse under long-day conditions (day/night cycle of 16/8 h, 22–25°C, light intensity of  $\sim 140 \mu\text{mol m}^{-2} \text{sec}^{-1}$ , maximal humidity of 60%). Plants were  $\sim 3.5$  weeks old when leaf discs were collected for immunity assays.

*Hordeum vulgare* and *Brachypodium distachyon*. Seeds of *H. vulgare* cv. Golden Promise were sown on soil and grown in a climate chamber with a day/night cycle of 16/8 h at 22/18°C, 60% humidity and a light intensity of  $108 \mu\text{mol m}^{-2} \text{sec}^{-1}$  for 2–3 weeks. Seeds of *B. distachyon* Bd21-3 were stratified on soil for 5 days. Pots were then transferred to a climate chamber and *B. distachyon* plants were cultivated for 4–5 weeks under the same conditions as *H. vulgare*.

*Oryza sativa*. Seeds of *Oryza sativa* (rice) L. *japonica* cv. Nipponbare Kanto BL no. 2 control (#53-Rev and #117-Rev) and *oscerk1* KO (#53-KO and #117-KO) lines were previously characterized (Kouzai *et al.*, 2014). Seeds were surface sterilized with 3.5% bleach for 30 min, extensively washed with sterile water and germinated in jars containing water with  $4 \text{ g L}^{-1}$  gelrite (Duchefa, Haarlem, the Netherlands). Plants were cultivated in a climate chamber (31°C, 70% humidity) before being transferred to pots with pure sand. After an acclimatization period of 2 weeks, plants were transferred onto a soil–sand–mix (8:1) and grown for a further 2–3 weeks before being used for ROS burst assays.

### Elicitors

Laminarin was purchased from Sigma-Aldrich (Taufkirchen, Germany), flg22 from GenScript (Piscataway, NJ, USA), and laminarihexaose, laminaritriose, laminaribiose and chitohexaose from Megazyme (Bray, Ireland). All elicitors were dissolved in autoclaved MilliQ-water and used at indicated concentrations without additional treatment.

### Calcium influx assay

Leaf discs or seedlings were placed into white 96-well plates filled with  $75 \mu\text{l}$  of distilled water. To each well,  $25 \mu\text{l}$  of a  $40 \mu\text{M}$  coelenterazine (Roth, Karlsruhe, Germany) solution (in 100% methanol) was added, and plates were kept in the dark at room temperature overnight. Luminescence measurements were carried out using a multiwell plate reader (TECAN SPARK 10M). Following 2 min baseline measurements,  $50 \mu\text{l}$  elicitor solutions [sterile water,  $250 \mu\text{M}$  laminarihexaose,  $100 \text{ nM}$  flg22 or  $2\text{--}4 \text{ mg ml}^{-1}$  laminarin ( $0.5\text{--}1 \text{ mM}$ ) final concentrations] were added to wells and luminescence was measured for 30 min. Remaining aequorin was discharged for 1 min with  $100 \mu\text{l}$  of  $2.5 \text{ M}$   $\text{CaCl}_2$  (in 25% ethanol). All measurements were performed with an integration time of 300 msec. To calculate the increase of intracellular calcium concentrations, discharge curves of each well were integrated. Integrated values were normalized to the maximal discharge integral upon all wells and treatments. The values for the baseline measurement and the measurement after elicitor treatment were then normalized according to the discharge integral.

### Oxidative burst assay

Oxidative burst measurements were performed on leaf discs or seedlings. Plant material was placed into white 96-well plates filled with 100  $\mu$ l of sterile distilled water. Following overnight incubation at room temperature on the bench, water was replaced with 50  $\mu$ l of fresh water containing 20  $\mu$ g ml<sup>-1</sup> horseradish peroxidase (Sigma-Aldrich) and 20  $\mu$ M L-012 (Wako Chemicals, Neuss, Germany). Following ~20 min incubation at room temperature in the dark, 50  $\mu$ l elicitor solutions [final concentrations: 250  $\mu$ M laminarihexaose, 100 nM flg22, 2–4 mg ml<sup>-1</sup> laminarin (0.5–1 mM), 10  $\mu$ M chitohexaose] or water were added. Measurements were started immediately and taken at 1 min intervals with an integration time of 300 msec using a TECAN SPARK 10M.

### MAPK assay

Twenty leaf discs (3 mm) or 15 seedlings for each treatment were floated in water overnight. The plant material was treated with water as control, 250  $\mu$ M laminarihexaose, 100 nM flg22 or 2–4 mg ml<sup>-1</sup> (0.5–1 mM) laminarin. Samples were collected after 0, 15 and 30 min, and snap-frozen in liquid nitrogen. Samples were ground using a tissue lyzer (TissueLyzer II, Qiagen) and metal beads. Homogenized samples were suspended in 150  $\mu$ l MAPK extraction buffer (Mine *et al.*, 2017). Samples were vortexed and pelleted at 13 000 rpm and 4°C for 10 min. Small aliquots of supernatants were used to determine total protein concentrations using Bradford reagent (Sigma-Aldrich) according to manufacturer's instructions. Remaining supernatants were diluted with 6  $\times$  sodium dodecyl sulfate buffer and boiled at 95°C for 5 min. Each sample (15  $\mu$ g total protein) was separated on 10% polyacrylamide gels and transferred onto nitrocellulose membranes with fast Western buffer (48 mM Tris, 20 mM HEPES, 1 mM EDTA, 1.3 mM DMF). Immunoblot analysis was performed with 1:2000 anti-phospho-p44/42 (ERK1/2) MAPK (Cell Signaling Technology, Danvers, USA) as primary antibody and 1:2000 HRP-conjugated anti-rabbit-IgG (Sigma-Aldrich) as secondary antibody. Bands were detected using SuperSignal West Femto Chemiluminescent Substrate (Thermo Scientific).

### Virus-induced gene silencing

Virus-induced gene silencing of *NbCERK1* and *NbBAK1* in *N. benthamiana* SLJR15 was performed (Liu *et al.*, 2002; Senthil-Kumar and Mysore, 2014) using previously generated pTRV2 vectors targeting *NbCERK1* and *NbBAK1* as well as the green fluorescent protein gene (*GFP*; Heese *et al.*, 2007; Gimenez-Ibanez *et al.*, 2009; Chaparro-Garcia *et al.*, 2011; Saur *et al.*, 2016). Cultures of *Agrobacterium tumefaciens* strain GV3101 containing either pTRV1 or pTRV2 constructs were pre-cultured overnight at 28°C and 200 rpm. Bacteria were then pelleted, washed and diluted to an OD<sub>600</sub> = 1 with MMA buffer (10 mM MgCl<sub>2</sub>, 10 mM MES pH 5.7, 200  $\mu$ M acetosyringone). After 3 h of incubation in the dark, bacterial suspensions with pTRV1 and pTRV2 constructs were mixed at a 1:1 ratio and infiltrated into leaves of 2-week-old *N. benthamiana* SLJR15 plants (four-leaf stage) using a 1-ml needleless syringe. Phenotypes were assessed 27 days after infiltration.

### Enzymatic treatments of laminarin

The  $\beta$ -1,6 side-chains of laminarin were removed by hydrolysis with the  $\beta$ -1,6-exoglucosidase *FbGH30* essentially as described previously (Wawra *et al.*, 2019). To generate substrates for ROS assays, 4 mg laminarin (in water) was digested using 4  $\mu$ M *FbGH30* overnight (16 h, 37°C).

For the complete hydrolysis of laminarin, 20 mg ml<sup>-1</sup> laminarin (in water) was treated with a glucanase mix consisting of an endo- $\beta$ -1,3-glucanase from *Helix pomatia* (Sigma, Taufkirchen, Germany), an exo- $\beta$ -1,3-glucanase from *Trichoderma virens* (Megazyme, Bray, Ireland) and an endo- $\beta$ -1,3-glucanase from *H. vulgare*: (Megazyme, Bray, Ireland) (each 0.1 mg ml<sup>-1</sup>). After overnight incubation (16 h) at 37°C, the enzymatic reaction was stopped by boiling at 95°C for 15 min. Precipitates were removed by centrifugation at 17 000 g for 20 min. The supernatant was used for TLC analysis and ROS assays.

### Thin-layer chromatography

A glass chamber was equilibrated with 8:4:1:1 ethyl acetate/acetic acid/methanol/formic acid/water. Twice, three spots of 0.4  $\mu$ l per sample were spotted on a line 2 cm above the lower edge of a plate of silica gel 60 F254 (Merck-Millipore, Darmstadt, Germany). After drying, the plate was placed into the equilibrated glass chamber. The solvent reached the top of the plate after approximately 2 h. Plates were dried under the fume hood and then sprayed with developer solution [82.6% ethanol (v/v), 10.7% H<sub>2</sub>SO<sub>4</sub> (v/v), 7.6% water, 1 mg ml<sup>-1</sup> 1-naphthol]. To visualize carbohydrate fragments, plates were developed in an oven at 99.9°C for 5–10 min.

### ACKNOWLEDGEMENTS

The authors thank Dennis Mahr and Tina Trautmann for technical assistance, and acknowledge Kenichi Tsuda for providing *C. rubella* seeds; Yoko Nishizawa and Uta Paskowski for providing seeds of mutant and wild-type rice lines; and Cyril Zipfel for sharing TRV constructs. AW was supported by the International Max Planck Research School (IMPRS) on 'Understanding Complex Plant Traits using Computational and Evolutionary Approaches' and the University of Cologne. AZ acknowledges support from the Max-Planck-Society and the Cluster of Excellence on Plant Sciences (CEPLAS) Funded by the Deutsche Forschungsgemeinschaft (DFG, German Research Foundation) under Germany's Excellence Strategy – EXC 2048/1 – Project ID: 390686111. SB and JHH acknowledge the support of this project through the Deutsche Forschungsgemeinschaft (DFG) project grant HE 7217/1-1 as well as the Max-Planck-Society.

### CONFLICTS OF INTEREST

All authors confirm that there are no conflicts of interest.

### AUTHOR CONTRIBUTIONS

AW, HR, JHH, SW and AZ conceived and planned experiments. AW, HR, FS, SV and SB carried out experiments and analyzed results. AW, HR and AZ wrote the manuscript.

### DATA AVAILABILITY STATEMENT

All relevant data can be found within the manuscript and its supporting materials.

### SUPPORTING INFORMATION

Additional Supporting Information may be found in the online version of this article.

**Figure S1.**  $\beta$ -Glucan triggered defense gene expression in *H. vulgare* and *N. benthamiana*.

1154 Alan Wanke *et al.*

**Figure S2.** Laminarihexase but not laminarin activates immune responses in *A. thaliana* Col-0 seedlings.

**Figure S3.** Laminarin-triggered ROS production is concentration dependent.

**Figure S4.** Qualitative characterization of different laminarin preparations.

**Figure S5.** Laminarihexase triggers ROS production in *C. rubella*.

**Figure S6.** *H. vulgare* produces ROS upon elicitation with short and long unbranched  $\beta$ -glucans.

**Figure S7.** Efficiency and specificity of *NbBAK1* and *NbCERK1* silencing in *N. benthamiana*.

**Figure S8.** *OsCERK1* is not involved in the recognition of laminarin in *O. sativa*.

**Table S1.** Primers used for gene expression analysis.

**Method S1.** Defense gene expression analysis and VIGS efficiency test.

**Method S2.** High-performance anion exchange chromatography with pulsed amperometric detection (HPAEC-PAD).

## REFERENCES

- Albersheim, P. and Valent, B.S. (1978) Host-pathogen interactions in plants. Plants, when exposed to oligosaccharides of fungal origin, defend themselves by accumulating antibiotics. *J. Cell Biol.* **78**, 627–643.
- Albersheim, P., Darvill, A.G., Roberts, K.A., Sederoff, R. and Staehlin, A. (2011) *Cell walls and plant-microbe interactions*. New York, NY, USA: Garland Science, Taylor & Francis.
- Alderkamp, A.C., van Rijssel, M. and Bolhuis, H. (2007) Characterization of marine bacteria and the activity of their enzyme systems involved in degradation of the algal storage glucan laminarin. *FEMS Microbiol. Ecol.* **59**, 108–117.
- Antolín-Llovera, M., Petutsching, E.K., Ried, M.K., Lipka, V., Nürnberger, T., Robatzek, S. and Parniske, M. (2014) Knowing your friends and foes—plant receptor-like kinases as initiators of symbiosis or defence. *New Phytol.* **204**, 791–802.
- Ao, Y., Li, Z., Feng, D., Xiong, F., Liu, J., Li, J.F., Wang, M., Wang, J., Liu, B. and Wang, H.B. (2014) OsCERK1 and OsRLCK176 play important roles in peptidoglycan and chitin signaling in rice innate immunity. *Plant J.* **80**, 1072–1084.
- Ayers, A.R., Ebel, J., Valent, B. and Albersheim, P. (1976) Host-pathogen interactions: X. Fractionation and biological activity of an elicitor isolated from the mycelial walls of *Phytophthora megasperma* var. *sojiae*. *Plant Physiol.* **57**, 760–765.
- de Azevedo Souza, C., Li, S., Lin, A.Z., Boutrot, F., Grossmann, G., Zipfel, C. and Somerville, S.C. (2017) Cellulose-derived oligomers act as damage-associated molecular patterns and trigger defense-like responses. *Plant Physiol.* **173**, 2383–2398.
- Aziz, A., Poinssot, B., Daire, X., Adrian, M., Bezier, A., Lambert, B., Joubert, J.M. and Pugin, A. (2003) Laminarin elicits defense responses in grapevine and induces protection against *Botrytis cinerea* and *Plasmopara viticola*. *Mol. Plant Microbe Interact.* **16**, 1118–1128.
- Beck, M., Zhou, J., Faulkner, C., MacLean, D. and Robatzek, S. (2012) Spatio-temporal cellular dynamics of the Arabidopsis flagellin receptor reveal activation status-dependent endosomal sorting. *Plant Cell*, **24**, 4205–4219.
- Becker, S., Scheffel, A., Polz, M.F. and Hehemann, J.H. (2017) Accurate quantification of laminarin in marine organic matter with enzymes from marine microbes. *Appl. Environ. Microbiol.* **83**, e03389–e03316.
- Boller, T. and Felix, G. (2009) A renaissance of elicitors: perception of microbe-associated molecular patterns and danger signals by pattern-recognition receptors. *Annu. Rev. Plant Biol.* **60**, 379–406.
- Bowman, S.M. and Free, S.J. (2006) The structure and synthesis of the fungal cell wall. *BioEssays*, **28**, 799–808.
- Brutus, A., Sicilia, F., Maccone, A., Cervone, F. and De Lorenzo, G. (2010) A domain swap approach reveals a role of the plant wall-associated kinase 1 (WAK1) as a receptor of oligogalacturonides. *Proc. Natl. Acad. Sci. USA*, **107**, 9452–9457.
- Burton, R.A., Wilson, S.M., Hrmova, M., Harvey, A.J., Shirley, N.J., Medhurst, A., Stone, B.A., Newbigin, E.J., Bacic, A. and Fincher, G.B. (2006) Cellulose synthase-like *Cs1F* genes mediate the synthesis of cell wall (1,3;1,4)-beta-D-glucans. *Science*, **311**, 1940–1942.
- Cao, Y., Liang, Y., Tanaka, K., Nguyen, C.T., Jedrejczak, R.P., Joachimiak, A. and Stacey, G. (2014) The kinase LYK5 is a major chitin receptor in Arabidopsis and forms a chitin-induced complex with related kinase CERK1. *Elife*, **3**. <https://doi.org/10.7554/eLife.03766>.
- Carbonero, E.R., Smiderle, F.R., Gracher, A.H.P., Mellinger, C.G., Torri, G., Ahti, T., Gorin, P.A.J. and Iacomini, M. (2006) Structure of two glucans and a galactofuranomannan from the lichen *Umbilicaria mammulata*. *Carbohydr. Pol.* **63**, 13–18.
- Chaparro-Garcia, A., Wilkinson, R.C., Gimenez-Ibanez, S., Findlay, K., Coffey, M.D., Zipfel, C., Rathjen, J.P., Kamoun, S. and Schornack, S. (2011) The receptor-like kinase SERK3/BAK1 is required for basal resistance against the late blight pathogen *Phytophthora infestans* in *Nicotiana benthamiana*. *PLoS ONE*, **6**, e16608.
- Choi, J., Tanaka, K., Cao, Y., Qi, Y., Qiu, J., Liang, Y., Lee, S.Y. and Stacey, G. (2014) Identification of a plant receptor for extracellular ATP. *Science*, **343**, 290–294.
- Chowdhury, J., Henderson, M., Schweizer, P., Burton, R.A., Fincher, G.B. and Little, A. (2014) Differential accumulation of callose, arabinoxylan and cellulose in nonpenetrated versus penetrated papillae on leaves of barley infected with *Blumeria graminis* f. sp. *hordei*. *New Phytol.* **204**, 650–660.
- Chuah, C.T., Sarko, A., Deslandes, Y. and Marchessault, R.H. (1983) Triple-helical crystalline structure of curdlan and paramylon hydrates. *Macromolecules*, **16**, 1375–1382.
- Cline, K., Wade, M. and Albersheim, P. (1978) Host-pathogen interactions: XV. Fungal glucans which elicit phytoalexin accumulation in soybean also elicit the accumulation of phytoalexins in other plants. *Plant Physiol.* **62**, 918–921.
- Cook, D.E., Mesarich, C.H. and Thomma, B.P. (2015) Understanding plant immunity as a surveillance system to detect invasion. *Annu. Rev. Phytopathol.* **53**, 541–563.
- Cosio, E.G., Feger, M., Miller, C.J., Antelo, L. and Ebel, J. (1996) High-affinity binding of fungal beta-glucan elicitors to cell membranes of species of the plant family *Fabaceae*. *Planta*, **200**, 92–99.
- Côté, F., Roberts, K.A. and Hahn, M.G. (2000) Identification of high-affinity binding sites for the hepta-beta-glucoside elicitor in membranes of the model legumes *Medicago truncatula* and *Lotus japonicus*. *Planta*, **211**, 596–605.
- Couto, D. and Zipfel, C. (2016) Regulation of pattern recognition receptor signalling in plants. *Nat. Rev. Immunol.* **16**, 537–552.
- Ebel, J., Ayers, A.R. and Albersheim, P. (1976) Host-pathogen interactions: XII. response of suspension-cultured soybean cells to the elicitor isolated from *Phytophthora megasperma* var. *sojiae*, a fungal pathogen of soybeans. *Plant Physiol.* **57**, 775–779.
- Erwig, J., Ghareeb, H., Kopischke, M., Hacke, R., Matei, A., Petutschnig, E. and Lipka, V. (2017) Chitin-induced and CHITIN ELICITOR RECEPTOR KINASE1 (CERK1) phosphorylation-dependent endocytosis of *Arabidopsis thaliana* LYSIN MOTIF-CONTAINING RECEPTOR-LIKE KINASE5 (LYK5). *New Phytol.* **215**, 382–396.
- Feng, F., Sun, J., Radhakrishnan, G.V. *et al.* (2019) A combination of chitoooligosaccharide and lipochitoooligosaccharide recognition promotes arbuscular mycorrhizal associations in *Medicago truncatula*. *Nat. Commun.* **10**, 5047.
- Fesel, P.H. and Zuccaro, A. (2016) Beta-glucan: crucial component of the fungal cell wall and elusive MAMP in plants. *Fungal Genet. Biol.* **90**, 53–60.
- Fliegmann, J., Mithöfer, A., Wanner, G. and Ebel, J. (2004) An ancient enzyme domain hidden in the putative beta-glucan elicitor receptor of soybean may play an active part in the perception of pathogen-associated molecular patterns during broad host resistance. *J. Biol. Chem.* **279**, 1132–1140.
- Gauthier, A., Trouvelot, S., Kelloniemi, J. *et al.* (2014) The sulfated laminarin triggers a stress transcriptome before priming the SA- and ROS-dependent defenses during grapevine's induced resistance against *Plasmopara viticola*. *PLoS ONE*, **9**, e88145.
- Gimenez-Ibanez, S., Hann, D.R., Ntoukakis, V., Petutschnig, E., Lipka, V. and Rathjen, J.P. (2009) AvrPtoB targets the LysM receptor kinase CERK1 to promote bacterial virulence on plants. *Curr. Biol.* **19**, 423–429.



- Gust, A.A. (2015) Peptidoglycan perception in plants. *PLoS Pathog.* **11**, e1005275.
- Hayafune, M., Berisio, R., Marchetti, R. *et al.* (2014) Chitin-induced activation of immune signaling by the rice receptor CEBiP relies on a unique sandwich-type dimerization. *Proc. Natl Acad. Sci. USA*, **111**, E404–E413.
- Heese, A., Hann, D.R., Gimenez-Ibanez, S., Jones, A.M., He, K., Li, J., Schroeder, J.I., Peck, S.C. and Rathjen, J.P. (2007) The receptor-like kinase SERK3/BAK1 is a central regulator of innate immunity in plants. *Proc. Natl Acad. Sci. USA*, **104**, 12 217–12 222.
- Hückelhoven, R. (2007) Cell wall-associated mechanisms of disease resistance and susceptibility. *Annu. Rev. Phytopathol.* **45**, 101–127.
- Hückelhoven, R. (2014) The effective papilla hypothesis. *New Phytol.* **204**, 438–440.
- Kanagawa, M., Satoh, T., Ikeda, A., Adachi, Y., Ohno, N. and Yamaguchi, Y. (2011) Structural insights into recognition of triple-helical  $\beta$ -glucans by an insect fungal receptor. *J. Biol. Chem.* **286**, 29 158–29 165.
- Kanzaki, H., Saitoh, H., Ito, A., Fujisawa, S., Kamoun, S., Katou, S., Yoshioaka, H. and Terachi, R. (2003) Cytosolic HSP90 and HSP70 are essential components of INF1-mediated hypersensitive response and non-host resistance to *Pseudomonas cichorii* in *Nicotiana benthamiana*. *Mol. Plant Pathol.* **4**, 383–391.
- Klarzynski, O., Plesse, B., Joubert, J.M., Yvin, J.C., Kopp, M., Kloareg, B. and Fritig, B. (2000) Linear  $\beta$ -1,3 glucans are elicitors of defense responses in tobacco. *Plant Physiol.* **124**, 1027–1038.
- Koch, M., Bishop, J. and Mitchell-Olds, T. (1999) Molecular systematics and evolution of Arabidopsis and Arabis. *Plant Biol.* **11**, 529–537.
- Kohorn, B.D., Johansen, S., Shishido, A., Todorova, T., Martínez, R., Defeo, E. and Obregon, P. (2009) Pectin activation of MAP kinase and gene expression is WAK2 dependent. *Plant J.* **60**, 974–982.
- Kombrink, A., Sánchez-Vallet, A. and Thomma, B.P.H.J. (2011) The role of chitin detection in plant–pathogen interactions. *Microbes Infect.* **13**, 1168–1176.
- Kouzai, Y., Mochizuki, S., Nakajima, K. *et al.* (2014) Targeted gene disruption of OsCERK1 reveals its indispensable role in chitin perception and involvement in the peptidoglycan response and immunity in rice. *Mol. Plant Microbe Interact.* **27**, 975–982.
- Kulicke, W.M., Lettau, A.I. and Thielking, H. (1997) Correlation between immunological activity, molar mass, and molecular structure of different (1 $\rightarrow$ 3)- $\beta$ -D-glucans. *Carbohydr. Res.* **297**, 135–143.
- Lahrmann, U., Strehmel, N., Langen, G., Frerigmann, H., Leson, L., Ding, Y., Scheel, D., Herklotz, S., Hilbert, M. and Zuccaro, A. (2015) Mutualistic root endophytism is not associated with the reduction of saprotrophic traits and requires a noncompromised plant innate immunity. *New Phytol.* **207**, 841–857.
- Latgé, J.P. (2007) The cell wall: a carbohydrate armour for the fungal cell. *Mol. Microbiol.* **66**, 279–290.
- Latgé, J.P. and Calderone, R. (2006) The fungal cell wall. In *The Mycota I. Growth, Differentiation and Sexuality* (Kües, U. and Fischer, R. eds). Heidelberg, Germany: Springer, pp. 73–104.
- Lee, J., Eschen-Lippold, L., Lassowskat, I., Bottcher, C. and Scheel, D. (2015) Cellular reprogramming through mitogen-activated protein kinases. *Front. Plant Sci.* **6**, 940.
- Limpens, E., van Zeijl, A. and Geurts, R. (2015) Lipochitoooligosaccharides modulate plant host immunity to enable endosymbioses. *Annu. Rev. Phytopathol.* **53**, 311–334.
- Liu, Y., Schiff, M., Marathe, R. and Dinesh-Kumar, S.P. (2002) Tobacco Rar1, EDS1 and NPR1/NIM1 like genes are required for N-mediated resistance to tobacco mosaic virus. *Plant J.* **30**, 415–429.
- Liu, B., Li, J.F., Ao, Y. *et al.* (2012a) Lysin motif-containing proteins LYP4 and LYP6 play dual roles in peptidoglycan and chitin perception in rice innate immunity. *Plant Cell*, **24**, 3406–3419.
- Liu, T., Liu, Z., Song, C. *et al.* (2012b) Chitin-induced dimerization activates a plant immune receptor. *Science*, **336**, 1160–1164.
- Ma, X., Xu, G., He, P. and Shan, L. (2016) SERKING co-receptors for receptors. *Trends Plant Sci.* **21**, 1017–1033.
- Macho, A.P. and Zipfel, C. (2015) Targeting of plant pattern recognition receptor-triggered immunity by bacterial type-III secretion system effectors. *Curr. Opin. Microbiol.* **23**, 14–22.
- Mélida, H., Sandoval-Sierra, J.V., Dieguez-Urbeondo, J. and Bulone, V. (2013) Analyses of extracellular carbohydrates in oomycetes unveil the existence of three different cell wall types. *Eukaryot. Cell*, **12**, 194–203.
- Mélida, H., Sopena-Torres, S., Bacete, L., Garrido-Arandia, M., Jordá, L., López, G., Muñoz-Barrios, A., Pacios, L.F. and Molina, A. (2018) Non-branched  $\beta$ -1,3-glucan oligosaccharides trigger immune responses in Arabidopsis. *Plant J.* **93**, 34–49.
- Ménard, R., Alban, S., de Ruffray, P., Jamois, F., Franz, G., Fritig, B., Yvin, J.C. and Kauffmann, S. (2004)  $\beta$ -1,3 glucan sulfate, but not  $\beta$ -1,3 glucan, induces the salicylic acid signaling pathway in tobacco and Arabidopsis. *Plant Cell*, **16**, 3020–3032.
- Meng, X. and Zhang, S. (2013) MAPK cascades in plant disease resistance signaling. *Annu. Rev. Phytopathol.* **51**, 245–266.
- Mine, A., Berens, M.L., Nobori, T., Anver, S., Fukumoto, K., Winkelmüller, T.M., Takeda, A., Becker, D. and Tsuda, K. (2017) Pathogen exploitation of an abscisic acid- and jasmonate-inducible MAPK phosphatase and its interception by Arabidopsis immunity. *Proc. Natl Acad. Sci. USA*, **114**, 7456–7461.
- Mishima, Y., Quintin, J., Amanianda, V. *et al.* (2009) The N-terminal domain of Drosophila Gram-negative binding protein 3 (GNBP3) defines a novel family of fungal pattern recognition receptors. *J. Biol. Chem.* **284**, 28 687–28 697.
- Mithöfer, A., Lottspeich, F. and Ebel, J. (1996) One-step purification of the  $\beta$ -glucan elicitor-binding protein from soybean (*Glycine max* L.) roots and characterization of an anti-peptide antiserum. *FEBS Lett.* **381**, 203–207.
- Mithöfer, A., Fliegmann, J., Neuhaus-Url, G., Schwarz, H. and Ebel, J. (2000) The hepta- $\beta$ -glucoside elicitor-binding proteins from legumes represent a putative receptor family. *Biol. Chem.* **381**, 705–713.
- Miya, A., Albert, P., Shinya, T., Desaki, Y., Ichimura, K., Shirasu, K., Narusaka, Y., Kawakami, N., Kaku, H. and Shibuya, N. (2007) CERK1, a LysM receptor kinase, is essential for chitin elicitor signaling in Arabidopsis. *Proc. Natl Acad. Sci. USA*, **104**, 19 613–19 618.
- Monaghan, J. and Zipfel, C. (2012) Plant pattern recognition receptor complexes at the plasma membrane. *Curr. Opin. Plant Biol.* **15**, 349–357.
- Nelson, T.E. and Lewis, B.A. (1974) Separation and characterization of the soluble and insoluble components of insoluble laminaran. *Carbohydr. Res.* **33**, 63–74.
- Nizam, S., Qiang, X., Wawra, S., Nostadt, R., Getzke, F., Schwanke, F., Dreyer, I., Langen, G. and Zuccaro, A. (2019) Serendipita indica E5'NT modulates extracellular nucleotide levels in the plant apoplast and affects fungal colonization. *EMBO Rep.* **20**, pii: e47430.
- Okobira, T., Miyoshi, K., Uezu, K., Sakurai, K. and Shinkai, S. (2008) Molecular dynamics studies of side chain effect on the  $\beta$ -1,3-D-glucan triple helix in aqueous solution. *Biomacromolecules*, **9**, 783–788.
- Oldroyd, G.E. (2013) Speak, friend, and enter: signalling systems that promote beneficial symbiotic associations in plants. *Nat. Rev. Microbiol.* **11**, 252–263.
- Pereyra, M.T., Prieto, A., Bernabé, M. and Leal, J.A. (2003) Studies of new polysaccharides from *Lasallia pustulata* (L.) Hoffm. *Lichenologist*, **35**, 177–185.
- Petutschnig, E.K., Jones, A.M., Serazetdinova, L., Lipka, U. and Lipka, V. (2010) The lysin motif receptor-like kinase (LysM-RLK) CERK1 is a major chitin-binding protein in *Arabidopsis thaliana* and subject to chitin-induced phosphorylation. *J. Biol. Chem.* **285**, 28 902–28 911.
- Pluinage, B., Fillo, A., Massel, P. and Boraston, A.B. (2017) Structural analysis of a family 81 glycoside hydrolase implicates its recognition of  $\beta$ -1,3-glucan quaternary structure. *Structure*, **25**, 1348–1359. e1343.
- Postma, J., Liebrand, T.W., Bi, G., Evrard, A., Bye, R.R., Mbengue, M., Kuhn, H., Joosten, M.H. and Robatzek, S. (2016) Avr4 promotes Cf-4 receptor-like protein association with the BAK1/SERK3 receptor-like kinase to initiate receptor endocytosis and plant immunity. *New Phytol.* **210**, 627–642.
- Rae, A.L., Harris, P.J., Bacic, A. and Clarke, A.E. (1985) Composition of the cell walls of *Nicotiana glauca* Link et Otto pollen tubes. *Planta*, **166**, 128–133.
- Ranf, S., Eschen-Lippold, L., Pecher, P., Lee, J. and Scheel, D. (2011) Interplay between calcium signalling and early signalling elements during defence responses to microbe- or damage-associated molecular patterns. *Plant J.* **68**, 100–113.
- Robatzek, S., Chinchilla, D. and Boller, T. (2006) Ligand-induced endocytosis of the pattern recognition receptor FLS2 in Arabidopsis. *Genes Dev.* **20**, 537–542.
- Romani, L. (2011) Immunity to fungal infections. *Nat. Rev. Immunol.* **11**, 275–288.

1156 Alan Wanke *et al.*

- Rovenich, H., Zuccaro, A. and Thomma, B.P.H.J. (2016) Convergent evolution of filamentous microbes towards evasion of glycan-triggered immunity. *New Phytol.* **212**, 896–901.
- Salomon, S. and Robatzek, S. (2006) Induced endocytosis of the receptor kinase FLS2. *Plant Signal. Behav.* **1**, 293–295.
- Sánchez-Vallet, A., Mesters, J.R. and Thomma, B.P.H.J. (2015) The battle for chitin recognition in plant-microbe interactions. *FEMS Microbiol. Rev.* **39**, 171–183.
- Saur, I.M., Kadota, Y., Sklenar, J., Holton, N.J., Smakowska, E., Belkadir, Y., Zipfel, C. and Rathjen, J.P. (2016) NbCSPR underlies age-dependent immune responses to bacterial cold shock protein in *Nicotiana benthamiana*. *Proc. Natl Acad. Sci. USA*, **113**, 3389–3394.
- Segonzac, C., Feike, D., Gimenez-Ibanez, S., Hann, D.R., Zipfel, C. and Rathjen, J.P. (2011) Hierarchy and roles of pathogen-associated molecular pattern-induced responses in *Nicotiana benthamiana*. *Plant Physiol.* **156**, 687–699.
- Senthil-Kumar, M. and Mysore, K.S. (2014) Tobacco rattle virus-based virus-induced gene silencing in *Nicotiana benthamiana*. *Nat. Protoc.* **9**, 1549–1562.
- Seybold, H., Trempel, F., Ranf, S., Scheel, D., Romeis, T. and Lee, J. (2014) Ca<sup>2+</sup> signalling in plant immune response: from pattern recognition receptors to Ca<sup>2+</sup> decoding mechanisms. *New Phytol.* **204**, 782–790.
- Sharp, J.K., McNeil, M. and Albersheim, P. (1984a) The primary structures of one elicitor-active and seven elicitor-inactive hexa(beta-D-glucopyranosyl)-D-glucitols isolated from the mycelial walls of *Phytophthora megasperma* f. sp. *glycinea*. *J. Biol. Chem.* **259**, 11 321–11 336.
- Sharp, J.K., Valent, B. and Albersheim, P. (1984b) Purification and partial characterization of a beta-glucan fragment that elicits phytoalexin accumulation in soybean. *J. Biol. Chem.* **259**, 11 312–11 320.
- Shen, Q.H., Saijo, Y., Mauch, S., Biskup, C., Bieri, S., Keller, B., Seki, H., Ulker, B., Somssich, I.E. and Schulze-Lefert, P. (2007) Nuclear activity of MLA immune receptors links isolate-specific and basal disease-resistance responses. *Science*, **315**, 1098–1103.
- Shimizu, T., Nakano, T., Takamizawa, D. *et al.* (2010) Two LysM receptor molecules, CEBiP and OsCERK1, cooperatively regulate chitin elicitor signaling in rice. *Plant J.* **64**, 204–214.
- Smith, A.J., Graves, B., Child, R., Rice, P.J., Ma, Z., Lowman, D.W., Ensley, H.E., Ryter, K.T., Evans, J.T. and Williams, D.L. (2018) Immunoregulatory activity of the natural product laminarin varies widely as a result of its physical properties. *J. Immunol.* **200**, 788–799.
- Sørensen, I., Pettolino, F.A., Wilson, S.M., Doblin, M.S., Johansen, B., Bacic, A. and Willats, W.G. (2008) Mixed-linkage (1→3), (1→4)-beta-D-glucan is not unique to the Poales and is an abundant component of Equisetum arvense cell walls. *Plant J.* **54**, 510–521.
- Spallek, T., Beck, M., Ben Khaled, S., Salomon, S., Bourdais, G., Schellmann, S. and Robatzek, S. (2013) ESCRT-I mediates FLS2 endosomal sorting and plant immunity. *PLoS Genet.* **9**, e1004035.
- Takahasi, K., Ochiai, M., Horiuchi, M., Kumeta, H., Ogura, K., Ashida, M. and Inagaki, F. (2009) Solution structure of the silkworm betaGRP/GNBP3 N-terminal domain reveals the mechanism for beta-1,3-glucan-specific recognition. *Proc. Natl Acad. Sci. USA*, **106**, 11 679–11 684.
- Trethewey, J.A., Campbell, L.M. and Harris, P.J. (2005) (1→3), (1→4)-beta-D-glucans in the cell walls of the Poales (*sensu lato*): an immunogold labeling study using a monoclonal antibody. *Am. J. Bot.* **92**, 1660–1674.
- Umemoto, N., Kakitani, M., Iwamatsu, A., Yoshikawa, M., Yamaoka, N. and Ishida, I. (1997) The structure and function of a soybean beta-glucan-elicitor-binding protein. *Proc. Natl Acad. Sci. USA*, **94**, 1029–1034.
- Unfried, F., Becker, S., Robb, C.S. *et al.* (2018) Adaptive mechanisms that provide competitive advantages to marine bacteroidetes during microalgal blooms. *ISME J.* **12**, 2894–2906.
- Wawra, S., Fesel, P., Widmer, H. *et al.* (2016) The fungal-specific beta-glucan-binding lectin FGB1 alters cell-wall composition and suppresses glucan-triggered immunity in plants. *Nat. Commun.* **7**, 13 188.
- Wawra, S., Fesel, P., Widmer, H., Neumann, U., Lahrmann, U., Becker, S., Hehemann, J.H., Langen, G. and Zuccaro, A. (2019) FGB1 and WSC3 are *in planta*-induced beta-glucan-binding fungal lectins with different functions. *New Phytol.* **222**, 1493–1506.
- Weishaupt, M.W., Hahn, H.S., Geissner, A. and Seeberger, P.H. (2017) Automated glycan assembly of branched beta-(1,3)-glucans to identify antibody epitopes. *Chem. Commun. (Camb.)* **53**, 3591–3594.
- Willmann, R., Lajunen, H.M., Erbs, G. *et al.* (2011) Arabidopsis lysin-motif proteins LYM1 LYM3 CERK1 mediate bacterial peptidoglycan sensing and immunity to bacterial infection. *Proc. Natl Acad. Sci. USA*, **108**, 19 824–19 829.
- Xu, J., Xie, J., Yan, C., Zou, X., Ren, D. and Zhang, S. (2014) A chemical genetic approach demonstrates that MPK3/MPK6 activation and NADPH oxidase-mediated oxidative burst are two independent signaling events in plant immunity. *Plant J.* **77**, 222–234.
- Yamaguchi, T., Yamada, A., Hong, N., Ogawa, T., Ishii, T. and Shibuya, N. (2000) Differences in the recognition of glucan elicitor signals between rice and soybean: beta-glucan fragments from the rice blast disease fungus *Pyricularia oryzae* that elicit phytoalexin biosynthesis in suspension-cultured rice cells. *Plant Cell*, **12**, 817–826.
- Yoshikawa, M., Keen, N.T. and Wang, M.C. (1983) A receptor on soybean membranes for a fungal elicitor of phytoalexin accumulation. *Plant Physiol.* **73**, 497–506.
- Young, S.H., Dong, W.J. and Jacobs, R.R. (2000) Observation of a partially opened triple-helix conformation in 1→3-beta-glucan by fluorescence resonance energy transfer spectroscopy. *J. Biol. Chem.* **275**, 11 874–11 879.
- Zipfel, C. and Oldroyd, G.E. (2017) Plant signalling in symbiosis and immunity. *Nature*, **543**, 328–336.



## Chapter 3: *Supplementary Material*

### **Plant species-specific recognition of long and short $\beta$ -1,3-linked glucans is mediated by different receptor systems**

Alan Wanke<sup>1,2,#</sup>, Hanna Rovenich<sup>1,3,#</sup>, Florian Schwanke<sup>1</sup>, Stefanie Velte<sup>1</sup>, Stefan Becker<sup>4,5</sup>, Jan-Hendrik Hehemann<sup>4,5</sup>, Stephan Wawra<sup>1,3</sup>, Alga Zuccaro<sup>1,3</sup>

<sup>1</sup> University of Cologne, Institute for Plant Sciences, 60679 Cologne, Germany

<sup>2</sup> Max Planck Institute for Plant Breeding Research, 50829 Cologne, Germany

<sup>3</sup> University of Cologne, Cluster of Excellence on Plant Sciences (CEPLAS), 50679 Cologne, Germany

<sup>4</sup> Center for Marine Environmental Sciences, University of Bremen, MARUM, 28359 Bremen, Germany

<sup>5</sup> Max Planck Institute for Marine Microbiology, 28359 Bremen, Germany

# equal contribution

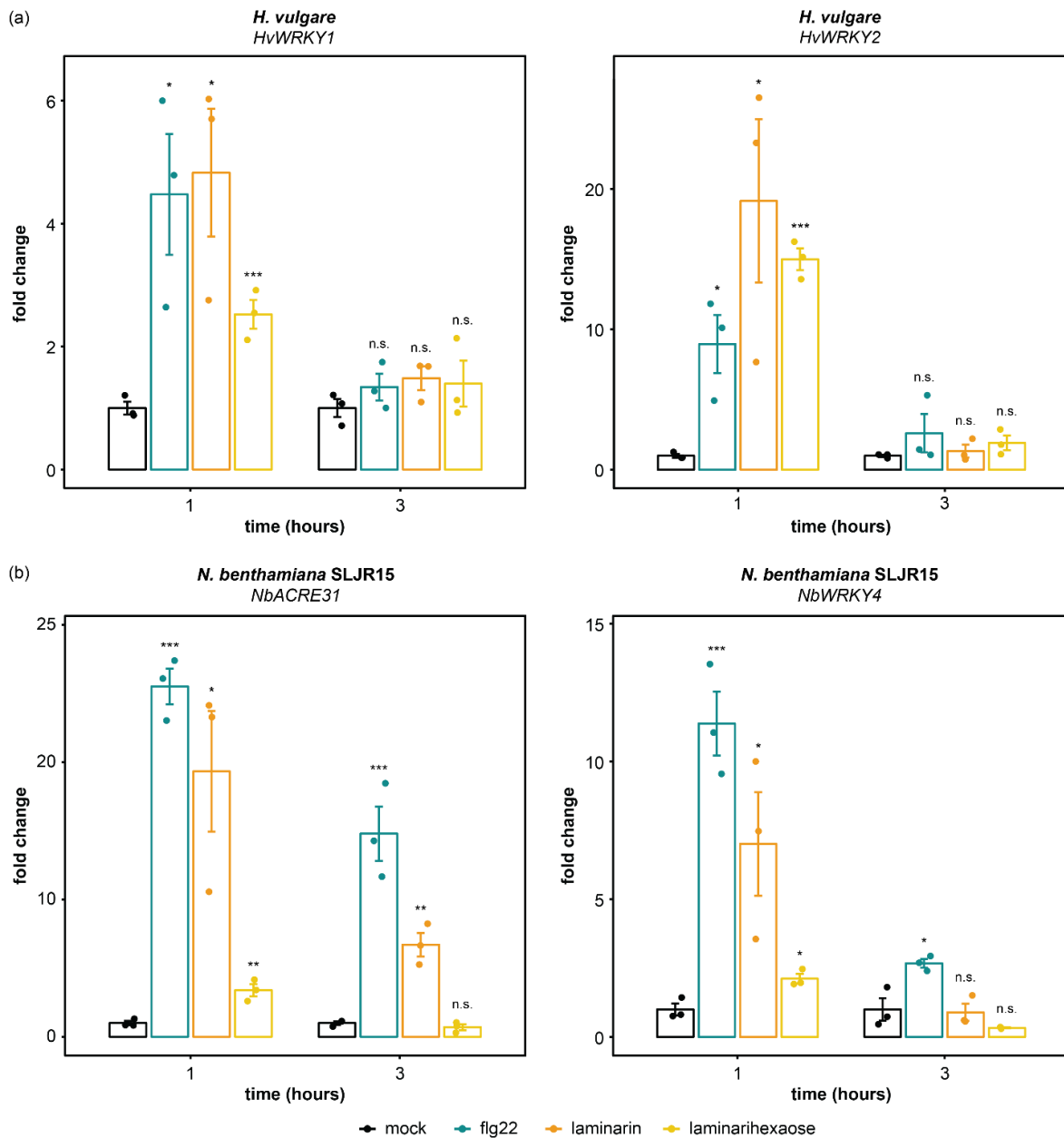


**Figure S1  $\beta$ -glucan triggered defense gene expression in *H. vulgare* and *N. benthamiana*.** Nine leaf discs of two barley (*H. vulgare*) (a) and *N. benthamiana* SLJR15 (b) plants were treated with water (mock), 100 nM flg22, or 250  $\mu$ M laminarihexaose. The final concentration of laminarin used to treat barley and *N. benthamiana* was 4 mg/mL (1 mM) and 2 mg/mL (0.5 mM), respectively. One and three hours after treatment, three samples were collected for each treatment. Elicitor-triggered changes in the expression of *HvWRKY1* (upper left), *HvWRKY2* (upper right), *NbACRE31* (lower left), and *NbWRKY4* (lower right) were determined by quantitative RT-PCR. Primers targeting *HvUBI* and *NbEF1 $\alpha$*  were used to calculate relative expression levels for barley and *N. benthamiana*, respectively. All expression levels were then normalized to the mock-treated controls at the respective time points. Significant differences to mock treatment were determined *via* two-tailed t-test analysis (\* =  $p < 0.05$ ; \*\* =  $p < 0.01$ ; \*\*\* =  $p < 0.001$ ; n.s. = not significant). Experiments were performed twice with similar results.

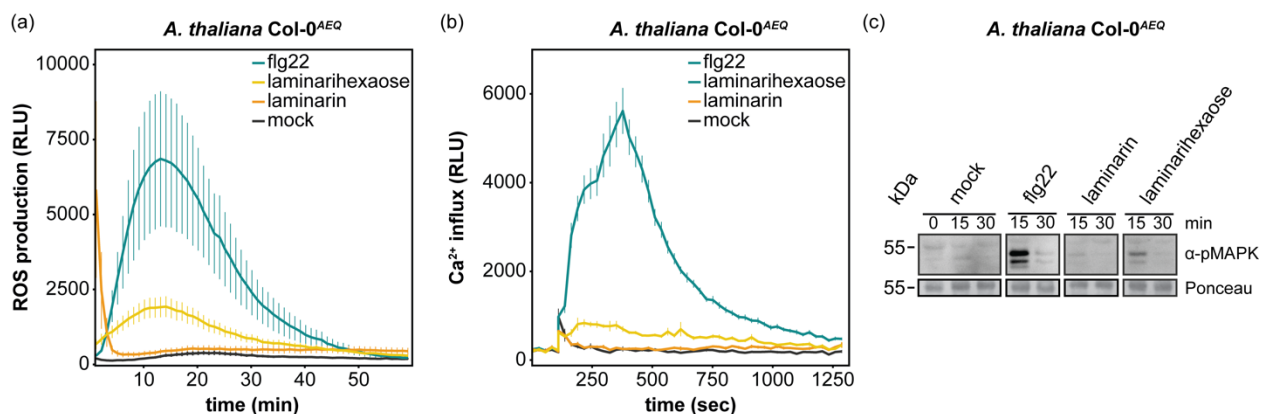


**Figure S2 Laminarihexaose but not laminarin activates immune responses in *A. thaliana* Col-0 seedlings.** Twelve-day-old *A. thaliana* Col-0<sup>AEQ</sup> seedlings were suspended in water or 10  $\mu$ M coelenterazine (for Ca<sup>2+</sup> influx assays) for overnight incubation in the dark. **(a)** Production of reactive oxygen species (ROS) was measured using luminol-based chemiluminescence for 60 min after treatment with 100 nM flg22, 4 mg/mL laminarin (1 mM) and 250  $\mu$ M laminarihexaose. Water (mock) served as negative control. ROS response intensity was measured as sum of photon counts in relative luminescence units (RLU). Values represent means  $\pm$  SE of 24 seedlings. **(b)** Elevations of cytosolic calcium concentrations (Ca<sup>2+</sup> influx) were measured as relative luminescence units following elicitor treatment of *A. thaliana* Col-0<sup>AEQ</sup> seedlings. Remaining aequorin was discharged by adding CaCl<sub>2</sub>. Discharge kinetics were integrated and used to normalize Ca<sup>2+</sup> kinetics in response to elicitor treatment. Values represent means  $\pm$  SE of 24 seedlings. **(c)** MAPK activation was detected using phospho-p44/42 MAPK (ERK1/2) antibody following elicitor treatment at indicated time points. Membranes were stained with PonceauS after Western blotting to confirm equal loading. All experiments were performed twice with similar results.

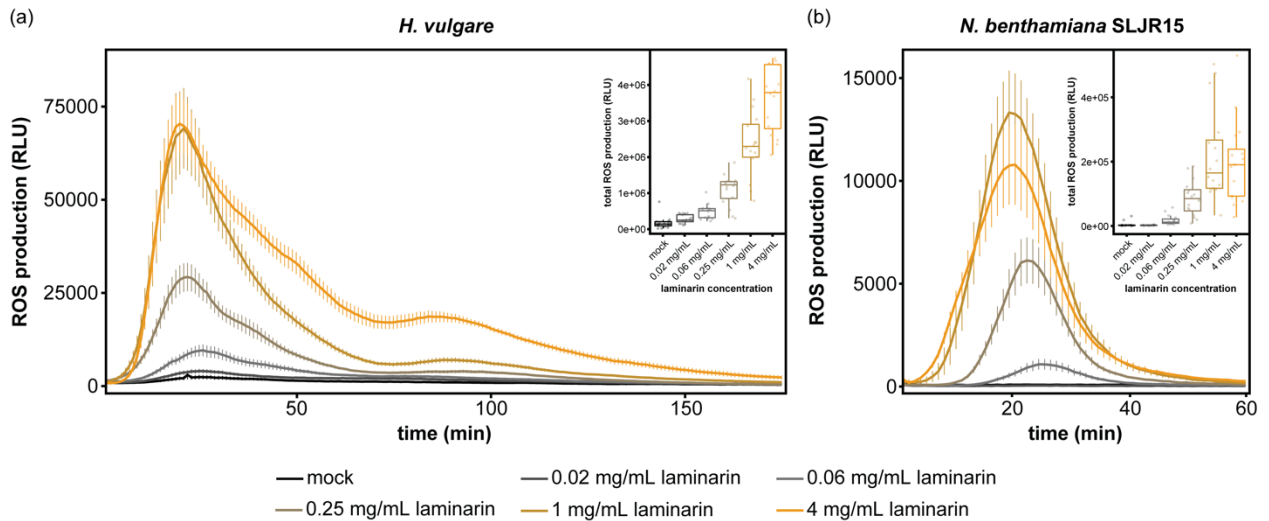


**Figure S3 Laminarin-triggered ROS production is concentration-dependent.** Leaf discs were collected from two to three-week-old barley (*H. vulgare*) and three- to four-week-old *N. benthamiana* SLJR15 plants. Laminarin was dissolved in sterile MilliQ water and a dilution series was aliquoted from a single stock. The generation of reactive oxygen species (ROS) was measured using a luminol-based chemiluminescence assay for 180 min and 60 min following the treatment of barley (a) and *N. benthamiana* SLJR15 (b) with laminarin at indicated concentrations. Water (mock) served as negative control. ROS response intensity was measured as sum of photon counts in relative luminescence units (RLU). Values represent means  $\pm$  SE of 16 leaf discs from four plants per treatment. Experiments were performed three times with similar results.

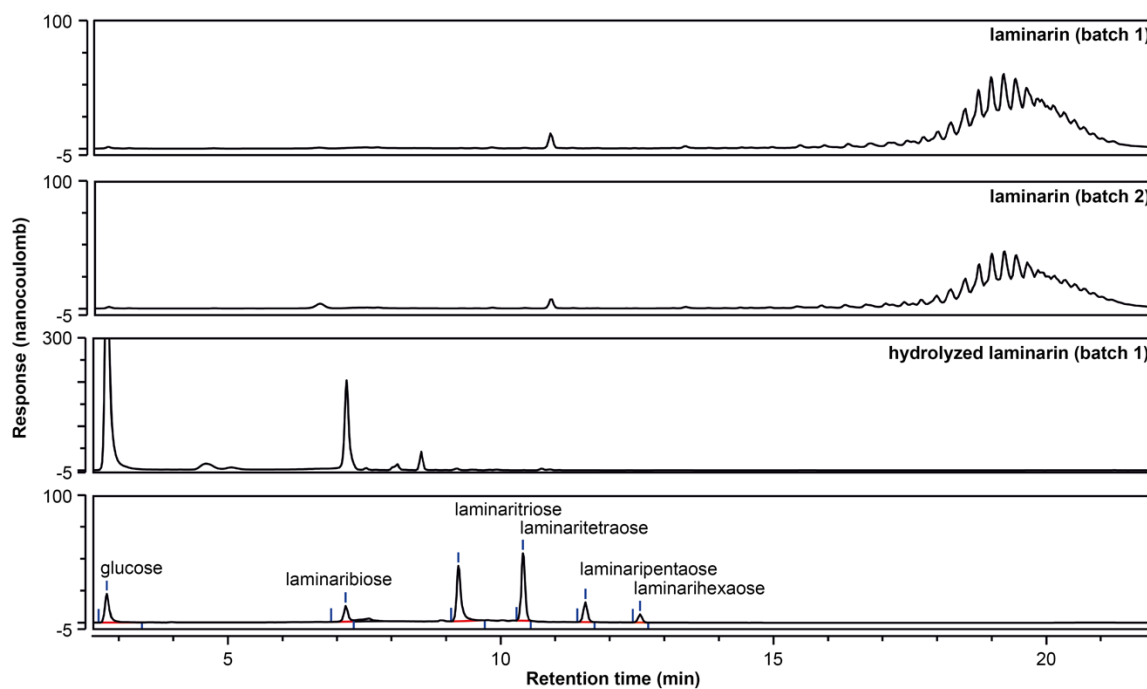


**Figure S4 Qualitative characterization of different laminarin preparations.** The glucan composition of two different laminarin batches and the enzymatically hydrolyzed laminarin was analyzed by HPAEC-PAD. Both laminarins were purchased from SIGMA (Lot # SLBP4829V). Hydrolyzed samples were incubated over night at 37°C with a glucanase mix consisting of an endo- $\beta$ -1,3-glucanase from *Helix pomatia* (Sigma), an exo- $\beta$ -1,3-glucanase from *Trichoderma virens* (Megazyme) and an endo- $\beta$ -1,3-glucanase from *H. vulgare* (each 0.1 mg/mL). Reactions were performed in water.

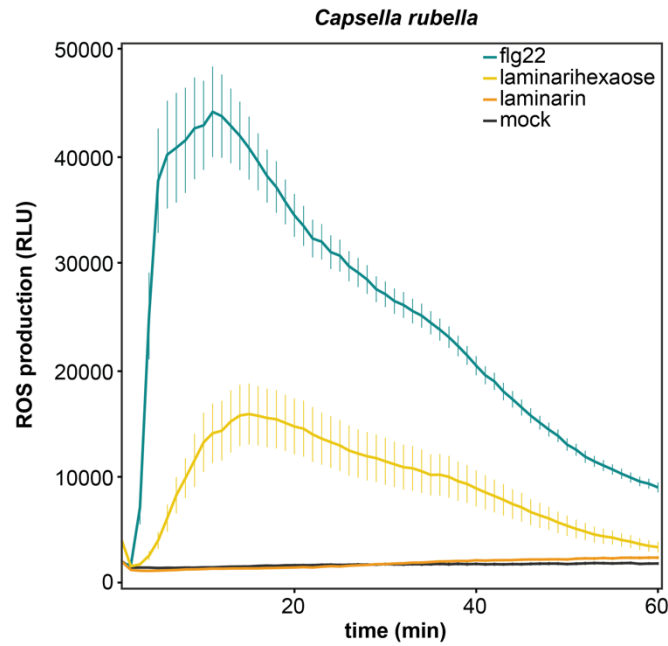


**Figure S5 Laminarihexaose triggers ROS production in *C. rubella*.** Leaf discs were collected from three-week-old *C. rubella*. Production of reactive oxygen species (ROS) was measured using luminol-based chemiluminescence for 60 min after treatment of leaf discs with 100 nM flg22, 4 mg/mL (1 mM) laminarin and 250  $\mu$ M laminarihexaose. Water (mock) served as negative control. ROS response intensity was measured as sum of photon counts in relative luminescence units (RLU). Values represent means  $\pm$  SE of 16 leaf discs from eight different plants. Experiments were performed twice with similar results.

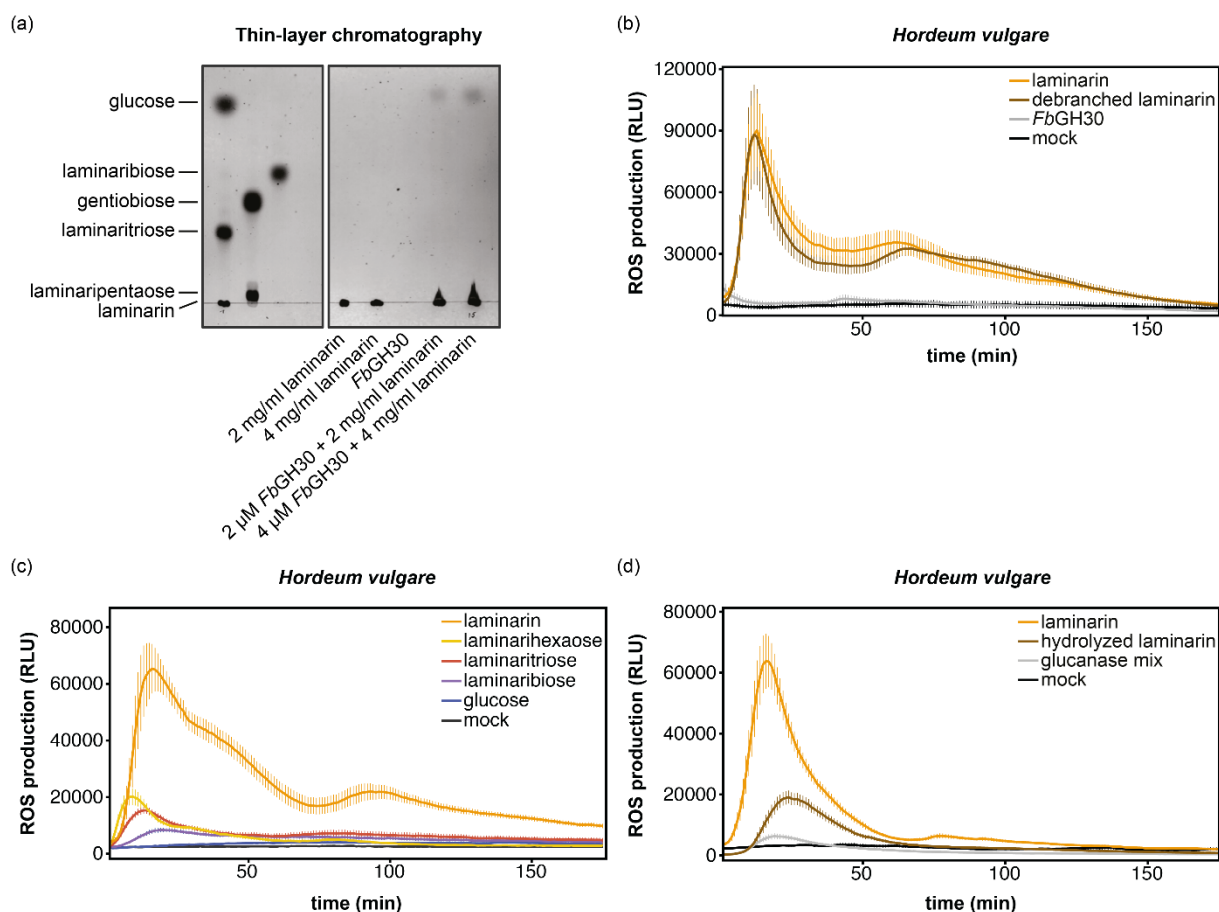


**Figure S6** *H. vulgare* produces ROS upon elicitation with short and long, unbranched  $\beta$ -glucans. Debranched laminarin was obtained as described previously (Becker *et al.*, 2017, Unfried *et al.*, 2018). (a) Thin-layer chromatography showing products of overnight laminarin hydrolysis by GH30 at two different concentrations. Glucose, laminaribiose, gentiobiose, laminaritriose, laminaripentaose and laminarin (each 1 mg/mL) were spotted as standards. Experiments were performed three times with similar results. (b) Production of reactive oxygen species (ROS) was measured using luminol-based chemiluminescence for 180 min after treatment of leaf discs with 4  $\mu$ M FbGH30 enzyme, 4 mg/mL laminarin and 4 mg/mL debranched laminarin. Water (mock) served as negative control. Values represent means  $\pm$  SE of 24 leaf discs from eight different plants. ROS response intensity was measured in relative luminescence units (RLU). (c) In order to analyze ROS production triggered by short and long glucans in barley, leaf discs were treated with glucose, laminaribiose, laminaritriose, laminarihexaose (each 250  $\mu$ M), laminarin (4 mg/mL, 1mM) and water (mock). Values represent means  $\pm$  SE of 16 leaf discs from four different plants. Experiments were performed three times with similar results. (d) Laminarin was hydrolyzed using an enzyme mix consisting of three commercially available exo- and endoglucanases. Both treated and untreated laminarin were tested on ROS production in barley leaf discs. Water and the crude enzyme mix (glucanase mix) were used as controls. Values represent means  $\pm$  SE of 16 leaf discs from four different plants.



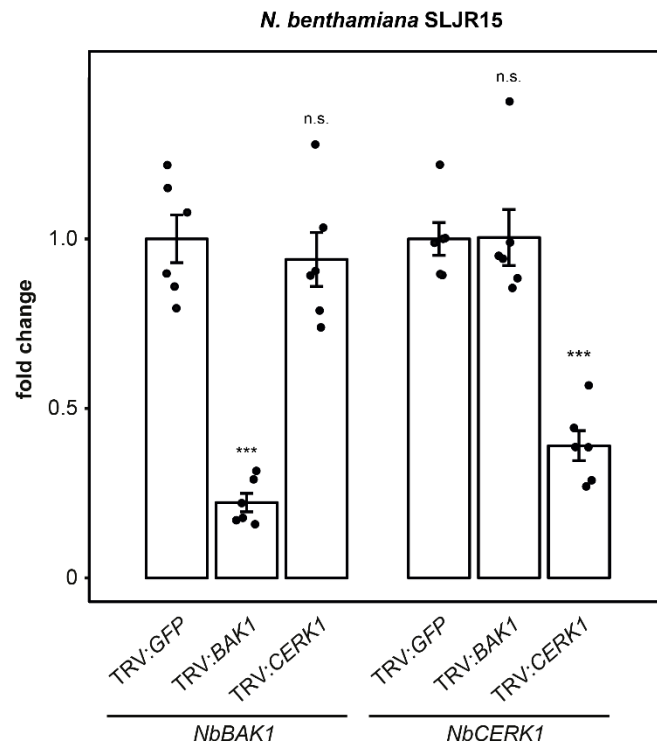


**Figure S7 Efficiency and specificity of *NbBAK1* and *NbCERK1* silencing in *N. benthamiana*.** Quantitative RT-PCR of *NbBAK1* and *NbCERK1* expression in *N. benthamiana* SLJR15 tissue treated with TRV:*NbBAK1* (TRV:*BAK1*), TRV:*NbCERK1* (TRV:*CERK1*) and TRV:*GFP*. Primers targeting *NbEF1 $\alpha$*  were used to calculate relative expression levels. All expression levels were then normalized to the *GFP*-silenced controls. Error bars indicate the standard error from six independent samples. Statistically significant differences between mRNA levels of gene targets compared to negative *GFP*-silenced controls were determined with a two-tailed t-test analysis (\*\*\*) =  $p < 0.001$ ; n.s. = not significant).

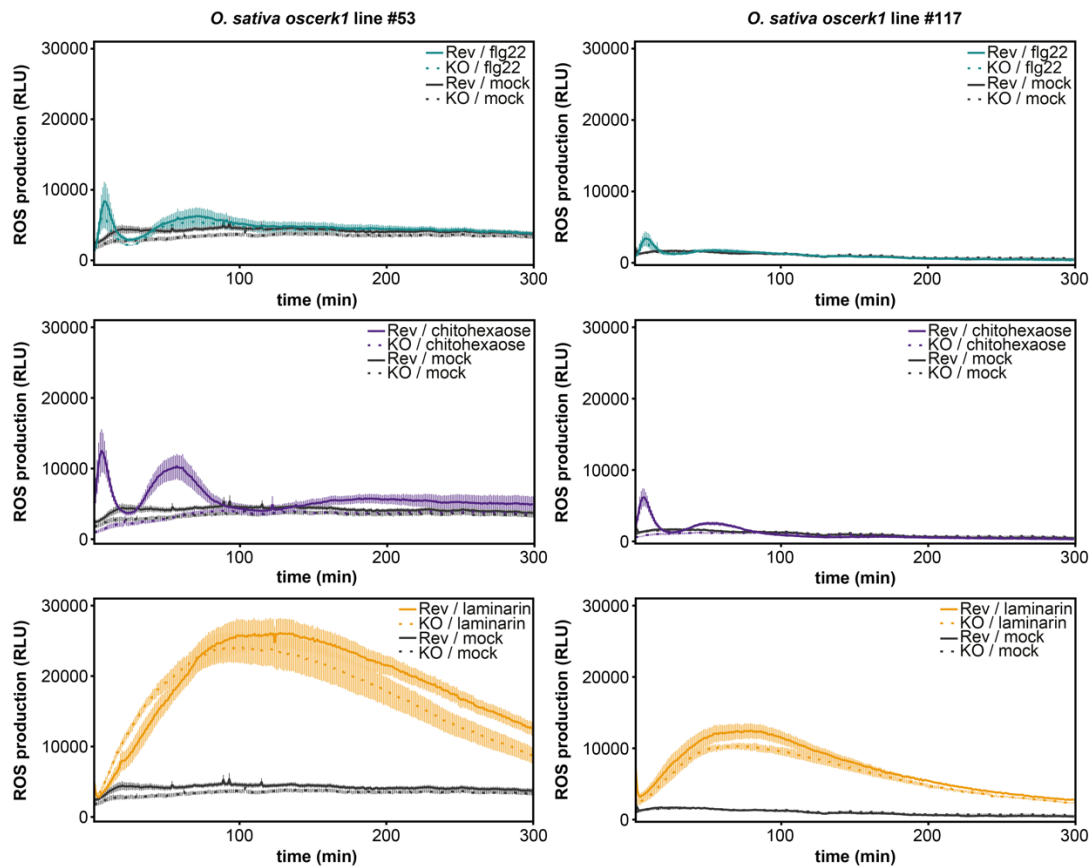


**Figure S8 *OsCERK1* is not involved in the recognition of laminarin in *O. sativa*.** Leaf discs were collected from six- to seven-week-old rice (*O. sativa*) plants of two segregated wild-type lines (Rev) #53 (left panels) and #117 (right panels) and corresponding *oscerk1* knockout lines (KO) (Kouzai *et al.*, 2014). Production of reactive oxygen species (ROS) was measured using luminol-based chemiluminescence for 300 min after treatment of leaf discs with 100 nM flg22, 10  $\mu$ M chitohexaose and 4 mg/mL (1 mM) laminarin. Water (mock) served as negative control. ROS response intensity was measured in relative luminescence units (RLU). Values represent means  $\pm$  SE of eight leaf discs from two different plants. Experiments were performed three times with similar results.

## REFERENCES

- Becker, S., Scheffel, A., Polz, M.F. and Hehemann, J.H. (2017) Accurate quantification of laminarin in marine organic matter with enzymes from marine microbes. *Appl Environ Microbiol*, 83, e03389-03316. DOI: 10.1128/AEM.03389-16.
- Kouzai, Y., Mochizuki, S., Nakajima, K., Desaki, Y., Hayafune, M., Miyazaki, H., Yokotani, N., Ozawa, K., Minami, E., Kaku, H., Shibuya, N. and Nishizawa, Y. (2014) Targeted gene disruption of OsCERK1 reveals its indispensable role in chitin perception and involvement in the peptidoglycan response and immunity in rice. *Mol Plant Microbe Interact*, 27, 975-982. DOI: 10.1094/MPMI-03-14-0068-R.
- Unfried, F., Becker, S., Robb, C.S., Hehemann, J.H., Markert, S., Heiden, S.E., Hinzke, T., Becher, D., Reintjes, G., Kruger, K., Avci, B., Kappelmann, L., Hahnke, R.L., Fischer, T., Harder, J., Teeling, H., Fuchs, B., Barbeyron, T., Amann, R.L. and Schweder, T. (2018) Adaptive mechanisms that provide competitive advantages to marine bacteroidetes during microalgal blooms. *ISME J*, 12, 2894-2906. DOI: 10.1038/s41396-018-0243-5.

Further supplementary data are available at *The Plant Journal* online.

**Table S1.** Primers used for gene expression analysis.

**Method S1.** Defense gene expression analysis and VIGS efficiency test.

**Method S2.** High-performance anion exchange chromatography with pulsed amperometric detection (HPAEC-PAD)

# Chapter 4

## **Fungi hijack a ubiquitous plant apoplastic endoglucanase to release a ROS scavenging $\beta$ -glucan decasaccharide to subvert immune responses**

Balakumaran Chandrasekar<sup>1,#</sup>, Alan Wanke<sup>1,2,#</sup>, Stephan Wawra<sup>1,#</sup>, Pia Saake<sup>1</sup>, Lisa Mahdi<sup>1</sup>, Nyasha Charura<sup>1</sup>, Miriam Neidert<sup>1</sup>, Gereon Poschmann<sup>3</sup>, Milena Malisic<sup>1</sup>, Meik Thiele<sup>1</sup>, Kai Stühler<sup>4</sup>, Murali Dama, Markus Pauly<sup>5</sup>, Alga Zuccaro<sup>1</sup>

<sup>1</sup> University of Cologne, Cluster of Excellence on Plant Sciences (CEPLAS), 50679 Cologne, Germany

<sup>2</sup> Max Planck Institute for Plant Breeding Research, 50829 Cologne, Germany

<sup>3</sup> Institute of Molecular Medicine, Proteome Research, University Hospital and Medical Faculty, Heinrich Heine University Düsseldorf, 40225 Düsseldorf, Germany

<sup>4</sup> Molecular Proteomics Laboratory, Biomedical Research Centre (BMFZ), Heinrich Heine University Düsseldorf, 40225 Düsseldorf, Germany

<sup>5</sup> Institute of Plant Cell Biology and Biotechnology, Heinrich Heine University Düsseldorf, 40225 Düsseldorf, Germany

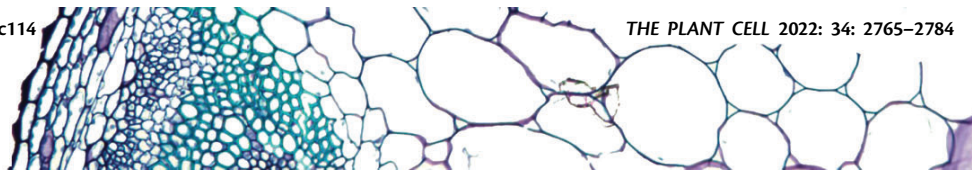
# equal contribution

This article was published in *The Plant Cell*, **72**: 15-35 (2021).  
DOI: <https://doi.org/10.1093/plcell/koac114>

<https://doi.org/10.1093/plcell/koac114>

THE PLANT CELL 2022: 34: 2765–2784

THE  
PLANT  
CELL



# Fungi hijack a ubiquitous plant apoplastic endoglucanase to release a ROS scavenging $\beta$ -glucan decasaccharide to subvert immune responses

Balakumaran Chandrasekar <sup>1,†</sup> Alan Wanke <sup>1,2</sup> Stephan Wawra <sup>1</sup> Pia Saake <sup>1</sup> Lisa Mahdi <sup>1,2</sup> Nyasha Charura <sup>1</sup> Miriam Neidert <sup>1</sup> Gereon Poschmann <sup>3</sup> Milena Malisic <sup>1</sup> Meik Thiele <sup>1</sup> Kai Stühler,<sup>4</sup> Murali Dama <sup>1</sup> Markus Pauly <sup>5</sup> and Alga Zuccaro <sup>1,\*†</sup>

- 1 Cluster of Excellence on Plant Sciences (CEPLAS), Institute for Plant Sciences, University of Cologne, 50679 Cologne, Germany
- 2 Max Planck Institute for Plant Breeding Research, 50829 Cologne, Germany
- 3 Institute of Molecular Medicine, Proteome Research, University Hospital and Medical Faculty, Heinrich-Heine University Düsseldorf, Universitätsstraße 1, 40225 Düsseldorf, Germany
- 4 Molecular Proteomics Laboratory, Biomedical Research Centre (BMFZ), Heinrich-Heine University Düsseldorf, Universitätsstraße 1, 40225 Düsseldorf, Germany
- 5 Institute of Plant Cell Biology and Biotechnology, Heinrich Heine University, 40225 Düsseldorf, Germany

\*Author for correspondence: [azuccaro@uni-koeln.de](mailto:azuccaro@uni-koeln.de)

These authors contributed equally (B.C., A.W. and S.W.).

†Present address: Department of Biological Sciences, Birla Institute of Technology & Science, Pilani (BITS Pilani), 333031, India.

‡Senior author.

B.C., A.W., S.W., and A.Z. conceived the study. S.W. established the protocols for the CW and EPS matrix extraction and performed the proteomics of EPS, CW, and culture filtrates together with G.P. and K.S. B.C. performed carbohydrate analytics (glycosyl linkage analysis of EPS and CW, MALDI-TOF, purification of  $\beta$ -GD for <sup>1</sup>H NMR, and ROS burst assay). A.W. performed DAB assays and gene expression analysis. A.W. and B.C. performed  $\beta$ -GD oxidation assays. A.W., S.W., P.S., M.N., M.M., M.T., N.C. performed the ROS burst assays, EPS and CW preparations, and enzymatic digestions. L.M. performed the colonization assays. M.D. contributed to the <sup>1</sup>H NMR result interpretation. M.P. directed and supervised the carbohydrate analytics. A.Z. supervised the project, designed the experiments, and wrote the paper with contribution of all the authors.

The author responsible for distribution of materials integral to the findings presented in this article in accordance with the policy described in the Instructions for Authors (<https://academic.oup.com/plcell>) is: Alga Zuccaro ([azuccaro@uni-koeln.de](mailto:azuccaro@uni-koeln.de)).

## Abstract

Plant pathogenic and beneficial fungi have evolved several strategies to evade immunity and cope with host-derived hydrolytic enzymes and oxidative stress in the apoplast, the extracellular space of plant tissues. Fungal hyphae are surrounded by an inner insoluble cell wall layer and an outer soluble extracellular polysaccharide (EPS) matrix. Here, we show by proteomics and glycomics that these two layers have distinct protein and carbohydrate signatures, and hence likely have different biological functions. The barley (*Hordeum vulgare*)  $\beta$ -1,3-endoglucanase *HvBGLUII*, which belongs to the widely distributed apoplastic glycoside hydrolase 17 family (GH17), releases a conserved  $\beta$ -1,3;1,6-glucan decasaccharide ( $\beta$ -GD) from the EPS matrices of fungi with different lifestyles and taxonomic positions. This low molecular weight  $\beta$ -GD does not activate plant immunity, is resilient to further enzymatic hydrolysis by  $\beta$ -1,3-endoglucanases due to the presence of three  $\beta$ -1,6-linked glucose branches and can scavenge reactive oxygen species. Exogenous application of  $\beta$ -GD leads to enhanced fungal colonization in barley, confirming its role in the fungal counter-defensive strategy to subvert host immunity. Our data highlight the hitherto undescribed capacity of this often-overlooked EPS matrix from plant-associated fungi to act as an outer protective barrier important for fungal accommodation within the hostile environment at the apoplastic plant–microbe interface.

## IN A NUTSHELL

**Background:** Plants secrete various hydrolytic enzymes into the apoplastic space to protect themselves against invading microbes. Some of these enzymes target the fungal cell wall polymer chitin. This enzymatic attack leads to the release of chitin oligomers, which can be perceived by the plant immune system, informing the plant to activate its defense machinery. However, chitin accounts for only a small part of most fungal cell walls. Recent studies have highlighted a largely uncharacterized,  $\beta$ -glucan-rich extracellular polysaccharide matrix (EPS) surrounding the cell wall of various plant-colonizing fungi.

**Question:** This EPS matrix is made of glucose and abundantly produced during colonization. As its secretion into the extracellular environment is costly for the fungus, we explored how this EPS matrix affects plant immunity and fungal colonization.

**Findings:** We demonstrated that EPS matrices from a symbiotic and pathogenic plant-colonizing fungus are distinct from the nonsoluble fungal cell walls with respect to their protein and carbohydrate composition. Enzymatic digests revealed that a secreted plant hydrolase from barley (*HvBGLUII*) acts on these EPS matrices and releases a highly branched  $\beta$ -glucan decasaccharide ( $\beta$ -GD) fragment. This fragment is not perceived by the plant immune system but instead detoxifies reactive oxygen species produced by the plant host as a defense mechanism and contributes to host colonization. We thus have shown that the outermost fungal EPS layer represents a protective shield against oxidative stress.

**Next steps:** The diversity of linkage types and branching patterns of  $\beta$ -glucans not only accounts for their different biochemical properties, but also makes them important messengers for the plant, potentially encoding specific information on the approaching fungal invader. Future studies should aim to identify other plant hydrolases and the elusive glucan receptors, to disentangle the contribution of  $\beta$ -glucans to the communication between plant hosts and fungi.

## Introduction

The fungal cell wall (CW) consists of repeatedly branched glycan polymers and proteins that adjust according to cell type, environmental conditions, and lifestyle phases (Geoghegan *et al.*, 2017; Gow *et al.*, 2017). The CW of animal pathogenic fungi is commonly surrounded by a soluble gel-like extracellular polysaccharide (EPS) matrix that can contain  $\beta$ -glucans, a heterogeneous group of glucose polymers (Gravelat *et al.*, 2013; Gow *et al.*, 2017; Kang *et al.*, 2018). Commonly, fungal  $\beta$ -glucans have a structure comprising a main chain of  $\beta$ -1,3 and/or  $\beta$ -1,4-glucopyranosyl units, decorated by side-chains with various branches and lengths (Han *et al.*, 2020). The immunomodulatory properties of  $\beta$ -glucans derived from animal pathogens have been long recognized (Goodridge *et al.*, 2009).  $\beta$ -glucans exhibit a broad spectrum of biological activities and have a dual role with respect to host immunity that depends on their chemophysical characteristics. On the one hand,  $\beta$ -glucans are important microbe-associated molecular patterns (MAMPs) that are detected upon fungal colonization to trigger host immune responses in both vertebrates and invertebrates (Brown and Gordon, 2005). On the other hand, certain soluble  $\beta$ -glucans do not possess high immunogenic properties but are implicated in antioxidant activities and scavenging of reactive oxygen species (ROS; Han *et al.*, 2020). Their immunological or antioxidant properties are rather complex

and could be influenced by modifications in their structural characteristics such as molecular weight, substitution pattern, solubility, polymer charge, and conformation in solution (Han *et al.*, 2020).

In plant–fungal interactions, carbohydrate metabolic processes mediated by carbohydrate-active enzymes (CAZymes) in the apoplast play a crucial role. Surface-exposed and accessible fungal polysaccharides are hydrolyzed by apoplastic CAZymes, such as chitinases and glucanases and the resulting oligosaccharides can act as elicitors to trigger a plant immune response known as pattern-triggered immunity (Silipo *et al.*, 2010; Rovenich *et al.*, 2016; Van Holle and Van Damme, 2018; Wanke *et al.*, 2020, 2021; Buscaill and van der Hoorn, 2021; Ngou *et al.*, 2021; Rebaque *et al.*, 2021; Yuan *et al.*, 2021). Recently, we described a soluble extracellular  $\beta$ -glucan matrix produced by endophytic fungi during root colonization of *Arabidopsis thaliana* (hereafter *Arabidopsis*) and *Hordeum vulgare* (hereafter barley; Wawra *et al.*, 2019). Little is known about the biochemical properties, composition, and function of this EPS matrix, but its detection in beneficial and pathogenic fungi strongly suggests a conserved role in counteracting environmental and immunological challenges during fungal growth and plant colonization (El Oirdi *et al.*, 2011; Mahdi *et al.*, 2021; Wanke *et al.*, 2021). It is therefore crucial to investigate the structure and function of these soluble  $\beta$ -glucans and the hydrolytic events



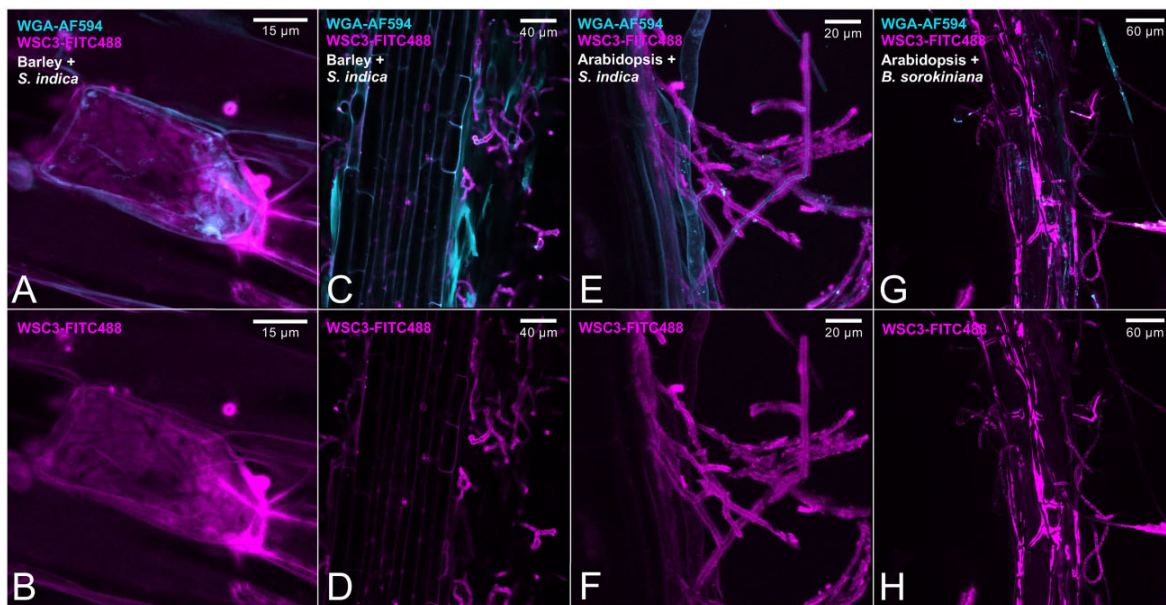


**Figure 1** Fungal EPS matrix revealed by the fluorescently labeled  $\beta$ -glucan binding lectin SiWSC3-His-FITC488 during root colonization. The  $\beta$ -glucan-binding SiWSC3-His and the chitin-binding WGA lectins were used as molecular probes to visualize the fungal EPS matrix and CW of *S. indica* and *B. sorokiniana*, respectively. Magenta pseudocolor corresponds to FITC488-labeled SiWSC3-His. Cyan pseudocolor corresponds to WGA-AF594. (A), (C), (E), and (G) are merged confocal microscopy images of SiWSC3-His-FITC488 and WGA-AF594. (B), (D), (F), and (H) display the EPS matrix of *S. indica* or *B. sorokiniana* stained by SiWSC3-His-FITC488 during colonization of Arabidopsis or barley roots. (A) and (B) show *S. indica* intracellular colonization of a barley root cell with abundant production of the  $\beta$ -glucan EPS matrix. The microscopy was repeated at least 10 times with two independent SiWSC3-His-FITC488 batches and independent Arabidopsis or barley plants colonized by *S. indica* or *B. sorokiniana*. The fungal matrix was not a sporadic observation but regularly observed with both fungi. WGA, wheat germ agglutinin.

mediated by host apoplastic CAZymes during plant–fungal interactions. In this study, we have characterized the CW and the soluble EPS matrix produced by two distantly related fungi, the beneficial root endophyte *Serendipita indica* (Basidiomycota), and the pathogenic fungus *Bipolaris sorokiniana* (Ascomycota), separated by over 649 million years of evolution (Taylor and Berbee, 2006; Lutzone *et al.*, 2018). Proteomics and glycomics revealed that  $\beta$ -glucan-binding proteins with cell wall integrity and stress response component (WSC) domains and  $\beta$ -1,3;1,6-glucan polysaccharides are enriched in the soluble EPS matrix compared to the CW layer. Treatment of the fungal EPS matrices with the apoplastic barley  $\beta$ -1,3-endoglucanase HvbGLUIII released a  $\beta$ -1,3;1,6-glucan decasaccharide ( $\beta$ -GD) with a mass/charge ( $m/z$ ) of 1661 Da. Proton nuclear magnetic resonance ( $^1\text{H}$  NMR) of  $\beta$ -GD is consistent with a heptameric  $\beta$ -1,3-glucan backbone substituted with three monomeric  $\beta$ -glucosyl residues at O-6. The  $\beta$ -GD is resilient to further enzymatic digestion by glycoside hydrolase 17 (GH17) family members and is immunologically inactive in a  $\beta$ -1,6-glucan side-branch-dependent manner. This low molecular weight soluble  $\beta$ -GD is able to efficiently scavenge ROS and to enhance colonization, corroborating its role as a previously undescribed fungal carbohydrate-class effector. The release of a conserved  $\beta$ -GD from the  $\beta$ -glucan-rich EPS matrix of a beneficial and a pathogenic fungus indicates that the utilization

of this outermost soluble polysaccharide layer as a protective shield against oxidative stress and ROS-mediated host signaling is a common fungal strategy to withstand apoplastic defense responses during plant colonization.

## Results

### Beneficial and pathogenic fungi produce a gel-like $\beta$ -glucan EPS matrix surrounding their CWs

We recently reported on a gel-like EPS matrix surrounding the hyphae of different fungi during colonization of plant hosts (Wawra *et al.*, 2019; Wanke *et al.*, 2021), suggesting that the secretion of soluble glycans is a common feature of plant-associated fungi independent of their lifestyle and taxonomy. This finding motivated us to investigate the biochemical characteristics, composition, and function of this matrix in the beneficial root endophyte *S. indica* and in the pathogenic fungus *B. sorokiniana*. To this end, we labeled the  $\beta$ -1,3-glucan-binding lectin PIIN\_05825 (SiWSC3-His-FITC488) from *S. indica* by applying an improved FITC488 conjugation protocol (see “Materials and methods”) and used it as a molecular probe for localization studies of the fungal EPS matrix in planta. SiWSC3-His-FITC488 signal accumulated around the wheat germ agglutinin-stained chitin layer in both fungi (Figure 1), strongly indicating that  $\beta$ -1,3-glucans are abundant in the outer EPS matrix. This expands the repertoire of fungal  $\beta$ -glucan-binding lectins that can be



used as molecular probes to fluorescently label the fungal EPS matrix during live cell imaging (Wawra *et al.*, 2016).

### The *S. indica* EPS matrix, CW, and culture filtrate represent three functionally distinct but interconnected compartments

To identify secreted proteins associated with the EPS matrix, the CW, and/or the culture filtrate, we performed quantitative proteomics with protein extracts from these three compartments from *S. indica* axenically grown in three different media (complete medium [CM], yeast-extract peptone dextrose [YPD], tryptic soy broth [TSB]; Supplemental Figure S1). We identified 1,724 proteins from all media and compartments (Supplemental Data Set S1; Figure 2A). Among those, 220 proteins carrying a predicted signal peptide were further analyzed for their domain architecture using the Pfam database (Supplemental Data Set S2; Figure 2A). Glucan-binding proteins with at least one WSC domain were more abundant or uniquely present in the EPS matrix compared to the CW (enrichment score 0.96, Benjamini–Hochberg corrected  $P = 0.00003$ ) or the culture filtrate (enrichment score 0.6, Benjamini–Hochberg corrected  $P = 0.02$ ), irrespective of the medium used (Figure 2B; Supplemental Figure S2 and Supplemental Data Set S3). Four of them, including SiWSC3 (PIIN\_08474, PIIN\_06786, PIIN\_03979, and PIIN\_05825), were among the most abundant proteins consistently found in this compartment (Figure 2B; Supplemental Figure S2), thereby confirming our in planta localization study (Figure 1). Gene expression analyses revealed an induction of these genes during *S. indica* colonization of barley and Arabidopsis over time (Wawra *et al.*, 2019; Supplemental Figure S3). Additionally, several *S. indica* proteases and CAZymes were more abundant in the EPS matrix and culture filtrate compared to the CW (Supplemental Figure S2 and Supplemental Data Set S3), suggesting that the matrix may serve as a transient storage depot for these enzymes. In the CW fraction, we identified two chitin-binding LysM proteins (PIIN\_02172 and PIIN\_02169) and several other lectin-like proteins, including the  $\beta$ -1,6-glucan-binding effector SiFGB1 (Wawra *et al.*, 2016; PIIN\_03211) and the ricin B lectin (PIIN\_01237). Most of these lectins were also present in the culture filtrate, indicating that besides their ability to bind to CW components, such as chitin and glucan, they also function as soluble lectins in the extracellular environment (Figure 2B; Supplemental Figure S2). This is in agreement with the function of SiFGB1, which has the potential to alter fungal CW composition and properties as well as suppress  $\beta$ -glucan-triggered immunity in the apoplast of different plant hosts (Wawra *et al.*, 2016). Proteins containing cellulose-binding CBM\_1 or starch-binding CBM\_20 domains were found at higher abundances in the culture filtrate (Supplemental Figure S2). Based on the distribution and nature of the carbohydrate-binding proteins, we propose that the EPS matrix, the

CW, and the culture filtrate represent three functionally distinct but interconnected compartments.

### *Serendipita indica* EPS matrix and CW have different sugar compositions

The different amount of glycan-binding proteins within the EPS matrix and CW layer prompted us to investigate the glycan composition of these two compartments. Protein-free EPS matrix and CW preparations from *S. indica* grown in TSB medium were subjected to glycosyl linkage analysis for neutral sugars (Ciucanu, 2006; Liu *et al.*, 2015). About 85% of the detected glycosidic linkages could be annotated based on the retention times and the mass spectra profile of the sugar residues (Supplemental Data Sets S4 and S5). Terminal glucose, 3-glucose, and 3,6-glucose were the dominant glycosidic linkages ( $\sim 35\%$ ) observed in the EPS matrix compared to other glycosidic sugar residues (Figure 2C; Supplemental Figure S4 and Supplemental Data Set S4). In contrast, in the CW fraction, 4-linked glucose was more abundant ( $\sim 45\%$ , Figure 2C; Supplemental Figure S4 and Supplemental Data Set S5) than in the EPS matrix. Further analyses are required to clarify the type of glycosidic linkages that can be  $\alpha$ -,  $\beta$ -, or mixed type.

Next, we treated the EPS matrix and CW with  $\beta$ -glucanases from *T. harzianum* (TLE) and *H. pomatia* and analyzed the digested products by thin-layer chromatography (TLC) and matrix-assisted laser desorption ionization time-of-flight mass (MALDI-TOF; Figure 3A). Several glucan fragments with various degrees of polymerization could be detected in the digested fraction confirming that  $\beta$ -glucans are present in both layers (Figure 3B; Supplemental Figure S5). Altogether, these data demonstrate that the EPS matrix and the CW of *S. indica* display major differences in the linkage compositions of their neutral sugars.

### A $\beta$ -glucan decasaccharide is released from the *S. indica* EPS matrix by a barley glucanase

We recently reported that several  $\beta$ -glucanases belonging to the GH17 family accumulate in the apoplast of barley roots during colonization by *S. indica* (Wawra *et al.*, 2016). Among them, the  $\beta$ -glucanase H $\nu$ BGLUII (P15737) was consistently found at different colonization stages but also in mock-treated plants (Wawra *et al.*, 2016; Supplemental Data Set S6), suggesting that this may be an ubiquitous apoplastic enzyme in root tissues. To investigate the activity of H $\nu$ BGLUII on the fungal CW and/or on the EPS matrix, we analyzed the digested fraction by TLC analysis after enzymatic incubation. Treatment of the EPS matrix with H $\nu$ BGLUII led to the release of a glucan fraction found at the sample origin spot that could not be further resolved under the TLC separation conditions used (Figure 3B). The corresponding band was not detected in the CW digestion (Figure 3B), indicating that H $\nu$ BGLUII is only active on the EPS matrix. Other  $\beta$ -1,3-glucanases (TLE and *H. pomatia*  $\beta$ -1,3-glucanase) were able to release oligosaccharides from both EPS and CW preparations, indicating that both preparations contain  $\beta$ -glucans

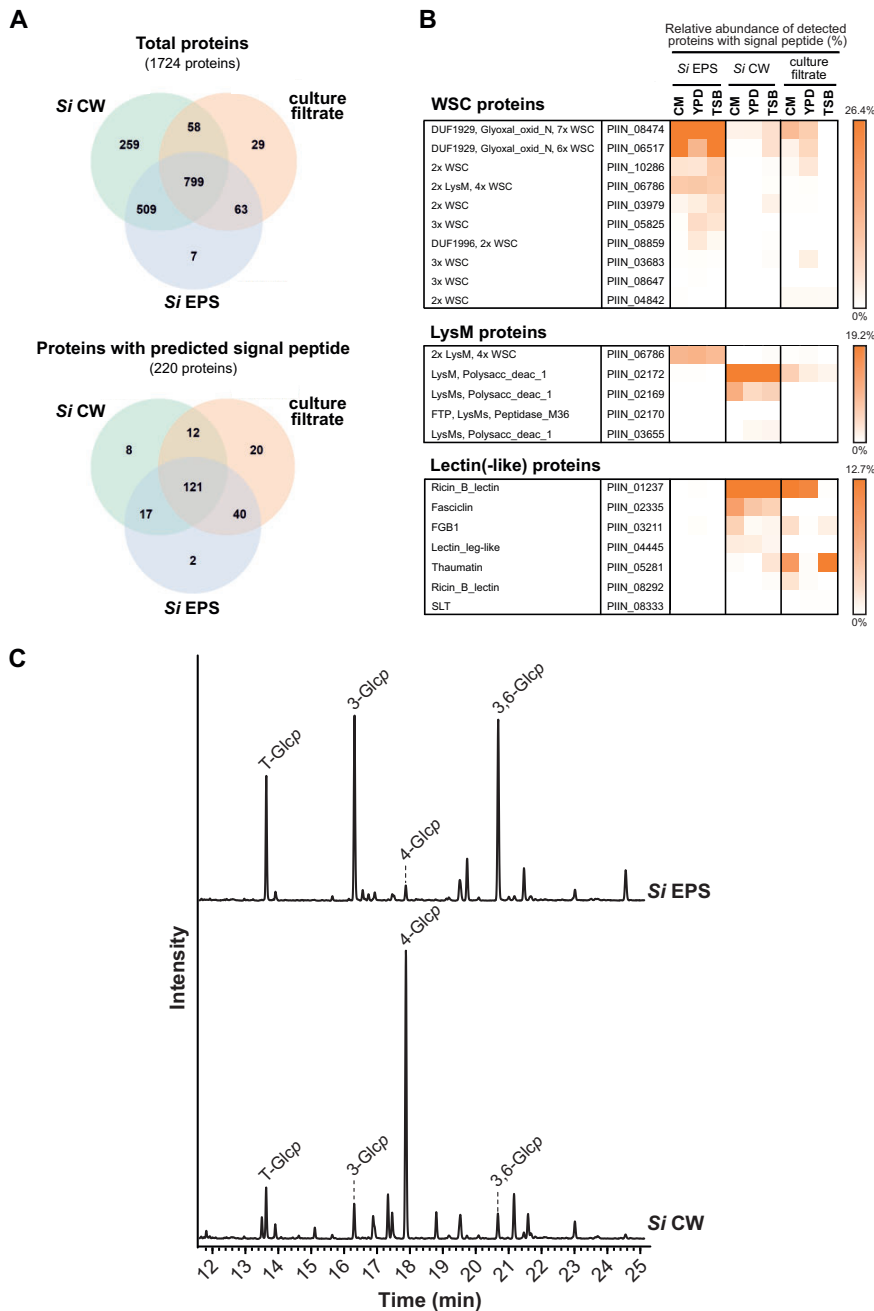


**Figure 2** Proteomics and glycosyl linkage analysis of *S. indica* EPS matrix and CW. A, Venn diagram of proteins identified in the EPS matrix, CW, and/or culture filtrate from three cultivation media (CM, YPD, and TSB). B, Proteins with WSC domain/s show higher abundances in the EPS matrix of *S. indica* (see also [Supplemental Figure S2](#) and [Supplemental Data Sets S1, S2, and S3](#)). The relative abundance of each protein was calculated using LFQ intensity values and is depicted in percentage. C, Glycosidic linkage analysis of *S. indica* EPS and CW preparations. 3-glucose and 3,6-glucose are abundant in the EPS matrix, whereas 4-glucose is abundant in the CW of *S. indica*. The experiment was performed with four independent biological replicates of Si EPS and Si CW and the TIC of one of the replicates is represented. TIC, total ion chromatogram; LysM, lysine motif; p, pyranose; Si, *Serendipita indica*.

that are enzyme accessible ([Figure 3B](#); [Supplemental Figure S5](#)).

To further characterize the structure of the compound released by *HvBGLUII* from the EPS matrix, we performed

MALDI-TOF and glycosyl linkage analyses. An oligosaccharide with a *m/z* of 1,661 Da, corresponding to 10 hexoses (referred to as  $\beta$ -glucan deca-saccharide [ $\beta$ -GD] fragment) with 3- and 3,6-linked glucoses was detected in high

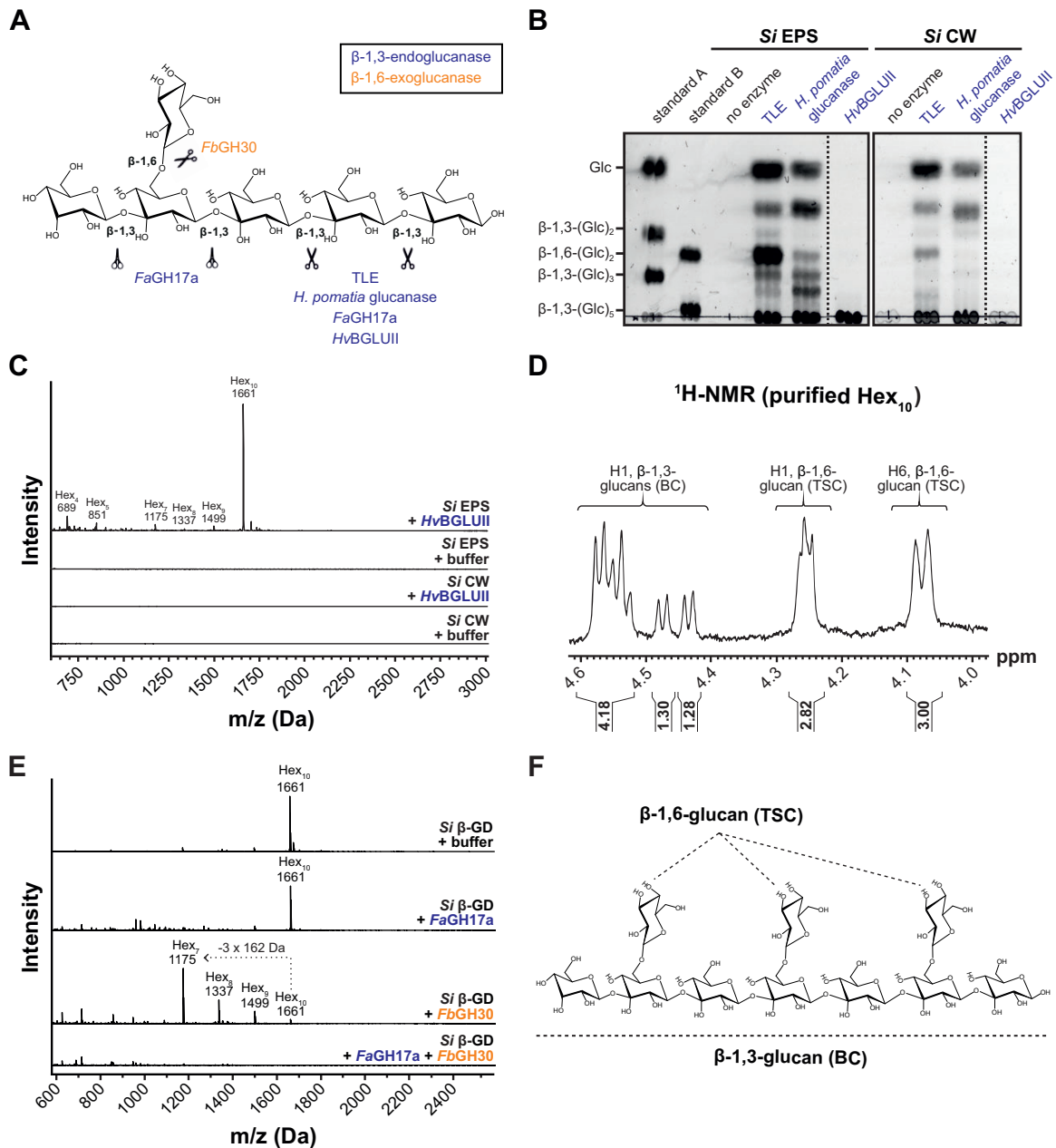


**Figure 3** The  $\beta$ -1,3;1,6-gluco-10-mer ( $\beta$ -GD) is released from the *S. indica* EPS matrix upon treatment with the barley apoplasmic glycosyl hydrolase HvBGLUII. **A**, Glycosyl hydrolases specific for  $\beta$ -1,3;1,6-gluco-10-mer were used for the characterization of the EPS matrix, CW, and  $\beta$ -GD. The  $\beta$ -1,3-endoglucanases from *T. harzianum* (TLE) and *H. pomatia* as well as FaGH17a and HvBGLUII are shown as open scissors (in blue). FaGH17a is represented as closed scissors because it does not hydrolyze glycosidic bonds of  $\beta$ -1,3-gluco-10-mer residues substituted with  $\beta$ -1,6-gluco-10-mer residues (in blue). FbGH30 is a  $\beta$ -1,6-exoglucanase (in orange). **B**, Analysis of digested EPS matrix or CW fractions by TLC. Several gluco-10-mer fragments with different lengths are released from the EPS matrix and CW by the action of TLE and *H. pomatia*  $\beta$ -1,3-gluco-10-mer. HvBGLUII releases a gluco-10-mer fraction from the  $\beta$ -gluco-10-mer-containing EPS matrix but not from the CW. The experiment was repeated twice with *Si* EPS and *Si* CW isolated under different medium conditions (YPD and CM) and similar results were obtained. **C**, Analysis of digested EPS or CW fractions by MALDI-TOF mass spectrometry. The 1,661 Da  $\beta$ -GD corresponding to 10 hexoses is released from the EPS matrix but not from the CW of *S. indica*. The representative DP of hexoses is indicated on top of the  $m/z$  ( $M + Na$ )<sup>+</sup> masses of oligosaccharides. The digestion of *Si* EPS with HvBGLUII was repeated independently more than three times with a similar result and the digestion of *Si* CW with HvBGLUII was performed two times with a similar result. **D**, <sup>1</sup>H NMR spectrum of HPLC purified  $\beta$ -GD. **E**, Treatment of  $\beta$ -GD with various hydrolases followed by MALDI-TOF analysis of the products. The loss of three hexoses ( $-3 \times 162$  Da) as a result of treatment with FbGH30 is indicated with a dotted arrow. The experiment was performed two times with a similar result. **F**, Structure of the  $\beta$ -GD based on the <sup>1</sup>H NMR spectrum.  $\beta$ -GD consists of a linear  $\beta$ -1,3-gluco-10-mer backbone substituted with  $\beta$ -1,6-gluco-10-mer moieties. *Si*, *Serendipita indica*; DP, degree of polymerization; Hex<sub>*n*</sub>, oligosaccharides with the indicated hexose composition; BC, backbone chain; TSC, terminal side-chain.

abundance compared to other oligosaccharides with various degrees of polymerization (DP4–DP9, [Figure 3C](#); [Supplemental Figure S6A](#)). Neither the  $\beta$ -GD nor the other oligosaccharides were detected in the supernatant of the digested CW preparation ([Figure 3C](#)), confirming the TLC result ([Figure 3B](#)). Furthermore, the  $\beta$ -GD was also released from the EPS matrix of *S. indica* grown in CM medium ([Supplemental Figure S6B](#)), suggesting that the growth conditions do not notably influence the release of the  $\beta$ -GD.

To further assess the structure of  $\beta$ -GD, the fragment was purified using reverse-phase chromatography ([Supplemental Figure S7](#)) and subjected to  $^1\text{H}$  NMR spectroscopy ([Figure 3D](#)).  $^1\text{H}$  NMR analysis displayed characteristic proton signals for  $\beta$ -1,3;1,6-glucan ([Kim et al., 2000](#); [Tada et al., 2009](#); [Lowman et al., 2011](#)). Since  $\beta$ -GD was reduced prior to the NMR analysis, only nine anomeric carbohydrate signals were present. The anomeric  $^1\text{H}$  NMR signals of the six internal  $\beta$ -1,3-glucan backbone moieties were identified at 4.4–4.6 ppm ([Figure 3D](#)). They appear as a multiplet due to overlapping proton doublet signals at 4.5–4.6 ppm (four protons), a doublet at 4.48 ppm ( $J$  7.8 Hz, one proton) representing the second glucose unit next to the reducing end and a doublet at 4.44 ppm ( $J$  7.8 Hz, one proton) representing the non-reducing end of the oligosaccharide backbone. Anomeric NMR signals were also observed for the  $\beta$ -1,6-D-side-chain substituents at 4.26 ppm (three protons), indicating that the oligosaccharide contains three individual monomeric substituents. This is confirmed by the H6 NMR signal of  $\beta$ -1,6-D-glucose substituents at 4.08 ppm (three protons). In conclusion, the  $^1\text{H}$  NMR analysis indicates that  $\beta$ -GD consists of seven  $\beta$ -1,3-linked D-glucose backbone units substituted with three terminal  $\beta$ -1,6-glucose units. The order of the substituents on the backbone could not be established by the NMR analysis performed here.

To validate the  $^1\text{H}$  NMR results, we took advantage of the two well-characterized glycosyl hydrolases, *FaGH17a* and *FbGH30* ([Becker et al., 2017](#); [Wanke et al., 2020](#)). *FaGH17a* is an endoglucanase specifically active on unsubstituted  $\beta$ -1,3-glucans and *FbGH30* is an exoglucanase specific for  $\beta$ -1,6-glycosidic linkages ([Figure 3A](#)). The  $\beta$ -GD was treated with *FaGH17a* or *FbGH30* or a combination of the two enzymes and the digested samples were analyzed using MALDI-TOF mass spectrometry ([Figure 3E](#)). Digestion with *FbGH30* resulted in ion signals that represent the enzymatic removal of one ( $m/z$  1,499), two ( $m/z$  1,337), or most pronounced three glucosyl moieties ( $m/z$  1,175), confirming the presence of three  $\beta$ -1,6-glucose units in  $\beta$ -GD. Digestion with *FaGH17a* alone did not alter the molecular weight of  $\beta$ -GD indicating that potential enzyme hydrolysis sites are blocked by its side-chain substituents. In contrast, the combined treatment with both enzymes led to complete hydrolysis of the  $\beta$ -GD ([Figure 3E](#)). Taken together, these results

demonstrate that the  $\beta$ -GD released from the EPS matrix by the action of *HvBGLUII* is a decasaccharide with seven  $\beta$ -1,3-glucosyl units substituted with three  $\beta$ -1,6-glucosyl units as depicted in [Figure 3F](#).

### The apoplastic *HvBGLUII* fosters MAMP-triggered immunity that is counteracted by the uncleavable $\beta$ -GD

Since  $\beta$ -glucans represent an important class of microbial cell surface glycans able to trigger plant immune responses ([Fesel and Zuccaro, 2016](#); [Wanke et al., 2020](#)), we performed ROS burst assays with *S. indica* CW and EPS matrix as well as with the enzymatically released  $\beta$ -GD to test their immunogenic potential on barley roots. Whereas the application of the fungal MAMP chitohexaose (positive control) triggered apoplastic ROS accumulation, incubation with *S. indica* CW and EPS matrix only marginally induced ROS accumulation ([Supplemental Figure S8](#)). Applications of the  $\beta$ -GD led to significantly lower ROS levels compared to the mock treatment ([Figure 4A](#); [Supplemental Figure S9](#)). This prompted us to test the ability of this fragment to affect ROS levels during co-treatment with different MAMPs ([Figure 4A](#); [Supplemental Figures S10 and S11](#)). The combined application of chitohexaose and  $\beta$ -GD led to a decreased accumulation of ROS with increasing concentrations of added  $\beta$ -GD ([Figure 4A](#); [Supplemental Figures S9 and S10](#)). Combined digestion of the  $\beta$ -GD with the endoglucanases *FaGH17a* and *FbGH30* restored the chitohexaose-triggered ROS burst ([Figure 4B](#)), thereby highlighting that the decreased accumulation of apoplastic ROS is linked to the presence of an—at least largely—intact  $\beta$ -GD. Impaired ROS accumulation was not observed with *S. indica* CW or EPS matrix preparations ([Figure S8](#)). Additionally, the application of the  $\beta$ -GD significantly reduced apoplastic ROS accumulation in barley roots treated with the  $\beta$ -1,3;1,6-glucan laminarin and in *Arabidopsis* seedlings treated with the flagellin-derived peptide flg22 ([Supplemental Figure S11](#)), substantiating a general function of the  $\beta$ -GD irrespective of plant species or elicitor.

To clarify whether the  $\beta$ -GD interferes with the MAMP perception machinery or detoxifies ROS, we tested its effect on further early and late immune responses triggered by chitohexaose. In barley, *HvWRKY2* has been demonstrated to act as a reliable marker for the onset of early immune responses among a wide range of elicitors applied to barley ([Shen et al., 2007](#); [Liu et al., 2014](#); [Wanke et al., 2020](#)). Despite the reduction of the oxidative burst, chitohexaose-triggered *HvWRKY2* expression was not reduced by the application of the  $\beta$ -GD ([Figure 4C](#); [Supplemental Figure S10C](#)). This shows that the  $\beta$ -GD does not prevent MAMP perception but acts on the released ROS. Furthermore, treatment with the  $\beta$ -GD alone did not lead to a significant increase in *HvWRKY2* expression, supporting the notion that this  $\beta$ -glucan fragment does not exhibit an immunogenic

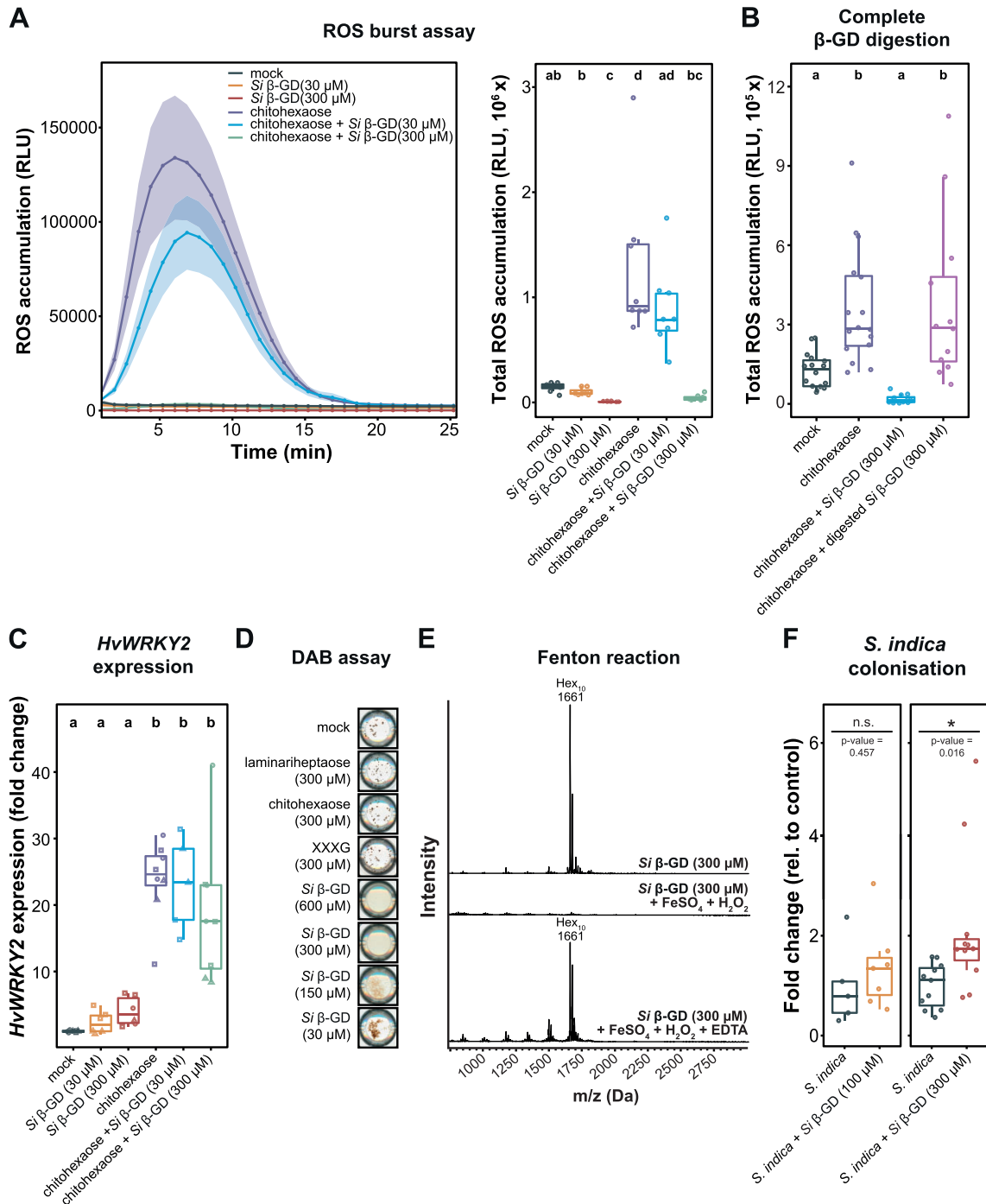


**Figure 4** The β-GD released from *S. indica* EPS matrix scavenges ROS and enhances host colonization. A, Apoplastic ROS accumulation after treatment of barley roots of 8-day-old plants with 25-μM chitohexaose and/or purified β-GD from *S. indica*. ROS accumulation was monitored via a luminol-based chemiluminescence assay. Treatment with Milli-Q water was used as mock control. Boxplot represents total ROS accumulation over the measured time period. Values represent mean ± SEM from eight wells, each containing four root pieces. In total, roots from 16 individual barley plants were used per experiment. The assay was performed at least four times with independent β-GD preparations. Letters represent statistically significant differences in expression based on a one-way ANOVA and Tukey's post hoc test (significance threshold:  $P \leq 0.05$ ). B, Prior to treatment of barley root pieces with the elicitors, β-GD was digested overnight (25°C, 500 rpm in heat block) with the glucanases FaGH17a and FbGH30, which led to complete digestion of β-GD (see also Figure 3E). As control, β-GD without the addition of enzymes (but instead with an equal volume of Milli-Q water) was treated similarly. Barley root pieces were treated with Milli-Q water ( $n = 16$ ) and 25-μM



activity in barley roots. In support of this, treatments of Arabidopsis seedlings with  $\beta$ -GD did not induce rapid intracellular calcium fluxes (Supplemental Figure S12), an early hallmark of plant immune responses (Boller and Felix, 2009). These results are surprising due to the structural similarity of  $\beta$ -GD to laminarihexaose and laminarin, two potent ROS elicitors in different plant species, including barley and Arabidopsis (Wanke *et al.*, 2020). Thus, the frequency and position of  $\beta$ -1,6-glucose substituents may define both their immunomodulatory potential as MAMP as well as their biochemical activity as ROS scavengers. To confirm this hypothesis, we treated laminariheptaose, the  $\beta$ -1,3-backbone of  $\beta$ -GD, with H $\nu$ BGLUII for 1 h or overnight and tested those preparations in ROS burst assays. Barley BGLUII was capable of digesting the laminariheptaose to glucose and laminaribiose (Supplemental Figure S13). The activity of H $\nu$ BGLUII on the laminariheptaose led to higher ROS accumulation compared to incubation with undigested laminariheptaose (Supplemental Figure S13). This demonstrates that H $\nu$ BGLUII is a host defense enzyme that releases potent MAMPs from unbranched  $\beta$ -1,3-glucan oligomers likely derived from the fungus (Figure 2C), playing a role in host glycan perception.

### The $\beta$ -GD scavenges apoplastic ROS

Numerous studies have highlighted the capability of sugars and specifically of  $\beta$ -glucans to act as ROS scavengers, contributing to the intracellular antioxidant system in different eukaryotes (Benaroudj *et al.*, 2001; Nishizawa *et al.*, 2008; Valluru and Van den Ende, 2008; Peshev *et al.*, 2013; Lei *et al.*, 2015; Boulos and Nystrom, 2017). To test whether the  $\beta$ -GD can directly act as an antioxidant, we performed an *in vitro* 3,3'-diaminobenzidine (DAB) assay. In the presence of hydrogen peroxide and horseradish peroxidase as catalyst, DAB is oxidized and polymerizes, ultimately leading to the formation of a brown, water-insoluble precipitate (Figure 4D). At low concentrations of  $\beta$ -GD (30–150  $\mu$ M), DAB still oxidizes but forms less precipitates compared to

the mock control. Formation of precipitates was completely inhibited at higher concentrations of  $\beta$ -GD (300–600  $\mu$ M; Figure 4D). The inhibition of DAB precipitation can be explained by the ability of  $\beta$ -GD to scavenge ROS in a concentration dependent manner. Other CW-associated sugars such as chitohexaose, laminariheptaose, and a xyloglucan heptasaccharide (XXXG) did not interfere with DAB precipitation (Figure 4D). Mechanistically, nonenzymatic scavenging of hydroxyl radicals by sugars is based on their oxidation, which can lead to cleavage of glycosidic linkages and the formation of less reactive sugar radicals that further cross-react with themselves or other sugars (Matros *et al.*, 2015). To validate if the oxidation of the decasaccharide contributes to ROS scavenging, we performed a Fenton reaction-based assay with the  $\beta$ -GD followed by MALDI-TOF analysis. In the presence of the Fenton reagents, the peak at 1,661 Da, corresponding to the  $\beta$ -GD, was no longer detected, suggesting that the fragment might have undergone oxidative degradation and/or have changed its chemo-physical properties by the activity of hydroxyl radicals produced by the Fenton reaction (Figure 4E). The oxidative degradation of the  $\beta$ -GD could be rescued in the presence of ethylenediaminetetraacetic acid (EDTA), which chelates the catalytic iron involved in the formation of hydroxyl radicals. Complete degradation was not observed for the structurally related laminariheptaose, chitohexaose, and XXXG (Supplemental Figure S14). Altogether, these results demonstrate that the activity of H $\nu$ BGLUII on the *S. indica* EPS matrix does not release a MAMP that initiates plant defense responses, but a fragment that can detoxify apoplastic ROS possibly via oxidative degradation. These results highlight a hitherto undescribed function of the fungal EPS matrix as a protective layer to mitigate oxidative stress during plant–microbe interaction.

To explore whether the  $\beta$ -GD can facilitate root colonization during early interaction, we performed colonization assays on barley roots in the presence of various  $\beta$ -GD concentrations (Figure 4F). The addition of  $\beta$ -GD slightly

#### Figure 4 (continued)

chitohexaose alone ( $n = 16$ ) or in combination with digested or undigested  $\beta$ -GD (300  $\mu$ M,  $n = 12$ ). The experiment was performed twice with similar results. Statistically significant differences are indicated by different letters based on a one-way ANOVA and Tukey's post hoc test (significance threshold:  $P \leq 0.05$ ). C, Barley root pieces were collected 1 h after elicitor treatment and further processed for RNA extraction and cDNA synthesis. Expression changes of the elicitor-responsive gene *HvWRKY2* were analyzed by RT-qPCR. Fold change expression were calculated by normalization to housekeeping gene expression (*HvUBI*) and mock treatment. Data from three independent experiments are indicated by different dot shapes. Letters represent statistically significant differences in expression based on two-way ANOVA (additive model, treatment + experiment) and Tukey's post hoc test (significance threshold:  $P \leq 0.05$ ). Significant differences were associated with different treatments ( $F = 11.629$ ,  $P = 1.58 \times 10^{-6}$ ), but not with independent experiments ( $F = 2.227$ ,  $P = 0.124$ ). D, The capability of different carbohydrates to prevent hydrogen peroxide-based and horseradish peroxidase-catalyzed oxidation and precipitation of DAB was monitored. Respective sugars (or Milli-Q water as mock control) were pre-incubated with 1-mM  $H_2O_2$  and 0.05- $\mu$ M horseradish peroxidase before DAB (50  $\mu$ M) was added. Scans of wells from 96-well plates were performed 16 h after DAB addition. The experiment was performed three times with similar results. E, Oxidative degradation of *S. indica* EPS matrix-derived  $\beta$ -GD (300  $\mu$ M) by  $H_2O_2$  was detected with an overnight Fenton reaction (1-mM  $H_2O_2$ , 100- $\mu$ M  $FeSO_4$ ) followed by MALDI-TOF mass spectroscopic analysis. As controls, either sugar alone or the samples supplemented with 100- $\mu$ M EDTA were used. F, Colonization of barley roots by *S. indica* upon daily application of sterile Milli-Q water (mock) or  $\beta$ -GD (100 or 300  $\mu$ M). Fungal colonization in each biological replicate was assessed by RT-qPCR comparing the expression of the fungal housekeeping gene *SiTEF* and the plant gene *HvUBI* ( $n = 5-11$ ). Boxplot elements in this figure: center line, median; box limits, upper and lower quartiles; whiskers,  $1.5 \times$  interquartile range. Statistical significance was determined on the nontransformed values (before normalization to *S. indica* control treatment) using a two-tailed Student's *t* test ( $*P \leq 0.05$ ). *Si*, *Serendipita indica*; RLU, relative light units; XXXG, xyloglucan heptasaccharide.



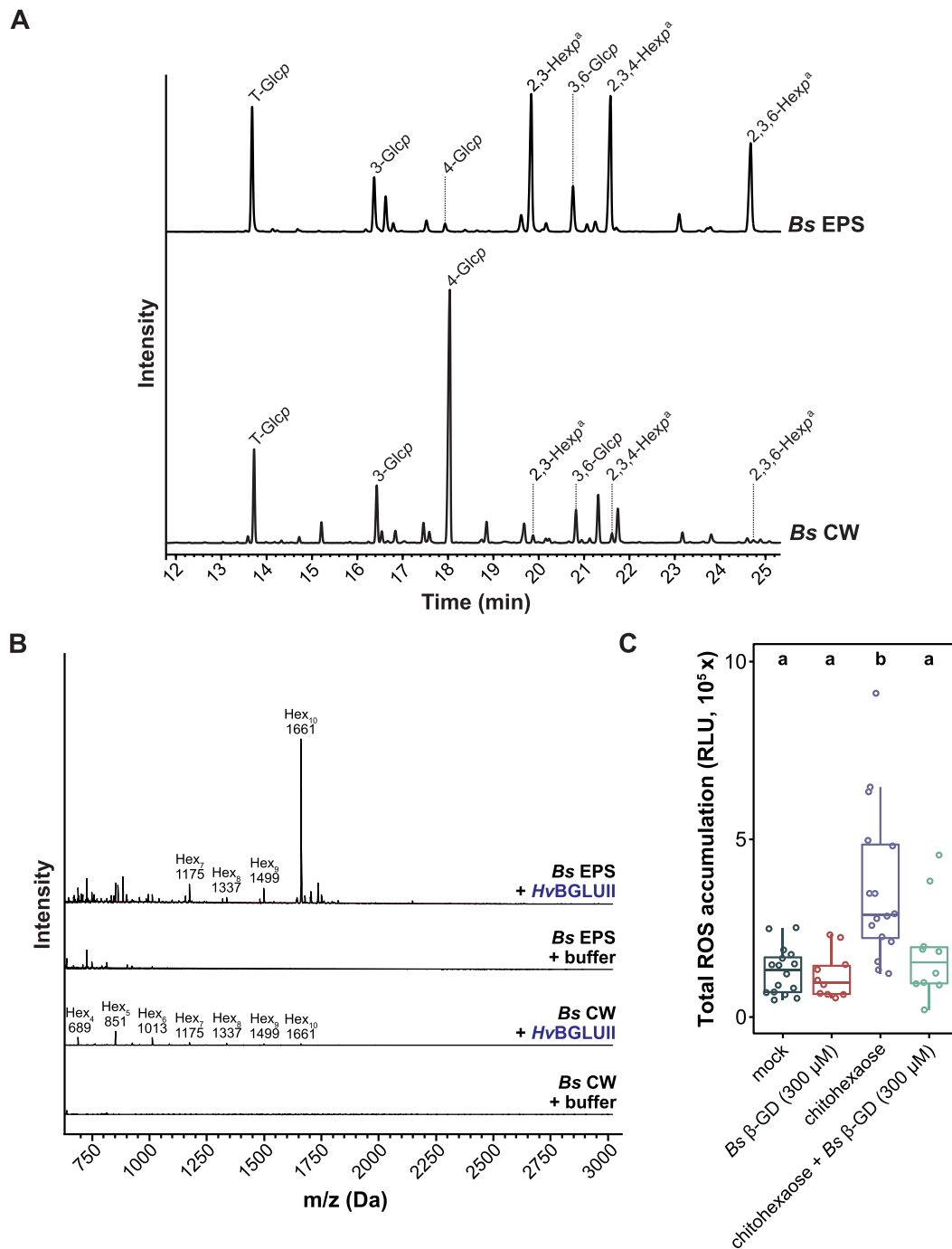


**Figure 5** The  $\beta$ -GD derived from the hydrolysis of *B. sorokiniana* EPS matrix exhibits antioxidative properties. A, Glycosidic linkage analysis of *B. sorokiniana* EPS matrix and CW preparations. 2,3-hexopyranose, 2,3,4-hexopyranose, and 2,3,6-hexopyranose are abundant in the EPS matrix, whereas 4-glucose is abundant in the CW of *B. sorokiniana*. The experiment was performed with three independent biological replicates of *Bs* EPS and *Bs* CW and the TIC from one of the replicates is represented. B, Analysis of digested EPS or CW fractions by MALDI-TOF mass spectrometry. The 1,661-Da  $\beta$ -GD corresponding to 10 hexoses is released from the EPS matrix but not from the CW of *B. sorokiniana*. The representative DP of hexoses is indicated on top of the  $m/z$  ( $M + Na$ )<sup>+</sup> masses of oligosaccharides. The digestion of *Bs* EPS with *HvBGLUII* was repeated independently three times with a similar result and the digestion of *Bs* CW with *HvBGLUII* was performed once. C, ROS burst assay was performed on barley roots treated with Milli-Q water (mock), chitohexaose (25  $\mu$ M), *Bs*  $\beta$ -GD (300  $\mu$ M), or a combination of chitohexaose and *Bs*  $\beta$ -GD. Boxplots represent total cumulative ROS accumulation over a measured time interval of 25 min. Each data point in the boxplot represents the integrated value from an individual well (center line, median; box limits, upper and lower quartiles; whiskers, 1.5  $\times$  interquartile range). The experiment was performed three times with similar results. Statistically significant differences are indicated by different letters based on a one-way ANOVA and Tukey's post hoc test (significance threshold:  $P \leq 0.05$ ). *Bs*, *Bipolaris sorokiniana*; DP, degree of polymerization; p, pyranose. <sup>a</sup>exact sugar moiety unknown; overrepresentation of linkages due to undermethylation cannot be excluded.

increased colonization at 100  $\mu\text{M}$  and led to an on average 2.15-fold increase of fungal colonization at 300  $\mu\text{M}$  after 3 days post inoculation (dpi). This demonstrates that an EPS matrix-resident decasaccharide that is released by a plant glucanase can act as a carbohydrate-class effector enhancing fungal colonization.

### The antioxidative properties of the $\beta$ -GD are conserved among pathogenic and beneficial fungi

To clarify whether the observed properties of the  $\beta$ -GD are conserved among fungi with different lifestyles and taxonomic positions, we performed glycosyl linkage analysis of the CW and EPS matrix of *B. sorokiniana* grown in YPD medium. As observed for *S. indica*, the relative abundance of 4-linked glucose in the *B. sorokiniana* CW was higher compared to other sugar residues (Figure 5A; Supplemental Figure S15 and Supplemental Data Set S7). In the *B. sorokiniana* EPS matrix, 3-glucose and 3,6-glucose represented only a minor fraction ( $\sim 10\%$ ) compared to 2,3-hexose, 2,3,4-hexose, and 2,3,6-hexose ( $\sim 40\%$ ) and this is different from the EPS matrix of *S. indica* (Figure 5A; Supplemental Figure S15 and Supplemental Data Set S8). However, the presence of 3- and 3,6-linked glucose suggests that  $\beta$ -glucans with similar structures to *S. indica* glucans are also present in the EPS matrix of *B. sorokiniana*. Indeed several glucan fragments with various degrees of polymerization (DP3–DP10) could be release from digestion with the TLE but not from the buffer control (Supplemental Figure S16), indicating that  $\beta$ -glucans are present in the EPS matrix.

Since *HvBGLUII* was detected in the apoplastic fluid of *B. sorokiniana* challenged barley roots and the gene is highly induced during *B. sorokiniana* root colonization (Supplemental Data Sets S6 and S9), we investigated whether *HvBGLUII* can also release oligosaccharides from the *B. sorokiniana* EPS matrix. We detected a 1,661 Da fragment in high abundance representing a decasaccharide (Figure 5B). To characterize the structure of the 1,661 Da fragment from *B. sorokiniana*, we incubated it with *FaGH17a* or *FbGH30* or a combination of the two enzymes. MALDI-TOF analysis revealed that this fragment has the same digestion profile and thus most likely the same structure as *S. indica*  $\beta$ -GD (Supplemental Figure S17), demonstrating that  $\beta$ -GD is conserved among distantly related fungi.

Next, to investigate the immunogenic properties of *B. sorokiniana*  $\beta$ -GD, we tested it in ROS burst assays using barley roots. Consistent with the data obtained from *S. indica*, the enzymatically released *B. sorokiniana*  $\beta$ -GD, but not crude EPS matrix or CW preparations, displayed a decrease in ROS accumulation when co-applied with chitohexaose (Figure 5C; Supplemental Figure S18). Collectively, our results indicate that the antioxidative property of the  $\beta$ -GD is a common feature among plant-associated fungi.

## Discussion

Fungi synthesize and secrete a wide range of glycans, which are crucial determinants of microbe–microbe and microbe–

host interactions. Despite variations in glycan structures and composition of the CW and the surrounding EPS matrix between fungal species,  $\beta$ -glucans are generally the most abundant and complex structural components. Their recognition by host receptors activates immune responses, such as accumulation of ROS and CAZymes in the extracellular apoplastic space, which hamper host colonization (El Oirdi *et al.*, 2011; Wanke *et al.*, 2020, 2021; Rebaque *et al.*, 2021). In order to overcome or bypass such responses, fungi employ different extracellular strategies (Buscaill and van der Hoorn, 2021). Common fungal countermeasures to prevent recognition and hydrolysis of their surface exposed glycans involve converting, depleting or masking highly immunoreactive CW components. Although effective, these countermeasures may not always be employed because some of these glycan structures mediate important processes that are beneficial to the fungus. This explains why some glycan structures are highly conserved and cannot be extensively modified. Thus, fungi have additionally evolved apoplastic glycan-binding effector proteins that either sequester immunoreactive CW-derived elicitors from the apoplast to prevent their recognition or shield them from hydrolysis. Additionally, fungi secrete CAZyme inhibitors and proteases that cleave host hydrolytic enzymes (Ham *et al.*, 1997; Rovenich *et al.*, 2016; Rocafort *et al.*, 2020). Less is known about fungal cytoplasmic effector proteins targeting the disruption of glycan signaling inside plant cells.

Here, we identified a previously undescribed extracellular fungal counterdefensive strategy to subvert host immunity that involves the hijacking of widely distributed plant apoplastic endoglucanases to release a conserved  $\beta$ -1,3;1,6-glucan decasaccharide with ROS scavenging properties from the extracellular polysaccharide matrix of different fungi (Figure 6). Several classes of plant proteins, called pathogenesis-related (PR) proteins, are induced in response to fungal colonization. Among these proteins the family of PR-2 proteins, which are  $\beta$ -1,3-endo-type glucanases, is long known (Stintzi *et al.*, 1993; Leubner-Metzger and Meins, 1999). In seed plants,  $\beta$ -1,3-glucanases are widely distributed, highly regulated and abundant in the apoplast or vacuoles. Besides their role in the plant response to microbial pathogens and wounding, these enzymes are also implicated in diverse physiological and developmental processes in the uninfected plant. The GH17 family member BGLUII is present in the apoplast of uninfected and infected barley roots and highly induced upon challenge with the pathogen *B. sorokiniana*. The activity of BGLUII on the fungal EPS matrix indicates that its substrate is available/exposed in this layer, the first physical site of contact with the plant defense components. The released  $\beta$ -GD is not immunoreactive in barley and *Arabidopsis* and has some specific properties, which include resilience to further digestion by GH17 family members as well as ROS scavenging abilities. These properties seem to depend on the presence of  $\beta$ -1,6-linked glucosyl substituents. In fact, the structurally related laminariheptaose, which has the same structure as the backbone of  $\beta$ -

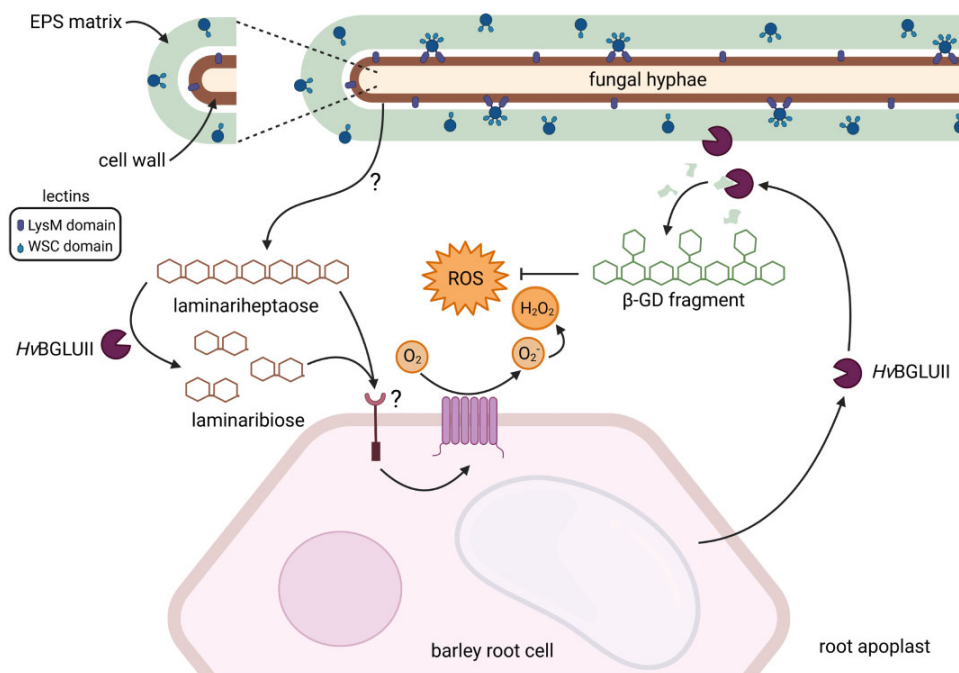


**Figure 6** Model for the production and function of the conserved fungal EPS-derived  $\beta$ -1,3;1,6-glucan deca-saccharide. The fungal-responsive GH17 family member *HvbGLUII* is found in the apoplast of barley roots and acts on  $\beta$ -1,3-glucan. Digestion of linear  $\beta$ -1,3-glucan (laminariheptaose) with *HvbGLUII* enhances ROS accumulation in barley roots, corroborating its role as a host defense enzyme with a function in  $\beta$ -glucan perception. To counteract the activity of *HvbGLUII*, plant-colonizing fungi produce a  $\beta$ -1,3;1,6-glucan-rich EPS matrix. The activity of *HvbGLUII* on the EPS matrix releases a conserved  $\beta$ -GD, which is resilient to further digestion by GH17 family members. The  $\beta$ -GD acts as a carbohydrate-class effector by scavenging ROS and enhancing fungal colonization. Lectins containing WSC domains are enriched in the outer EPS matrix and lectins containing LysM domains are enriched in the CW of *S. indica*. Graphical illustration was designed with the BioRender online tool.

GD, is highly sensitive to digestion by *HvbGLUII* and other GH17 family members, is immunoactive in barley, is not significantly degraded/modified in the Fenton reaction and does not display ROS scavenging capabilities (Figure 4D; Supplemental Figures S13 and S14). The removal of the side-branches from the  $\beta$ -GD by a microbial-derived  $\beta$ -1,6-gluco-nase makes it sensitive to further digestion by GH17 family members, confirming the protective effect displayed by the side-branches. In planta, the  $\beta$ -GD most likely corresponds to a host glucanase-resistant structure because plants are not known to produce  $\beta$ -1,6-gluco-nases (Fliegmann *et al.*, 2004; Nars *et al.*, 2013).

Additionally, the branching frequency might also be crucial for the immunomodulating activities of  $\beta$ -glucans. In animal systems, glucans are sensed by the well-characterized receptor Dectin-1. The minimal glucan subunit structure for Dectin-1 activation is a  $\beta$ -1,3-glucan oligo-saccharide containing a backbone with at least seven glucose subunits and a single  $\beta$ -1,6-linked side-chain branch at the nonreducing end (Adams *et al.*, 2008). We recently have shown that in plants  $\beta$ -1,3-glucan oligomers are perceived in a host species and length-dependent manner. While the monocots barley and *Brachypodium distachyon* can recognize longer (laminarin) and shorter (laminari-hexaose)  $\beta$ -1,3-glucans with responses of varying intensity, duration and timing, the dicot *Nicotiana benthamiana*

activates immunity in response to long  $\beta$ -1,3-glucans, whereas *Arabidopsis* and *Capsella rubella* perceive short  $\beta$ -1,3-glucans. The hydrolysis of the  $\beta$ -1,6 side-branches of laminarin did not affect recognition, demonstrating that not the glycosidic decoration but rather the degree of polymerization plays a pivotal role in the recognition of long-chain  $\beta$ -glucans in plants. Our data do not unambiguously demonstrate the glucosyl position of the substituents on the heptasaccharide backbone of the  $\beta$ -GD, but a possible explanation to the observed differences between the immune properties of laminarin (1:10 branching) and the  $\beta$ -GD (1:2.3 branching) might be that in barley roots  $\beta$ -glucans with a higher degree of branching could stereo-chemically interfere with each other, leading to less binding by specific receptors. It could well be that the  $\beta$ -GD has different immune properties depending on the plant species and this requires further investigation. However, here we show that upon incubation of  $\beta$ -GD with two unrelated plant species, *Arabidopsis* and barley, no accumulation of ROS was detected. It should also be mentioned that the antioxidant value of  $\beta$ -GD seems to be strictly “single use” and the  $\beta$ -GD pool may be easily depleted in planta. Nevertheless, a temporary dampening of the oxidative burst may be all that is required to support colonization and/or hamper ROS signaling. The immunomodulatory properties of the  $\beta$ -GD resemble those of

fungal effector proteins, suggesting that carbohydrate-class effectors also play an important role in fungal accommodation.

In conclusion, our data demonstrate that the fungal EPS matrix is a source of soluble  $\beta$ -glucans that leads to ROS scavenging properties important for host colonization and represents a distinct outer fungal layer with well-defined protein and carbohydrate signatures.  $\beta$ -glucans can form complex higher order structures depending on the conformation of sugar residues, molecular weight, inter- and intra-chain hydrogen bonding, and environmental conditions—all effecting their properties. This is different to the immune perception of the MAMP chitin, which is solely based on the length of the released oligomers by, for instance, the activity of chitinases. In plants,  $\beta$ -glucans are considered “orphan MAMPs” as their direct immune receptors have so far not been unambiguously identified. One of the remaining challenges is to fully elucidate the  $\beta$ -glucans’ functions and receptors. Information on the structure, solubility, molecular weight, side-chain branching frequency, and conformation is of paramount importance and should be provided in studies dealing with fungal  $\beta$ -glucans and their effects on the plant immune system.

## Materials and methods

Biological assays were performed with barley (*H. vulgare* L. cv Golden Promise) and *A. thaliana* Col-0 or aequorin-expressing Col-0 lines (Choi et al., 2014). Barley seeds were surface sterilized with 6% bleach for 1 h, followed by five washing steps with 30 mL of sterile Milli-Q water (each 30 min, two quick rinses for a couple of seconds between longer incubation steps). Sterilized seeds were germinated for 3 days on wet filter paper at room temperature in the dark under sterile conditions. Seedlings were transferred to sterile jars containing solid 1/10 plant nutrition medium (PNM), 0.4% gelrite (Duchefa, Haarlem, the Netherlands) (Lahrmann et al., 2013) and cultivated in a growth chamber with a day/night cycle of 16 h/8 h (light intensity,  $108 \mu\text{mol m}^{-2} \text{s}^{-1}$ ) and temperatures of 22°C/18°C. Seedlings were grown for 4 more days before being used for immunity assays.

Arabidopsis seeds were surface sterilized (10 min 70% ethanol, 7 min 100% ethanol) and sown on half-strength Murashige and Skoog (MS) medium (pH 5.7) supplemented with 0.5% sucrose and 0.4% Gelrite (Duchefa, Haarlem, the Netherlands). Plates were transferred to climate chambers with 8-h/16-h light/dark regime (light intensity of  $110 \mu\text{mol m}^{-2} \text{s}^{-1}$ ) at 22°C/18°C. Seven-day-old seedlings were transferred into petri dishes filled with 30-mL fresh half-strength MS liquid medium and grown for 7 additional days under the same conditions.

## Commercial enzymes

The commercial  $\beta$ -glucanases used in this study are the *Trichoderma harzianum* lysing enzymes (TLE, Sigma L1412), the *Helix pomatia*  $\beta$ -1,3-glucanase (Sigma 67138) and the *H. vulgare*  $\beta$ -1,3-endoglucanase (GH17 family HvBGLUII, E-

LAMHV in 50% (v/v) glycerol, Megazyme). TLE or *H. pomatia*  $\beta$ -1,3-glucanase were prepared in a stock concentration of  $1.25 \text{ mg}\cdot\text{mL}^{-1}$  in respective buffers: TLE (2-mM sodium acetate, pH 5.0), *H. pomatia*  $\beta$ -1,3-glucanase (2-mM MES, pH 5.0). The GH17A family  $\beta$ -1,3-endoglucanase from *Formosa agariphila* (FaGH17a) and the GH30 family  $\beta$ -1,6-exoglucanase from *Formosa* sp. nov strain Hel1\_33\_131 (FbGH30) were obtained from Prof. Dr Jan-Hendrik Hehemann (Center for Marine Environmental Sciences, University of Bremen, Germany) at a concentration of  $5 \mu\text{g}\cdot\text{mL}^{-1}$  in water (Becker et al., 2017). For testing residual glycogen,  $\alpha$ -amylase (E-BAASS, Megazyme) was prepared in a stock concentration of  $1.25 \text{ mg}\cdot\text{mL}^{-1}$  using 50% (v/v) glycerol.

## FITC488 labeling and confocal microscopy

FITC488 labeling of SiWSC3 and SiFGB1 and confocal laser scanning microscopy was done as described previously (Wawra et al., 2019) using the KPL SureLink Fluorescein-X (FAM-X) labeling kit (#82-00-02) by Sera Care with the following modification for SiWSC3 labeling: 20-min incubation time at 20°C with half of the recommended concentration. The reaction was stopped by adding 1-M TRIS (pH 7.5) to a final concentration of 50 mM and then dialyzed overnight against 3 L of Milli-Q water. Modifications to the standard labeling protocol were necessary because over labeling reduced the ability of the SiWSC3 to bind to its substrate (Wawra et al., 2019).

## Microbial strains and culture conditions for EPS matrix production in *S. indica* and *B. sorokiniana*

The EPS matrix was isolated from the *S. indica* strain expressing GFP in the dikaryotic wild-type background DSM11827 (Wawra et al., 2016) and from the *B. sorokiniana* wild-type strain ND90r. *Serendipita indica* spores were isolated from 3-week-old cultures grown on solid complex medium (Si\_CM) using 0.002% (v/v) Tween water (Zuccaro et al., 2011). For the preculture, 2 mL of *S. indica* spores at a concentration of  $500,000 \text{ mL}^{-1}$  were inoculated in 100 mL of TSB medium containing 1% (w/v) sucrose and shaking at 120 rpm at 28°C. After 48 h, the pre-cultures were transferred to 400 mL of TSB containing 1% sucrose and shaken at 120 rpm at 28°C for 72 h. *Bipolaris sorokiniana* spores were isolated from 10-day-old cultures grown on solid complete medium (Bs\_CM), using 0.002% (v/v) Tween water (Sarkar et al., 2019). The spores were inoculated at a final concentration of  $250 \text{ spores}\cdot\text{mL}^{-1}$  in 250 mL of YPD medium and these samples were shaken at 28°C for 36 h.

## Isolation of EPS matrix from *S. indica* and *B. sorokiniana* culture supernatant

Culture supernatants from axenically grown *S. indica* or *B. sorokiniana* were collected by filtering the mycelia using Miracloth (Merck Millipore). The EPS matrix was isolated from the culture media using cryogelation. Briefly, the culture media were frozen overnight at  $-20^\circ\text{C}$  and slowly thawed at room temperature for 16 h. The precipitated EPS



matrix (Supplemental Figure S1) present in the culture medium was isolated using a pipette controller and washed four times with 30 mL of Milli-Q water and either used for proteome analyses (see section “Proteome analysis of *S. indica* EPS matrix, CW, and culture filtrate”) or washed one more time with 30 mL of 8.3-mM EDTA (pH 8.0) to remove metal ions potentially present in the EPS. The proteins present in the EPS matrix were removed by treatment with 30 mL of protein denaturation solution (containing 8-M urea, 2-M thiourea, 4% [w/v] sodium dodecyl sulfate [SDS], 100-mM Tris-HCl, pH 7.5) and boiling at 95°C for 15 min. The SDS present in the EPS matrix was removed by boiling the material with 30 mL of Milli-Q water at 95°C for 10 min and centrifuging at 10,000g for 10 min at room temperature. The latter step was repeated approximately 15 times until no further foaming occurred. The resulting protein-free EPS matrix was lyophilized and used for glycosyl linkage, TLC or MALDI-TOF analyses.

#### Proteome analysis of *S. indica* EPS matrix, CW, and culture filtrate

The proteins were isolated from the EPS matrix, CW, and the culture filtrate obtained from axenic cultures of *S. indica* strain expressing GFP grown in different media (CM, YPD, and TSB).

#### Protein isolation from the CW

Mycelium collected from the *S. indica* GFP strain was ground in liquid N<sub>2</sub> and resuspended in PBS buffer containing 1-mM PMSF and 1% (v/v) NP-40 using an ULTRA-TURRAX (IKA, Staufen, Germany). The resuspended mixture was incubated at 4°C in a rotating wheel for 30 min. The pellet obtained after centrifugation at 8,000g for 15 min at 4°C was resuspended in PBS buffer containing 1-mM PMSF and 0.1% (v/v) IGEPAL using an ULTRA-TURRAX. The pellet obtained after centrifugation at 8,000g for 15 min at 4°C was washed three times with Milli-Q water. Finally, the pellet was resuspended in Laemmli buffer containing 8-M urea, 2-M thiourea, and β-mercaptoethanol and boiled at 95°C for 10 min.

#### Protein isolation from the EPS matrix

The EPS matrix obtained from the culture media by cryogelation was washed four times with Milli-Q water and was directly boiled in Laemmli buffer containing 8-M urea, 2-M thiourea, and β-mercaptoethanol at 95°C for 10 min.

#### Protein isolation from the culture filtrate

The culture supernatant left over from the EPS matrix isolation step was first filtered using a Whatman filter paper and then using a 0.22-μm syringe filter. Approximately 30 mL of EPS matrix depleted culture supernatant was treated with 5 mL of 95% (v/v) trichloroacetic acid and incubated overnight at 4°C. The precipitated proteins were collected by centrifugation (10,000g) for 1 h at 4°C. The isolated proteins were washed at least three times with 100% (v/v) acetone.

The dried protein pellet was resuspended in Laemmli buffer containing 8-M urea, 2-M thiourea, and β-mercaptoethanol and boiled at 95°C for 10 min.

#### Liquid chromatography coupled mass spectrometric protein identification and quantification

The proteins isolated from the EPS matrix, CW and culture filtrate were separated using a 10% (v/v) SDS-polyacrylamide gel electrophoresis gel for 15 min and subsequently stained with Coomassie Brilliant Blue. Protein-containing bands from Coomassie-stained gels were prepared for mass spectrometric analysis as described elsewhere (Poschmann *et al.*, 2014). Briefly, bands were destained and the proteins were reduced with dithiothreitol and alkylated with iodoacetamide and subjected to tryptic digestion. The resulting peptides were extracted and reconstituted in 0.1% (v/v) trifluoroacetic acid in water. Peptides were separated on an Ultimate 3000 Rapid Separation Liquid Chromatography system (Thermo Fisher Scientific) on a 25-cm length C18 column using a 1-h gradient and subsequently analyzed by a QExactive Plus mass spectrometer (Thermo Fisher Scientific) as described with minor modifications (Poschmann *et al.*, 2014). First, survey scans were carried out at a resolution of 140,000 and up to 22- and 3-fold charged precursors selected by the quadrupole (4 *m/z* isolation window), fragmented by higher energy collisional dissociation and fragment spectra recorded at a resolution of 17,500. Mass spectrometric data were further processed by MaxQuant 1.6.12.0 (Max-Planck Institute for Biochemistry, Planegg, Germany) with standard parameters if not otherwise stated. Label-free quantification, “match between runs” and iBAQ quantification were enabled. Searches were carried out based on *S. indica* reference protein entries (UP000007148), downloaded on 15 May 2020 from the UniProt Knowledge Base. Carbamidomethylation at cysteines was considered as fixed and methionine oxidation and proteins N-terminal acetylation as variable modifications. Peptides and proteins were accepted at a false discovery rate of 1% and only proteins further considered were identified with at least two different peptides. The identified proteins were grouped into families using the Pfam database (Mistry *et al.*, 2021). The mass spectrometry proteomics data have been deposited to the ProteomeXchange Consortium via the PRIDE partner repository with the dataset identifier PXD025640.

#### Proteome analysis of *S. indica* EPS matrix, CW, and culture filtrate

Further calculations were done on label-free quantification (LFQ) intensity values. Only proteins were considered showing at least two valid intensity values at least in one group. LFQ intensity values were log<sub>2</sub> transformed and missing values imputed with values drawn from a downshifted normal distribution (width 0.3, downshift 1.8) before statistical and enrichment analysis. Statistical analysis was done for selected protein groups using the significance analysis of microarrays method (Tusher *et al.*, 2001; 5% false discovery rate,

$S_0 = 0.1$ ) and Student's *t* test. To identify proteins containing certain domains showing a higher abundance in the EPS matrix, we performed an annotation enrichment analysis (Cox and Mann, 2012) based on the differences of mean values of log<sub>2</sub> transformed LFQ intensities.

The percentage relative abundance of signal peptide containing proteins detected in the three components (EPS matrix, CW, and culture filtrate) was calculated using LFQ intensities.

#### Large scale digestion and enrichment of the $\beta$ -GD released from the EPS matrix of *S. indica* and *B. sorokiniana*

Five milligram of freeze-dried EPS matrix obtained from *S. indica* or *B. sorokiniana* were ground with two stainless steel beads (5 mm) using a TissueLyser (Qiagen, Hilden, Germany) at 30 Hz for 1 min at room temperature and soaked in 1 mL of 100-mM sodium acetate buffer (pH 5.0) at 70°C overnight. The soaked material was incubated with 20  $\mu$ L (50 U) of H $\nu$ BGLUII in a total reaction volume of 1 mL using 100-mM sodium acetate buffer (pH 5.0). The digestion was performed at 40°C with shaking at 500 rpm for 48 h. The supernatant containing the  $\beta$ -GD was collected by centrifugation at 10,000g for 5 min at room temperature. The digested pellet was additionally suspended in 1 mL of water and heated at 80°C for 10 min to solubilize additional  $\beta$ -GD. The resulting supernatant was combined with the initial digested material and boiled at 95°C for 15 min. The precipitated proteins were removed by centrifugation at 10,000g for 20 min at room temperature and the debris were removed using a 0.45- $\mu$ m syringe filter. The clear supernatant fraction was freeze-dried. The freeze-dried material was dialyzed against 3 L of Milli-Q water at 4°C using a 1-kDa cutoff dialysis tubing (Repligen Spectra/Por 6 Pre-Wetted Regenerated Cellulose, cat. no. 888-11461). The dialyze was lyophilized before further use.

#### Preparation of alcohol insoluble residue and protein-free CW from *S. indica* and *B. sorokiniana*

The mycelium collected from axenic cultures of *S. indica* or *B. sorokiniana* was washed twice with Milli-Q water and freeze-dried overnight. The freeze-dried material was powdered in liquid N<sub>2</sub> using a pestle and mortar and stored at -20°C until use. Twenty milligrams of the material was resuspended in 1 mL of 70% (v/v) aqueous ethanol with a stainless steel bead (5 mm) using a TissueLyser at 30 Hz for 1 min. After centrifugation at 10,000g for 20 min at room temperature, the pellet was washed with chloroform/methanol (1:1), then acetone and subsequently air-dried. Protein-free fungal wall material was prepared as mentioned previously (Wawra *et al.*, 2016).

#### Glycosyl linkage analysis of EPS matrices and CW preparations

EPS matrix (2 mg) or CW preparation of *S. indica* or *B. sorokiniana* were ground with a stainless steel bead (5 mm)

using a TissueLyser mill at 30 Hz for 1 min. The powdered material was subjected to glycosyl linkage analysis as described (Liu *et al.*, 2015). Briefly, a methylation reaction was performed using NaOH/DMSO. The methylated compounds were hydrolyzed in 1 M trifluoroacetic acid, reduced using sodium borodeuteride (ACROS Organics, cat.no. 194950050) and per-*o*-acetylated. The resulting partially methylated alditol acetates were analyzed using an Agilent 5977A GC/MSD System equipped with a SP-2380 Fused Silica Capillary Column (Supelco). The glycosidic linkages were assigned based on retention time and mass spectrum fragmentation patterns compared to the CCRC spectral database (<https://www.ccrucga.edu/specdb/ms/pmaa/pframe.html>).

#### Digestion of EPS matrix and CW and TLC analysis

Freeze-dried EPS matrix (1 mg) or CW preparation (1 mg) from *S. indica* or *B. sorokiniana* were suspended in 400  $\mu$ L of 2-mM sodium acetate (pH 5.0; for TLE), 2-mM MES (pH 5.0; for *H. pomatia*  $\beta$ -1,3-glucanase), or 100-mM sodium acetate (pH 5.0; for H $\nu$ BGLUII) at 70°C overnight. The excess buffer was removed and the suspended material was treated with 5  $\mu$ L of the glucanase enzymes (0.125 mg·mL<sup>-1</sup> or 12.5 U for H $\nu$ BGLUII) in the respective buffers, containing 1  $\mu$ L of BSA (100 mg·mL<sup>-1</sup>) in a total reaction volume of 50  $\mu$ L and incubated at 40°C by shaking at 500 rpm for 16 h. The digestion reaction was stopped by incubating the samples at 95°C for 10 min. An aliquot was subjected to TLC using a silica gel 60 F254 aluminum TLC plate (Merck Millipore, cat. no. 105554), with a running buffer containing ethyl acetate/acetic acid/methanol/formic acid/water in a ratio of 80:40:10:10:10 (v/v). D-glucose, laminaribiose  $\beta$ -1-3-(Glc)<sub>2</sub>, laminaritriose  $\beta$ -1-3-(Glc)<sub>3</sub>, gentiobiose  $\beta$ -1-6-(Glc)<sub>2</sub>, and laminaripentaose  $\beta$ -1-3-(Glc)<sub>5</sub> with a concentration of 1.5 mg·mL<sup>-1</sup> were used as standards. The glucan fragments were visualized by spraying the TLC plate with glucan developer solution (containing 45-mg N-naphthol, 4.8-mL H<sub>2</sub>SO<sub>4</sub>, 37.2-mL ethanol, and 3-mL water) and heating the TLC plate to 100°C until the glucan bands were visible (~4–5 min).

#### MALDI-TOF analysis

##### Analysis of the $\beta$ -GD from *S. indica*

Freeze-dried  $\beta$ -GD was solubilized in water at 70°C for 10 min.

##### Structural characterization of the $\beta$ -GD from *S. indica* and *B. sorokiniana*

Ten microliters of  $\beta$ -GD (2 mg·mL<sup>-1</sup>) was treated with 2  $\mu$ L of FaGH17a or 2- $\mu$ L FbGH30 or 1  $\mu$ L of FaGH17a + 1  $\mu$ L FbGH30 in 50  $\mu$ L of Milli-Q water. The digestion reaction was carried out at 40°C for 16 h and the reaction was stopped by incubation at 95°C for 5 min.

##### Analysis of oligosaccharides released from the EPS matrix and CW of *S. indica*

Freeze-dried EPS matrix (1 mg) or CW preparation (1 mg) isolated from *S. indica* were suspended in 400  $\mu$ L of a 2-mM



sodium acetate buffer, pH 5.0 (TLE), 2-mM MES buffer, pH 5.0 (*H. pomatia*  $\beta$ -1,3-glucanase), or 25-mM sodium acetate buffer, pH 5.0 (*HvBGLUII*) and incubated at 70°C overnight. The suspended material was treated with 2.5  $\mu$ L of TLE, 2.5  $\mu$ L of *H. pomatia*  $\beta$ -1,3-glucanase, or 1  $\mu$ L of *HvBGLUII* in the respective buffers, as described before, in a total reaction volume of 50  $\mu$ L. The digestion was performed at 40°C with shaking at 500 rpm for 16 h. The digestion reaction was stopped at 95°C for 10 min and centrifuged at 11,000g for 5 min at room temperature.

#### Analysis of oligosaccharides released from the EPS matrix and CW of *B. sorokiniana*

Freeze-dried EPS matrix (1 mg) or CW preparation (1 mg) isolated from *B. sorokiniana* were solubilized in 400  $\mu$ L of 2-mM sodium acetate, pH 5.0 (TLE) or 25-mM sodium acetate, pH 5.0 (*HvBGLUII*). The solubilized material was treated with 1  $\mu$ L of TLE or 1  $\mu$ L of *HvBGLUII* in a total reaction volume of 50  $\mu$ L. The digestion was performed at 40°C with shaking at 500 rpm for 16 h. The digestion reaction was stopped at 95°C for 10 min.

#### Mass spectrometrical analysis

The oligosaccharides present in the prepared samples were analyzed by Oligosaccharide Mass Profiling as described (Günl *et al.*, 2011). Briefly, the samples were spotted onto a dried spot of dihydroxy benzoic acid matrix (10 mg·mL<sup>-1</sup>) and analyzed by MALDI-TOF mass spectrometry (Bruker rapifleX instrument). The machine was set to linear, positive reflectron mode with an accelerating voltage of 20,000 V. The spectra from the samples were analyzed using flexanalysis software 4.0 (Bruker Daltonics).

#### Reduction and purification of *S. indica* $\beta$ -GD

Enriched  $\beta$ -GD (40 mg) was reduced with sodium borodeuteride (20 mg·mL<sup>-1</sup>; ACROS Organics, cat.no. 194950050) in 1-M ammonium hydroxide for 90 min at room temperature. The reaction was neutralized by addition of glacial acetic acid and 9:1 (v/v) methanol:acetic acid. The solvents were evaporated under N<sub>2</sub> gas. The dried material was washed once with 9:1 (v/v) methanol:acetic acid and three times with methanol. In each washing step, the methanol:acetic acid or methanol were evaporated under N<sub>2</sub> gas. The dried material was dissolved in 6% (v/v) aqueous methanol, vortexed, and centrifuged at 4,000g for 15 min at room temperature, to remove any occurring debris. The supernatant (50  $\mu$ L) was subjected to reverse-phase chromatography using a Vydac 238 TP C18 column (Vydac, Hesperia, CA, USA) eluting with a linear gradient from 6% (v/v) to 12% (v/v) methanol in 10 min, followed by 12% (v/v) to 50% (v/v) methanol in 10 min and equilibrated back to 6% (v/v) methanol in 10 min with a flow rate of 0.5 mL·min<sup>-1</sup>. The eluting compounds were detected by an evaporative light scattering detector (ERC GmbH, Munich, Germany) at 38°C and simultaneously collected for MALDI-TOF analyses. Collected fractions containing the  $\beta$ -GD were pooled and freeze-dried.

#### <sup>1</sup>H NMR analysis

Reduced  $\beta$ -GD (1 mg) was dissolved in D<sub>2</sub>O (100% atom D, ACROS Organics, 320700075) at 80°C for 10 min and subsequently freeze-dried overnight. The freeze-dried material was dissolved in 300  $\mu$ L of 6:1 (v/v) of methyl sulphoxide D6 (99.9% atom D + 1% tetramethylsilane, ACROS Organics):D<sub>2</sub>O (100% atom D, ACROS Organics, 320700075) at 80°C for 10 min. The <sup>1</sup>H NMR spectrum of the reduced  $\beta$ -GD was measured using a 600 MHz Bruker NMR spectrometer at 80°C (Kim *et al.*, 2000). The chemical shift signal was referred to the internal standard tetramethylsilane at 0 ppm and the <sup>1</sup>H NMR spectrum was processed using Bruker's Topspin software.

#### Purification of native $\beta$ -GD for the ROS burst assay

Enriched  $\beta$ -GD (40 mg) was dissolved in 6% (v/v) aqueous methanol, vortexed, and centrifuged to remove any debris. The  $\beta$ -GD was purified as described above but without reduction and used for the ROS burst assays if not otherwise stated in the legend.

#### Preparation of crude fungal CW substrates for immunity assays

For crude extraction of soluble fragments from the fungal CW and EPS matrix, 5 mg of the respective fungal substrate was transferred to a 2-mL Eppendorf tube with three stainless steel beads (5 mm), snap-frozen in liquid nitrogen and ground with a TissueLyser (1 min, 30 Hz). The ground substrate was resuspended in 2 mL of Milli-Q water, incubated at 70°C for 16 h (700 rpm), and then boiled at 95°C for 10 min. The volume was filled up to 5 mL for a final concentration of 1 mg·mL<sup>-1</sup>. The suspension was centrifuged at 13,000g for 10 min at room temperature and the supernatant was further used in plant immunity assays.

#### Plant immunity assays

##### Preparation of immunity assays

For immunity assays using barley, roots were separated from 7-day-old seedlings (cut 2 cm below seed), root tips were removed (first 1 cm), and residual roots were cut into 5-mm pieces. Each assay was performed with randomized root pieces from 16 barley seedlings. Four root pieces were transferred into each well of a 96-well plate microtiter plate containing Milli-Q water. For immunity assays with Arabidopsis (wild-type or aequorin-expressing lines), intact 14-day-old seedlings were transferred into a 96-well plate (one seedling/well) filled with Milli-Q water.

##### Elicitors

Chitohexase was purchased from Megazyme (Bray, Ireland), flg22 from GenScript (Piscataway, NJ, USA), and laminarin from Sigma-Aldrich (Taufkirchen, Germany). All commercial substrates were dissolved in Milli-Q water without additional treatment. Substrates derived from fungal CW and EPS were prepared as described earlier. The elicitor solutions had the following pH  $\pm$  SD ( $n = 3$ ): Milli-Q water = 7.20  $\pm$  0.125; EPS

matrix prep1 =  $7.30 \pm 0.322$ ; EPS matrix prep2 =  $7.37 \pm 0.167$ ;  $\beta$ -GD =  $6.96 \pm 0.212$ ; Chit6 =  $7.32 \pm 0.106$ .

#### Cytosolic calcium influx measurements

The solution in the 96-well plates containing the plant material (*Arabidopsis* seedlings expressing aequorin, see above) was exchanged for 100  $\mu$ L of a 10- $\mu$ M coelenterazine solution (Roth, Karlsruhe, Germany). After overnight incubation in the dark, the plates were transferred to a TECAN SPARK 10M multi-well plate reader. After baseline measurement (5 min), 50  $\mu$ L of a three-fold concentrated elicitor solution was manually added to the wells and luminescence was measured for 30 min. Residual aequorin was discharged with 100  $\mu$ L of 2.5-m CaCl<sub>2</sub> (in 25% [v/v] ethanol) and luminescence was detected for 1 min. All measurements were performed with an integration time of 300 ms. Baseline luminescence and elicitor-triggered luminescence were normalized according to the maximal integrated discharge value obtained from individual wells.

#### ROS assay

The ROS assay is based on previously published protocols (Felix et al., 1999; Wanke et al., 2020; Ngou et al., 2021). In detail, 96-well plate with plant material (see above) were incubated overnight at room temperature on the bench to remove ROS and other contaminants originating from the mechanical damage of the tissue during preparation. The next day, water was replaced by 100  $\mu$ L of fresh Milli-Q water containing 20  $\mu$ g·mL<sup>-1</sup> horseradish peroxidase (Sigma-Aldrich, Taufkirchen, Germany) and 20- $\mu$ M L-012 (Wako Chemicals, Neuss, Germany). Following a short incubation time (~15 min), 100  $\mu$ L of double-concentrated elicitor solutions were added to the wells. Measurements of elicitor-triggered apoplastic ROS production were started immediately and taken continuously with an integration time of 450 ms using a TECAN SPARK 10 M multi-well plate reader. Horseradish peroxidase catalyzes the oxidation of the luminol derivative L-012 by the plant-produced ROS species upon elicitation with MAMPs. This leads to a chemiluminescent signal that is detected by the plate reader.

#### Gene expression analysis

After the ROS burst assay (1 h after elicitor addition), plant material from three to four wells was pooled, dried on tissue paper and snap-frozen in liquid nitrogen for further analysis of gene expression changes. Total RNA was extracted using TRIzol reagent (Invitrogen, Karlsruhe, Germany) and contaminating gDNA was digested during a DNaseI treatment (Thermo Fisher Scientific, Schwerte, Germany) according to manufacturers' instructions. Synthesis of cDNA was carried out using the First Strand cDNA Synthesis Kit (Thermo Fisher Scientific, Schwerte, Germany) without changes to the manufacturer's protocol. Target gene expression was analyzed by reverse transcription-quantitative polymerase chain reaction (RT-qPCR) as described previously (Wawra et al., 2019). Relative expression of elicitor-responsive *HvWRKY2* gene

(Shen et al., 2007) compared to *H. vulgare* ubiquitin gene (Sarkar et al., 2019) was determined using the following primer pairs: *HvUBI\_F* (5'-ACCCTCGCCGACTACAACAT-3') with *HvUBI\_R* (5'-CAGTAGTGGCGGTCTGAAGT-3') and *HvWRKY2\_F* (5'-AACAACCACCACCAGTCGTT-3') with *HvWRKY2\_R* (5'-TCACCTTCTGCCCGTACTTC-3'). Gene expression levels in elicitor-treated samples were normalized to the expression levels in mock-treated samples.

#### In vitro DAB oxidation assay

DAB assay was performed as previously described (Nostadt et al., 2020). Sugar substrates (concentrations as indicated) were mixed with 0.05- $\mu$ M horseradish peroxidase (Sigma-Aldrich, Taufkirchen, Germany) and 1-mM H<sub>2</sub>O<sub>2</sub> (Sigma-Aldrich, Taufkirchen, Germany) in reaction buffer (50-mM sodium acetate, 150-mM NaCl, pH 5) and incubated for 10 min at room temperature in a 96-well plate. Then, an equal volume of a 200- $\mu$ M DAB solution was added to the wells. After 16 h of incubation in the dark, plates were scanned on a flatbed scanner (transmissive light mode).

#### Fenton reaction-based oxidation of sugars

The assay was performed as previously described (Matros et al., 2015). Carbohydrate samples (300  $\mu$ M) were mixed with Fenton reagents (1-mM H<sub>2</sub>O<sub>2</sub> [Sigma], 100- $\mu$ M FeSO<sub>4</sub> [Sigma]) and incubated overnight at 30°C. Control samples with an additional 100- $\mu$ M EDTA (Sigma) or without Fenton reagents were treated in the same way. Samples were centrifuged at 13,000g for 10 min at room temperature and the supernatant was further analyzed by MALDI-TOF.

#### Colonization assay with $\beta$ -GD

Roots of 4-day-old barley seedlings were inoculated with 3 mL of *S. indica* spores at a concentration of 500,000 mL<sup>-1</sup> and grown at a day/night cycle of 16 h/8 h at 22°C/18°C, 60% humidity, and 108  $\mu$ mol m<sup>-2</sup> s<sup>-1</sup> light intensity. At 1 and 2 dpi, 1 mL of sterile water as a control or 100- or 300- $\mu$ M  $\beta$ -GD were added to the jars which contained four seedlings each. The seedlings of each jar were pooled and harvested at 3 dpi. The roots were washed in ice water to remove extraradical hyphae, cut as previously described (Nizam et al., 2019), frozen in liquid nitrogen and used for RNA extraction. RNA extraction for fungal colonization, cDNA generation, and RT-qPCR was performed as previously described (Sarkar et al., 2019). For quantification of endophytic fungal colonization by RT-qPCR, the following primers were used: 5'-GCAAGTTCTCCGAGCTCATC-3' and 5'-CCAAGTGGTGGTACTCGTT-3' for *S. indica* translation-elongation factor (*SiTEF*) and 5'-ACCCTCGCCGACTACAACAT-3' and 5'-CAGTAGTGGCGGTCTGAAGTG-3' for barley ubiquitin (*HvUbi*).

#### Expression analysis of selected genes with WSC domains

Gene expression of *S. indica* WSC domain-containing proteins during root colonization of barley and *Arabidopsis* was monitored via RT-qPCR as previously described (Wawra

*et al.*, 2019) at 3, 7, and 14 dpi. For each biological replicate ( $n = 3$ ), roots from several individual plants were pooled (Arabidopsis: 60 plants; barley: 4 plants).

### Statistical analyses

A summary of statistical analyses is given in [Supplemental Data Set S10](#).

### Accession numbers

*Hordeum vulgare* BGLU2: P15737 (UniProt), HORVU.MOREX.r3.3HG0319100.1 (MorexV3\_pseudomolecules\_assembly, EnsemblePlants).

### Supplemental data

The following materials are available in the online version of this article.

**Supplemental Figure S1.** EPS matrix isolated from *S. indica* grown in CM medium using a cryogelation approach.

**Supplemental Figure S2.** Proteome analysis of *S. indica* EPS matrix, CW, and culture filtrate.

**Supplemental Figure S3.** Expression analysis of selected genes with WSC domains in *S. indica* during plant colonization at 3, 7, and 14 dpi.

**Supplemental Figure S4.** Glycosyl linkage analysis of *Si* EPS and *Si* CW.

**Supplemental Figure S5.** Analysis of oligosaccharides released from the EPS or protein-free CW of *S. indica* by the action of  $\beta$ -1,3-glucanases.

**Supplemental Figure S6.** Glycosyl linkage and MALDI-TOF analysis of the glucan fraction ( $\beta$ -GD) released from the EPS matrix of *S. indica*.

**Supplemental Figure S7.** Purification of the  $\beta$ -GD fragment for  $^1\text{H}$  NMR analysis.

**Supplemental Figure S8.** Mechanically released fragments from *S. indica* EPS matrix and CW layer do not exhibit ROS scavenging activity.

**Supplemental Figure S9.** Chitohexaose-triggered ROS accumulation is decreased by *S. indica*  $\beta$ -GD treatment in a concentration-dependent manner.

**Supplemental Figure S10.** Purification of native  $\beta$ -GD and immunogenic characterization.

**Supplemental Figure S11.** Detoxification of apoplastic ROS by *S. indica*  $\beta$ -GD is independent of elicitor treatment and plant species.

**Supplemental Figure S12.** *Serendipita indica*  $\beta$ -GD treatment does not trigger cytosolic calcium influx in *A. thaliana* seedlings.

**Supplemental Figure S13.** Digestion of laminariheptaose with *Hv*BGLUII enhances ROS production in barley roots.

**Supplemental Figure S14.** Glycan controls are not degraded by hydrogen peroxide during Fenton reaction.

**Supplemental Figure S15.** Glycosyl linkage analysis of *B. sorokiniana* EPS matrix and CW.

**Supplemental Figure S16.** Analysis of oligosaccharides released from the EPS of *B. sorokiniana* by the action of *Trichoderma harzianum* lysing enzymes.

**Supplemental Figure S17.** The  $\beta$ -GD released from the EPS matrix of *B. sorokiniana* consists of a seven unit  $\beta$ -1,3-linked glucan backbone substituted with three  $\beta$ -1,6-glucosyl residues.

**Supplemental Figure S18.** Mechanically released fragments from *B. sorokiniana* EPS matrix or CW do not scavenge ROS.

**Supplemental Data Set S1.** Total proteins detected in the proteome analysis of the EPS matrix, CW, and culture filtrate isolated from *S. indica* grown in CM, TSB, or YPD liquid media.

**Supplemental Data Set S2.** Relative abundance of signal peptide (SP) containing proteins detected in the EPS matrix, CW, and culture filtrate isolated from the *S. indica* under three culture mediums: CM, TSB, and YPD. LFQ intensities of the proteins were used to calculate their relative abundance.

**Supplemental Data Set S3.** Statistics, enrichment score, Benjamini–Hochberg corrected *P*-value.

**Supplemental Data Set S4.** Glycosyl sugar residues detected in the total ion chromatogram of EPS matrix isolated from *S. indica*,  $n = 4$  independent biological replicates.

**Supplemental Data Set S5.** Glycosyl sugar residues detected in the total ion chromatogram of alcohol insoluble residue (cell wall) isolated from *S. indica*,  $n = 4$  independent biological replicates.

**Supplemental Data Set S6.** List of Barley CAZymes detected in the root apoplastic fluids (AFs) of barley after mock, *S. indica* or *B. sorokiniana* treatments.

**Supplemental Data Set S7.** Glycosyl sugar residues detected in the total ion chromatogram of alcohol insoluble residue (cell wall) isolated from *B. sorokiniana*,  $n = 3$  independent biological replicates.

**Supplemental Data Set S8.** Glycosyl sugar residues detected in the total ion chromatogram of EPS matrix isolated from *B. sorokiniana*,  $n = 3$  independent biological replicates.

**Supplemental Data Set S9.** List of Barley CAZymes differentially regulated during *B. sorokiniana* infection.

**Supplemental Data Set S10.** Summary of statistical analyses.

### Acknowledgments

The authors would like to thank Katharina Lufen, Institute for Plant Cell Biology and Biotechnology, Heinrich Heine University, Düsseldorf for excellent technical assistance and Alba Silipo Department of Chemical Sciences, University of Napoli Federico II for initial support with the sugar analyses. We thank Gereon Poschmann, Anja Stefanski, Thomas Lenz and Kai Stühler, Institute of Molecular Medicine, Proteome research facility, Medical Faculty and University Hospital Düsseldorf for excellent proteomics. NMR analysis was performed at the Center for Molecular and Structural Analytics at the Heinrich Heine University, Düsseldorf. We further thank Jan-Hendrik Hehemann for providing aliquots of *Fa*GH17a and *Fb*GH30.



## Funding

A.Z. and L.M. acknowledge support from the Cluster of Excellence on Plant Sciences (CEPLAS) funded by the Deutsche Forschungsgemeinschaft (DFG, German Research Foundation) under Germany's Excellence Strategy–EXC 2048/1–Project ID: 390686111 and projects ZU 263/11-1 (SPP 2125 DECrypT).

*Conflict of interest statement.* The authors have no conflicts of interest.

## References

- Adams EL, Rice PJ, Graves B, Ensley HE, Yu H, Brown GD, Gordon S, Monteiro MA, Papp-Szabo E, Lowman DW, et al. (2008) Differential high-affinity interaction of dectin-1 with natural or synthetic glucans is dependent upon primary structure and is influenced by polymer chain length and side-chain branching. *J Pharmacol Exp Therap* **325**: 115–123
- Becker S, Scheffel A, Polz MF, Hehemann J-H (2017) Accurate quantification of laminarin in marine organic matter with enzymes from marine microbes. *Appl Environ Microbiol* **83**: e03389–16
- Benaroudj N, Lee DH, Goldberg AL (2001) Trehalose accumulation during cellular stress protects cells and cellular proteins from damage by oxygen radicals. *J Biol Chem* **276**: 24261–24267
- Boller T, Felix G (2009) A renaissance of elicitors: perception of microbe-associated molecular patterns and danger signals by pattern-recognition receptors. *Annu Rev Plant Biol* **60**: 379–406
- Boulos S, Nystrom L (2017) Complementary sample preparation strategies for analysis of cereal beta-glucan oxidation products by UPLC-MS/MS. *Front Chem* **5**: 90
- Brown GD, Gordon S (2005) Immune recognition of fungal  $\beta$ -glucans. *Cell Microbiol* **7**: 471–479
- Buscaill P, van der Hoorn RAL (2021) Defeated by the nines: nine extracellular strategies to avoid MAMP recognition in plants. *Plant Cell* (in press)
- Choi J, Tanaka K, Cao Y, Qi Y, Qiu J, Liang Y, Lee SY, Stacey G (2014) Identification of a plant receptor for extracellular ATP. *Science* **343**: 290–294
- Ciucanu I (2006) Per-O-methylation reaction for structural analysis of carbohydrates by mass spectrometry. *Analyt Chim Acta* **576**: 147–155
- Cox J, Mann M (2012) 1D and 2D annotation enrichment: a statistical method integrating quantitative proteomics with complementary high-throughput data. *BMC Bioinform* **13** (Suppl 16): S12
- El Oirdi M, El Rahman TA, Rigano L, El Hadrami A, Rodriguez MC, Daayf F, Vojnov A, Bouarab K (2011) Botrytis cinerea manipulates the antagonistic effects between immune pathways to promote disease development in tomato. *Plant Cell* **23**: 2405–2421
- Felix G, Duran JD, Volko S, Boller T (1999) Plants have a sensitive perception system for the most conserved domain of bacterial flagellin. *Plant J* **18**: 265–276
- Fesel PH, Zuccaro A (2016)  $\beta$ -glucan: crucial component of the fungal cell wall and elusive MAMP in plants. *Fungal Genet Biol* **90**: 53–60
- Fliegmann J, Mithofer A, Wanner G, Ebel J (2004) An ancient enzyme domain hidden in the putative beta-glucan elicitor receptor of soybean may play an active part in the perception of pathogen-associated molecular patterns during broad host resistance. *J Biol Chem* **279**: 1132–1140
- Geoghegan I, Steinberg G, Gurr S (2017) The role of the fungal cell wall in the infection of plants. *Trends Microbiol* **25**: 957–967
- Goodridge HS, Wolf AJ, Underhill DM (2009) Beta-glucan recognition by the innate immune system. *Immunol Rev* **230**: 38–50
- Gow NAR, Latge JP, Munro CA (2017) The fungal cell wall: structure, biosynthesis, and function. *Microbiol Spectr* **5**
- Gravelat FN, Beauvais A, Liu H, Lee MJ, Snarr BD, Chen D, Xu W, Kravtsov I, Hoareau CM, Vanier G, et al. (2013). Aspergillus galactosaminogalactan mediates adherence to host constituents and conceals hyphal beta-glucan from the immune system. *PLoS Pathog* **9**: e1003575
- Günl M, Kraemer F, Pauly M (2011) Oligosaccharide mass profiling (OLIMP) of cell wall polysaccharides by MALDI-TOF/MS. *Methods Mol Biol* **715**: 43–54
- Ham K-S, Wu S-C, Darvill AG, Albersheim P (1997) Fungal pathogens secrete an inhibitor protein that distinguishes isoforms of plant pathogenesis-related endo- $\beta$ -1,3-glucanases. *Plant J* **11**: 169–179
- Han B, Baruah K, Cox E, Vanrompay D, Bossier P (2020) Structure-functional activity relationship of  $\beta$ -glucans from the perspective of immunomodulation: a mini-review. *Front Immunol* **11**: 658
- Kang X, Kirui A, Muszynski A, Widanage MCD, Chen A, Azadi P, Wang P, Mentink-Vigier F, Wang T (2018) Molecular architecture of fungal cell walls revealed by solid-state NMR. *Nat Commun* **9**: 2747
- Kim YT, Kim EH, Cheong C, Williams DL, Kim CW, Lim ST (2000) Structural characterization of beta-D-(1  $\rightarrow$  3, 1  $\rightarrow$  6)-linked glucans using NMR spectroscopy. *Carbohydr Res* **328**: 331–341
- Lahrmann U, Ding Y, Banhara A, Rath M, Hajirezaei MR, Döhlemann S, Wirén Nv, Parniske M, Zuccaro A (2013) Host-related metabolic cues affect colonization strategies of a root endophyte. *Proc Natl Acad Sci USA* **110**: 13965–13970
- Lei N, Wang M, Zhang L, Xiao S, Fei C, Wang X, Zhang K, Zheng W, Wang C, Yang R, Xue F (2015) Effects of low molecular weight yeast beta-glucan on antioxidant and immunological activities in mice. *Int J Mol Sci* **16**: 21575–21590
- Leubner-Metzger G, Meins F (1999) Functions and regulation of plant  $\beta$ -1,3-glucanases (PR-2): pathogenesis-related proteins in plants. In SK Datta, S Muthukrishnan, eds, Pathogenesis-related Proteins in Plants. CRC Press LLC, Boca Raton, FL, pp 49–76
- Liu D, Leib K, Zhao P, Kogel K-H, Langen G (2014) Phylogenetic analysis of barley WRKY proteins and characterization of HvWRKY1 and -2 as repressors of the pathogen-inducible gene HvGER4c. *Mol Genet Genomics* **289**: 1331–1345
- Liu L, Paulitz J, Pauly M (2015) The presence of fucogalactoxyloglucan and its synthesis in rice indicates conserved functional importance in plants. *Plant Physiol* **168**: 549–560
- Lowman DW, West LJ, Bearden DW, Wempe MF, Power TD, Ensley HE, Haynes K, Williams DL, Kruppa MD (2011) New insights into the structure of (1 $\rightarrow$ 3,1 $\rightarrow$ 6)- $\beta$ -D-glucan side chains in the *Candida glabrata* cell wall. *PLoS One* **6**: e27614
- Lutzoni F, Nowak MD, Alfaro ME, Reeb V, Miadlikowska J, Krug M, Arnold AE, Lewis LA, Swofford DL, Hibbett D, et al. (2018) Contemporaneous radiations of fungi and plants linked to symbiosis. *Nat Commun* **9**: 5451
- Mahdi LK, Miyauchi S, Uhlmann C, Garrido-Oter R, Langen G, Wawra S, Niu Y, Guan R, Robertson-Albertyn S, Bulgarelli D, et al. (2021) The fungal root endophyte *Serendipita vermifera* displays inter-kingdom synergistic beneficial effects with the microbiota in *Arabidopsis thaliana* and barley. *ISME J* (in press)
- Matros A, Peshev D, Peukert M, Mock H-P, Ende WVd (2015) Sugars as hydroxyl radical scavengers: proof-of-concept by studying the fate of sucralose in *Arabidopsis*. *Plant J* **82**: 822–839
- Mistry J, Chuguransky S, Williams L, Qureshi M, Salazar GA, Sonnhammer ELL, Tosatto SCE, Paladin L, Raj S, Richardson LJ, et al. (2021) Pfam: the protein families database in 2021. *Nucleic Acids Res* **49**: D412–D419
- Nars A, Lafitte C, Chabaud M, Drouillard S, Mélida H, Danoun S, Le Costauouëc T, Rey T, Benedetti J, Bulone V, et al. (2013) *Aphanomyces euteiches* cell wall fractions containing novel glucan-chitosaccharides induce defense genes and nuclear calcium

- oscillations in the plant host *Medicago truncatula*. *PLoS One* **8**: e75039
- Ngou BPM, Ahn HK, Ding P, Jones JDG** (2021) Mutual potentiation of plant immunity by cell-surface and intracellular receptors. *Nature* **592**: 110–115
- Nishizawa A, Yabuta Y, Shigeoka S** (2008) Galactinol and raffinose constitute a novel function to protect plants from oxidative damage. *Plant Physiol* **147**: 1251–1263
- Nizam S, Qiang X, Wawra S, Nostadt R, Getzke F, Schwanke F, Dreyer I, Langen G, Zuccaro A** (2019) *Serendipita indica* E5'NT modulates extracellular nucleotide levels in the plant apoplast and affects fungal colonization. *EMBO Rep* **20**: e47430
- Nostadt R, Hilbert M, Nizam S, Rovenich H, Wawra S, Martin J, Küpper I, Mijovilovich A, Ursinus A, Langen G, et al.** (2020) A secreted fungal histidine- and alanine-rich protein regulates metal ion homeostasis and oxidative stress. *New Phytol* **227**: 1174–1188
- Peshev D, Vergauwen R, Moglia A, Hideg E, Van den Ende W** (2013) Towards understanding vacuolar antioxidant mechanisms: a role for fructans? *J Exp Bot* **64**: 1025–1038
- Poschmann G, Seyfarth K, Besong Agbo D, Klafki H-W, Rozman J, Wurst W, Wiltfang J, Meyer HE, Klingenspor M, Stühler K** (2014) High-fat diet induced isoform changes of the Parkinson's disease protein DJ-1. *J Proteome Res* **13**: 2339–2351
- Rebaque D, Del Hierro I, Lopez G, Bacete L, Vilaplana F, Dallabernardina P, Pfrengle F, Jorda L, Sanchez-Vallet A, Perez R, et al.** (2021) Cell wall-derived mixed-linked beta-1,3/1,4-glucans trigger immune responses and disease resistance in plants. *Plant J* (in press)
- Rocafort M, Fudal I, Mesarich CH** (2020) Apoplastic effector proteins of plant-associated fungi and oomycetes. *Curr Opin Plant Biol* **56**: 9–19
- Rovenich H, Zuccaro A, Thomma BPHJ** (2016) Convergent evolution of filamentous microbes towards evasion of glycan-triggered immunity. *New Phytol* **212**: 896–901
- Sarkar D, Rovenich H, Jeena G, Nizam S, Tissier A, Balcke GU, Mahdi LK, Bonkowski M, Langen G, Zuccaro A** (2019) The inconspicuous gatekeeper: endophytic *Serendipita vermifera* acts as extended plant protection barrier in the rhizosphere. *New Phytol* **224**: 886–901
- Shen Q-H, Saijo Y, Mauch S, Biskup C, Bieri S, Keller B, Seki H, Ulker B, Somssich IE, Schulze-Lefert P** (2007) Nuclear activity of MLA immune receptors links isolate-specific and basal disease-resistance responses. *Science (New York, N.Y.)* **315**: 1098–1103
- Silipo A, Erbs G, Shinya T, Dow JM, Parrilli M, Lanzetta R, Shibuya N, Newman MA, Molinaro A** (2010) Glyco-conjugates as elicitors or suppressors of plant innate immunity. *Glycobiology* **20**: 406–419
- Stintzi A, Heitz T, Prasad V, Wiedemann-Merdinoglu S, Kauffmann S, Geoffroy P, Legrand M, Fritig B** (1993) Plant 'pathogenesis-related' proteins and their role in defense against pathogens. *Biochimie* **75**: 687–706
- Tada R, Adachi Y, Ishibashi K-i, Ohno N** (2009) An unambiguous structural elucidation of a 1,3-beta-D-glucan obtained from liquid-cultured *Grifola frondosa* by solution NMR experiments. *Carbohydr Res* **344**: 400–404
- Taylor JW, Berbee ML** (2006) Dating divergences in the Fungal Tree of Life: review and new analyses. *Mycologia* **98**: 838–849
- Tusher VG, Tibshirani R, Chu G** (2001) Significance analysis of microarrays applied to the ionizing radiation response. *Proc Natl Acad Sci USA* **98**: 5116–5121
- Valluru R, Van den Ende W** (2008) Plant fructans in stress environments: emerging concepts and future prospects. *J Exp Bot* **59**: 2905–2916
- Van Holle S, Van Damme EJM** (2018) Signaling through plant lectins: modulation of plant immunity and beyond. *Biochem Soc T* **46**: 217–233
- Wanke A, Malisic M, Wawra S, Zuccaro A** (2021) Unraveling the sugar code: the role of microbial extracellular glycans in plant-microbe interactions. *J Exp Bot* **72**: 15–35
- Wanke A, Rovenich H, Schwanke F, Velte S, Becker S, Hehemann J-H, Wawra S, Zuccaro A** (2020) Plant species-specific recognition of long and short  $\beta$ -1,3-linked glucans is mediated by different receptor systems. *Plant J* **102**: 1142–1156
- Wawra S, Fesel P, Widmer H, Neumann U, Lahrmann U, Becker S, Hehemann J-H, Langen G, Zuccaro A** (2019) FGB1 and WSC3 are in planta-induced  $\beta$ -glucan-binding fungal lectins with different functions. *New Phytol* **222**: 1493–1506
- Wawra S, Fesel P, Widmer H, Timm M, Seibel J, Leson L, Kesseler L, Nostadt R, Hilbert M, Langen G, et al.** (2016) The fungal-specific  $\beta$ -glucan-binding lectin FGB1 alters cell-wall composition and suppresses glucan-triggered immunity in plants. *Nat Commun* **7**: 13188
- Yuan M, Jiang Z, Bi G, Nomura K, Liu M, Wang Y, Cai B, Zhou JM, He SY, Xin XF** (2021) Pattern-recognition receptors are required for NLR-mediated plant immunity. *Nature* **592**: 105–109
- Zuccaro A, Lahrmann U, Güldener U, Langen G, Pfiffi S, Biedenkopf D, Wong P, Samans B, Grimm C, Basiewicz M, et al.** (2011) Endophytic life strategies decoded by genome and transcriptome analyses of the mutualistic root symbiont *Piriformospora indica*. *PLOS Pathogens* **7**: e1002290

## Chapter 4: *Supplementary Material*

### **Fungi hijack a ubiquitous plant apoplastic endoglucanase to release a ROS scavenging $\beta$ -glucan decasaccharide to subvert immune responses**

Balakumaran Chandrasekar<sup>1,#</sup>, Alan Wanke<sup>1,2,#</sup>, Stephan Wawra<sup>1,#</sup>, Pia Saake<sup>1</sup>, Lisa Mahdi<sup>1</sup>, Nyasha Charura<sup>1</sup>, Miriam Neidert<sup>1</sup>, Gereon Poschmann<sup>3</sup>, Milena Malisic<sup>1</sup>, Meik Thiele<sup>1</sup>, Kai Stühler<sup>4</sup>, Murali Dama, Markus Pauly<sup>5</sup>, Alga Zuccaro<sup>1</sup>

<sup>1</sup> University of Cologne, Cluster of Excellence on Plant Sciences (CEPLAS), 50679 Cologne, Germany

<sup>2</sup> Max Planck Institute for Plant Breeding Research, 50829 Cologne, Germany

<sup>3</sup> Institute of Molecular Medicine, Proteome Research, University Hospital and Medical Faculty, Heinrich Heine University Düsseldorf, 40225 Düsseldorf, Germany

<sup>4</sup> Molecular Proteomics Laboratory, Biomedical Research Centre (BMFZ), Heinrich Heine University Düsseldorf, 40225 Düsseldorf, Germany

<sup>5</sup> Institute of Plant Cell Biology and Biotechnology, Heinrich Heine University Düsseldorf, 40225 Düsseldorf, Germany

# equal contribution

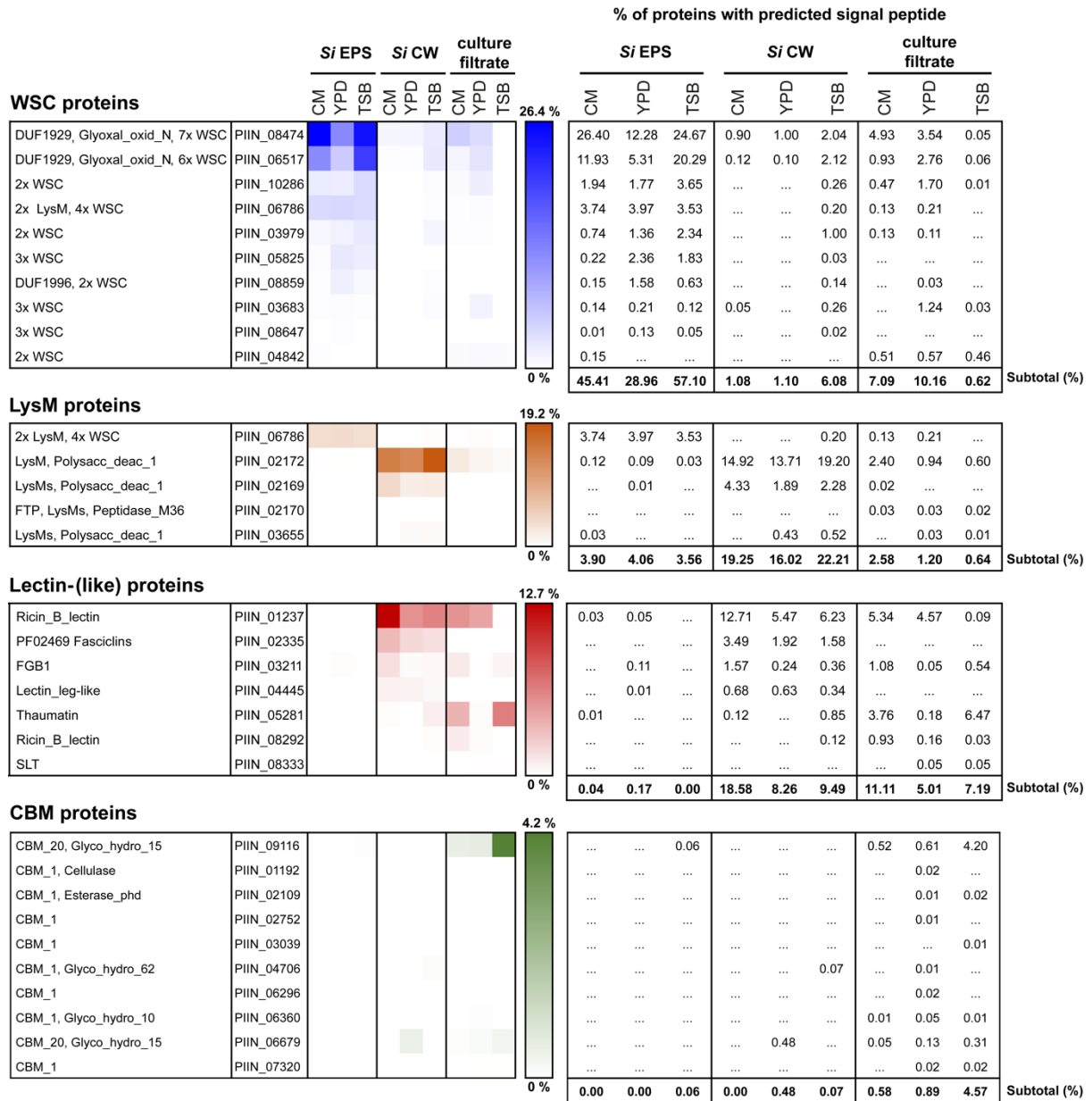
\





**Soluble  
extracellular  
polysaccharide  
(EPS) matrix**

**Supplemental Figure S1. EPS matrix isolated from *S. indica* grown in CM medium using a cryogelation approach. Supports Figure 2. Air bubbles were embedded in the gel-like EPS matrix after stirring to make the EPS matrix visible.**



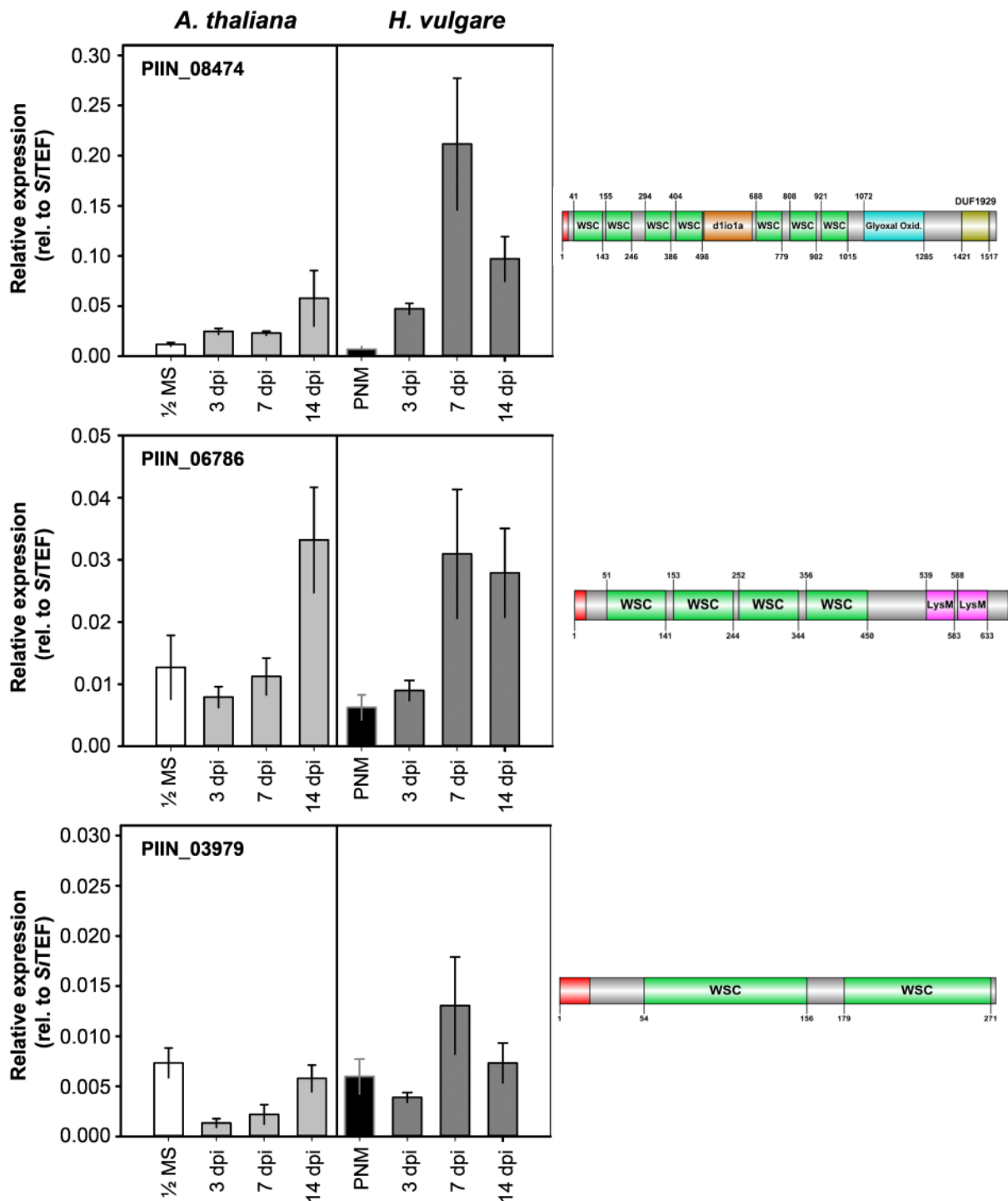
**% of proteins with predicted signal peptide**

Proteases	PIIN ID	Si EPS			Si CW			culture filtrate			6.17 %	Si EPS			Si CW			culture filtrate			Subtotal (%)	
		CM	YPD	TSB	CM	YPD	TSB	CM	YPD	TSB		CM	YPD	TSB	CM	YPD	TSB	CM	YPD	TSB		
		fn3_5, Peptidase_S8	PIIN_02492													0.68	5.50	6.17	0.16	...		0.41
Peptidase_S10	PIIN_07689												0.04	0.10	...	0.38	...	...	1.47	0.76	0.46	
Peptidase_S8	PIIN_04017												0.29	0.24	0.15	...	...	0.03	0.35	0.35	0.17	
Peptidase_M28	PIIN_04685												...	...	...	0.01	...	...	0.12	0.02	0.09	
FTP, Peptidase_M36	PIIN_11737												...	...	...	...	...	...	0.09	0.05	0.04	
Peptidase_M43	PIIN_07555												...	...	...	0.01	...	...	0.06	0.14	0.12	
fn3_5, Peptidase_S8	PIIN_05468												0.75	1.45	0.13	...	...	0.10	0.06	0.04	0.01	
Peptidase_S41	PIIN_10082												1.18	2.26	0.12	0.04	...	...	0.04	2.41	4.11	
FTP, LysMs, Peptidase_M36	PIIN_02170												...	...	...	...	...	...	0.03	0.03	0.02	
Peptidase_S28s	PIIN_01377												1.00	1.82	1.33	...	...	0.04	0.03	0.06	0.92	
Peptidase_S10	PIIN_06875												...	...	...	...	...	...	0.03	0.05	0.02	
Inhibitor_I9, Peptidase_S8	PIIN_07492												0.02	...	...	...	...	...	0.02	0.02	0.03	
FTP, Peptidase_M36	PIIN_00424												...	...	...	...	...	...	0.01	0.01	0.17	
Peptidase_M28	PIIN_04932												...	...	...	0.06	...	...	0.01	0.01	0.08	
FTP, Peptidase_M36	PIIN_09051												0.02	...	0.03	...	...	...	0.01	0.01	0.71	
Peptidase_M35	PIIN_06258												...	...	...	0.01	...	...	...	...	0.03	
Peptidase_M14, Propep_M14	PIIN_00112												...	...	...	...	0.02	...	...	...	0.23	
Peptidase_M28	PIIN_04931												...	...	...	...	...	...	...	...	0.14	
Peptidase_M43	PIIN_02952												...	...	...	...	...	...	...	...	0.13	
FTP, Peptidase_M36	PIIN_02992												0.01	...	...	...	...	0.01	...	0.02	0.04	
FTP, Peptidase_M36	PIIN_05476												0.07	0.02	...	...	...	0.05	...	...	0.02	
Inhibitor_I9, Peptidase_S8	PIIN_07598												...	...	...	...	...	...	...	...	0.01	
Peptidase_M28	PIIN_01065												0.05	...	...	0.28	...	...	...	...	...	
Peptidase_M28	PIIN_00565												...	0.01	...	...	...	0.08	...	...	...	
Peptidase_S8	PIIN_04374												...	...	...	...	...	...	...	...	...	
Peptidase_S66, Peptidase_S66C	PIIN_00863												0.01	...	...	...	...	...	...	...	...	
											0 %											
												4.12	11.40	7.95	0.87	0.09	0.73	5.05	5.89	8.60	Subtotal (%)	

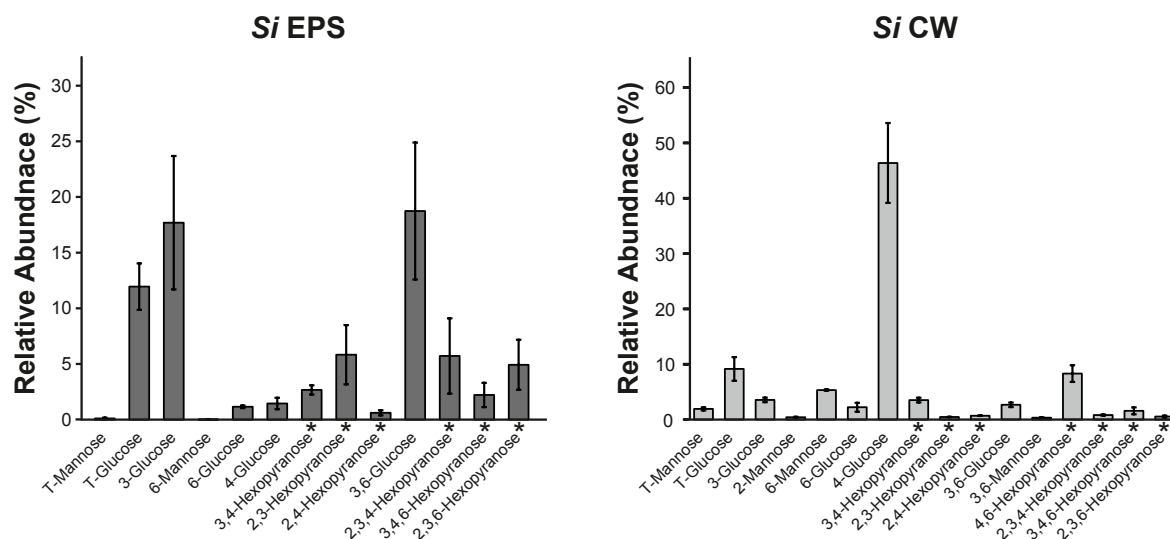
**% of proteins with predicted signal peptide**

CAZymes	PIIN ID	Si EPS			Si CW			culture filtrate			38.3 %	Si EPS			Si CW			culture filtrate			Subtotal (%)	
		CM	YPD	TSB	CM	YPD	TSB	CM	YPD	TSB		CM	YPD	TSB	CM	YPD	TSB	CM	YPD	TSB		
		Alginate_lyase	PIIN_08266													1.87	2.66	0.27	...	0.27		...
Alginate_lyase	PIIN_08262												0.02	...	...	...	...	...	10.96	0.44	0.47	
Cellulase	PIIN_05371												0.01	...	...	...	...	...	...	...	...	
Cellulase	PIIN_01558												9.04	0.27	0.01	9.41	9.14	9.05	0.23	2.20	0.16	
Cellulase	PIIN_01733												...	...	...	...	...	0.07	0.04	0.04	0.13	
Cellulase	PIIN_05555												1.01	0.08	...	...	...	0.09	...	0.05	0.11	
DIE2_ALG10	PIIN_06071												...	...	...	0.11	...	...	...	...	...	
Fn3-like, Glyco_hydro_3,	PIIN_04111												6.95	38.30	24.37	0.36	0.51	1.29	2.32	19.19	6.35	
Fn3-like, Glyco_hydro_3,	PIIN_00201												0.09	...	...	...	...	0.05	0.04	0.06	0.05	
GH115_C, Glyco_hydro_115	PIIN_04084												0.07	...	...	...	...	...	...	0.01	0.01	
GH131_N	PIIN_01141												0.05	0.07	...	...	0.05	...	...	...	0.02	
Glyco_hydro_10	PIIN_05057												...	...	...	0.01	...	...	...	...	...	
Glyco_hydro_10	PIIN_04364												0.02	0.02	...	...	...	...	0.01	0.08	0.03	
Glyco_hydro_16	PIIN_05222												...	...	...	...	...	...	1.78	1.84	0.71	
Glyco_hydro_16	PIIN_09220												0.30	1.82	0.05	...	...	...	0.03	0.21	0.09	
Glyco_hydro_16	PIIN_06486												...	...	...	0.02	...	...	0.07	0.06	0.03	
Glyco_hydro_16	PIIN_00239												...	...	...	...	...	...	0.04	0.01	0.01	
Glyco_hydro_20, Glycohydro_20b2	PIIN_04767												0.11	0.02	...	0.14	...	...	...	0.08	0.07	
Glyco_hydro_28	PIIN_09677												...	0.05	...	...	...	...	...	0.02	0.01	
Glyco_hydro_32	PIIN_08245												...	...	...	...	0.01	...	0.08	0.04	0.08	
Glyco_hydro_6	PIIN_00353												0.05	0.29	0.03	...	...	...	...	...	0.01	
Glyco_hydro_72, X8	PIIN_04585												0.44	...	...	0.35	0.48	0.39	0.42	0.21	0.20	
Glyco_hydro_88	PIIN_01829												3.40	0.19	1.54	0.04	...	...	...	0.34	0.60	
Glyco_hydro_88	PIIN_01867												0.06	...	0.01	...	...	...	...	0.02	0.01	
Glyco_hydro_cc	PIIN_01066												1.17	1.03	0.72	0.55	...	0.32	...	7.85	4.65	
Glyco_hydro_cc	PIIN_01067												1.81	0.68	0.18	...	...	0.22	...	5.79	2.30	
Pectate_lyase_3s	PIIN_01508												...	...	...	...	...	...	...	0.01	0.02	
PNCaseA	PIIN_01737												0.09	0.08	...	...	...	...	...	...	0.05	
Polysacc_deac_1	PIIN_08301												0.03	0.01	0.03	0.32	0.42	1.49	0.70	0.65	1.96	
Polysacc_deac_1	PIIN_05728												1.09	0.16	0.03	3.97	2.29	1.48	1.03	1.50	0.86	
Polysacc_deac_1	PIIN_02364												...	...	...	...	...	...	...	...	0.01	
											0 %											
												27.69	45.71	27.24	15.15	13.27	14.45	17.87	40.95	19.73	Subtotal (%)	

**Supplemental Figure S2. Proteome analysis of *S. indica* EPS matrix, CW and culture filtrate.** Supports Figure 2. *S. indica* spores were inoculated into three different liquid culture media: CM, YPD and TSB. The EPS matrix and CW proteins were isolated and solubilized by adding SDS-gel loading buffer and boiling at 95°C. The proteins present in the culture filtrate were precipitated using trichloroacetic acid and solubilized by boiling in SDS-gel loading buffer. The proteins were separated using a 10% SDS PAGE gel for 15 minutes and subsequently stained with Coomassie Brilliant Blue. The visible protein band in each sample was cut out and prepared for trypsin digest. The peptides were analyzed using LC-MS. Proteins with a predicted signal peptide were annotated using the protein family database Pfam. The relative abundance was calculated using the label-free quantification intensities values and expressed as a percentage (%). The proteome analysis of the EPS matrix and CW revealed that several WSC domain-containing proteins, including SWSC3 (PIIN\_05825), are abundant in the matrix compared to the CW. Additionally, two polysaccharide deacetylases with a LysM domain are enriched in the CW of *S. indica*. This suggests that the detected polysaccharide deacetylases with LysM domain might be involved in chitin remodeling within the CW of *S. indica*. Furthermore, a thaumatin family protein (PIIN\_05281) is enriched in the culture filtrate. Thaumatin family proteins have been shown to exhibit antifungal activity through their  $\beta$ -1,3-glucanase activity. It is possible that PIIN\_05281 exhibits an antimicrobial function against fungal competitors. Likewise, peptidases and glycosyl hydrolases with fibronectin type III module (Fn3) domains are enriched in the matrix and the culture medium but not in the CW. Fn3 domains are versatile domains in proteins that play a major role in mediating protein–protein interactions. CW: cell wall; EPS: extracellular polysaccharide; Fn3: fibronectin type III module; LysM: lysine motive; *Si*: *Serendipita indica*; WSC: cell wall integrity and stress response component.



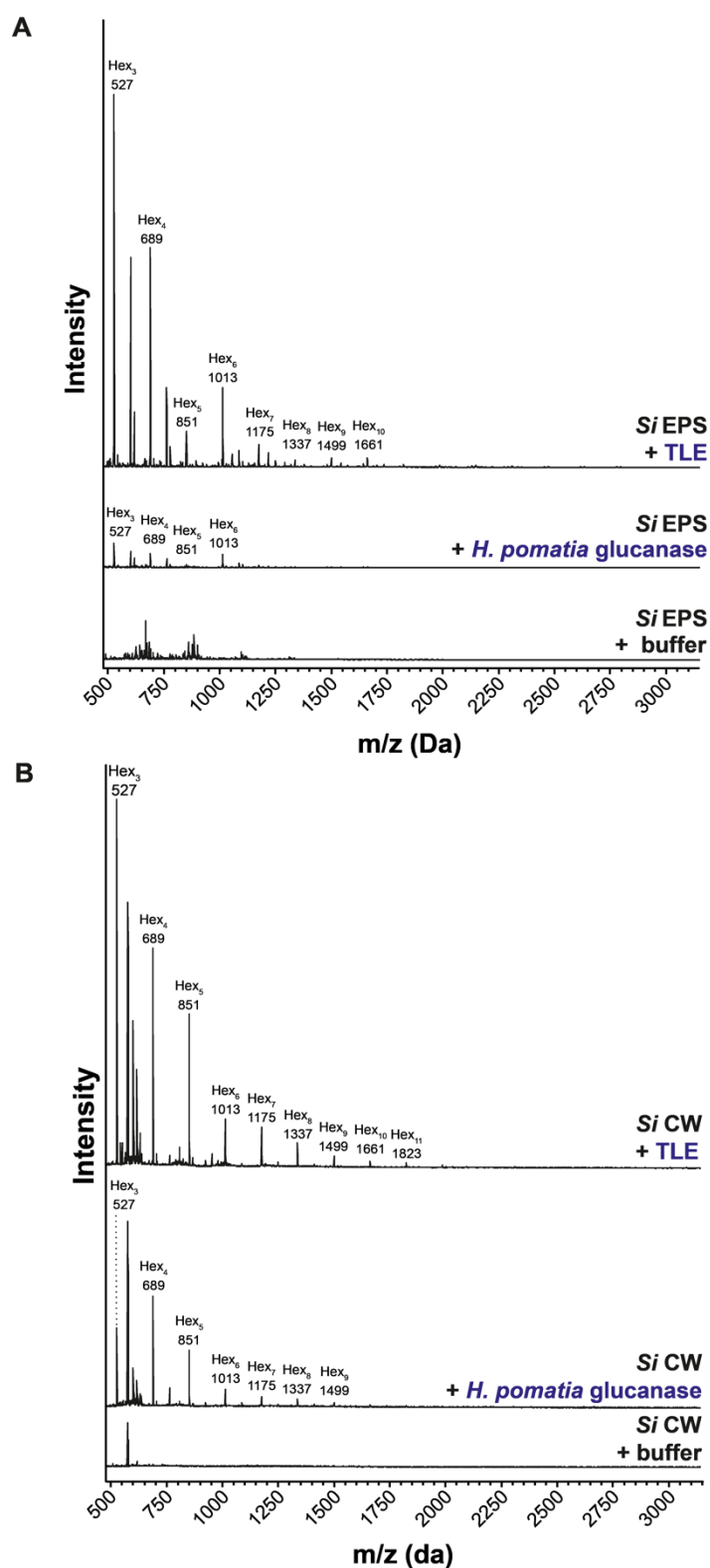
**Supplemental Figure S3. Expression analysis of selected genes with WSC domains in *S. indica* during plant colonization at 3-, 7- and 14-days post inoculation (dpi).** Supports Figure 2. The gene expression of *S. indica* WSC domain-containing proteins during root colonization of barley and Arabidopsis was monitored via quantitative reverse transcription PCR (RT-qPCR) as previously described (Wawra *et al.*, 2019). Average and standard deviation of three independent biological replicates ( $n=3$ ) are shown. For each biological replicate, roots from several individual plants were pooled (Arabidopsis: 60 plants; barley: 4 plants). LysM: lysine motive; MS: Murashige-Skoog medium; PNM: plant nutrition medium; WSC: cell wall integrity and stress response component.



#### Supplemental Figure S4. Glycosyl linkage analysis of *Si* EPS and *Si* CW.

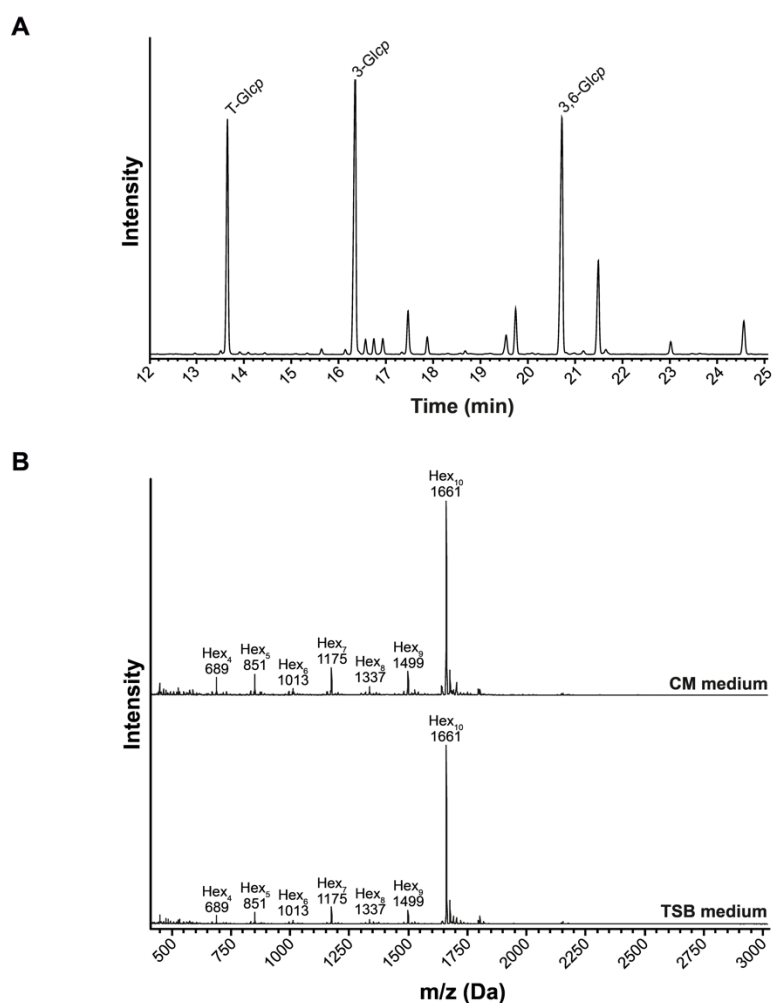
Supports Figure 2. Ground EPS matrix or the alcohol insoluble residue (CW fraction) isolated from *S. indica* grown in TSB medium containing 1% sucrose was subjected to glycosyl linkage analysis as previously described (Liu et al., 2015). The sugar residues were derivatized into partially methylated alditol acetates and analyzed using GC-MS. The glycosidic linkages were assigned based on the retention time and the mass spectrum available at the publicCCRC spectral database. The annotated glycosyl residues detected in the EPS matrix or CW are expressed as a percentage of the total glycosyl peak areas. The other minor unannotated glycosyl residues are listed in Supplemental Data Set S4 and S5. Average and standard deviation of four independent biological replicates (n=4) are presented. CW: cell wall; EPS: extracellular polysaccharide matrix; *Si*: *Serendipita indica*; \*exact sugar moiety unknown; overrepresentation of linkages due to undermethylation cannot be excluded.



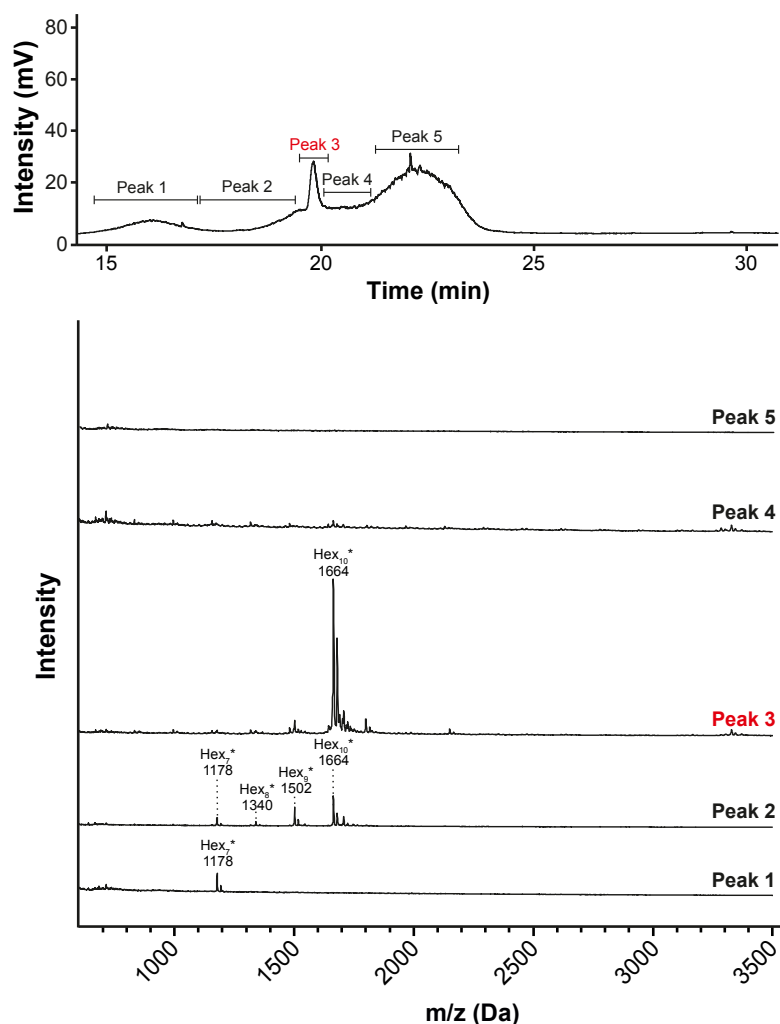


**Supplemental Figure S5. Analysis of oligosaccharides released from the EPS or protein-free CW of *S. indica* by the action of  $\beta$ -1,3-glycosidases.** Supports Figure 3. 1 mg of freeze-dried EPS (A) or CW (B) obtained from *S. indica* was soaked in 2 mM sodium acetate, pH 5.0 (TLE), or 2 mM MES pH 5.0 (*H. pomatia* glucanase) at 70°C overnight. The soaked material was incubated with TLE or *H. pomatia*  $\beta$ -1,3-glycosidase at 40°C for 16 hours. The supernatant fraction from the digested EPS matrix and CW

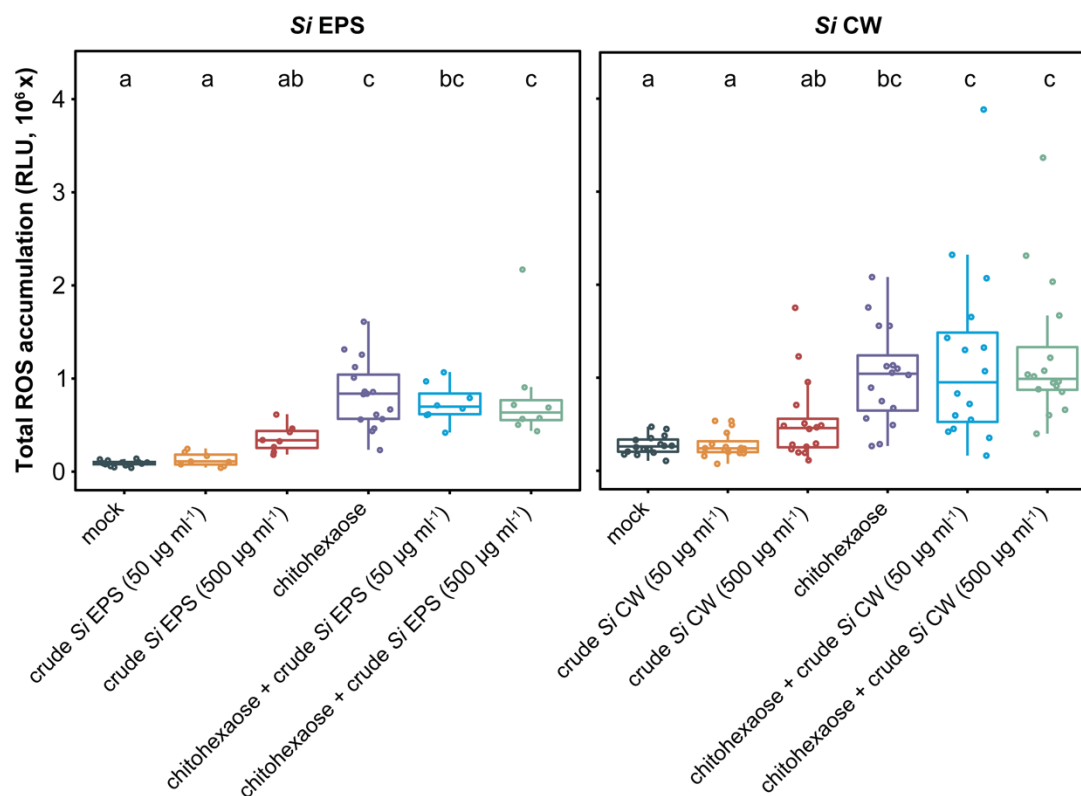
were analyzed by MALDI-TOF. The  $m/z$   $(M+Na)^+$  Da of oligosaccharides resulting from the digestion of the samples are labeled with their hexose composition. The digestion of *Si* EPS with TLE or *H. pomatia* glucanase was repeated independently two times with a similar result and the digestion of *Si* CW with TLE or *H. pomatia* was performed once. CW: cell wall; EPS: extracellular polysaccharide; Hex<sub>n</sub>: oligosaccharides with the indicated hexose composition; *Si*: *Serendipita indica*; TLE: *Trichoderma harzianum* lysing enzymes.



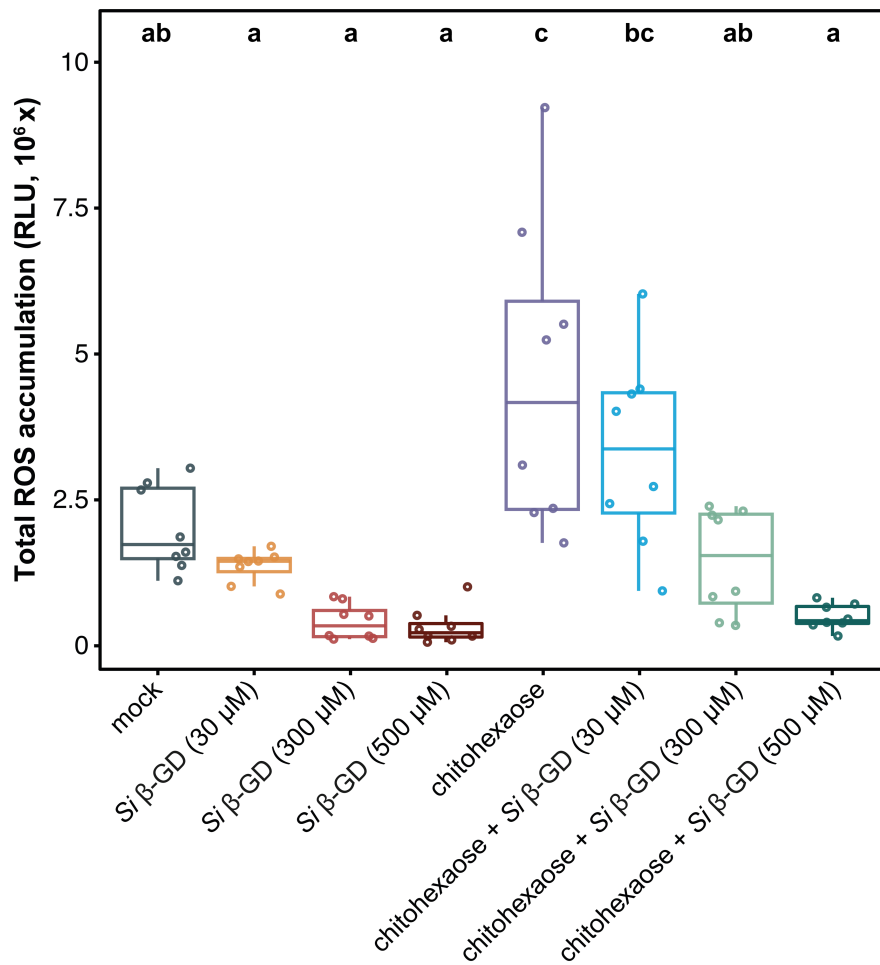
**Supplemental Figure S6. Glycosyl linkage and MALDI-TOF analysis of the glucan fraction ( $\beta$ -GD) released from the EPS matrix of *S. indica*.** Supports Figure 3. (A) Glycosyl linkage analysis of  $\beta$ -GD released from the EPS matrix of *S. indica*. The experiment was performed with three independent biological replicates of  $\beta$ -GD and the total ion chromatogram (TIC) of one of the replicates is represented. (B) *S. indica* was grown either in liquid CM or TSB medium containing 1% sucrose.  $\beta$ -GD was isolated and subjected to MALDI-TOF mass spectrometry. The ions corresponding to oligosaccharides with varying degree of polymerization are labelled with their hexose composition. The experiment performed with the TSB medium was repeated independently more than three times with a similar result and the experiment performed with the CM medium was performed once. CM: complex Hill-Käfer medium; EPS: extracellular polysaccharide; Hex<sub>n</sub>: oligosaccharides with the indicated hexose composition; TSB: Tryptic Soy Broth.



**Supplemental Figure S7. Purification of the  $\beta$ -GD fragment for  $^1\text{H}$  NMR analysis.** Supports Figure 3. 40 mg of the  $\beta$ -GD enriched fraction was reduced using  $\text{NaBD}_4$ . The reduced fraction was neutralized with acetic acid, washed with methanol and air-dried. The dried material was dissolved in 2 ml of 6% methanol and 50  $\mu\text{l}$  of the sample was subjected to liquid chromatography using a reverse-phase column (Vydac, Hesperia, CA, USA) connected to an evaporative light scattering detector. The detected peaks were collected and analyzed using MALDI-TOF. The samples were injected multiple times (24x) and peak 3 (shown in red) containing the reduced 1661 Da fragment was pooled and freeze-dried. The freeze-dried material was used for the  $^1\text{H}$  NMR analysis.  $\beta$ -GD:  $\beta$ -1,3;1,6-glucan deca-saccharide;  $\text{Hex}_n$ : oligosaccharides with the indicated hexose composition; \* represents the increase by +3 Da in the detected oligosaccharides due to the reduction of the anomeric C1 atom.

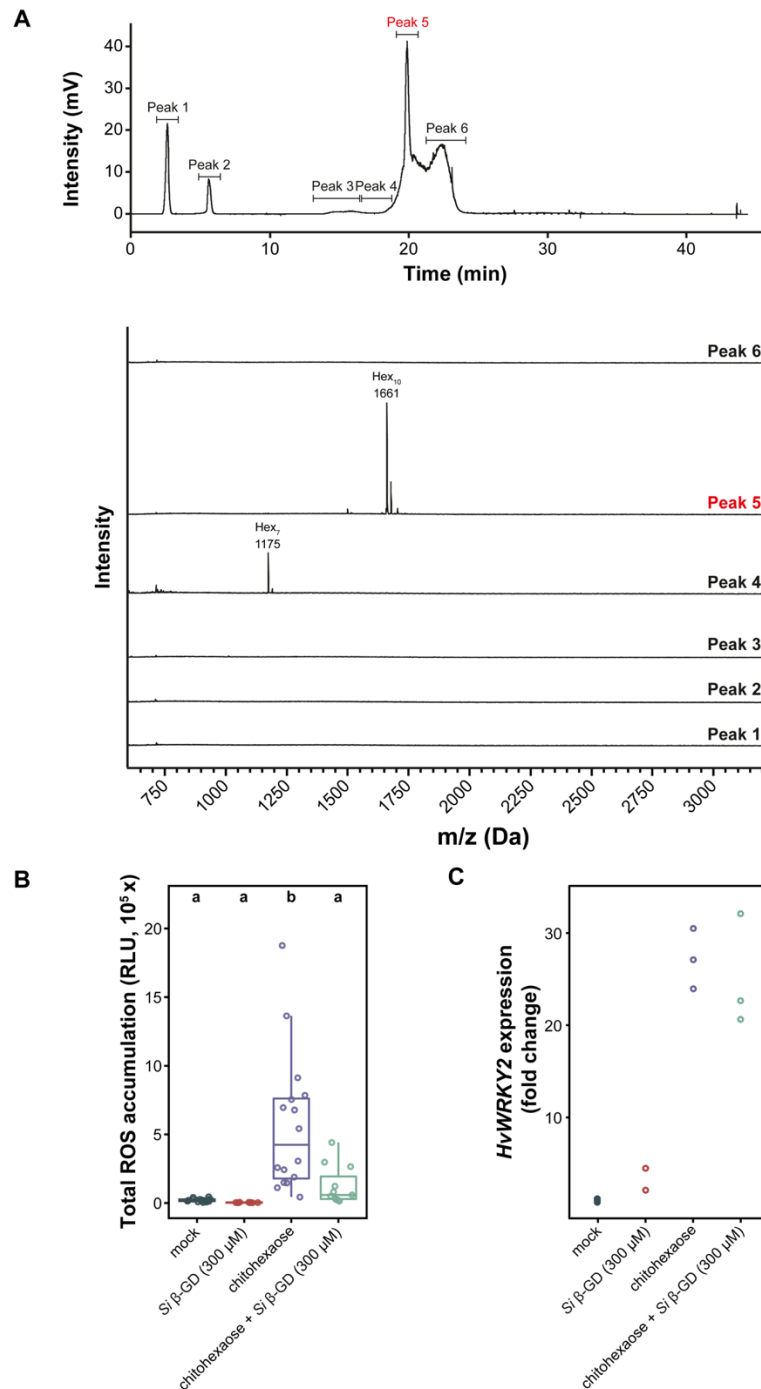


**Supplemental Figure S8. Mechanically released fragments from *S. indica* EPS matrix and CW layer do not exhibit ROS scavenging activity.** Supports Figure 4. (A) *S. indica* EPS matrix and CW substrates were ground, heat-treated and sonicated prior to application to barley roots. Roots were treated with Milli-Q water (mock, n=16), chitohexaose (25 µM, n=16), crude EPS matrix or CW preparations (n=8-16) and combinations of chitohexaose and EPS matrix or CW preparations (n=8-16). Total cumulative ROS was calculated from a measured time interval of 60 minutes. Each data point in the boxplot represents the integrated value from an individual well (center line, median; box limits, upper and lower quartiles; whiskers, 1.5x interquartile range). Experiments were performed two times with similar results. Different letters indicate statistically significant differences based on a one-way ANOVA and Tukey's post-hoc test (significance threshold: p-value ≤ 0.05). CW: cell wall; EPS: extracellular polysaccharide; RLU: relative light units; ROS: reactive oxygen species; *Si*: *Serendipita indica*.



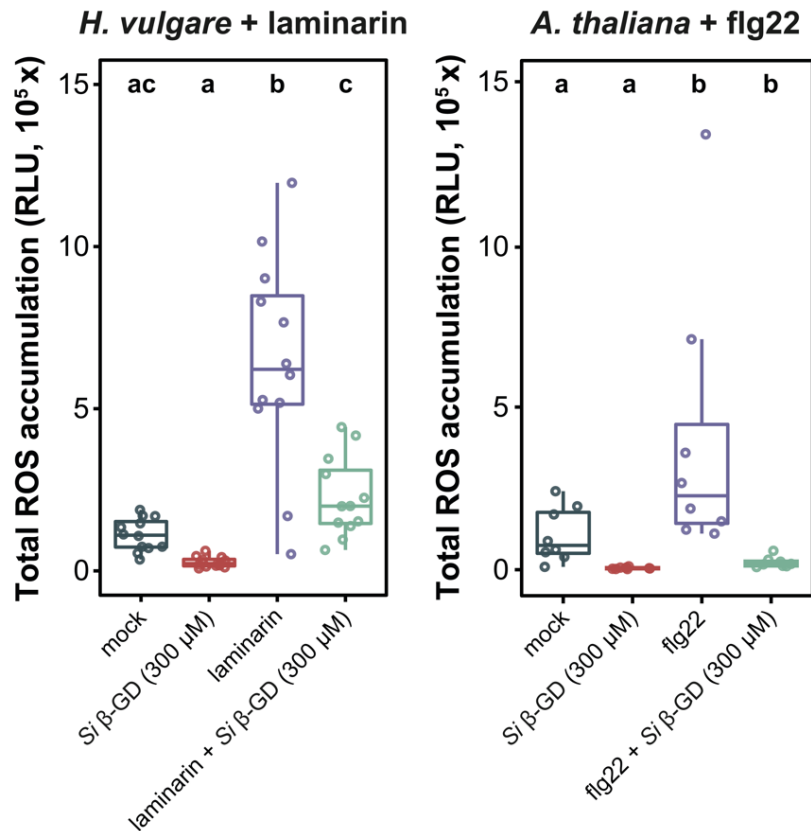
**Supplemental Figure S9. Chitohexaose-triggered ROS accumulation is decreased by *S. indica* β-GD treatment in a concentration-dependent manner.** Supports Figure 4. Apoplastic ROS accumulation after treatment of eight-day-old barley roots with 25 μM chitohexaose and/or purified β-GD from *S. indica*. Treatment with Milli-Q water was used as mock control. Boxplots represents total ROS accumulation over the measured time period (center line, median; box limits, upper and lower quartiles; whiskers, 1.5x interquartile range). Each data point represents measurement of an individual well containing four root pieces. In total, roots from 16 individual barley plants were used per experiment. This assay represents one out of four experiments with independent β-GD preparations. Letters represent statistically significant differences in expression based on a one-way ANOVA and Tukey's post-hoc test (significance threshold: p-value ≤ 0.05).



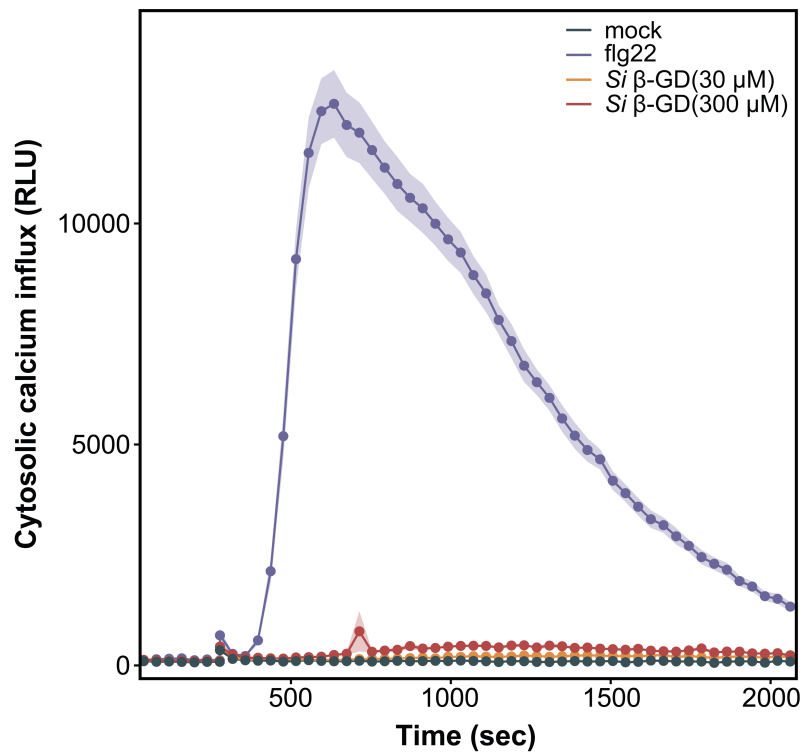


**Supplemental Figure S10. Purification of native  $\beta$ -GD and immunogenic characterization.** Supports Figure 4. (A) 40 mg of the  $\beta$ -GD enriched fraction was dissolved in 2 ml of 6% methanol and 50  $\mu$ l of the sample was subjected to liquid chromatography using a reverse-phase column (Vydac, Hesperia, CA, USA) connected to an evaporative light scattering detector. The detected peaks were collected and analyzed using MALDI-TOF. The samples were injected multiple times (24x) and peak 5 (shown in red) containing the 1661 Da fragment was pooled and freeze-dried. HPLC-purified  $\beta$ -GD fraction was used in the ROS burst assay (B) and the quantitative reverse transcription PCR gene expression analysis (C) was performed using root pieces obtained from eight-day-old barley plants. (B) The

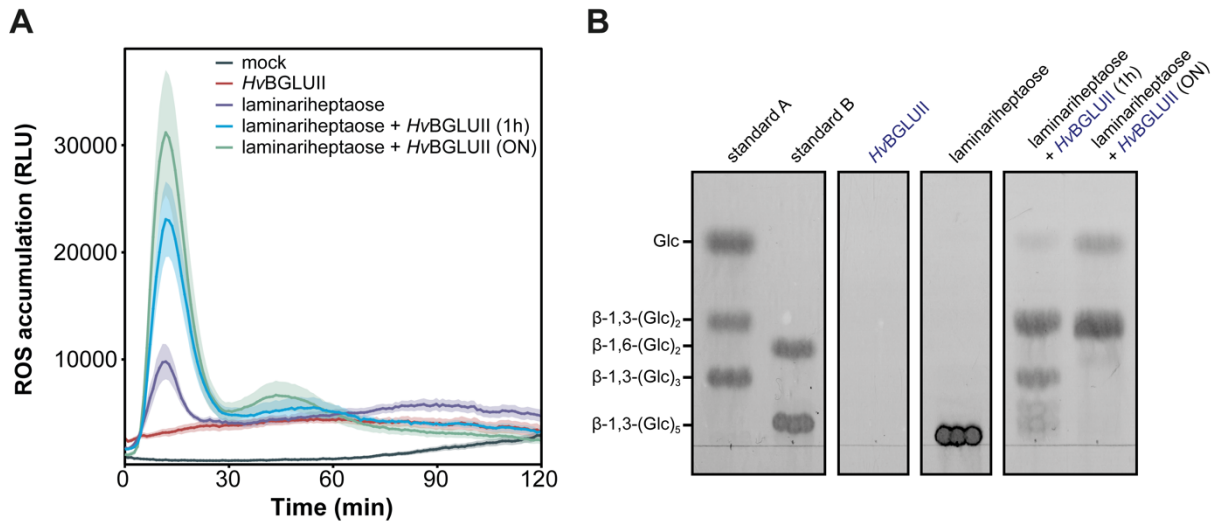
following treatments were applied in the ROS burst assay: mock treatment with Milli-Q water (n=16),  $\beta$ -GD (300  $\mu$ M, n=8), chitohexaose (25  $\mu$ M, n=16) and combined  $\beta$ -GD/chitohexaose treatments (concentrations as in previous treatments, n=11). ROS production was measured for 25 minutes. Each data point in the boxplot represents the integrated value from an individual well (center line, median; box limits, upper and lower quartiles; whiskers, 1.5x interquartile range). Different letters indicate statistically significant differences based on a one-way ANOVA and Tukey's post-hoc test (significance threshold: p-value  $\leq$  0.05). (C) Samples for quantitative reverse transcription PCR were collected after 1 hour of treatment. Applied elicitor concentrations were as described above for the ROS burst assay (n=2-3). Gene expression of elicitor-responsive *HvWRKY2* was calculated relative to housekeeping gene expression (*HvUBI*) and normalized to mock treatment. Calculation of statistical significance was not performed due to low sample number.  $\beta$ -GD:  $\beta$ -1,3:1,6-glucan decasaccharide; RLU: relative light units; ROS: reactive oxygen species; *Si*: *Serendipita indica*.



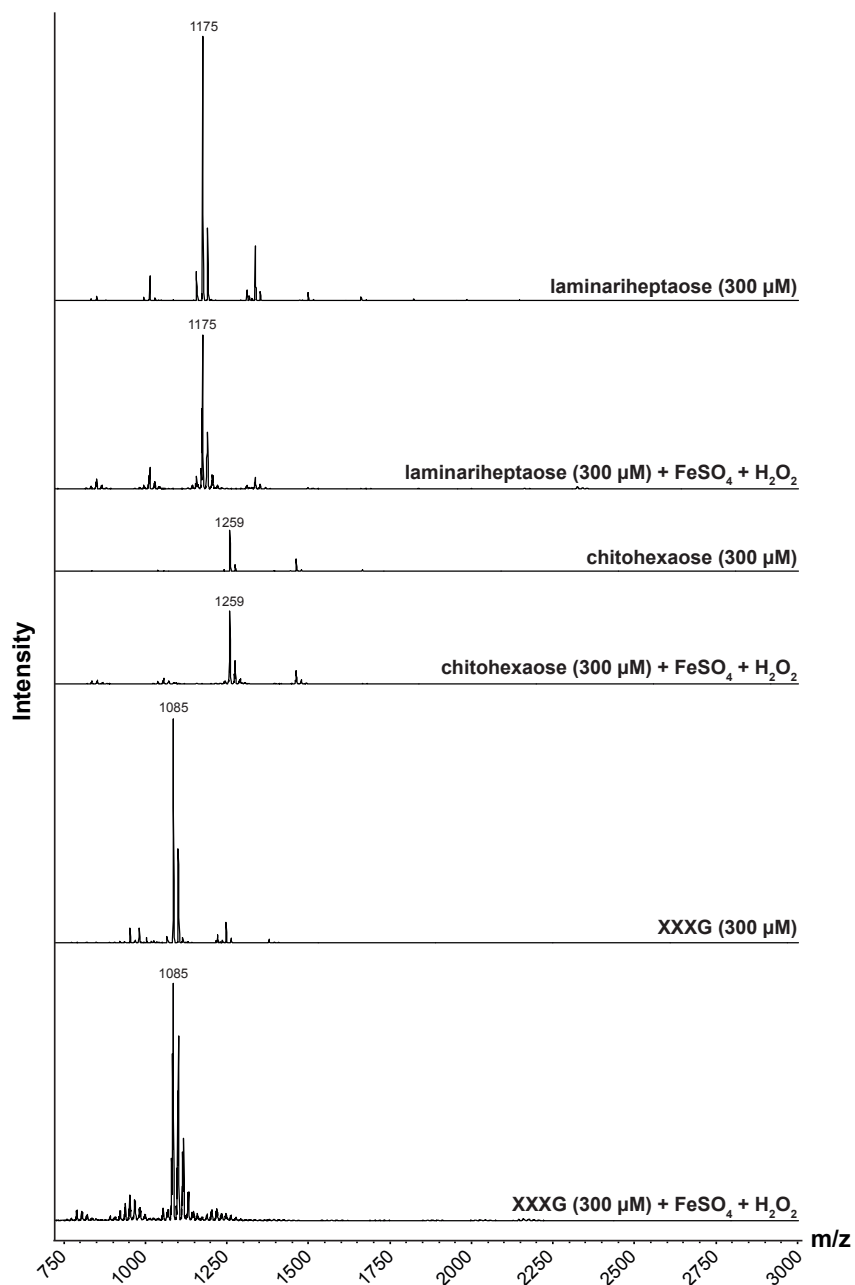
**Supplemental Figure S11. Detoxification of apoplastic ROS by *S. indica* β-GD is independent of elicitor treatment and plant species.** Supports Figure 4. ROS burst assays were performed with the roots of eight-day-old barley plants (n=12, data shown from one out of two independent experiments) and two-week-old *Arabidopsis* seedlings (n=8, single experiment). Plants were treated with Milli-Q water (mock), 2 mg/ml laminarin, 100 nM flg22, 300 μM β-GD and combinations of laminarin or flg22 and β-GD. Each data point in the boxplot represents the integrated value from an individual well (center line, median; box limits, upper and lower quartiles; whiskers, 1.5x interquartile range). Different letters indicate statistically significant differences based on a one-way ANOVA and Tukey's post-hoc test (significance threshold: p-value ≤ 0.05). β-GD: β-1,3:1,6-glucan deacasaccharide; RLU: relative light units; ROS: reactive oxygen species; *Si*: *Serendipita indica*.



**Supplemental Figure S12. *S. indica* β-GD treatment does not trigger cytosolic calcium influx in *A. thaliana* seedlings.** Supports Figure 4. Calcium influx assays were performed with two-week-old *A. thaliana* seedlings expressing the calcium reporter protein aequorin in the cytosol. After an initial baseline measurement (5 min), seedlings were treated with Milli-Q water (mock), 100 nM flg22, 300 μM β-GD and β-GD. β-GD: β-1,3:1,6-glucan decasaccharide; RLU: relative light units; *Si*: *Serendipita indica*. The experiment was performed once with 16 *A. thaliana* seedlings (n=16) per treatment.

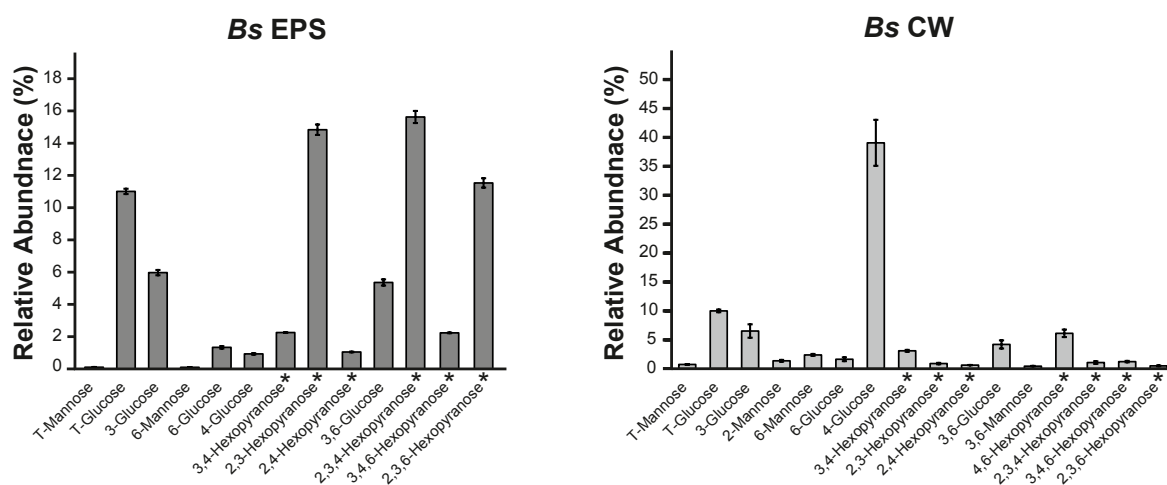


**Supplemental Figure S13: Digestion of laminariheptaose with *HvBGLUII* enhances ROS production in barley roots.** Supports Figure 4. (A) Before treatment of barley roots, 3 mM laminariheptaose was digested with *HvBGLUII* (10 units in total digestion volume of 200  $\mu$ l) for one hour or overnight (ON) at 40°C, 450 rpm. As controls, Milli-Q water with *HvBGLUII* and laminariheptaose without *HvBGLUII* were treated in a similar way. Digestion was stopped by incubation at 90°C (10 minutes, 450 rpm) followed by centrifugation (10 min, 13000xg, room temperature). Supernatants were used in ROS burst assays with the roots of eight-day-old barley plants ( $n=8$ , three root pieces per replicate). Plants were treated with Milli-Q water (mock), Milli-Q water with *HvBGLUII* or 300  $\mu$ M laminariheptaose (digested or non-digested). (B) Digestion of substrates used in the ROS burst assay was analyzed via thin-layer chromatography. Glc: glucose; ON: overnight; RLU: relative light units; ROS: reactive oxygen species. The experiment was repeated 3 times with similar results.

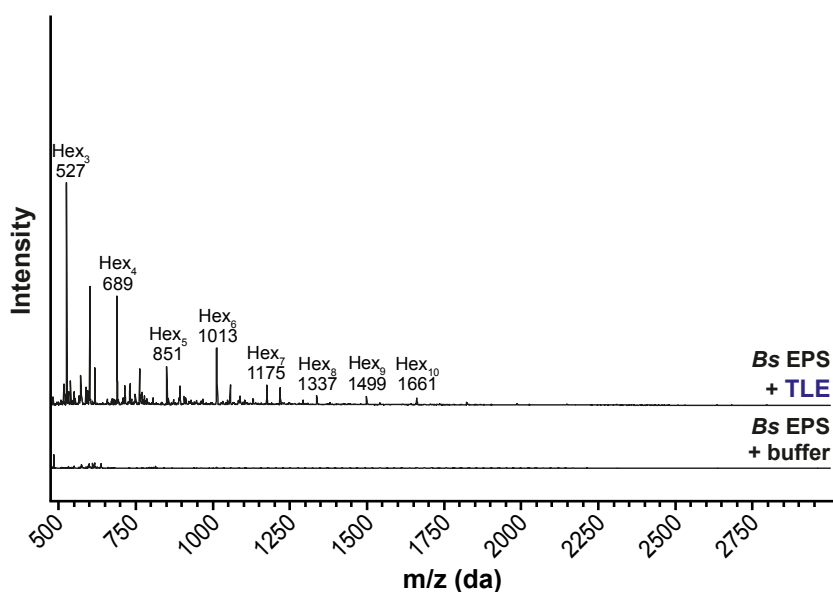


**Supplemental Figure S14. Glycan controls are not degraded by hydrogen peroxide during Fenton reaction.** Supports Figure 4. Laminariheptaose, chitohexaose and xyloglucan heptasaccharide (XXXG) were tested for oxidative degradation by overnight Fenton reaction (1 mM H<sub>2</sub>O<sub>2</sub>, 100  $\mu$ M FeSO<sub>4</sub>) followed by MALDI-TOF analysis. The experiment was repeated independently two times with similar results.

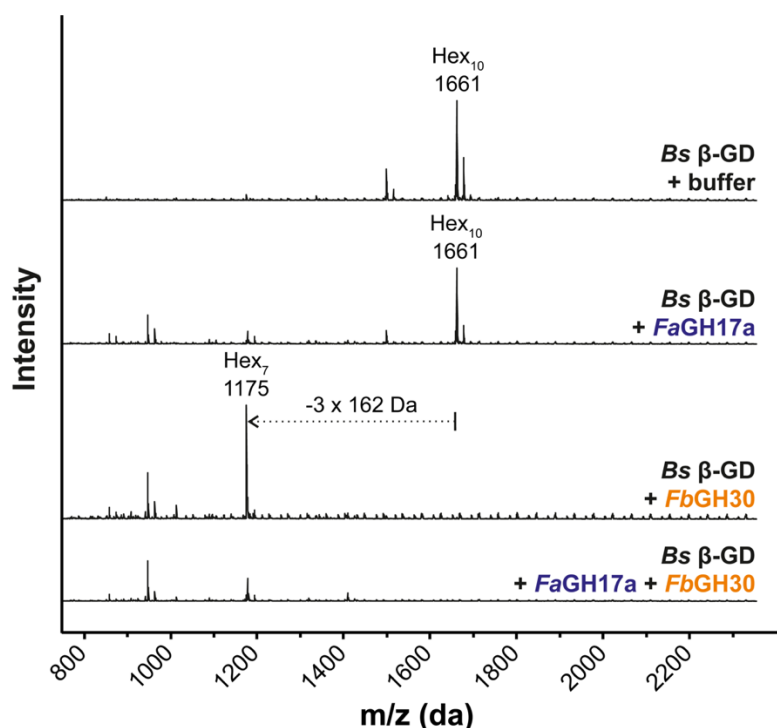




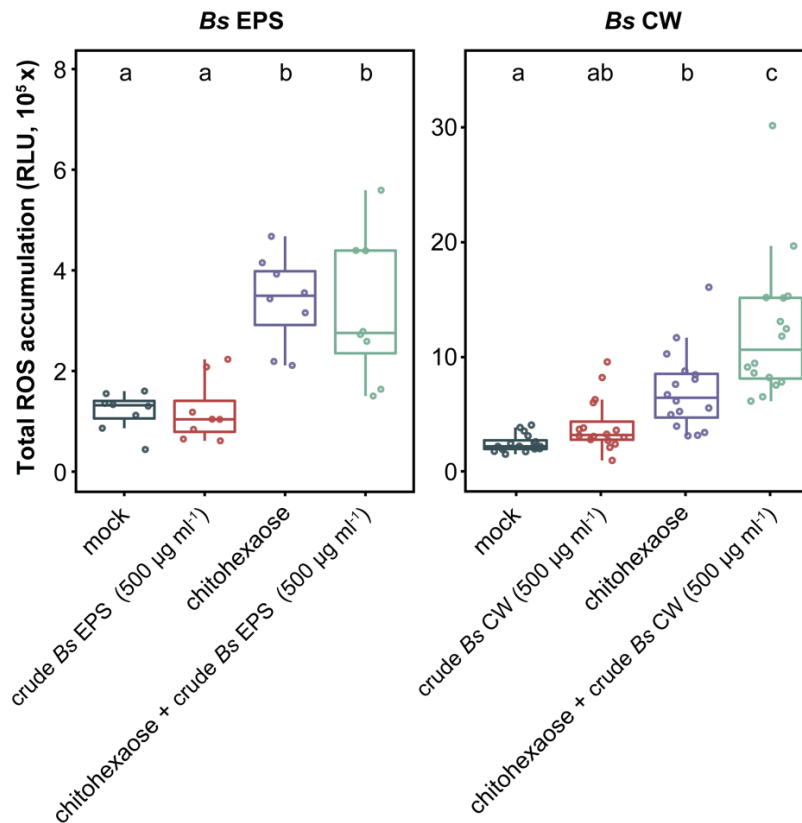
**Supplemental Figure S15. Glycosyl linkage analysis of *B. sorokiniana* EPS matrix and CW.** Supports Figure 5. 2 mg of ground EPS matrix or the alcohol insoluble residue (CW fraction) isolated from the cultures of *B. sorokiniana* grown in YPD medium was subjected to glycosyl linkage analysis as previously described (Liu *et al.*, 2015). The sugar residues were derivatized into partially methylated alditol acetates and analyzed using GC-MS. The glycosidic linkages were assigned based on the retention time and the mass spectrum available at CCRC spectral database. The annotated glycosyl residues detected in the EPS matrix or CW are expressed as a percentage of total glycosyl peak areas. The other minor unannotated glycosyl residues can be found in Supplemental Data Set S7 and S8. Average and standard deviation of three independent biological replicates ( $n=3$ ) are presented. *Bs*: *Bipolaris sorokiniana*; CW: cell wall; EPS: extracellular polysaccharide; \*exact sugar moiety unknown; overrepresentation of linkages due to undermethylation cannot be excluded.



**Supplemental Figure S16. Analysis of oligosaccharides released from the EPS of *B. sorokiniana* by the action of *Trichoderma harzianum* lysing enzymes.** Supports Figure 5. 1 mg of freeze-dried EPS obtained from *B. sorokiniana* was soaked in 2 mM sodium acetate, pH 5.0 at 70°C overnight. The soaked material was incubated with TLE at 40°C for 16 hours. The supernatant fraction from the digested EPS matrix was analyzed by MALDI-TOF. The m/z (M+Na)<sup>+</sup> Da of oligosaccharides resulting from the digestion of EPS is indicated along with their hexose composition. The experiment was performed once. *Bs*: *Bipolaris sorokiniana*; EPS: extracellular polysaccharide; Hex<sub>n</sub>: oligosaccharides with the indicated hexose composition; TLE: *Trichoderma harzianum* lysing enzymes.



**Supplemental Figure S17.** The  $\beta$ -GD released from the EPS matrix of *B. sorokiniana* consists of a seven-unit  $\beta$ -1,3-linked glucan backbone substituted with three  $\beta$ -1,6-glucosyl residues. Supports Figure 5.  $\beta$ -GD was treated with *FaGH17a* and/or *FbGH30* at 40°C overnight. The digested  $\beta$ -GD fragment was analyzed by MALDI-TOF. The loss of three hexoses ( $-3 \times 162 \text{ Da}$ ) as a result of *FbGH30* (orange) treatment is indicated with a dotted arrow.  $\beta$ -GD:  $\beta$ -1,3;1,6-glucan deca-saccharide; *Bs*: *Bipolaris sorokiniana*; EPS: extracellular polysaccharide. The experiment was performed once.



**Supplemental Figure S18. Mechanically released fragments from *B. sorokiniana* EPS matrix or CW do not scavenge ROS.** Supports Figure 5. Assays were performed and analyzed as described in Figure S8. Total cumulative ROS was calculated from a measured time interval of 60 minutes. Each data point in the boxplot represents the integrated value from an individual well (center line, median; box limits, upper and lower quartiles; whiskers, 1.5x interquartile range). The experiment was performed two times with similar results. *Bs*: *Bipolaris sorokiniana*; CW: cell wall; EPS: extracellular polysaccharide; RLU: relative light units; ROS: reactive oxygen species.

### Supplemental References

Liu, L., Paulitz, J., and Pauly, M. (2015). The Presence of Fucogalactoxyloglucan and Its Synthesis in Rice Indicates Conserved Functional Importance in Plants. *Plant Physiology* **168**, 549-560.

Wawra, S., Fesel, P., Widmer, H., Neumann, U., Lahrmann, U., Becker, S., Hehemann, J.-H., Langen, G., and Zuccaro, A. (2019). FGB1 and WSC3 are in planta-induced  $\beta$ -glucan-binding fungal lectins with different functions. *New Phytologist* **222**, 1493-1506.

**Further supplementary data are available at *The Plant Cell* online:**

**Supplemental Data Set S1.** Total proteins detected in the proteome analysis of the EPS matrix, CW, and culture filtrate isolated from *S. indica* grown in CM, TSB, or YPD liquid media.

**Supplemental Data Set S2.** Relative abundance of signal peptide (SP) containing proteins detected in the EPS matrix, CW, and culture filtrate isolated from the *S. indica* under three culture mediums: CM, TSB, and YPD. LFQ intensities of the proteins were used to calculate their relative abundance.

**Supplemental Data Set S3.** Statistics, enrichment score, Benjamini–Hochberg corrected *P*-value.

**Supplemental Data Set S4.** Glycosyl sugar residues detected in the total ion chromatogram of EPS matrix isolated from *S. indica*, *n* = 4 independent biological replicates.

**Supplemental Data Set S5.** Glycosyl sugar residues detected in the total ion chromatogram of alcohol insoluble residue (cell wall) isolated from *S. indica*, *n* = 4 independent biological replicates.

**Supplemental Data Set S6.** List of Barley CAZymes detected in the root apoplastic fluids (AFs) of barley after mock, *S. indica* or *B. sorokiniana* treatments.

**Supplemental Data Set S7.** Glycosyl sugar residues detected in the total ion chromatogram of alcohol insoluble residue (cell wall) isolated from *B. sorokiniana*, *n* = 3 independent biological replicates.

**Supplemental Data Set S8.** Glycosyl sugar residues detected in the total ion chromatogram of EPS matrix isolated from *B. sorokiniana*, *n* = 3 independent biological replicates.

**Supplemental Data Set S9.** List of Barley CAZymes differentially regulated during *B. sorokiniana* infection.

**Supplemental Data Set S10.** Summary of statistical analyses.

# Chapter 5

## **A GH81-type $\beta$ -glucan-binding protein facilitates colonization by mutualistic fungi in barley**

Alan Wanke<sup>1,2</sup>, Sarah van Boerdonk<sup>1</sup>, Lisa Mahdi<sup>1</sup>, Stephan Wawra<sup>1</sup>, Miriam Neidert<sup>1</sup>, Balakumaran Chandrasekar<sup>1</sup>, Pia Saake<sup>1</sup>, Isabel Saur<sup>2</sup>, Ivan F. Acosta<sup>2</sup>, Markus Pauly<sup>3</sup>, Alga Zuccaro<sup>1</sup>

<sup>1</sup> University of Cologne, Cluster of Excellence on Plant Sciences (CEPLAS), 50679 Cologne, Germany

<sup>2</sup> Max Planck Institute for Plant Breeding Research, 50829 Cologne, Germany

<sup>3</sup> Institute of Plant Cell Biology and Biotechnology, Heinrich Heine University Düsseldorf, 40225 Düsseldorf, Germany



## Abstract

Cell walls are important interfaces of plant-fungal interactions. Host cell walls act as robust physical and chemical barriers against fungal invaders, making them an essential line of defense. Upon fungal colonization, plants deposit phenolics and callose at the sites of fungal penetration to reinforce their walls and prevent further fungal progression. Alterations in the composition of plant cell walls significantly impact host susceptibility. Furthermore, plants and fungi secrete glycan hydrolases acting on each other's cell walls. These enzymes release a wide range of sugar oligomers into the apoplast, some of which trigger the activation of host immunity *via* host surface receptors. Recent characterization of cell walls from plant-colonizing fungi have emphasized the abundance of  $\beta$ -glucans in different cell wall layers, which makes them suitable targets for recognition. To characterize host components involved in immunity against fungi, we performed a protein pull-down with biotinylated laminarin. Thereby, we identified a glycoside hydrolase family 81-type  $\beta$ -1,3-endoglucanase as the major  $\beta$ -glucan interactor. Mutation of *GBP1* and its only paralogue *GBP2* in barley lead to decreased colonization by the beneficial root endophytes *Serendipita indica* and *S. vermifera*, as well as the arbuscular mycorrhizal fungus *Rhizophagus irregularis*. The reduction of symbiotic colonization was accompanied by enhanced responses at the host cell wall. Moreover, *GBP* mutation in barley also increased resistance to fungal infections in roots and leaves by the hemibiotrophic pathogen *Bipolaris sorokiniana* and the obligate biotrophic pathogen *Blumeria graminis* f. sp. *hordei*, respectively. These results indicate that *GBP1* is involved in the establishment of symbiotic associations with beneficial fungi, a role that has potentially been appropriated by barley-adapted pathogens.

## Introduction

Cell walls (CWs) are key interfaces in plant-fungal interactions, representing the first point of physical contact between the invading fungus and its potential host. Plant CWs consist of adaptable networks of cellulose microfibrils embedded in a matrix of hemicellulose (mostly xyloglucan, mannan and xylans), pectins and hydrophobic polymers such as cutin, lignin and suberin. Their architecture and composition are highly responsive to external and internal cues (Cosgrove, 2005; Cosgrove & Jarvis, 2012). Plant CWs act as scaffolds for hydrolytic enzymes and reservoirs for antimicrobial substances such as secondary metabolites and reactive oxygen species (ROS) (Aist, 1977; Brown *et al.*, 1998; Bednarek *et al.*, 2009; Underwood, 2012). To gain access to the nutritional resources of the host, fungi need to trespass these chemical and physical barriers. They do so by employing either carbohydrate active enzymes (CAZymes) and/or specialized pressure-driven penetration structures like appressoria. Plants counteract those strategies by forming carbohydrate-enriched CW appositions (CWAs), so-called papillae, which act as CW reinforcements at the sites of fungal penetrations (Hückelhoven, 2007). Although the relevance of papillae in halting or delaying fungal colonization has been discussed over the last decades, many studies correlated papillae effectiveness with the timing of deposition, papillae size and architecture, as well as composition (Aist, 1977; Zeyen *et al.*, 2002; Chowdhury *et al.*, 2014; Hückelhoven, 2014). Systematic screenings of *Arabidopsis thaliana* CW mutants have shown that interference with the structure and composition of plant CWs severely impacts fungal compatibility (Molina *et al.*, 2021). Besides the direct effects of changes in CW architecture, compromised CW integrity can indirectly prime host defenses and alter phytohormone levels, which ultimately impact fungal colonization success (Nishimura *et al.*, 2003; Hernández-Blanco *et al.*, 2007; Escudero *et al.*, 2017; Molina *et al.*, 2021).

Both fungi and plants secrete a plethora of CAZymes upon confrontation. These host and fungal hydrolases not only physically damage each other's CWs, but also release carbohydrate oligomers as degradation products that can inform the host's immune system about the invading microbe. Fungal chitin and its deacetylated derivative chitosan are well studied microbe-associated molecular patterns (MAMPs) that upon perception by cell surface receptor-like kinases mount a range of defense responses such as the production of ROS and the secretion of antimicrobials (Yin *et al.*, 2016;

Albert *et al.*, 2020). Furthermore, fungal hydrolases and mechanical forces exerted during fungal penetration release a variety of plant CW-derived fragments, functioning as damage-associated molecular patterns (DAMPs) (Hahn *et al.*, 1981). This recognition of modified self similarly initiates immune signaling pathways. Examples for unequivocal plant CW-derived DAMPs are cellulose oligomers, pectin oligogalacturonides, as well as mannan, xyloglucan and arabinoxylan fragments (Aziz *et al.*, 2007; Galletti *et al.*, 2008; Ferrari *et al.*, 2013; Claverie *et al.*, 2018; Zang *et al.*, 2019; Mélida *et al.*, 2020).

In the context of fungal colonization,  $\beta$ -glucans perform different functions in enhancing or suppressing immune responses, depending on their structure and branch decorations and cannot be clearly categorized as MAMPs or DAMPs. They represent the major component of most fungal cell surface glycans, being part of both the outer layer of the rigid fungal CW as well as the surrounding gel-like extracellular polysaccharide (EPS) matrix loosely attached to the CW (Wawra *et al.*, 2019; Wanke *et al.*, 2021). Plants secrete various carbohydrate hydrolases, amongst them  $\beta$ -glucanases, that target these fungal glycans (Rovenich *et al.*, 2016; Perrot *et al.*, 2022). The potential of some glycans to act as MAMPs and elicit pattern-triggered immunity has been demonstrated for a wide range of host plants (Fesel & Zuccaro, 2016). Notably, plants respond differentially to short-chain and long-chain  $\beta$ -1,3-glucans (Wanke *et al.*, 2020). While *Arabidopsis thaliana* Col-0 mounts immune responses such as ROS production, cytosolic calcium influx, MAPK activation and PR gene expression induction upon treatment with short-chain  $\beta$ -1,3-glucans like laminarihexaose, it does not respond to long-chain  $\beta$ -1,3-glucans. In contrast, immune responses in *Nicotiana benthamiana* are only activated upon treatment with long-chain  $\beta$ -1,3-glucans. The monocots *Hordeum vulgare* (barley) and *Brachypodium distachyon* are able to perceive both types of  $\beta$ -1,3-glucan independent of their degree of polymerization (Mélida *et al.*, 2018; Wanke *et al.*, 2020). While the responses to laminarihexaose in *Arabidopsis* are mediated by the central carbohydrate lysin motif (LysM) receptor-like kinase CERK1, perception of long-chain  $\beta$ -1,3-glucans in *N. benthamiana* and *Oryza sativa* is CERK1 independent (Mélida *et al.*, 2018; Wanke *et al.*, 2020). It was recently suggested that  $\beta$ -glucan oligomers from fungal cell surface glycans do not function only as MAMPs. Upon fungal colonization, barley secretes the  $\beta$ -1,3-glucanase BGLUII which releases a highly substituted and specific  $\beta$ -1,3-glucan

decasaccharide ( $\beta$ -GD) from the fungal EPS matrix (Chandrasekar *et al.*, 2022). Instead of activating immune responses in its host,  $\beta$ -GD exhibits antioxidative properties that help to overcome the hostile oxidative environment and, thereby, facilitate host colonization. In addition to their occurrence in fungal CWs,  $\beta$ -1,3-glucan polymers are major components of callose in host CWAs (Hückelhoven, 2007). Since the release of callose fragments from papillae by mechanical force or enzymatic digest is conceivable,  $\beta$ -1,3-glucan oligomers can serve a dual function as DAMPs and/or MAMPs (Mélida *et al.*, 2018). A similar dual role has been recently attributed to immunogenic mixed-linked  $\beta$ -1,3/1,4-glucans that can be found in the CWs of grasses as well as fungi and other microbes (Rebaque *et al.*, 2021; Barghahn *et al.*, 2021).

To detect novel components linked to  $\beta$ -glucan signaling in barley, we performed a protein pull-down with biotinylated laminarin, which has the  $\beta$ -1,6-branched  $\beta$ -1,3-glucans also found in fungal cell walls. Thereby, we identified the GH81  $\beta$ -1,3-endoglucanase GBP1 as a major interactor of  $\beta$ -1,3/1,6-glucans. Purified GBP1 specifically hydrolyzes  $\beta$ -1,3-linked glucans and can modulate ROS responses in *N. benthamiana* and *H. vulgare*. CRISPR/Cas9-generated mutation of the two *GBP* gene copies decreased the colonization efficiency of the beneficial root endophytes *Serendipita indica* and *S. vermifera* (Basidiomycota) as well as the arbuscular mycorrhizal (AM) fungus *Rhizophagus irregularis* (Glomeromycotina). This phenotype was accompanied by a hyperresponse of the host CW during fungal colonization. Additionally, *gbp* double mutants were more resistant to root infection with the hemibiotrophic pathogen *Bipolaris sorokiniana* and leaf infection with *Blumeria graminis* f. sp. *hordei* (hereafter, *B. graminis*) (Ascomycota). Altogether, this demonstrates a previously undescribed role of  $\beta$ -1,3-endoglucanases as tissue-independent broad range compatibility factors for fungal colonization.

## Material and methods

### *Plant material and growth conditions*

#### *Hordeum vulgare*

All experiments, including the generation of CRISPR/Cas9 knock-out lines, were performed with the spring barley (*H. vulgare* L.) Golden Promise Fast, an introgression line carrying the *Ppd-H1* allele that confers fast flowering (Gol *et al.*, 2021). From here on, we use “control” to name this non-mutagenized cultivar that carries normal copies of *GBP1* and *GBP2*. For ROS burst assays, barley seeds were surface sterilized with 6% bleach for 1 hour and then washed extensively (5 × 30 mL sterile water). Seeds were germinated on wet filter paper at room temperature in the dark under sterile conditions for three days before transfer to sterile jars containing solid 1/10 plant nutrition medium (PNM) and 0.4% Gelrite (Duchefa, Haarlem, the Netherlands) (Lahrmann *et al.*, 2013). Seedlings were cultured for four days in a growth chamber under long-day conditions (day/night cycle of 16/8 h, 22°C/18°C, light intensity of 108  $\mu\text{mol}\cdot\text{m}^{-2}\cdot\text{s}^{-1}$ ).

#### *Nicotiana benthamiana*

Seeds of *N. benthamiana* wild-type lines were sown on soil and grown for 3 weeks in the greenhouse under long-day conditions (day/night cycle of 16/8 h, 22–25°C, light intensity of ~140  $\mu\text{mol}\cdot\text{m}^{-2}\cdot\text{s}^{-1}$ , maximal humidity of 60%).

### *Carbohydrate substrates for immunity and enzymatic digestion assays*

All laminarioligomeres, gentiobiose, chitohexaose, cellohexaose and xyloglucan oligomers (XXXG) were purchased from Megazyme (Bray, Ireland). Laminarin from *Laminaria digitata* was purchased from Sigma-Aldrich (Taufkirchen, Germany) and laminarin from *Eisenia bicyclis* was purchased from Biosynth (Staad, Switzerland). Substrates derived from *Serendipita indica* CW and EPS matrix were purified and prepared as previously described (Chandrasekar *et al.*, 2022).

*Identification of protein candidates interacting with laminarin**Biotinylation of laminarin*

Laminarin (final concentration ~ 60 mM) was incubated with biotin-hydrazide (120 mM) and sodium cyanoborohydride (1 M) for 2 h at 65°C. The product was purified on a PD MidiTrap G-10 column (GE Healthcare) according to the manufacturer's description. Success of biotinylation was validated via mass spectrometry. The immunogenic capacity of biotinylated laminarin was confirmed via ROS burst assays.

*Protein pull-down with biotinylated laminarin*

Barley leaves from 2-week-old plants were treated for 15 min with biotinylated laminarin, followed by vacuum infiltration for 2 min. Untreated laminarin and a biotinylated version of the bacterial elongation factor Tu peptide (elf18) were used as controls. The tissue was frozen in liquid nitrogen and ground to fine powder. Then, 10 mg·ml<sup>-1</sup> of extraction buffer (10mM MES, 50mM NaCl, 10mM MgCl<sub>2</sub>, 1mM DTT, 1% IGEPAL, proteinase inhibitor cocktail) were added to the powder. To avoid pH-dependent binding effects to the NeutrAvidin beads, two buffer conditions (pH 5.6 and pH 8.0) were used for all treatments. Samples were incubated rotating at 4°C for 60 min and centrifuged at 10,000 rpm, 4°C for 15 min. Supernatant was filtered to remove pieces, mixed with 50 µL of high-capacity Neutravidin agarose resin (Thermo Fisher Scientific, Schwerte, Germany), and incubated (inverting) at 4°C for 3 h. The sample was briefly centrifuged at 700 rpm for 1 min. After discarding the supernatant, the beads were washed four times with 10 mL of wash buffer (10mM MES [pH 5.6 or pH 8.0], 50mM NaCl, 10mM MgCl<sub>2</sub>, 0.5% IGEPAL). Proteins were eluted by boiling the beads with 50-70 µL of 2 x SDS loading (including reducing agent) for 5 min. Proteins were separated by SDS-PAGE (NuPAGE; Invitrogen, Waltham, United States) after staining with Coomassie brilliant Blue G-250, cut out for mass spectrometric analysis and digested with trypsin.

*Tandem mass spectrometric (MS-MS) analysis of the pull-down proteins*

LC-MS/MS analysis was performed using an LTQ-Orbitrap mass- spectrometer (Thermo Fisher Scientific, Schwerte, Germany) and a nanoflow-HPLC system (nanoAcquity; Waters, Wilmslow, United Kingdom) as described previously (Ntoukakis *et al.*, 2009). The entire *Hordeum vulgare* Morex v1.0 database (IBSC\_v2, IPK



Gatersleben) was searched using Mascot (Matrix Science) (with the inclusion of sequences of common contaminants, such as keratins and trypsin).

*Plasmid construction for the heterologous expression of barley GBP1 in N. benthamiana*

For *in planta* protein production in *N. benthamiana*, we used the binary vector pXCScpmv-HAStrep (Witte *et al.*, 2004; Myrach *et al.*, 2017) characterized by a 35S promoter cassette, modified 5'- and 3'-UTRs of RNA-2 from the cowpea mosaic virus as translational enhancers, and C-terminal hemagglutinin (HA) and StrepII tags. The codon-optimized GBP1 coding sequence was amplified with the primer pair *Clal*\_GBP1\_F (5'-gacggtatcgataaaATGCCGCCACATGGTAGACG-3') and GBP1\_noSTOP\_*Xmal*\_R (5'-ataactcccgggATGGCCATATTGACGATACCAACAGC-3') and directionally cloned into the *Clal* and *Xmal* sites of the binary vector to produce pXCScpmv-GBP1-HAStrep. To generate a catalytically inactive version of GBP1, the first glutamate residue of the catalytic center (E500) was exchanged to an alanine residue via site-directed mutagenesis PCR with the primer pair GBP1\_E500A\_F (5'-CAGGCATCAACATCAGAAGCAGTG-3') and GBP1\_E500A\_R (5'-GTTCCCTACCATCTCCAAACTCAGTC-3'). The linearized, mutated plasmid was purified after gel electrophoresis using the NucleoSpin Gel and PCR Clean-up Kit (Machery-Nagel, Düren, Germany). The isolated DNA fragment was treated with a self-made KLD mixture (1,000 units·ml<sup>-1</sup> T4 polynucleotide kinase, 40,000 T4 DNA ligase units·ml<sup>-1</sup> ligase 2,000 units·ml<sup>-1</sup> DpnI, 1 × T4 DNA ligase buffer; all enzymes were purchased from New England Biolabs, Ipswich, USA) for 1 hour at room temperature before transformation into *Escherichia coli* MachI cells. Plasmids were isolated using the NucleoSpin Plasmid Kit (Machery-Nagel, Düren, Germany) and sequenced to confirm the introduced mutation. Both plasmids (pXCScpmv-GBP1-HAStrep and pXCScpmv-GBP1\_E500A-HAStrep) were introduced into *Agrobacterium tumefaciens* GV3101::pMP90RK strains for transient transformation of *N. benthamiana* leaf tissue.

*Heterologous protein production and purification from N. benthamiana*

*A. tumefaciens* GV3101::pMP90RK strains carrying the binary vectors for protein production (antibiotic selection: 30 µg·mL<sup>-1</sup> Rifampicin, 25 µg·mL<sup>-1</sup> Kanamycin, 50

$\mu\text{g}\cdot\text{mL}^{-1}$  Carbenicillin) and *A. tumefaciens* GV3101 strains carrying the binary vector for viral p19 silencing inhibitor expression (antibiotic selection:  $30\ \mu\text{g}\cdot\text{mL}^{-1}$  Rifampicin,  $30\ \mu\text{g}\cdot\text{mL}^{-1}$  Gentamicin,  $100\ \mu\text{g}\cdot\text{mL}^{-1}$  Carbenicillin) were grown in selection LB liquid medium at  $28^\circ\text{C}$ , 180 rpm for three days. The cultures were centrifuged ( $3,500\ \text{g}$  for 15 min), resuspended in infiltration buffer (10 mM MES pH 5.5, 10 mM  $\text{MgCl}_2$ , 200  $\mu\text{M}$  acetosyringone) to an  $\text{OD}_{600}$  of 1 and incubated for 1 h in the dark at  $28^\circ\text{C}$ , 180 rpm. Each of the two *A. tumefaciens* strains carrying the GBP1 production constructs was mixed with the *A. tumefaciens* strain carrying the p19-expressing construct in a 1:1 ratio. The bacterial suspensions were infiltrated into the four youngest, fully developed leaves of four-week-old *N. benthamiana* plants with a needleless syringe. Five days after infiltration, the leaves were detached from the plant and ground in liquid nitrogen. Protein purification was carried out according to Werner *et al.* (2008) with minor modifications: The ground plant material (up to the 5 mL mark of 15-mL tube) was thoroughly resuspended in 5 mL of ice-cold extraction buffer (100 mM Tris pH 8.0, 100 mM NaCl, 5 mM EDTA, 0.5% Triton X-100, 10 mM DTT,  $100\ \mu\text{g}\cdot\text{mL}^{-1}$  Avidin) and centrifuged at  $10,000\ \text{g}$ ,  $4^\circ\text{C}$  for 10 min. The supernatant was filtered through a PD-10 desalting column (Sigma-Aldrich, Taufkirchen, Germany), transferred to a new tube, and supplemented with  $75\ \mu\text{L}\cdot\text{mL}^{-1}$  Strep-Tactin Macroprep (50% slurry) (IBA Lifesciences GmbH, Göttingen, Germany). Samples were incubated in a rotary wheel at  $4^\circ\text{C}$  for one hour, followed by centrifugation for 30 s at 700 g. The supernatant was discarded, and the beads were washed three times with 2 mL of washing buffer (50 mM Tris pH 8.0, 100 mM NaCl, 0.5 mM EDTA, 0.005% Triton X-100, 2 mM DTT). Proteins were eluted from the beads by adding 100  $\mu\text{L}$  of elution buffer (wash buffer containing 10 mM biotin) and incubating at 800 rpm for 5 min at  $25^\circ\text{C}$ . The samples were centrifuged at 700 g for 20 s and the elution was repeated two more times. The elution fractions were pooled and dialyzed overnight against cold MilliQ water (dialysis tubing with 6-8 kDa cut-off). Proteins were stored on ice at  $4^\circ\text{C}$  for further use. The success of protein purification was analyzed by SDS PAGE and Western Blotting (Werner *et al.*, 2008).

### *Oxidative burst assay*

#### Preparation of the plant material

For immunity assays in barley, the roots and shoots of seven-day-old seedlings were separated. The root tissue between 2 cm below the seed and 1 cm above the tip was cut into 5 mm pieces. Each assay was carried out with randomly selected root pieces from 16 barley seedlings. Four root pieces were transferred to each well of a 96-well microtiter plate containing 150  $\mu\text{L}$  of sterile Milli-Q water. Barley shoot assays were performed on 3-mm leaf discs punched from the youngest leaves of eight individual barley seedlings.

For immunity assays in *N. benthamiana*, 3-mm leaf discs from the youngest, fully developed leaf of eight three-week-old plants were transferred to a 96-well plate filled with 150  $\mu\text{L}$  of sterile Milli-Q water.

#### Assay protocol

The ROS burst assay was based on previously published protocols (Chandrasekar *et al.*, 2022; Felix *et al.*, 1999). In brief, a 96-well plate containing water and plant material (as described above) was incubated overnight at RT to remove unstable contaminants that had resulted from mechanical damage to the tissue during preparation (e.g. ROS). The next day, the water was replaced with 100  $\mu\text{L}$  of fresh Milli-Q water containing 20  $\mu\text{g}\cdot\text{mL}^{-1}$  horseradish peroxidase (Sigma-Aldrich, Taufkirchen, Germany) and 20  $\mu\text{M}$  L-012 (Wako Chemicals, Neuss, Germany). After a short incubation period ( $\sim 15$  min), 100  $\mu\text{L}$  of double-concentrated elicitor solutions were added to the wells. All elicitors were dissolved in Milli-Q water without additional treatment. Measurements of elicitor-triggered apoplastic ROS production were started immediately and performed continuously with an integration time of 450 ms in a TECAN SPARK 10 M multiwell plate reader (Männedorf, Switzerland).

#### *Enzymatic carbohydrate digestion and thin layer chromatography (TLC)*

Carbohydrate digestion assays were performed using either purified barley GBP (heterologously expressed in *N. benthamiana*) or barley BGLUII (Chandrasekar *et al.*, 2022; available from Megazyme, E-LAMHV). Preparations of the fungal CW and EPS matrix were incubated overnight in sterile MilliQ water at 65°C prior to enzymatic

digestion. Substrate and enzyme concentrations, buffer compositions, digestion temperature and time are described in the figure captions. Digestion was stopped by denaturing the enzymes at 95°C for 10 min and the digestion products were stored at -20 °C prior to use. An aliquot of each sample was subjected to TLC using a silica gel 60 F254 aluminum TLC plate (Merck Millipore, Burlington, USA), using a running buffer containing ethyl acetate/acetic acid/methanol/formic acid/water at a ratio of 80:40:10:10:10 (v/v). D-glucose, laminaribiose  $\beta$ -1-3-(Glc)<sub>2</sub>, laminaritriose  $\beta$ -1-3-(Glc)<sub>3</sub>, gentiobiose  $\beta$ -1-6-(Glc)<sub>2</sub>, and laminaripentaose  $\beta$ -1-3-(Glc)<sub>5</sub> at a concentration of 1.5 mg·mL<sup>-1</sup> were used as standards (Megazyme, Bray, Ireland). To visualize the glucan fragments, the TLC plate was sprayed with glucan developer solution (45 mg N-naphthol, 4.8 mL H<sub>2</sub>SO<sub>4</sub>, 37.2 mL ethanol and 3 mL water) and baked at 95°C until the glucan bands became visible (approximately 4-5 min).

#### *MALDI TOF analysis*

The digested products of GBP1 were analyzed using Oligosaccharide Mass Profiling as previously described (Günl *et al.*, 2011). Briefly, 2  $\mu$ l of the samples were spotted onto a dihydroxy benzoic acid matrix (10 mg · mL<sup>-1</sup>) and analyzed by MALDI-TOF mass spectrometry (Bruker rapifleX instrument). The linear positive reflectron mode with an accelerating voltage of 20,000 V was used for the analysis of the sample by MALDI-TOF mass spectrometry (Bruker rapifleX instrument). The spectra of the samples were analyzed using the Flexanalysis software 4.0 (Bruker Daltonics, Billerica, USA).

#### *CRISPR/Cas9-based mutagenesis of GBP homologues in barley*

The CRISPOR web tool (version 4.97, Concordet and Haeussler, 2018) was used to design two single guide RNAs for each *GPB1* and *GBP2*:

GBP1\_gRNA1: 5'-CCCGGCACGCTTCTTCGCGCCGG-3'

GBP1\_gRNA2: 5'-TGGCGCCTTCGGATGAACAGCGG-3'

GBP2\_gRNA1: 5'-TAAGATCCGTCGAGGCAGTATGG-3'

GBP2\_gRNA2: 5'-GTACAGCCGTTGCTACCCGACGG-3'

Golden Gate cloning was used to load each guide sequence from complementary oligonucleotides into shuttle vectors pMGE625, pMGE626, pMGE628, pMGE629. The four guide expression cassettes were then assembled into binary vector pMGE599 to create pMP202. Vectors and cloning protocols have been previously described (Kumar *et al.*, 2018) and were kindly provided by Johannes Stuttmann. Stable transformation of pMP202 in Golden Promise Fast was performed as described (Amanda *et al.*, 2022).

### *Fungal colonization assays*

#### *Serendipita vermifera*, *Serendipita indica* and *Bipolaris sorokiniana*

The growth conditions for barley, *Serendipita vermifera* (MAFF305830, Sv), *Serendipita indica* (DSM11827, Si) and *Bipolaris sorokiniana* (ND90Pr, Bs) and the preparation of fungal suspensions for plant inoculation have been described previously (Sarkar *et al.*, 2019; Mahdi *et al.*, 2021). Four-day-old barley seedlings were transferred to sterile jars on 1/10 PNM (Plant Nutrition Medium, pH 5.7) and inoculated with 3 mL of either sterile water as control, Sv mycelium (1 g per 50 mL), Bs conidia (5,000 spores·mL<sup>-1</sup>) or Si chlamydospores (500,000 spores·mL<sup>-1</sup>). plants were grown on a day/night cycle of 16/8 h at 22/18 °C and 60 % humidity under a light intensity of 108 μmol·m<sup>-2</sup>·s<sup>-1</sup>. Plant roots were harvested six days after inoculation (dpi), washed thoroughly to remove extraradical fungal hyphae, and frozen in liquid nitrogen. Four barley plants were pooled per biological replicate. RNA extraction to quantify endophytic fungal colonization, cDNA generation and RT-PCR were performed as previously described (Sarkar *et al.*, 2019). The primers used are listed in Supplementary Table 1.

#### *Blumeria graminis* f. sp. *hordei*

Control and *gbp* knock-out lines were grown in soil in a growth chamber (Polyclimate) at 19 °C, 60 % relative humidity and a photoperiod of 14 h with a light intensity of 100 μmol m<sup>-2</sup> s<sup>-1</sup>. Primary leaves of seven-day-old plants were cut and placed adaxial side down on 1% plant agar plates before gravity inoculation with *Blumeria graminis* f. sp. *hordei* isolate K1 at a conidial density of about 20 conidia per mm. Ten- to 14-day-old plants were infected with *Blumeria graminis* f. sp. *hordei* K1 for five to seven days.

Leaves were harvested at the indicated time points and cleared in 70 % ethanol before staining of the fungal structures with Coomassie brilliant blue solution (0.1 % [w/v] Coomassie Brilliant Blue R250 in 50 % ethanol and 10 % acetic acid) for 10 to 15 seconds. Bright field microscopy was used to assess secondary hyphae formation in 50 germinated conidia spores in the tip area and 50 germinated conidia in the middle of the leaf. At least six independent leaves were examined at 48 h after infection for fungal penetration success.

### *Rhizophagus irregularis*

Barley control and mutant seeds were sterilized and germinated as described previously (Mahdi *et al.*, 2021). Germinated seedlings were transferred to 9 × 9 cm pots containing autoclaved 1:1 silica sand:vermiculite mixture inoculated with 700 mg *R. irregularis* spore inoculum (10,000 spores·g<sup>-1</sup> moist diatomaceous earth powder [50% water]) (Symplanta, Darmstadt, Germany). Approximately 500 mg of the inoculum was evenly mixed into the lower two-third substrate layer, further 200 mg were evenly sprinkled into a hole in the upper third of the substrate layer, into which the seedlings were transplanted. The seedlings were grown in the greenhouse and watered weekly with 30 mL of deionized water and tap water in a 1:1 ratio. Roots were harvested at 28 dpi and stored in 50% EtOH at 4°C until staining.

Roots were stained according to a previously published protocol (Vierheilig *et al.*, 1998). Briefly, roots were incubated for 15 min at 95°C in 10% KOH, washed with 10% acetic acid and incubated for 5 min at 95°C with a staining solution of 5% ink (Pelikan, Falkensee, Germany) in 5% acetic acid. After staining, the roots were carefully washed with tap water, then incubated in 5% acetic acid at 4°C for at least 20 minutes. The ink-stained root tissue was cut into 1 cm segments with a scalpel and 30 segments of similar diameter were randomly selected from each genotype. Cross-section points were determined from 10 random cuts per root segment. Ink-stained *R. irregularis* structures such as intraradical hyphae (IRH), extraradical hyphae (ERH), arbuscules and vesicles were visualized with a light microscope (AxioStar, Carl Zeiss, Jena, Germany) at 10× magnification. Colonization with *R. irregularis* was scored as positive if IRH, arbuscules or vesicles were present. The roots of four biological replicates per genotype were examined.



*Staining for confocal microscopy*

Root tissue of barley control and mutant plants colonized by *S. indica* was harvested at 6 dpi and then stained as previously described (Hilbert *et al.*, 2019). Briefly, roots were incubated at 95 °C for 2 min in 10% KOH, washed 3 times for 30 min in deionized water and 3 times for 30 min in PBS (pH 7.4). The roots were stained for 5 min under vacuum and then washed three times with deionized water. Fungal structures were visualized using 10 µg·mL<sup>-1</sup> fluorescently labeled wheat germ agglutinin (WGA-AF488, Invitrogen, Thermo Fisher Scientific, Schwerte, Germany) in PBS (pH 7.4) and imaging was conducted with an excitation wavelength of 488 nm and emission detection between 500-540 nm. Papillae and root cell wall appositions were stained with 10 µg·mL<sup>-1</sup> fluorescently labeled Concanavalin A (ConA-AF633, Invitrogen, Thermo Fisher Scientific, Schwerte, Germany) in PBS (pH 7.4) and imaged by excitation at 633 nm and detection at 650-690 nm.

Images were taken with a Leica TCS SP8 confocal microscope (Wetzlar, Germany). The percentage area of ConA staining was quantified using Fiji (Schneider *et al.*, 2012) in maximum intensity projections of 10-slice Z-stacks with an image depth of 10 µm. At least 24 different root regions of each genotype were analyzed.

## Deposit numbers

*Hordeum vulgare* GBP1: HORVU5Hr1G059430.56 (*Hordeum vulgare* Morex v1.0, IBSC\_v2, IPK Gatersleben),

*Hordeum vulgare* GBP2: HORVU6Hr1G034610.3

(*Hordeum vulgare* Morex v1.0, IBSC\_v2, IPK Gatersleben),

*Hordeum vulgare* BGLU2: P15737 (UniProt), HORVU3Hr1G105630.7

(*Hordeum vulgare* Morex v1.0, IBSC\_v2, IPK Gatersleben).

## Results

### *Barley GBP-type enzymes mediate compatibility to leaf and root colonization by fungi with different lifestyles*

Leaf and root tissues of barley express the cellular machinery necessary to sense the long-chain  $\beta$ -1,3/ $\beta$ -1,6 branched glucan laminarin (Supplementary Figure 1). To discover interactors of long-chain  $\beta$ -glucans, we performed a protein pull-down approach using biotinylated laminarin as bait. The biotinylated and non-biotinylated versions of laminarin induced similar ROS burst responses in barley (Supplementary Figure 2A), confirming that biotinylation of laminarin does not alter its immunogenic potential. Non-biotinylated laminarin and biotinylated elf18 were included as control treatments. Elf18 is a peptide derived from the prokaryotic elongation factor Tu, a well characterized immunogenic peptide solely perceived by *Brassicaceae* members. Eluted proteins were separated by SDS-PAGE (Supplementary Figure 2B), extracted from the gel, and further subjected to tandem mass spectrometric analysis. A total of 101 proteins was identified across the three treatments, based on strict criteria for candidate selection (i.e. proteins detected in three out of four replicates). The only interactor detected exclusively in the biotinylated laminarin treatment (Figure 1A) was the  $\beta$ -glucan-binding protein GBP1 (HORVU5Hr1G059430.56). Despite the absence of a predicted signal peptide in its gene sequence, GBP1 was previously identified in barley apoplastic fluids following colonization by the mutualistic root endophyte *S. indica* (Nizam *et al.*, 2019). In support of this, another study demonstrates that a GBP ortholog in soybean is secreted into the apoplastic space even in the absence of a signal peptide (Umemoto *et al.*, 1997). GBPs are found in the genomes of most land plants, including bryophytes, ferns and angiosperms (Supplementary Figure 3). They have been duplicated several times throughout the evolution of plants, with a large expansion in legumes. Barley has two GBP copies (GBP1 and GBP2, HORVU6Hr1G034610.3) but only GBP1 is expressed according to publicly available transcriptomic data sets (Supplementary Figure 4).

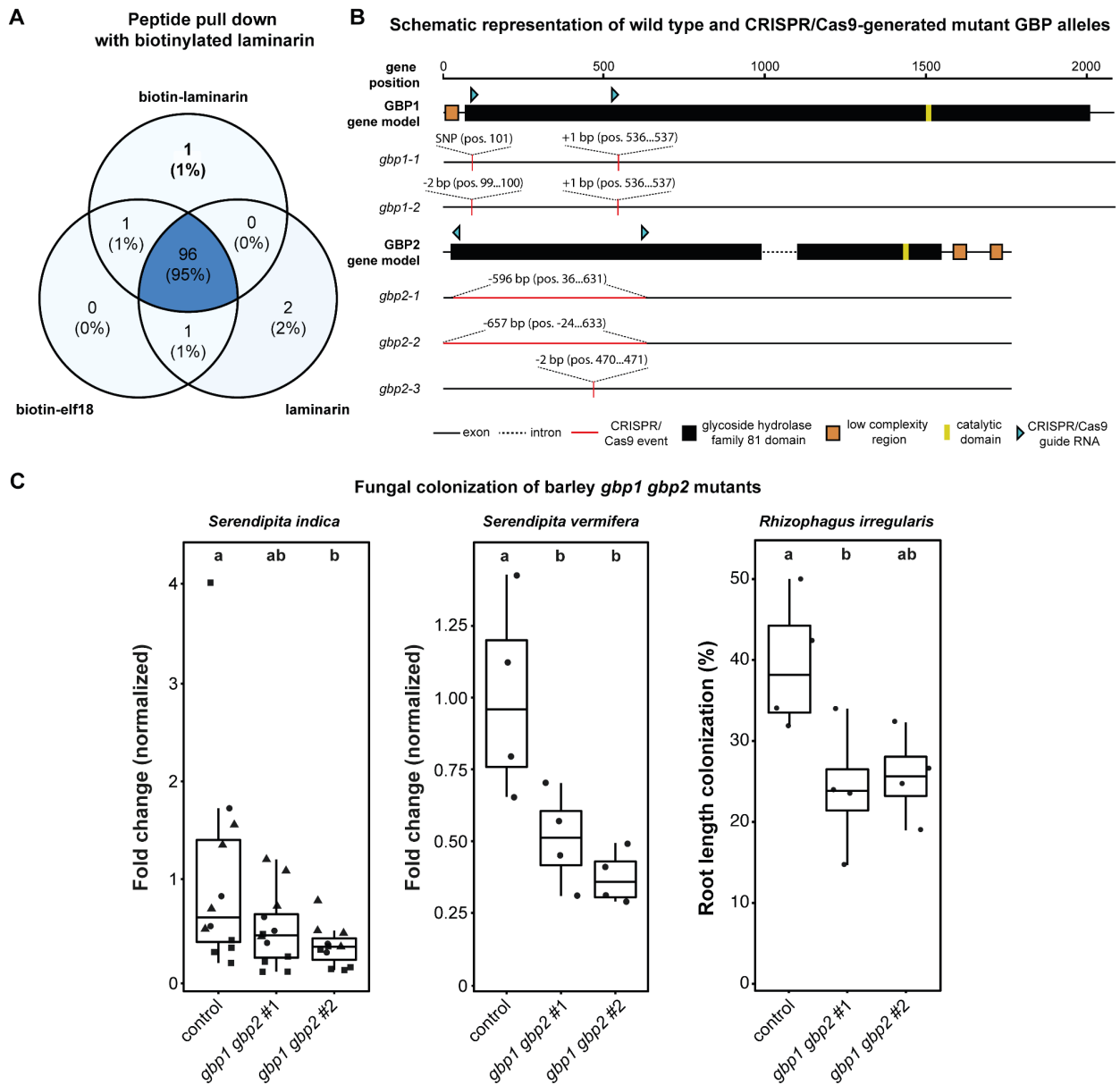


**Figure 1. GBP1 is a compatibility factor identified *via* protein pull-down with biotinylated laminarin in barley.** (A) Distribution of barley proteins identified by LC-MS/MS analysis with biotinylated laminarin, biotinylated elf18 or laminarin as bait. Only the proteins whose peptides were identified in three out of four replicates are listed. (B) Schematic overview of CRISPR/Cas9-generated mutant alleles in *GBP1* and *GBP2*. (C) Colonization of control and *gbp1 gbp2* barley lines by *S. indica*, *S. vermifera* and *R. irregularis*. Boxplot elements in this figure: center line, median; box limits, upper and lower quartiles; whiskers,  $1.5 \times$  interquartile range. Data points from independent experiments are indicated by data point shape. Letters represent statistically significant differences in expression based on a one-way ANOVA and Tukey's post hoc test (significance threshold:  $P \leq 0.05$ ). elf18, peptide derived from bacterial elongation factor Tu.

To investigate the contribution of barley GBPs to fungal colonization, we used a CRISPR/Cas9 approach to generate plants mutated in both *GBP* genes (*gbp1 gbp2*, Figure 1B). The first mutant line (*gbp1 gbp2* #1) is homozygous for the mutant alleles *gbp1-1* and *gbp2-1*, and the second mutant line (*gbp1 gbp2* #2) is homozygous for the *gbp1-2* allele and biallelic for *gbp2-2* and *gbp2-3*. The seedlings of the two independent mutant lines showed no differences in root and shoot biomass compared to the control lines (Supplementary Figure 5). To survey colonization by fungi with different lifestyles and colonization strategies, we inoculated the control and both mutant lines with the beneficial root endophytes *S. indica* and *S. vermifera* as well as the AM fungus *R. irregularis* (Figure 1C, Supplementary Figure 6). In all three cases, total fungal colonization was reduced in both *gbp1 gbp2* mutant lines compared to the control lines, with at least one mutant line presenting a significant reduction in colonization. To expand the range of surveyed fungal lifestyles, we additionally tested colonization by the hemibiotrophic root pathogen *Bipolaris sorokiniana* and the obligate biotrophic foliar pathogen *Blumeria graminis* (Supplementary Figure 7). Both *B. sorokiniana* and *B. graminis* showed a significant decrease of fungal biomass and penetration success, respectively. In conclusion, the *gbp1 gbp2* mutant lines showed increased resistance to fungal colonization compared to the control plants, irrespective of the taxonomic position of the fungus, its lifestyle or the host tissue inoculated. Although we cannot rule out the possibility that GBP2 is also involved in mediating compatibility, the fact that we did not detect any expression of GBP2 (Supplementary Figure 4) suggests that the observed phenotype mainly depends on the role of GBP1 as a compatibility factor for fungal colonization of root and leaf tissues.

*GBP1 is an active  $\beta$ -1,3-endoglucanase hydrolyzing  $\beta$ -1,3-glucans with a low degree of  $\beta$ -1,6 substitutions*

We further biochemically characterized the laminarin-interactor GBP1, which belongs to the GH81 family of the carbohydrate active enzymes (CAZymes). These enzymes are characterized by their endoglycosidic activity on substituted and unsubstituted  $\beta$ -1,3-linked glucans. Their catalytic center is highly conserved across bacteria, fungi, and plants. GH81 family glycosyl hydrolases follow an inverting hydrolysis mechanism that requires a glutamate residue acting as nucleophiles (Fig. 2A).

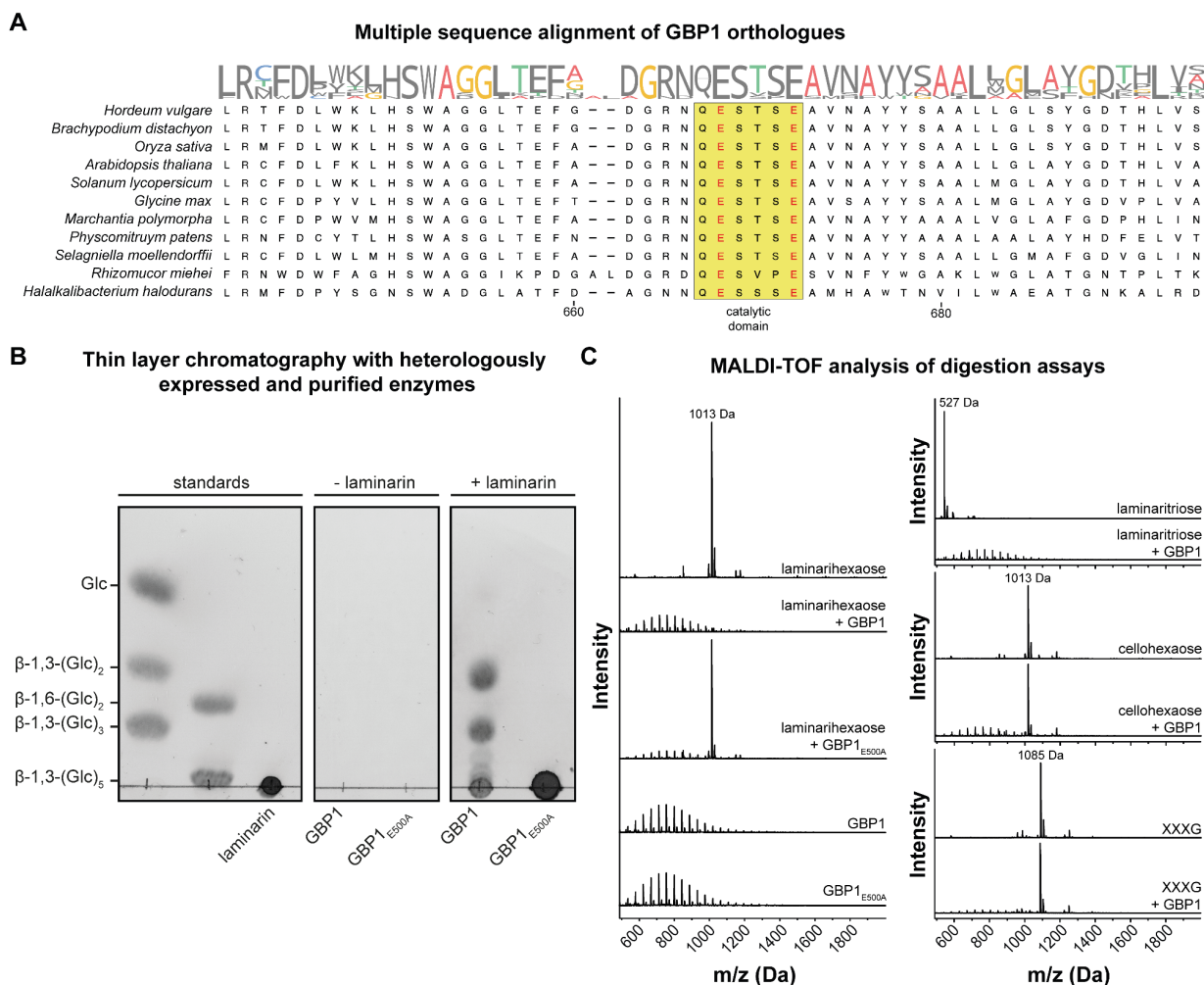


**Figure 2. Barley GBP1 has a conserved GH81 catalytic center that specifically mediates the hydrolysis of  $\beta$ -1,3-glucans.** (A) Multiple sequence alignment with sequences from different domains of life shows conservation of the catalytic domain (yellow box), which contains the previously described glutamate residues (red letters) that act as nucleophiles in carbohydrate hydrolysis (Fliegmann *et al.*, 2004). (B) Analysis of the  $\beta$ -1,3-glycosidic activity of heterologously expressed and purified GBP1 and mutant GBP1<sub>E500A</sub> on laminarin from *Laminaria digitata*. After overnight incubation at 25°C, the digestion products were analyzed by thin layer chromatography. Only the wild-type but not the mutated version of GBP1 exhibited hydrolytic activity on laminarin. The experiment was repeated more than four times with similar results. (C) The activity of GBP1 and GBP1<sub>E500A</sub> was tested on laminarihexaose ( $\beta$ -1,3-glucan hexamer), cellohexaose ( $\beta$ -1,4-glucan hexamer) and XXXG (xyloglucan heptamer). After overnight digestion at 25°C, the products were analyzed by MALDI-TOF mass spectrometry. Among the tested substrates, the hydrolytic activity of laminarin is specific to  $\beta$ -1,3-glucans. Digestion assays were performed twice with similar results. UT, untreated; XXXG, xyloglucan heptasaccharide.

To verify the predicted  $\beta$ -1,3-endoglycosidic activity of GBP1, we overexpressed and purified a codon-optimized, C-terminally HA-StrepII-tagged version of barley GBP1 from *N. benthamiana* leaves (Supplementary Figure 8). Digestion assays with laminarin as a substrate confirmed the  $\beta$ -1,3-endoglycosidase activity of GBP1 (Figure 2B). Furthermore, site-directed mutagenesis of the predicted catalytically active site of GBP1 by replacing the first glutamate residue (putative nucleophile, E500) with an alanine (GBP1<sub>E500A</sub>) abolished its enzymatic activity (Figure 2B). This confirms that the observed digestion of laminarin is specific to the conserved catalytic site of GBP1. Activity assays with laminarin showed that GBP1 is highly active over a wide range of pH values (pH 5-9) and has the highest hydrolytic activity at 60°C (Supplementary Figure 9). GBP1 activity is specific to  $\beta$ -1,3-linked glucans (laminarihexaose, laminaritriose and laminarin), while MALDI-TOF analysis revealed that GBP1 is unable to digest other oligosaccharides such as  $\beta$ -1,4-linked cellobiohexaose and xyloglucan (XXXG) (Figure 2B+C).

To further test whether GBP1 is able to process complex substrates derived from the CW and extracellular polysaccharide (EPS) matrix of fungi, we performed digestion assays with crude *S. indica* CW and EPS matrix preparations as well as the previously characterized  $\beta$ -GD (Chandrasekar *et al.*, 2022).  $\beta$ -GD is a glucan fragment that is highly enriched during digestion of the *S. indica* matrix with the barley glucanase BGLUII. While GBP1 does not hydrolyze the highly  $\beta$ -1,6-branched glucans in the EPS matrix of *S. indica* and the derived  $\beta$ -GD, it can act to a minor extent on *S. indica* CWs (Supplementary Figure 10). This is consistent with the inability of GBP1 to digest the highly substituted laminarin from the brown alga *Eisenia bicyclis* (Supplementary Figure 11). This verifies that frequent  $\beta$ -1,6-branching patterns of glucans protect against hydrolytic degradation and activation of plant immunity as previously demonstrated for the EPS matrices of plant-colonizing fungi (Chandrasekar *et al.*, 2022).

Secreted plant hydrolases are known to modulate the activation of immunity by releasing, tailoring and increasing the accessibility of fragments from invading microbes (Rovenich *et al.*, 2016; Buscaill *et al.*, 2019). To test to what extent the observed hydrolytic activity of GBP1 on  $\beta$ -1,3-glucans alters their immunogenic potential, we treated *N. benthamiana* and barley with gradually digested laminarin (Figure 3A+B).

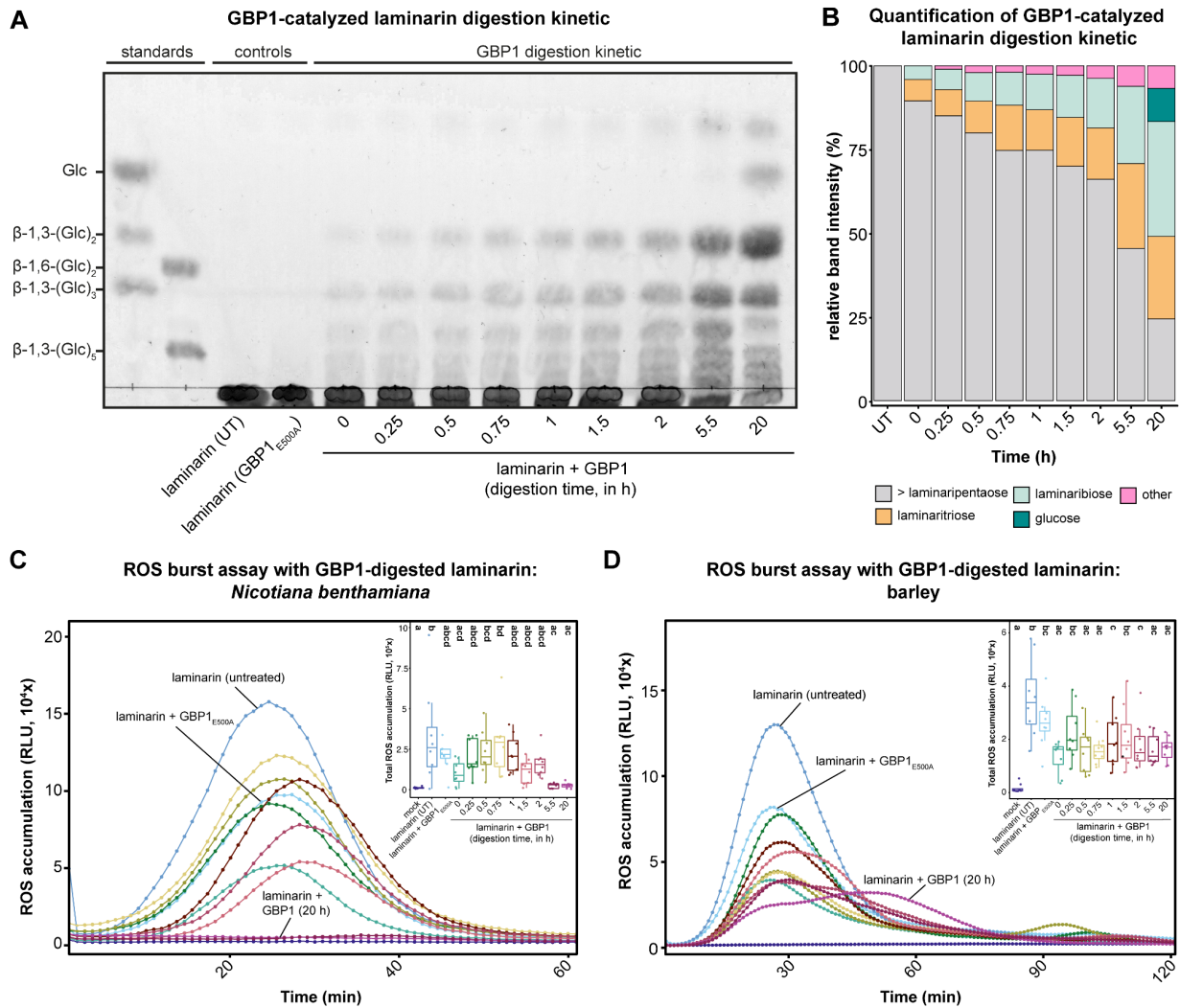


**Figure 3. GBP1 treatment of long-chain  $\beta$ -1,3-linked glucans modulate ROS production.** To investigate the effects of gradual hydrolysis of  $\beta$ -glucans by GBP1 on ROS bursts in *N. benthamiana* and barley, a digestion time series was performed with laminarin. (A) The digestion products were analyzed by thin layer chromatography. Untreated (UT) and GBP<sub>E500A</sub>-treated laminarin (20 hours) served as controls. Digestion was performed at 25°C. (B) Quantification of TLC band intensity using the ImageJ software. (C+D) Apoplastic ROS accumulation after treatment of *N. benthamiana* (C) and barley (D) with gradually digested laminarin (1 mg·ml<sup>-1</sup>) was monitored using a luminol-based chemiluminescence assay. Milli-Q water (mock) treatment, untreated laminarin (UT) and GBP<sub>E500A</sub> were used as controls. Values represent mean  $\pm$  SEM from eight wells. Boxplots display total ROS accumulation over the measured period of time. Boxplot elements in this figure: center line, median; box limits, upper and lower quartiles; whiskers, 1.5  $\times$  interquartile range. Letters represent statistically significant differences in expression based on a one-way ANOVA and Tukey's post hoc test (significance threshold:  $P \leq 0.05$ ). The assays were performed two times with independent laminarin digestions. ROS, reactive oxygen species; TLC, thin layer chromatography; UT, untreated.



To assess changes in early immune signaling, we used  $\beta$ -glucan-triggered ROS production, one of the first defense mechanisms triggered by MAMPs, as a readout. *N. benthamiana* and barley differ in terms of their perceived  $\beta$ -glucan substrates (Wanke *et al.*, 2020). The dicotyledonous *N. benthamiana* activates immune responses only when treated with long-chain  $\beta$ -1,3-glucans. As digestion of laminarin by GBP1 progressed, the intensity of the triggered oxidative burst gradually decreased to the level of mock treatment (20 hours) (Figure 3C). In contrast to *N. benthamiana*, barley responds to both short- and long-chain  $\beta$ -1,3-glucans. Accordingly, incubation of laminarin with GBP1 reduced the intensity of the oxidative burst but did not completely abolish it due to the recognition of the released short-chain hydrolysis products (Figure 3D). Treatment with the inactive version GBP1<sub>E500A</sub> (20 hours) did not affect laminarin perception in either species (Figure 3C+D).

#### *Barley GBPs are not essential for $\beta$ -glucan-triggered ROS production*

Previous studies on perception of a  $\beta$ -1,3/1,6-heptaglucoside from oomycetes in legumes have led to the suggestion that GBPs may be a part of the corresponding  $\beta$ -glucan perception machinery (Fliegmann *et al.*, 2004; Umemoto *et al.*, 1997). Since oomycete-derived heptaglucoside perception is specific to legumes (Fliegmann *et al.*, 2004), we investigated whether barley GBPs are involved in  $\beta$ -glucan-triggered ROS production upon treatment with short- and long-chain  $\beta$ -glucans. Since ROS burst production still occurred in both *gbp* double mutant lines (Supplementary Figure 12), we conclude that GBPs are not essential for the immune perception of  $\beta$ -glucan in barley.

#### *Barley GBP mutants exhibit hyperresponsive CW reaction upon colonization by endophytic fungi*

Previous studies have shown that broad-spectrum resistance to fungi can be mediated by the enhanced formation of CWAs, so called papillae, which are predominantly formed at the sites of hyphal penetration (Hilbert *et al.*, 2019). A major component of these CW reinforcements is callose, a linear  $\beta$ -1,3-linked glucan that could serve as a substrate for GBPs. To investigate the effect of GBPs on the formation of CWAs upon colonization by the root endophytes *S. indica* and *S. vermifera*, we monitored and quantified CWAs using a fluorescent version of the carbohydrate-binding lectin concanavalin A (ConA).

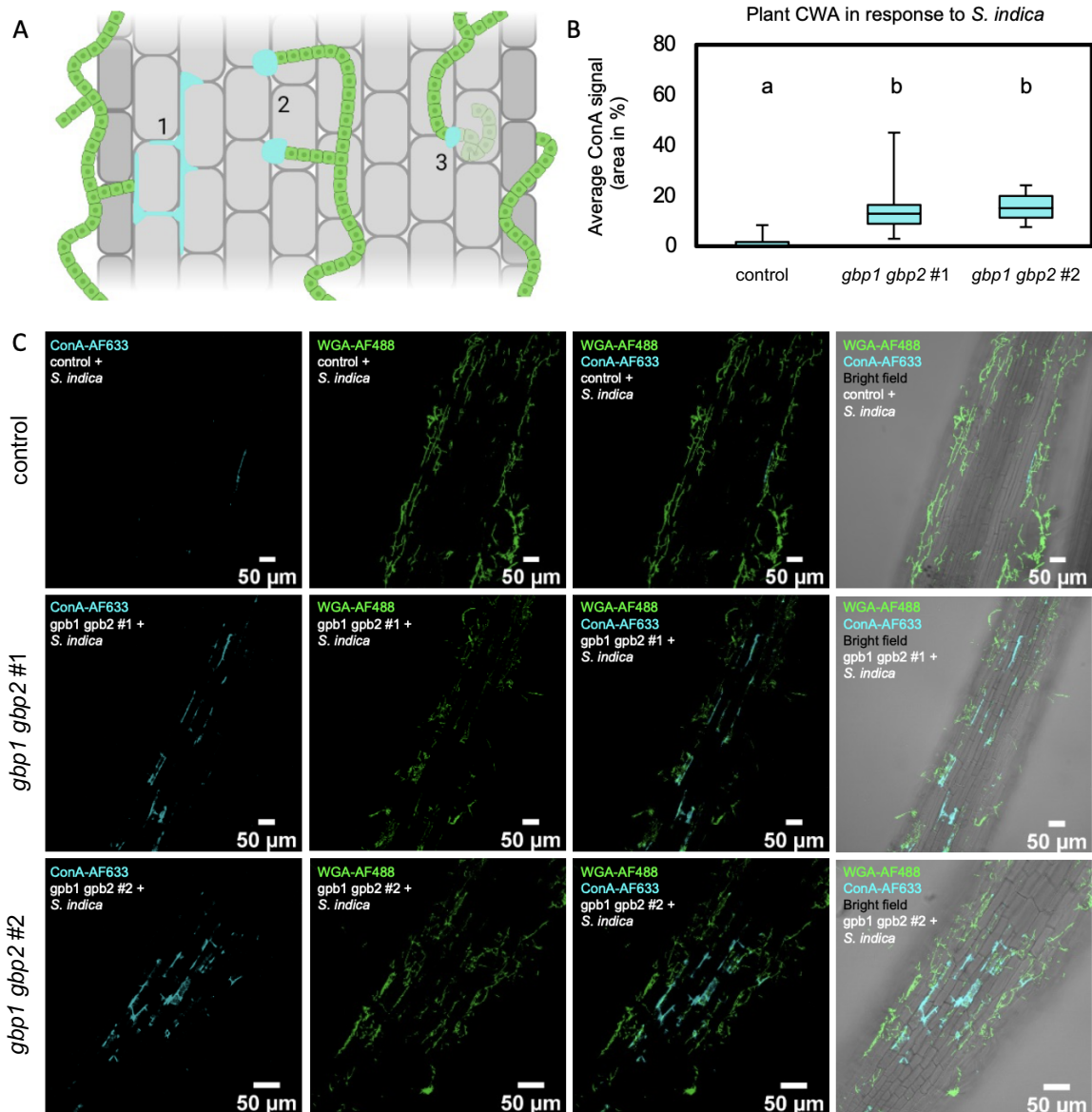


**Figure 4: Colonization of barley *gbp1 gbp2* mutant lines by *S. indica* results in hyperaccumulation of amorphous root CWAs.** (A) Schematic representation of different forms of CWAs in barley roots in response to fungal colonization, including extensive CWA along CWs (1), papillae formation at the sites of attempted (2) and successful (3) penetration. (B) Area of root CWA in barley control lines and *gbp1 gbp2* mutant lines in percent. Letters represent statistically significant differences in ConA signal based on a one-way ANOVA and Tukey's post hoc test (significance threshold:  $P \leq 0.05$ ). (C) Roots of Barley control line and *gbp1 gbp2* mutant lines inoculated with *S. indica* and stained with  $10 \mu\text{g mL}^{-1}$  concanavalin A (ConA-AF633, cyan) and wheat germ agglutinin (WGA-AF488, green) for visualization of CWAs and fungal structures, respectively. ConA, concanavalin A, CW(A), cell wall (appositions), WGA, wheat germ agglutinin.

Papilla formation was observed in all barley lines tested after colonization with the fungus, with no differences in papilla size or frequency between the control line and the two *gbp1 gbp2* mutant lines (Supplementary Figure 13). However, in addition to round-shaped papillae, inoculated mutant roots exhibited a unique type of CWAs, that lined extensively the CWs of the epidermal root cells (Figure 4) These CWAs occurred exclusively when colonized by the fungus and not in plants grown without the fungus under control conditions (Supplementary Figure 14).

## Discussion

The success of fungal colonization is largely determined by the environmental conditions (e.g. nutrient availability) and genetic factors of the host. Depending on the type of plant-fungal interaction, these genetic factors are referred to as susceptibility factors (pathogenic interaction) or compatibility factors (beneficial interaction). Their mutation can interfere with fungal colonization at different stages by hampering tissue penetration and early establishment, by modulating the plant immune system or by removal of structural and metabolic components that are required for fungal maintenance (van Schie & Takken, 2014). While compatibility factors are crucial for efficiently engaging in beneficial interactions with some fungi, they often represent weak spots that can be exploited by other fungi. In AM symbiosis, compatibility is scrutinized and mediated by a set of evolutionary conserved genes that are exclusively present in AM host species (Bravo *et al.*, 2016; Radhakrishnan *et al.*, 2020). In cooperation with membrane-integral LysM receptor-like kinases, these components are responsible for the signal transduction and decoding of nuclear calcium spiking signatures triggered by microbial chitin-derived oligomers. While this pathway is considered to be specific for the accommodation of AM fungi, many endophytes and pathogens have been shown to exploit it at least partially to ensure their own establishment within the host (Wang *et al.*, 2012; Rey *et al.*, 2013, 2015; Gobbato *et al.*, 2013; Skiada *et al.*, 2020). Furthermore, many fungi have adapted their colonization strategies to fundamental developmental processes, for example by relying on the host's CW structure and membrane dynamics for successful establishment within host tissue. Interferences of these processes can massively impact fungal compatibility (van Schie & Takken, 2014).

In this study, we present a previously undescribed role of GBPs, a family of GH81-type  $\beta$ -1,3-endoglucanases, as tissue-independent, broad-spectrum compatibility factors for fungal colonization. Barley GBP1 was identified as the major  $\beta$ -glucan interactor by a pull-down approach using laminarin as  $\beta$ -1,3-glucan bait (Figure 1A). Laminarin is an algal storage carbohydrate which commonly serves as a commercially available surrogate substrate for fungal cell surface glycans due to its  $\beta$ -1,3/1,6-linkage pattern (Fesel & Zuccaro, 2016; Wanke *et al.*, 2021). Plant  $\beta$ -1,3-glucanases have been known to be involved in plant development and plant-microbe interactions for a long time (Perrot *et al.*, 2022). In the context of plant immunity,  $\beta$ -1,3-endoglucanases became known as pathogenesis-related group 2 (PR-2) proteins due to their crucial role in plant defense. Contrasting with the primary role of  $\beta$ -1,3-endoglucanases in plant resistance, we here show that knocking out the only two GBP paralogues in barley leads to reduced colonization by the mutualistic root endophytes *S. indica* and *S. vermifera* as well as the AM fungus *R. irregularis* (Figure 1). This suggests that barley GBPs serve as compatibility factors for colonization by beneficial root fungi. Surprisingly, this compatibility principle could be extended beyond mutualistic fungi, as colonization by the hemibiotrophic root pathogen *B. sorokiniana* as well as the biotrophic foliar pathogen *B. graminis* was similarly hindered (Supplementary Figure 7). A closer look at the formation of CWAs during colonization by the mutualistic fungus *S. indica* showed that reduced colonization in the *gbp1 gbp2* mutants was accompanied by hyperaccumulation of CWAs stained with the lectin ConA (Figure 4). Strikingly, these CWAs were not spatially restricted to the sites of fungal penetration but instead excessively and amorphously spread along the host CW within the colonized area (Figure 4). Since spontaneous CWA formation in mock-treated plants was not observed, constitutive activation of these defense responses upon *gbp1 gbp2* mutation can be excluded (Supplementary Figure 14). Although the contribution of papillae formation to fungal resistance has been controversially discussed over the last decades, several studies reported that early, increased papillae formation can protect hosts from fungal penetration (Hückelhoven, 2007, 2014). Arabidopsis plants constitutively expressing the callose synthase PMR4 produced enlarged callose depositions at the inner and outer side of the cellulosic CW at early time points of fungal infection (Ellinger *et al.*, 2013; Eggert *et al.*, 2014). This mediates complete penetration resistance to adapted and non-adapted powdery mildew strains without the induction of either SA- or JA-dependent pathways (Ellinger

*et al.*, 2013). Another study reported that callose depositions induced by defense priming also enhance resistance to the necrotrophic pathogens *Alternaria brassicicola* and *Plectosphaerella cucumerina* in *Arabidopsis* (Ton & Mauch-Mani, 2004). Furthermore, *mlo1*-dependent resistance of barley to *B. graminis* and *S. indica* is accompanied by a faster formation of larger papillae in leaves or roots, respectively (Skou *et al.*, 1984; Jørgensen, 1992; Chowdhury *et al.*, 2014; Hilbert *et al.*, 2019). Similar to our observations for the *gbp1 gbp2* mutants, barley *mlo1* mutants also exhibited impaired colonization by AM fungi during early stages of interaction (Jacott *et al.*, 2020). This decrease in colonization by mutualistic fungi may partially explain why genes contributing to pathogen infection have been conserved throughout evolution. Furthermore, mutations of compatibility genes often bring along developmental penalties (e.g. growth, yield) or increased susceptibility to pathogens with other infection strategies (van Schie & Takken, 2014). However, we did not observe any differences in root and shoot fresh weight between the control lines and the *gbp1 gbp2* mutants (Supplementary Figure 5). While barley *mlo* mutants were more susceptible to necrotrophic and hemibiotrophic foliar pathogens due to the spontaneous occurrence of cell death (Jarosch *et al.*, 1999; McGrann *et al.*, 2014), barley *gbp1 gbp2* mutants exhibited reduced colonization by the aggressive hemibiotrophic root pathogen *B. sorokiniana*. To explore the limitations of *gbp* mutations in mediating fungal resistance, future studies should survey colonization rates of root (e.g. *Fusarium graminearum*, *Rhizoctonia solani*) and leaf (e.g. *Pyrenophora teres* f. sp. *teres*, *Rhynchosporium secalis*) necrotrophs.

The causal link between the *gbp1 gbp2* mutations and reduced fungal compatibility remains yet to be clarified. Barley GBP1 could process  $\beta$ -glucan-based host- or microbe-associated molecular patterns released during fungal colonization to modulate immune response activation as fungal colonization progresses. Missing GBP activity could lead to an overaccumulation of long-chain  $\beta$ -glucan elicitors in the host apoplast, possibly explaining the large-scale induction of CWAs observed in the *gbp1 gbp2* mutant background upon *S. indica* colonization. A related homeostasis principle was recently demonstrated for berberine bridge enzyme-like oxidases that counteract the deleterious accumulation of active oligogalacturonides and cellodextrins as DAMPs in the host apoplast during microbial colonization (Benedetti *et al.*, 2018; Locci *et al.*, 2019). Alternatively, GBPs could be involved in the release

or tailoring of a yet undescribed  $\beta$ -glucan-derived signaling molecule that dampens immunity to facilitate colonization of mutualistic fungi. Similar to  $\beta$ -glucans, symbiotic signals such as short chitooligosaccharides (e.g. chitotetraose) and lipochitooligosaccharides are abundantly found in both symbiotic and pathogenic fungi and fulfill various functions relevant for inter-kingdom interactions (Feng *et al.*, 2019; Rush *et al.*, 2020). Alternatively, GBP1 could be an important factor in CWA dynamics. The  $\beta$ -1,3-glucan callose is - along with phenolic substances and other CW carbohydrates - a major component of CWAs (Chowdhury *et al.*, 2014; Hückelhoven, 2014). GBPs could directly act on defense-triggered CWAs by degradation of their  $\beta$ -glucan components, thus acting as a negative regulator of the formation of CWA. While all of these proposed mechanisms for dynamic adjustment of plant defense persistence may be crucial for mutualistic fungi to effectively colonize plant roots, they also provide possible loopholes for pathogenic fungi to invade host tissues.

In the apoplastic space, the hydrolytic activity of  $\beta$ -1,3-endoglucanases contributes to host immunity in multiple ways (Perrot *et al.*, 2022). Secreted  $\beta$ -1,3-glucanases directly process the  $\beta$ -glucan-containing surface glycans of invading fungi and oomycetes. Furthermore, this hydrolytic activity leads to the release of glucan fragments that can act as elicitors of plant defense responses. Since the outermost layer of fungal cell surface glycans mainly consists of  $\beta$ -1,3-glucans (Wanke *et al.*, 2021), hydrolysis by  $\beta$ -1,3-glucanases renders the inner chitin layer more accessible to secreted plant chitinases, which in turn act on the exposed fungal CW. Although GH81 family members are not categorized as PR-2 proteins, previous studies focusing on GBPs from soybean and other legumes have shown their importance in defense against oomycetes (Fliegmann *et al.*, 2004; Leclercq *et al.*, 2008). To better understand the contribution of GBP1 to hydrolysis of fungal surface glycan substrates, we performed substrate characterization assays with heterologously purified barley GBP1. GBP1 specifically hydrolyzes linear  $\beta$ -1,3-glucans as short as laminaritriose (Figure 2C), whereas it did not effectively act on preparations of the extracellular polysaccharide matrix and CW isolated from the root endophyte *S. indica* (Supplementary Figure 10). EPS matrices from a variety of plant-colonizing fungi consist of a  $\beta$ -1,3-linked glucan backbone heavily substituted with  $\beta$ -1,6-linked glucose (Wawra *et al.*, 2019; Chandrasekar *et al.*, 2022). Barley BGLUII, an enzyme secreted upon confrontation with fungi, has been shown to release a  $\beta$ -glucan decasaccharide with antioxidative properties from this EPS matrix that facilitates fungal colonization (Chandrasekar *et*

*al.*, 2022). Since GBP1 was unable to digest highly substituted laminarin from *E. bicyclis* (Pang *et al.*, 2005; Mystkowska *et al.*, 2018), we conclude that the high degree of branching in the EPS matrix similarly protects this cell surface glycan from hydrolysis by GBP1 (Supplementary Figure 11). However, we cannot exclude that cell surface glycans from other fungi or oomycetes might serve as better substrates for GBP1. Although GBP1 from barley did not exhibit a pioneering hydrolytic role on the tested preparations, in a more complex scenario with a variety of secreted host hydrolases, GBP1 could belong to a second set of hydrolytic enzymes acting on the predigested cell surface glycans of microbial invaders. In the performed ROS burst assays, we observed that treatment of the long  $\beta$ -glucan laminarin with GBP1 differentially modulated ROS production in the two tested species (Figure 3C+D), demonstrating that GBP1 has the potential to fine-tune ROS responses.

Soybean GBPs contain two carbohydrate-associated domains: an endoglycosidic domain and a high-affinity binding site for a *Phytophthora sojae*-derived  $\beta$ -glucan heptagluco-side (Fliegmann *et al.*, 2004). Inhibition of elicitor binding to GBP with a specific antibody prevented the production of phytoalexins, which prompted the authors to conclude that soybean GBP may be part of the  $\beta$ -glucan-heptagluco-side receptor complex (Umemoto *et al.*, 1997). Since we identified GBP1 using a pull-down approach with laminarin, we hypothesize that GBP1 has a  $\beta$ -glucan binding domain in addition to the hydrolytic domain. However, barley *gbp1 gbp2* ROS production is not reduced upon treatment with various  $\beta$ -glucan elicitors, ruling out the long-standing assumption that barley GBPs are necessary components of a  $\beta$ -1,3-glucan receptor complex (Fliegmann *et al.*, 2004). Functional differences between barley and legume GBPs are not surprising given the massive expansion of GBPs in the legume family, suggesting that legume GBPs may have diversified in terms of their role upon a multitude of various abiotic and biotic stresses. Consistent with the facilitative role of barley BGLUIII in fungal colonization, our findings provide new insights of how spatiotemporal dynamics in perception and hydrolysis of host and microbial  $\beta$ -glucans modulate fungal establishment in the host tissue.

For decades, plant  $\beta$ -1,3-glucanases were predominantly considered to be deployed as a defensive strategy to hinder microbial invasion. Our work shows that  $\beta$ -1,3-glucanases such as barley GBPs can play a previously undescribed role as



compatibility factors for colonization by fungi of different phylogenetic origins and lifestyles. Consistent with the facilitative role of barley BGLUII in fungal colonization, our findings provide new insights into the contribution of host  $\beta$ -glucanases to spatiotemporal dynamics in perception and degradation of host and microbial  $\beta$ -glucans that promote fungal establishment in the host tissue.

## References

- Aist, J.R.** (1977) Papilla Formation: Timing and Significance during Penetration of Barley Coleoptiles by *Erysiphe graminis hordei*. *Phytopathology*, **77**, 455..
- Albert, I., Hua, C., Nürnberger, T., Pruitt, R.N. and Zhang, L.** (2020) Surface Sensor Systems in Plant Immunity. *Plant Physiol.*, **182**, 1582–1596.
- Amanda, D., Frey, F.P., Neumann, U., et al.** (2022) Auxin boosts energy generation pathways to fuel pollen maturation in barley. *Curr. Biol.*, **32**, 1798–1811.e8.
- Aziz, A., Gauthier, A., Bézier, A., Poinssot, B., Joubert, J.-M., Pugin, A., Heyraud, A. and Baillieul, F.** (2007) Elicitor and resistance-inducing activities of beta-1,4 cellodextrins in grapevine, comparison with beta-1,3 glucans and alpha-1,4 oligogalacturonides. *J. Exp. Bot.*, **58**, 1463–1472.
- Barghahn, S., Arnal, G., Jain, N., Petutschnig, E., Brumer, H. and Lipka, V.** (2021) Mixed Linkage  $\beta$ -1,3/1,4-Glucan Oligosaccharides Induce Defense Responses in *Hordeum vulgare* and *Arabidopsis thaliana*. *Front. Plant Sci.*, **12**, 682439.
- Bednarek, P., Pislewska-Bednarek, M., Svatos, A., et al.** (2009) A glucosinolate metabolism pathway in living plant cells mediates broad-spectrum antifungal defense. *Science*, **323**, 101–106.
- Benedetti, M., Verrascina, I., Pontiggia, D., Locci, F., Mattei, B., De Lorenzo, G. and Cervone, F.** (2018) Four *Arabidopsis* berberine bridge enzyme-like proteins are specific oxidases that inactivate the elicitor-active oligogalacturonides. *The Plant Journal*, **94**, 260–273. t: <http://dx.doi.org/10.1111/tpj.13852>.
- Bernard, A. and Joubès, J.** (2013) *Arabidopsis* cuticular waxes: advances in synthesis, export and regulation. *Prog. Lipid Res.*, **52**, 110–129.
- Bravo, A., York, T., Pumplin, N., Mueller, L.A. and Harrison, M.J.** (2016) Genes conserved for arbuscular mycorrhizal symbiosis identified through phylogenomics. *Nature Plants*, **2**, 1–6. Available at: [Accessed December 7, 2022].
- Brown, I., Trethowan, J., Kerry, M., Mansfield, J. and Bolwell, G.P.** (1998) Localization of components of the oxidative cross-linking of glycoproteins and of callose synthesis in papillae formed during the interaction between non-pathogenic strains of *Xanthomonas campestris* and French bean mesophyll cells. *Plant J.*, **15**, 333–343.
- Buscaill, P., Chandrasekar, B., Sanguankiattichai, N., et al.** (2019) Glycosidase and glycan polymorphism control hydrolytic release of immunogenic flagellin peptides. *Science*, **364**. Available at: <http://dx.doi.org/10.1126/science.aav0748>.
- Chandrasekar, B., Wanke, A., Wawra, S., et al.** (2022) Fungi hijack a ubiquitous plant apoplastic endoglucanase to release a ROS scavenging  $\beta$ -glucan decasaccharide to subvert immune responses. *Plant Cell*, **34**, 2765–2784.
- Chowdhury, J., Henderson, M., Schweizer, P., Burton, R.A., Fincher, G.B. and Little, A.** (2014) Differential accumulation of callose, arabinoxylan and cellulose in nonpenetrated versus penetrated papillae on leaves of barley infected with *Blumeria graminis f. sp. hordei*. *New Phytol.*, **204**, 650–660.
- Claverie, J., Balacey, S., Lemaître-Guillier, C., et al.** (2018) The Cell Wall-Derived Xyloglucan Is a New DAMP Triggering Plant Immunity in *Vitis vinifera* and *Arabidopsis thaliana*. *Front. Plant Sci.*, **9**, 1725.
- Concordet, J.-P. and Haeussler, M.** (2018) CRISPOR: intuitive guide selection for CRISPR/Cas9 genome editing experiments and screens. *Nucleic Acids Res.*, **46**, W242–W245.
- Cosgrove, D.J.** (2005) Growth of the plant cell wall. *Nat. Rev. Mol. Cell Biol.*, **6**, 850–861.

- Cosgrove, D.J. and Jarvis, M.C.** (2012) Comparative structure and biomechanics of plant primary and secondary cell walls. *Front. Plant Sci.*, **3**, 204.
- Eggert, D., Naumann, M., Reimer, R. and Voigt, C.A.** (2014) Nanoscale glucan polymer network causes pathogen resistance. *Sci. Rep.*, **4**, 4159.
- Ellinger, D., Naumann, M., Falter, C., Zwikowics, C., Jamrow, T., Manisseri, C., Somerville, S.C. and Voigt, C.A.** (2013) Elevated early callose deposition results in complete penetration resistance to powdery mildew in Arabidopsis. *Plant Physiol.*, **161**, 1433–1444.
- Escudero, V., Jordá, L., Sopena-Torres, S., et al.** (2017) Alteration of cell wall xylan acetylation triggers defense responses that counterbalance the immune deficiencies of plants impaired in the  $\beta$ -subunit of the heterotrimeric G-protein. *Plant J.*, **92**, 386–399.
- Felix, G., Duran, J.D., Volko, S. and Boller, T.** (1999) Plants have a sensitive perception system for the most conserved domain of bacterial flagellin. *Plant J.*, **18**, 265–276.
- Feng, F., Sun, J., Radhakrishnan, G.V., et al.** (2019) A combination of chitoooligosaccharide and lipochitoooligosaccharide recognition promotes arbuscular mycorrhizal associations in *Medicago truncatula*. *Nat. Commun.*, **10**, 1–12. Available at: [Accessed January 23, 2023].
- Ferrari, S., Savatin, D.V., Sicilia, F., Gramegna, G., Cervone, F. and Lorenzo, G.D.** (2013) Oligogalacturonides: plant damage-associated molecular patterns and regulators of growth and development. *Front. Plant Sci.*, **4**, 49.
- Fesel, P.H. and Zuccaro, A.** (2016)  $\beta$ -glucan: Crucial component of the fungal cell wall and elusive MAMP in plants. *Fungal Genet. Biol.*, **90**, 53–60.
- Fliegmann, J., Mithofer, A., Wanner, G. and Ebel, J.** (2004) An ancient enzyme domain hidden in the putative beta-glucan elicitor receptor of soybean may play an active part in the perception of pathogen-associated molecular patterns during broad host resistance. *J. Biol. Chem.*, **279**, 1132–1140.
- Galletti, R., Denoux, C., Gambetta, S., Dewdney, J., Ausubel, F.M., De Lorenzo, G. and Ferrari, S.** (2008) The AtrbohD-mediated oxidative burst elicited by oligogalacturonides in Arabidopsis is dispensable for the activation of defense responses effective against *Botrytis cinerea*. *Plant Physiol.*, **148**, 1695–1706.
- Gobbato, E., Wang, E., Higgins, G., Bano, S.A., Henry, C., Schultze, M. and Oldroyd, G.E.D.** (2013) RAM1 and RAM2 function and expression during arbuscular mycorrhizal symbiosis and *Aphanomyces euteiches* colonization. *Plant Signal. Behav.*, **8**. Available at: <http://dx.doi.org/10.4161/psb.26049>.
- Gol, L., Haraldsson, E.B. and Korff, M. von** (2021) Ppd-H1 integrates drought stress signals to control spike development and flowering time in barley. *J. Exp. Bot.*, **72**, 122–136.
- Günl, M., Kraemer, F. and Pauly, M.** (2011) Oligosaccharide mass profiling (OLIMP) of cell wall polysaccharides by MALDI-TOF/MS. *Methods Mol. Biol.*, **715**, 43–54.
- Hahn, M.G., Darvill, A.G. and Albersheim, P.** (1981) Host-Pathogen Interactions: XIX. THE ENDOGENOUS ELICITOR, A FRAGMENT OF A PLANT CELL WALL POLYSACCHARIDE THAT ELICITS PHYTOALEXIN ACCUMULATION IN SOYBEANS. *Plant Physiol.*, **68**, 1161–1169.
- Hansjakob, A., Riederer, M. and Hildebrandt, U.** (2011) Wax matters: absence of very-long-chain aldehydes from the leaf cuticular wax of the glossy11 mutant of maize compromises the prepenetration processes of *Blumeria graminis*. *Plant Pathology*, **60**, 1151–1161. Available at: <http://dx.doi.org/10.1111/j.1365-3059.2011.02467.x>.
- Hernández-Blanco, C., Feng, D.X., Hu, J., et al.** (2007) Impairment of cellulose synthases required for Arabidopsis secondary cell wall formation enhances disease resistance. *Plant Cell*, **19**, 890–903.

- Hilbert, M., Novero, M., Rovenich, H., Mari, S., Grimm, C., Bonfante, P. and Zuccaro, A.** (2019) MLO Differentially Regulates Barley Root Colonization by Beneficial Endophytic and Mycorrhizal Fungi. *Front. Plant Sci.*, **10**, 1678.
- Hückelhoven, R.** (2007) Cell wall-associated mechanisms of disease resistance and susceptibility. *Annu. Rev. Phytopathol.*, **45**, 101–127.
- Hückelhoven, R.** (2014) The effective papilla hypothesis. *New Phytol.*, **204**, 438–440.
- Jacott, C.N., Charpentier, M., Murray, J.D. and Ridout, C.J.** (2020) Mildew Locus O facilitates colonization by arbuscular mycorrhizal fungi in angiosperms. *New Phytol.*, **227**, 343–351.
- Jarosch, B., Kogel, K.-H. and Schaffrath, U.** (1999) The Ambivalence of the Barley Mlo Locus: Mutations Conferring Resistance Against Powdery Mildew (*Blumeria graminis* f. sp. hordei) Enhance Susceptibility to the Rice Blast Fungus *Magnaporthe grisea*. *Mol. Plant. Microbe Interact.*, **12**, 508–514.
- Jørgensen, I.H.** (1992) Discovery, characterization and exploitation of Mlo powdery mildew resistance in barley. *Euphytica*, **63**, 141–152.
- Kumar, N., Galli, M., Ordon, J., Stuttmann, J., Kogel, K.-H. and Imani, J.** (2018) Further analysis of barley MORC1 using a highly efficient RNA-guided Cas9 gene-editing system. *Plant Biotechnol. J.*, **16**, 1892–1903.
- Lahrmann, U., Ding, Y., Banhara, A., Rath, M., Hajirezaei, M.R., Döhlemann, S., Wirén, N. von, Parniske, M. and Zuccaro, A.** (2013) Host-related metabolic cues affect colonization strategies of a root endophyte. *Proc. Natl. Acad. Sci. U. S. A.*, **110**, 13965–13970.
- Leclercq, J., Fliegmann, J., Tellström, V., Niebel, A., Cullimore, J.V., Niehaus, K., Küster, H., Ebel, J. and Mithöfer, A.** (2008) Identification of a multigene family encoding putative beta-glucan-binding proteins in *Medicago truncatula*. *J. Plant Physiol.*, **165**, 766–776.
- Locci, F., Benedetti, M., Pontiggia, D., Citterico, M., Caprari, C., Mattei, B., Cervone, F. and De Lorenzo, G.** (2019) An *Arabidopsis* berberine bridge enzyme-like protein specifically oxidizes cellulose oligomers and plays a role in immunity. *Plant J.*, **98**, 540–554.
- Mahdi, L.K., Miyauchi, S., Uhlmann, C., et al.** (2021) The fungal root endophyte *Serendipita vermifera* displays inter-kingdom synergistic beneficial effects with the microbiota in *Arabidopsis thaliana* and barley. *ISME J.*, **16**, 876–889. Available at: [Accessed December 26, 2022].
- McGrann, G.R.D., Stavrinides, A., Russell, J., Corbitt, M.M., Booth, A., Chartrain, L., Thomas, W.T.B. and Brown, J.K.M.** (2014) A trade off between mlo resistance to powdery mildew and increased susceptibility of barley to a newly important disease, *Ramularia* leaf spot. *J. Exp. Bot.*, **65**, 1025–1037.
- Mélida, H., Bacete, L., Ruprecht, C., Rebaque, D., Hierro, I. del, López, G., Brunner, F., Pfrengle, F. and Molina, A.** (2020) Arabinoxylan-Oligosaccharides Act as Damage Associated Molecular Patterns in Plants Regulating Disease Resistance. *Front. Plant Sci.*, **11**. Available at: <https://www.frontiersin.org/articles/10.3389/fpls.2020.01210>.
- Mélida, H., Sopena-Torres, S., Bacete, L., Garrido-Arandia, M., Jordá, L., López, G., Muñoz-Barrios, A., Pacios, L.F. and Molina, A.** (2018) Non-branched  $\beta$ -1,3-glucan oligosaccharides trigger immune responses in *Arabidopsis*. *Plant J.*, **93**, 34–49.
- Molina, A., Miedes, E., Bacete, L., et al.** (2021) *Arabidopsis* cell wall composition determines disease resistance specificity and fitness. *Proc. Natl. Acad. Sci. U. S. A.*, **118**. Available at: <http://dx.doi.org/10.1073/pnas.2010243118>.
- Myrach, T., Zhu, A. and Witte, C.-P.** (2017) The assembly of the plant urease activation complex and the essential role of the urease accessory protein G (UreG) in delivery of nickel to urease. *J. Biol. Chem.*, **292**, 14556–14565.

- Mystkowska, A.A., Robb, C., Vidal-Melgosa, S., Vanni, C., Fernandez-Guerra, A., Höhne, M. and Hehemann, J.-H.** (2018) Molecular recognition of the beta-glucans laminarin and pustulan by a SusD-like glycan-binding protein of a marine Bacteroidetes. *FEBS J.*, **285**, 4465–4481.
- Nishimura, M.T., Stein, M., Hou, B.-H., Vogel, J.P., Edwards, H. and Somerville, S.C.** (2003) Loss of a callose synthase results in salicylic acid-dependent disease resistance. *Science*, **301**, 969–972.
- Nizam, S., Qiang, X., Wawra, S., Nostadt, R., Getzke, F., Schwanke, F., Dreyer, I., Langen, G. and Zuccaro, A.** (2019) *Serendipita indica* E5'NT modulates extracellular nucleotide levels in the plant apoplast and affects fungal colonization. *EMBO Rep.*, **20**, e47430.
- Ntoukakis, V., Mucyn, T.S., Gimenez-Ibanez, S., Chapman, H.C., Gutierrez, J.R., Balmuth, A.L., Jones, A.M.E. and Rathjen, J.P.** (2009) Host inhibition of a bacterial virulence effector triggers immunity to infection. *Science*, **324**, 784–787.
- Pang, Z., Otaka, K., Maoka, T., Hidaka, K., Ishijima, S., Oda, M. and Ohnishi, M.** (2005) Structure of beta-glucan oligomer from laminarin and its effect on human monocytes to inhibit the proliferation of U937 cells. *Biosci. Biotechnol. Biochem.*, **69**, 553–558.
- Perrot, T., Pauly, M. and Ramirez, V.** (2022) Emerging Roles of  $\beta$ -Glucanases in Plant Development and Adaptive Responses. *Plants*, **11**. Available at: <http://dx.doi.org/10.3390/plants11091119>.
- Radhakrishnan, G.V., Keller, J., Rich, M.K., et al.** (2020) An ancestral signalling pathway is conserved in intracellular symbioses-forming plant lineages. *Nature Plants*, **6**, 280–289. Available at: [Accessed December 7, 2022].
- Rebaque, D., Del Hierro, I., López, G., et al.** (2021) Cell wall-derived mixed-linked  $\beta$ -1,3/1,4-glucans trigger immune responses and disease resistance in plants. *Plant J.*, **106**, 601–615.
- Rey, T., Chatterjee, A., Buttay, M., Toulotte, J. and Schornack, S.** (2015) *Medicago truncatula* symbiosis mutants affected in the interaction with a biotrophic root pathogen. *New Phytol.*, **206**, 497–500.
- Rey, T., Nars, A., Bonhomme, M., et al.** (2013) NFP, a LysM protein controlling Nod factor perception, also intervenes in *Medicago truncatula* resistance to pathogens. *New Phytol.*, **198**, 875–886.
- Rovenich, H., Zuccaro, A. and Thomma, B.P.H.J.** (2016) Convergent evolution of filamentous microbes towards evasion of glycan-triggered immunity. *New Phytol.*, **212**, 896–901.
- Rush, T.A., Puech-Pagès, V., Bascaules, A., et al.** (2020) Lipo-chitooligosaccharides as regulatory signals of fungal growth and development. *Nat. Commun.*, **11**, 3897.
- Sarkar, D., Rovenich, H., Jeena, G., et al.** (2019) The inconspicuous gatekeeper: endophytic *Serendipita vermifera* acts as extended plant protection barrier in the rhizosphere. *New Phytol.*, **224**, 886–901.
- Schie, C.C.N. van and Takken, F.L.W.** (2014) Susceptibility genes 101: how to be a good host. *Annu. Rev. Phytopathol.*, **52**, 551–581.
- Schneider, C.A., Rasband, W.S. and Eliceiri, K.W.** (2012) NIH Image to ImageJ: 25 years of image analysis. *Nat. Methods*, **9**, 671–675.
- Skiada, V., Avramidou, M., Bonfante, P., Genre, A. and Papadopoulou, K.K.** (2020) An endophytic *Fusarium-legume* association is partially dependent on the common symbiotic signalling pathway. *New Phytol.*, **226**, 1429–1444.
- Skou, J.P., Jørgensen, J.H. and Lilholt, U.** (1984) Comparative studies on callose formation in powdery mildew compatible and incompatible barley. *J. Phytopathol.*, **109**, 147–168.

- Ton, J. and Mauch-Mani, B.** (2004) Beta-amino-butyric acid-induced resistance against necrotrophic pathogens is based on ABA-dependent priming for callose. *Plant J.*, **38**, 119–130.
- Umemoto, N., Kakitani, M., Iwamatsu, A., Yoshikawa, M., Yamaoka, N. and Ishida, I.** (1997) The structure and function of a soybean beta-glucan-elicitor-binding protein. *Proc. Natl. Acad. Sci. U. S. A.*, **94**, 1029–1034.
- Underwood, W.** (2012) The Plant Cell Wall: A Dynamic Barrier Against Pathogen Invasion. *Front. Plant Sci.*, **3**. Available at: <https://www.frontiersin.org/articles/10.3389/fpls.2012.00085>.
- Vierheilig, H., Coughlan, A.P., Wyss, U. and Piche, Y.** (1998) Ink and vinegar, a simple staining technique for arbuscular-mycorrhizal fungi. *Appl. Environ. Microbiol.*, **64**, 5004–5007.
- Wang, E., Schornack, S., Marsh, J.F., Gobbato, E., Schwessinger, B., Eastmond, P., Schultze, M., Kamoun, S. and Oldroyd, G.E.D.** (2012) A Common Signaling Process that Promotes Mycorrhizal and Oomycete Colonization of Plants. *Curr. Biol.*, **22**, 2242–2246.
- Wanke, A., Malisic, M., Wawra, S. and Zuccaro, A.** (2021) Unraveling the sugar code: the role of microbial extracellular glycans in plant-microbe interactions. *J. Exp. Bot.*, **72**, 15–35.
- Wanke, A., Rovenich, H., Schwanke, F., Velte, S., Becker, S., Hehemann, J.-H., Wawra, S. and Zuccaro, A.** (2020) Plant species-specific recognition of long and short  $\beta$ -1,3-linked glucans is mediated by different receptor systems. *Plant J.*, **102**, 1142–1156.
- Wawra, S., Fesel, P., Widmer, H., Neumann, U., Lahrmann, U., Becker, S., Hehemann, J.-H., Langen, G. and Zuccaro, A.** (2019) FGB1 and WSC3 are in planta-induced  $\beta$ -glucan-binding fungal lectins with different functions. *New Phytol.*, **222**, 1493–1506.
- Werner, A.K., Sparkes, I.A., Romeis, T. and Witte, C.-P.** (2008) Identification, biochemical characterization, and subcellular localization of allantoin amidohydrolases from Arabidopsis and soybean. *Plant Physiol.*, **146**, 418–430.
- Witte, C.-P., Noël, L.D., Gielbert, J., Parker, J.E. and Romeis, T.** (2004) Rapid one-step protein purification from plant material using the eight-amino acid StrepII epitope. *Plant Mol. Biol.*, **55**, 135–147.
- Yin, H., Du, Y. and Dong, Z.** (2016) Chitin Oligosaccharide and Chitosan Oligosaccharide: Two Similar but Different Plant Elicitors. *Front. Plant Sci.*, **7**, 522.
- Zang, H., Xie, S., Zhu, B., Yang, X., Gu, C., Hu, B., Gao, T., Chen, Y. and Gao, X.** (2019) Mannan oligosaccharides trigger multiple defence responses in rice and tobacco as a novel danger-associated molecular pattern. *Mol. Plant Pathol.*, **20**, 1067–1079.
- Zeyen, R.J., Carver, T.L.W., Lyngkjær, M.F.** (2002) Epidermal cell papillae. *The powdery mildews: a comprehensive treatise*, 107–125.

## Chapter 5: *Supplementary Material*

### **A GH81-type $\beta$ -glucan-binding protein facilitates colonization by mutualistic fungi in barley**

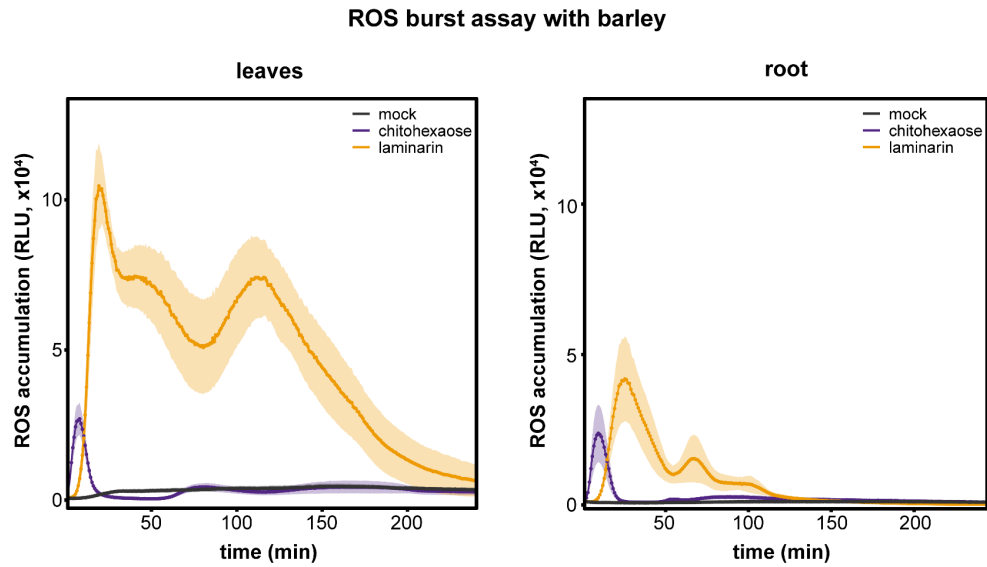
Alan Wanke<sup>1,2</sup>, Sarah van Boerdonk<sup>1</sup>, Lisa Mahdi<sup>1</sup>, Stephan Wawra<sup>1</sup>, Miriam Neidert<sup>1</sup>, Balakumaran Chandrasekar<sup>1</sup>, Pia Saake<sup>1</sup>, Isabel Saur<sup>2</sup>, Ivan F. Acosta<sup>2</sup>, Markus Pauly<sup>3</sup>, Alga Zuccaro<sup>1</sup>

<sup>1</sup> University of Cologne, Cluster of Excellence on Plant Sciences (CEPLAS), 50679 Cologne, Germany

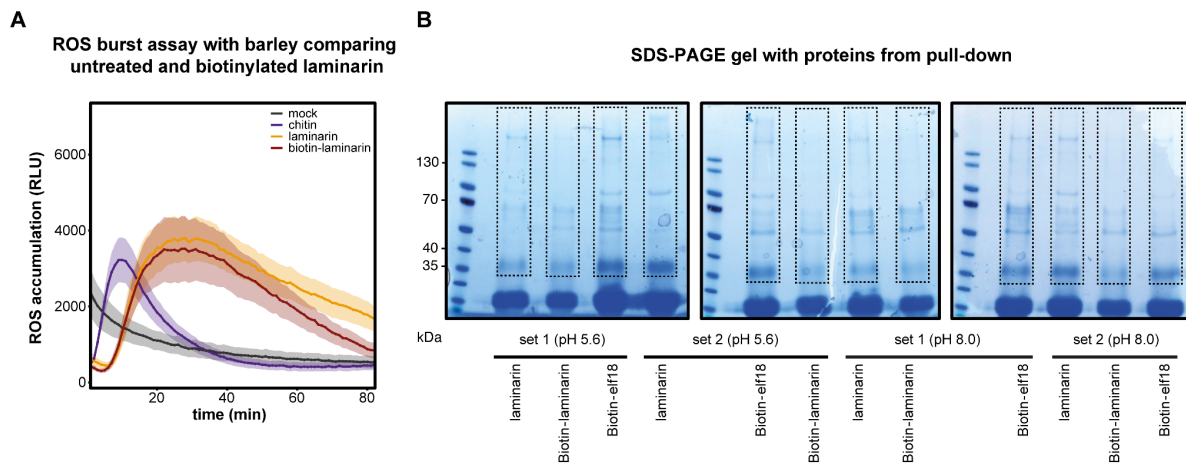
<sup>2</sup> Max Planck Institute for Plant Breeding Research, 50829 Cologne, Germany

<sup>3</sup> Institute of Plant Cell Biology and Biotechnology, Heinrich Heine University Düsseldorf, 40225 Düsseldorf, Germany

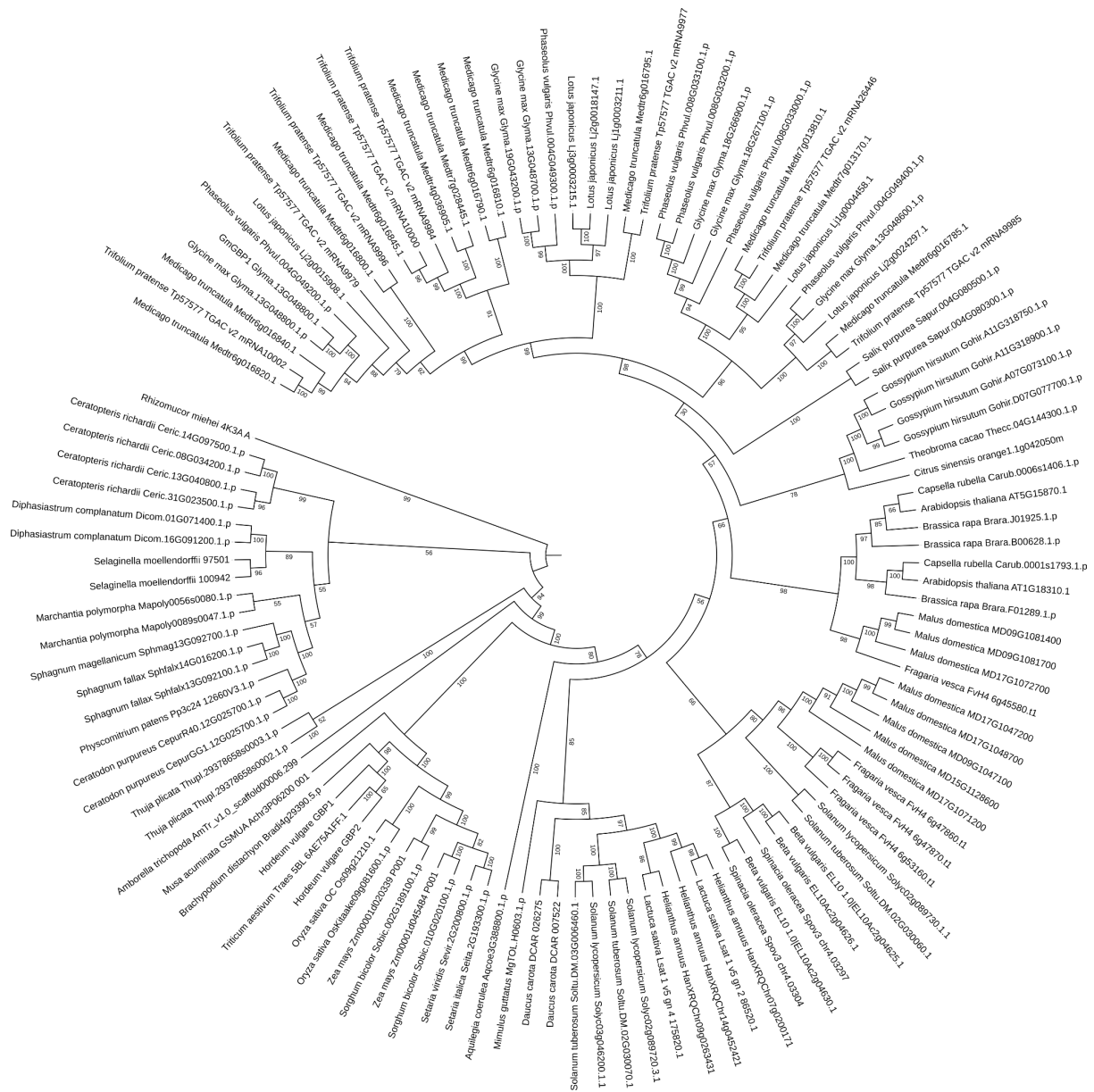




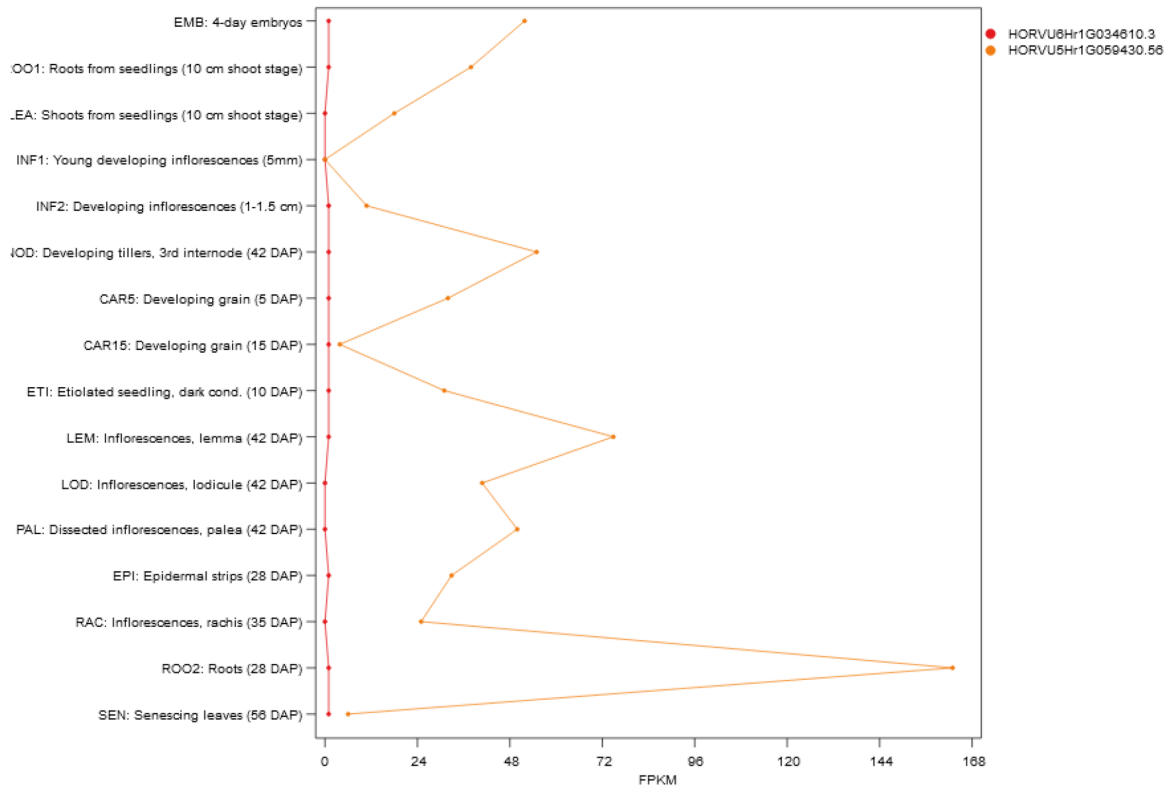
**Supplementary Figure 1. Barley leaf and root tissue responds similarly to laminarin treatment.** Apoplastic ROS accumulation after treatment of seven-day-old barley root pieces and leaf discs with chitohexaose (10  $\mu\text{M}$ ) and laminarin (4  $\text{mg}\cdot\text{mL}^{-1}$ ). Treatment with Milli-Q water was used as mock control. Values represent mean  $\pm$  SEM from 16 wells. Experiment was repeated at least three times. ROS, reactive oxygen species.



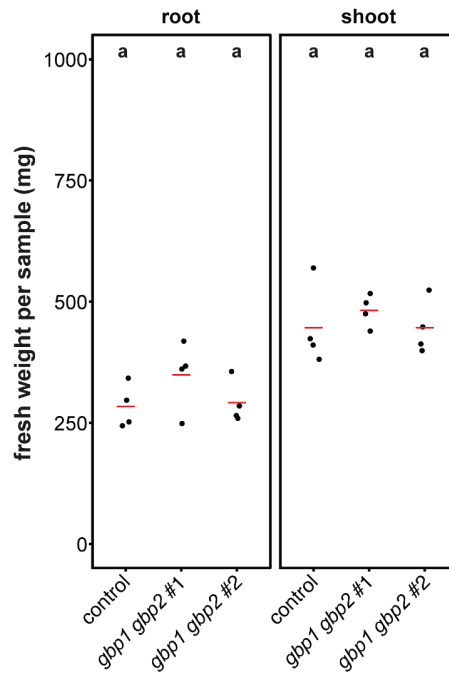
**Supplementary Figure 2. Protein pull-down with biotinylated laminarin in barley leaves.** (A) Apoplastic ROS accumulation after treatment of two-week-old barley leaf discs with untreated and biotinylated laminarin (each  $6 \text{ mg} \cdot \text{mL}^{-1}$ ). Treatment with Milli-Q water was used as mock control. Values represent mean  $\pm$  SEM from 8 wells. (B) Separation of pull-down samples on SDS-PAGE gel prior to submission for mass spectrometry. Pull-down was performed with untreated laminarin, biotinylated laminarin and biotinylated elf18 at two different pH values. Areas indicated by dotted lines were excised from the gel and further processed for mass spectrometric analyses. Elf18, peptide from bacterial elongation factor Tu; ROS, reactive oxygen species.



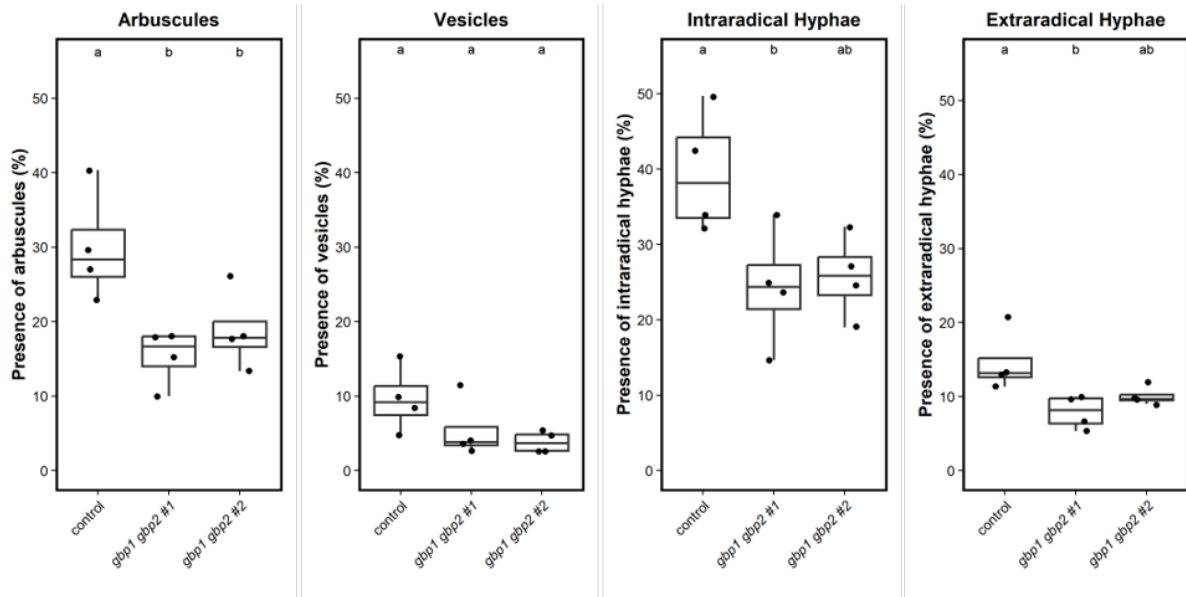
**Supplementary Figure 3. Duplication and expansion of GBP orthologues occurred in various plant lineages.** Homologues of barley GBP1 and GBP were obtained from Phytozome database (min. half of query protein sequence covered,  $e$ -value $\leq$ 0.001). Sequences were aligned with MAFFT (version 7.515), alignment was trimmed with trimal (version 1.4, *automated1* setting) and phylogenetic tree was constructed with IQ-TREE 2.2.0.3 (version, combined ModelFinder, tree search, SH-aLRT test with 10000 repetitions). Visualization of phylogenetic tree was performed with iTOL online software.



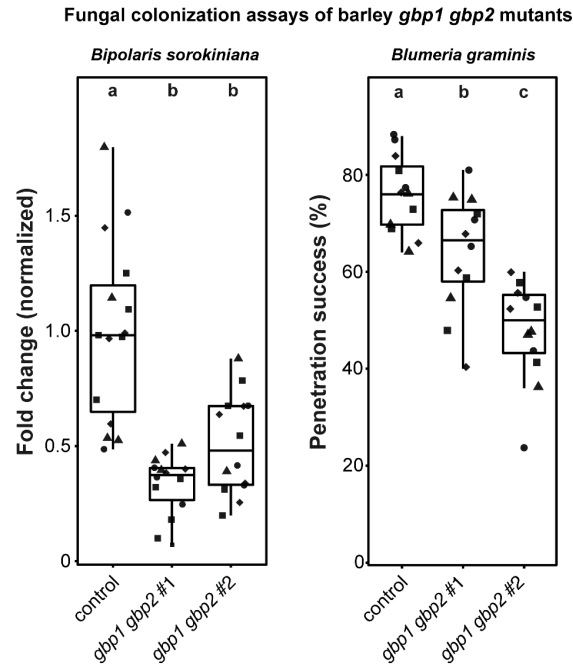
**Supplementary Figure 4. *GBP1* but not *GBP2* is expressed in different barley tissues.** Figure based on expression datasets curated by GENEINVESTIGATOR.



**Supplementary Figure 5. Fresh weight of root and shoot tissue of barley control lines and *gbp1 gbp2* mutant lines.** The barley control line and both mutant lines (*gbp1 gbp2 #1* and *gbp1 gbp2 #2*) were germinated on wet filter paper for 4 days and then grown on 1/10 PNM medium for 6 days under sterile conditions. Root and shoot fresh weight of the 10-day-old barley plants were measured. Black dots represent biological replicates and the red bar indicates the average fresh weight ( $n = 4$ , each replicate consists of 4 barley plants). Data were analyzed by one-way ANOVA ( $p < 0.05$ ).

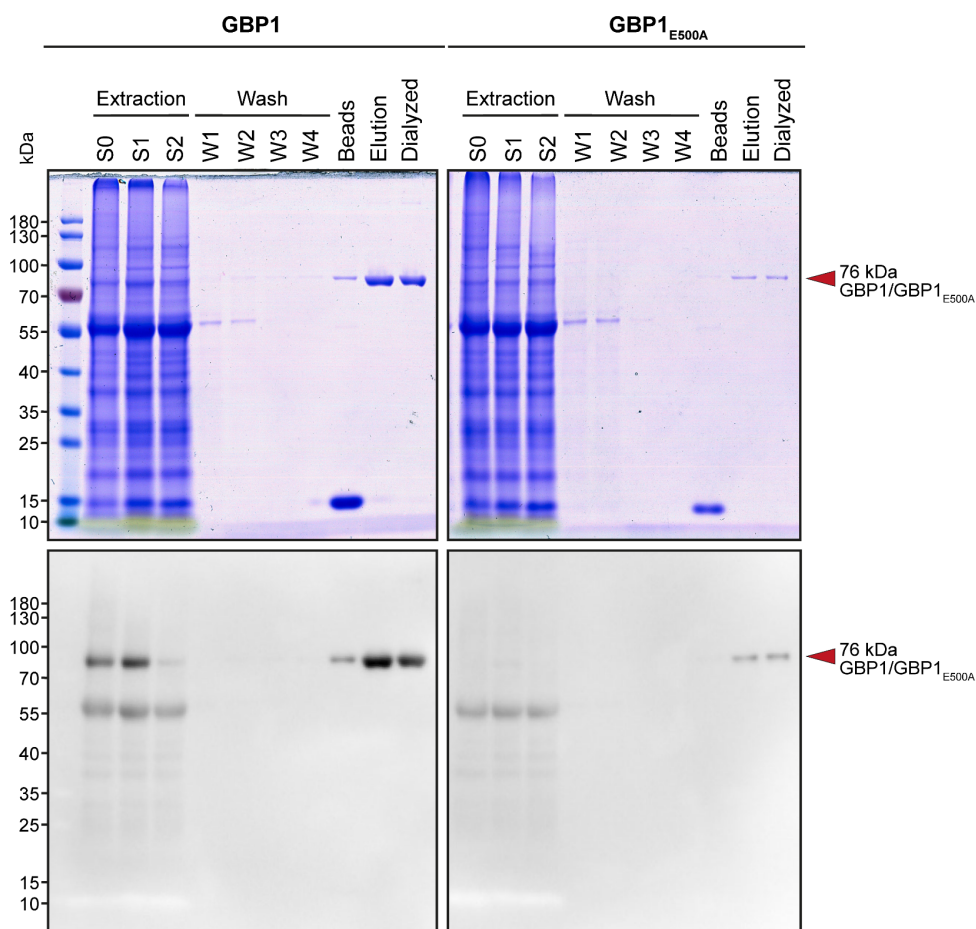


**Supplementary Figure 6. Abundance of *R. irregularis* structures observed during colonization assay of barley control and *gbp1 gbp2* mutant lines.** The barley control line and *gbp1 gbp2* mutant line seedlings were inoculated with *R. irregularis* and roots were harvested at 28 dpi. Using a light microscope (AxioStar, Carl Zeiss, Jena, Germany), barley roots were analyzed at 300 random sections (covering 30 cm of root length) for the presence of ink-stained *R. irregularis* structures including arbuscules, vesicles, intraradical hyphae (IRH), and extraradical hyphae (ERH). All data points are plotted on graphs as circles (n=4). Boxplot elements in this figure: center line, median; box limits, upper and lower quartiles; whiskers, 1.5 × interquartile range. Letters represent statistically significant differences in *R. irregularis* structure presence based on a one-way ANOVA and Tukey's post hoc test using a 95% confidence interval.



**Supplementary Figure 7. Colonization of control and *gpb1 gpb2* barley lines by *B. sorokiniana* and *B. graminis* f.sp. *hordei*.** Boxplot elements in this figure: center line, median; box limits, upper and lower quartiles; whiskers,  $1.5 \times$  interquartile range. Data points from independent experiments are indicated by data point shape. Letters represent statistically significant differences in expression based on a one-way ANOVA and Tukey's post hoc test (significance threshold:  $P \leq 0.05$ ).

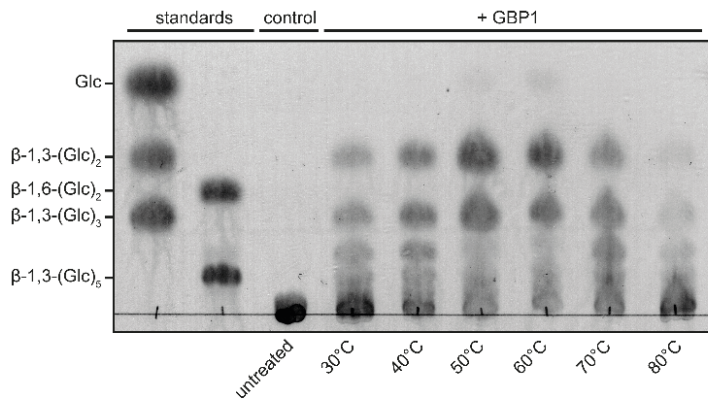




**Supplementary Figure 8. Purification of heterologously produced wildtype GBP1 and the mutated version GBP1<sub>E500A</sub> from *N. benthamiana* leaves.** Proteins were heterologously produced (Agrobacterium-mediated transient transformation) and purified from *N. benthamiana* leaves using StrepII-tag-based affinity chromatography. Protein purification success was analyzed via SDS-PAGE (upper row) and Western Blotting using an HRP-conjugated Strep-tagII antibody (lower row). S0, crude sample; S1, sample after initial centrifugation; S2, sample after passing desalting column; W1-W4, washing steps; beads, Strep-Tactin beads after elution; elution, eluted fraction; dialysed, eluted fraction after dialysis.

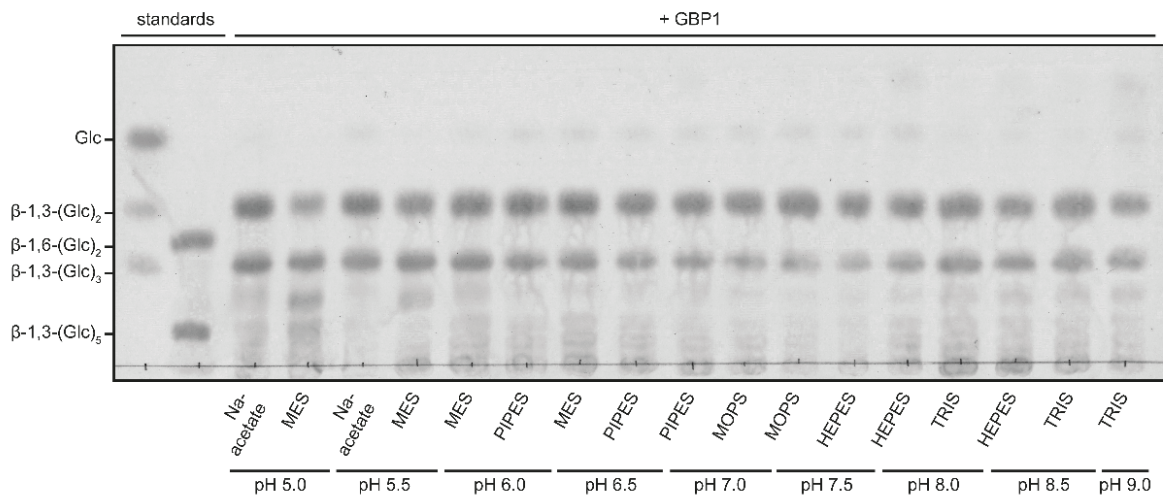
A

Thin layer chromatography of temperature-dependent digestion of laminarin



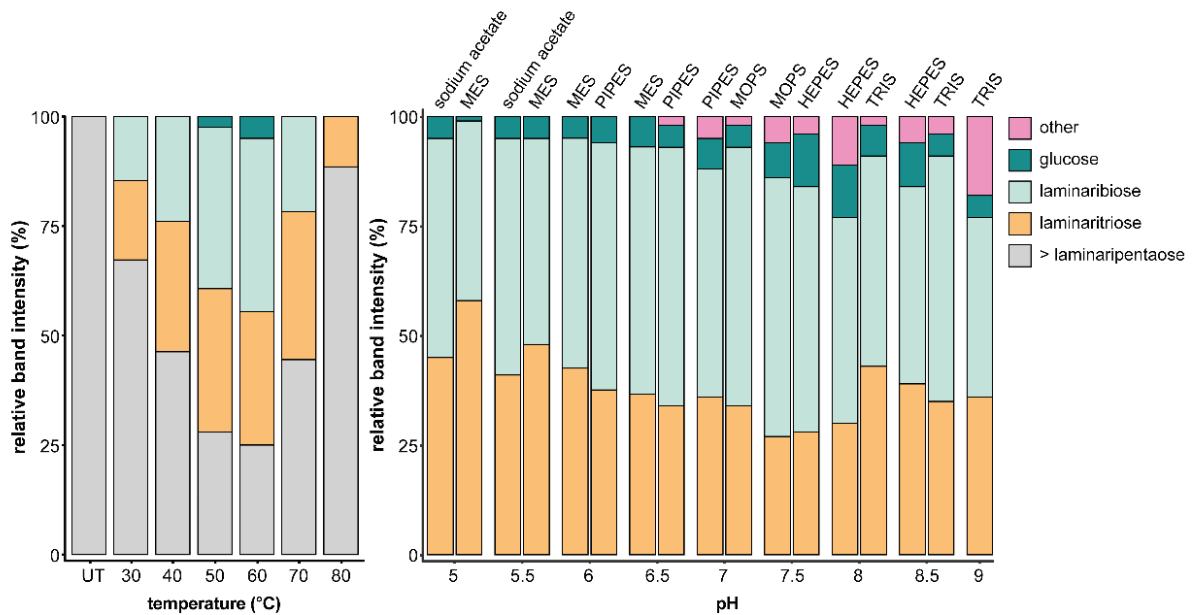
B

Thin layer chromatography of buffer-dependent digestion of laminarin

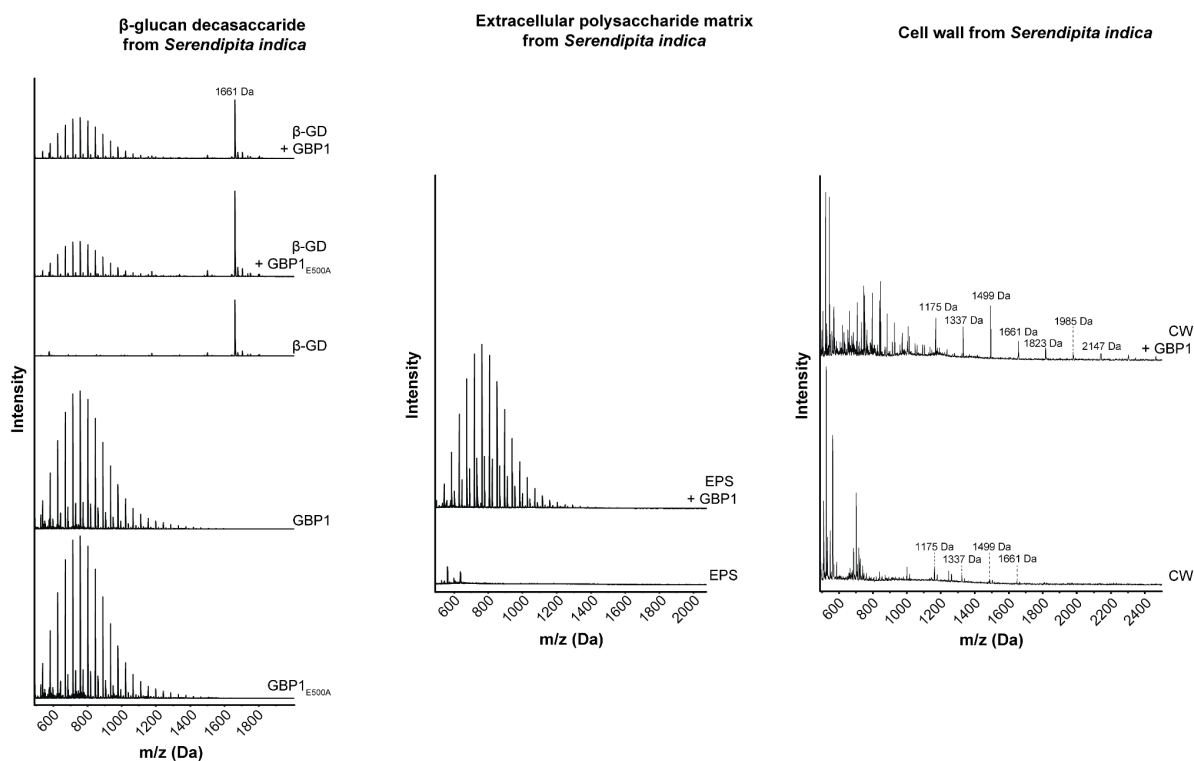


C

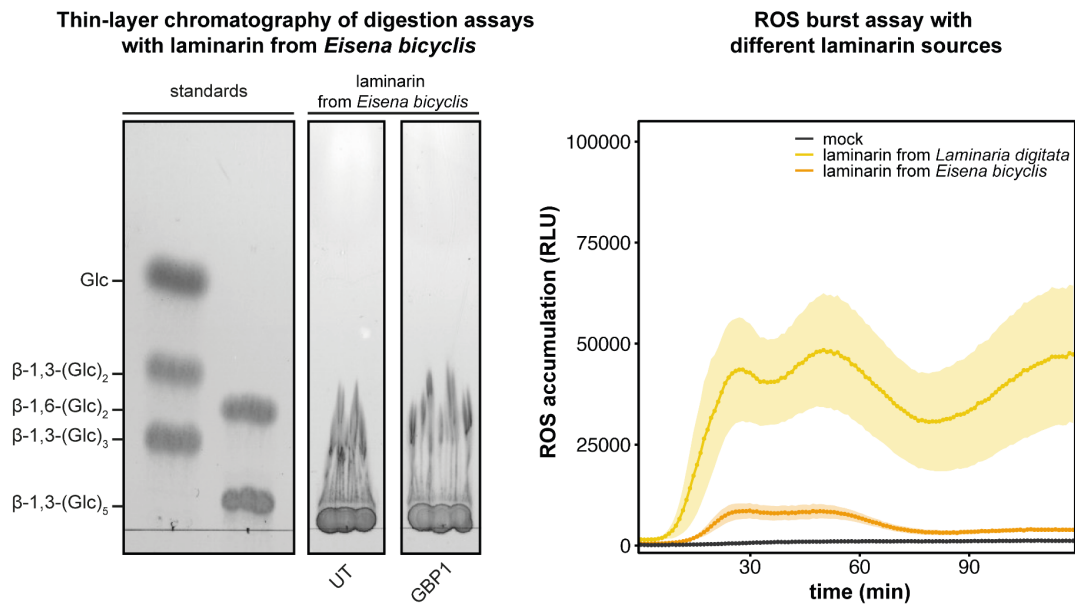
Quantification of thin layer chromatography



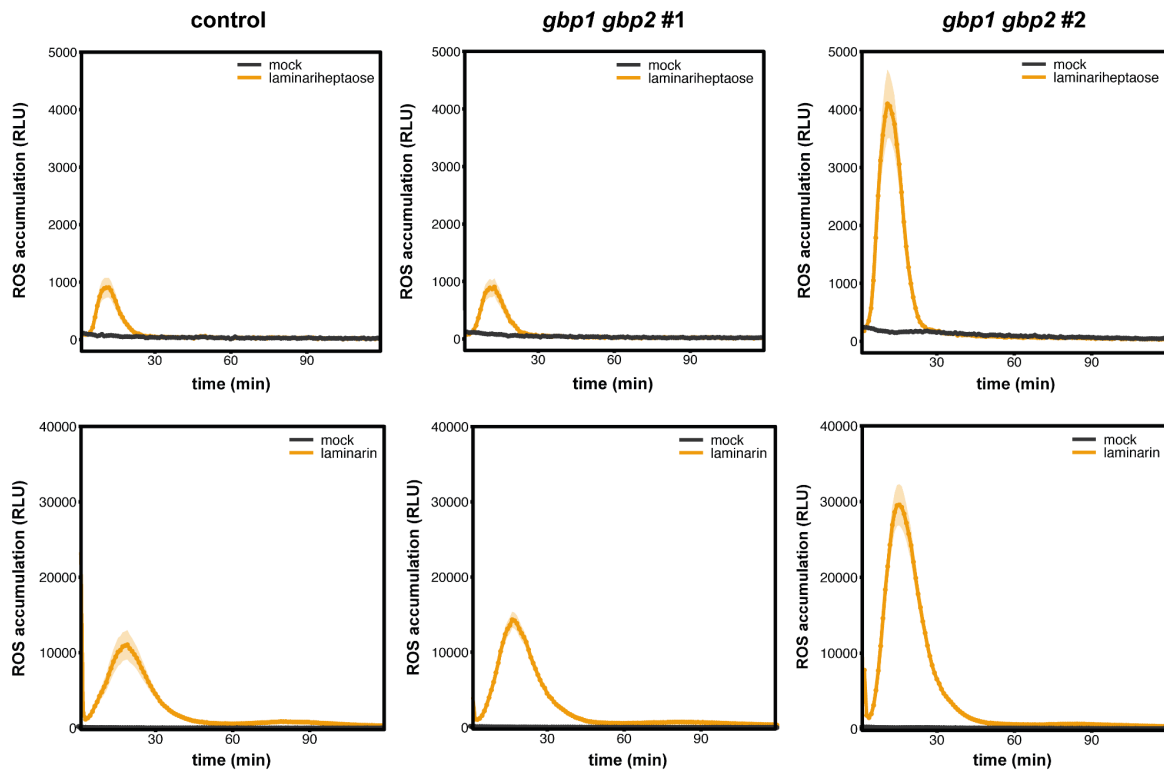
**Supplementary Figure 9. Temperature- and buffer-dependency of GBP1 activity on laminarin.** Products from GBP1-catalyzed laminarin digestion assays were separated by thin layer chromatography (A+B). (A) Laminarin ( $4 \text{ mg}\cdot\text{mL}^{-1}$ ) was digested with GBP1 (70 nM) for 10 min at different temperatures. Sample without enzymes (UT) was mock digested at  $80^\circ\text{C}$ . (B) Laminarin ( $4 \text{ mg}\cdot\text{mL}^{-1}$ ) was digested with purified GBP1 (70 nM) in different buffers (10 mM, pH 5-9). Digestions were performed at  $60^\circ\text{C}$  for 10 min. (C) Quantification of thin layer chromatography band intensities using the ImageJ software. UT, untreated sample.



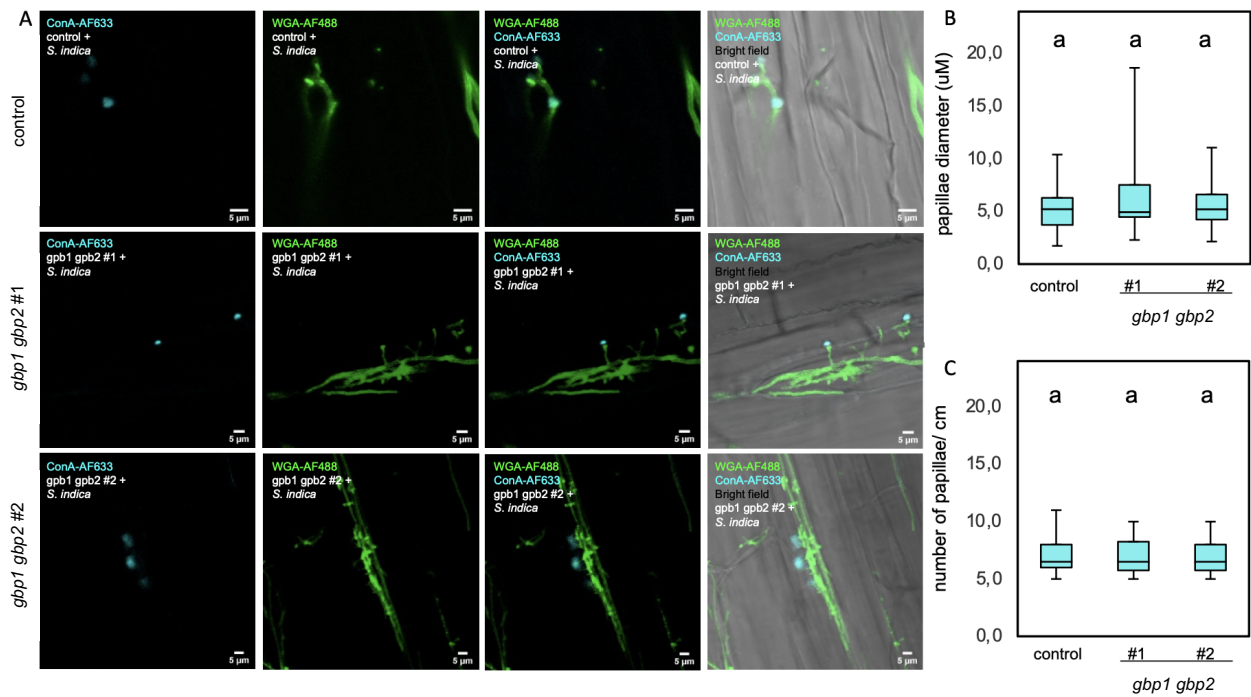
**Supplementary Figure 10.** Analysis of GBP1-digested  $\beta$ -GD, EPS, or CW fractions from *Serendipita indica* by MALDI-TOF mass spectrometry. While GBP1 does not act on the EPS matrix and the derived  $\beta$ -GD from *S. indica*, it releases minor oligosaccharide fractions from the CW. Oligosaccharide peaks of interest were labeled with  $m/z$  (M+Na)<sup>+</sup> masses. The digestion assays using the  $\beta$ -GD were performed two times with similar results and the digestion assays using the EPS and CW were performed once.  $\beta$ -GD,  $\beta$ -glucan decasaccharide; CW, cell wall; EPS, extracellular polysaccharides.



**Supplementary Figure 11. Highly branched laminarin from *Eisena bicyclis* is inert to GBP1 hydrolysis and triggers only low production of ROS in barley roots.** (A) Laminarin from *E. bicyclis* (2.4 mM) was digested with GBP1 (72 nM) for 1 h at 60°C. The digestion products were analyzed by thin layer chromatography. (B) Apoplastic ROS accumulation after treatment of barley root pieces with laminarin from either *Laminaria digitata* (low  $\beta$ -1,3-branching frequency) or *E. bicyclis* (high  $\beta$ -1,3-branching frequency) was monitored by ROS burst assay. Treatment with Milli-Q water (mock) was used as control. Values represent mean  $\pm$  SEM from eight wells. ROS, reactive oxygen species. UT, untreated.

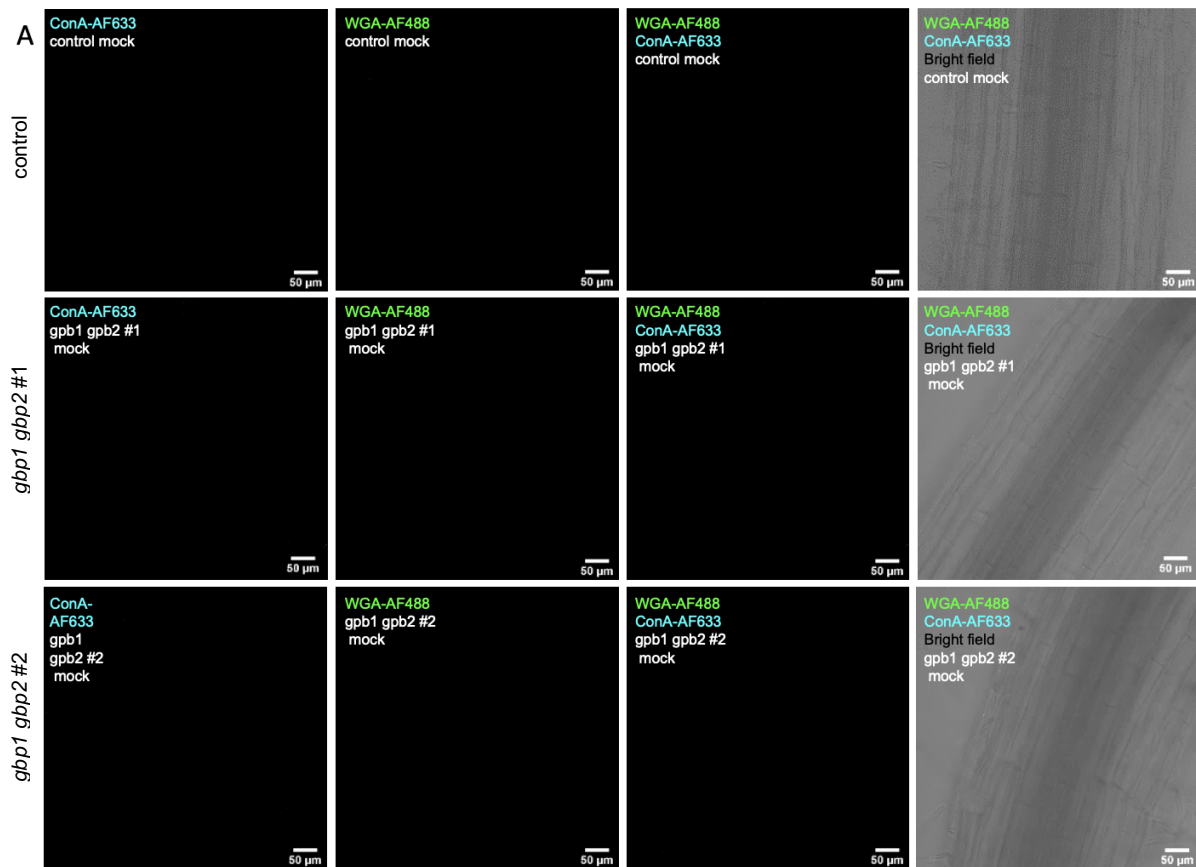


**Supplementary Figure 12. ROS burst assays in *gbp1 gbp2* mutant lines.** Apoplastic ROS accumulation after treatment of barley roots with laminariheptaose (250  $\mu\text{M}$ ) and laminarin (4  $\text{mg}\cdot\text{mL}^{-1}$ ) was tested in control and *gbp1 gbp2* mutant lines. Treatment with Milli-Q water (mock) was used as control. Values represent mean  $\pm$  SEM from 16 wells. Experiment was performed twice with similar results. ROS, reactive oxygen species.



**Supplementary Figure 13. The number and size of papillae upon *S. indica* colonization does not differ between the control and *gbp1 gbp2* mutant lines.** (A) *S. indica*-colonized roots of the barley control line and *gbp1 gbp2* mutant lines were stained with  $10 \mu\text{g mL}^{-1}$  concanavalin A (ConA-AF633, cyan) and wheat germ agglutinin (WGA-AF488, green) for visualization of papillae and fungal structures, respectively. Images were acquired using a confocal microscope. (B) The diameter of papillae found in barley control lines and *gbp1 gbp2* mutant lines colonized by *S. indica*. Data was analyzed using a one-way ANOVA ( $p = 0.05$ ). (C) Data were analyzed using a one-way ANOVA ( $p = 0.05$ ). ConA, concanavalin A, CW(A), cell wall (appositions), WGA, wheat germ agglutinin.





**Supplementary Figure 14. Control and *gpb1 gpb2* mutant lines do not form spontaneous papillae or CWAs in absence of fungal inoculation.** Roots of the barley control line and *gpb1 gpb2* mutant lines treated with water only were stained with  $10 \mu\text{g mL}^{-1}$  concanavalin A (ConA-AF633, cyan) and wheat germ agglutinin (WGA-AF488, green) for visualization of CWAs and fungal structures, respectively. Images were acquired using a confocal microscope. ConA, concanavalin A, CW(A), cell wall (appositions), WGA, wheat germ agglutinin.

**Supplementary Table 1.** Oligonucleotides used in this study.

<b>Oligo Name</b>	<b>Sequence</b>	<b>Purpose</b>
Clal_GBP1_F	5'-GACGGTATCGATAAAATGCCGCCACATGGTAGACG-3'	Cloning
GBP1_noSTOP_XmaI_R	5'-ATAACTCCGGGATGGCCATATTGACGATACCAACAGC-3'	Cloning
GBP1_E500A_F	5'-CAGGCATCAACATCAGAAGCAGTG-3'	Site-directed mutagenesis
GBP1_E500A_R	5'-GTTTCCTACCATCTCCAAACTCAGTC-3'	Site-directed mutagenesis
GBP1_gRNA1	5'-CCCCGGCAGCCTTCTTCGCGCCGG-3'	CRISPR/Cas9 gRNA
GBP1_gRNA2	5'-TGGCGCCTTCGGATGAACAGCGG-3'	CRISPR/Cas9 gRNA
GBP2_gRNA1	5'-TAAGATCCGTCGAGGCAGTATGG-3'	CRISPR/Cas9 gRNA
GBP2_gRNA2	5'-GTACAGCCGTTGCTACCCGACGG-3'	CRISPR/Cas9 gRNA
SvTEF_F	5'-ATCCCAAGCAAGCCAATGTG-3'	<i>Serendipita vermifera</i> colonization
SvTEF_R	5'-TGCCGTCAGTCTTCTCAACA-3'	<i>Serendipita vermifera</i> colonization
BsTEF_F	5'-CGCCGTACCGGAAAGTCTG-3'	<i>Bipolaris sorokiniana</i> colonization
BsTEF_R	5'-GGCGAAACGACCAAGAGGA-3'	<i>Bipolaris sorokiniana</i> colonization
HvUBI_F	5'-ACCCTCGCCGACTACAACAT-3'	qPCR primer for barley colonization
HvUBI_R	5'-CAGTAGTGGCGGTCGAAAGTG-3'	qPCR primer for barley colonization

# **Chapter 6**

## **Concluding Discussion**

In times of a steadily increasing population and climate change, food security is one of the hardest challenges of this century. With the additional rising *per capita* requirement for crops, current estimates project a surge of 100-110% in crop demand from 2005 to 2050 (Tilman *et al.*, 2011; Alexandratos & Bruinsma, 2012). Moreover, climate change burdens our agroecosystems in multiple ways. Increases in average temperature, elevated carbon dioxide levels as well as changes in irrigation frequency and intensity directly impact plant physiology and growth, contributing to lower nutritional quality with regards to protein and nutrient concentrations (Fernando *et al.*, 2014; Myers *et al.*, 2014; Dietterich *et al.*, 2015; Toreti *et al.*, 2020). Furthermore, extreme weather conditions in combination with our extensive management of crop- and grazing land are the main factors driving progressive land degradation, effectively decreasing the area suitable for agricultural purposes (IPBES, 2018). A recent model mapping agricultural suitability (“safe climatic spaces”) onto geographical zones predicts that drastic changes in aridity, temperature and precipitation will put a third (31%) of our current global food crop production at stake (Kummu *et al.*, 2021). Another emerging risk is the spread of plant pathogens into previously unaffected regions. While plant pathogens accounted for 17-31% of global crop production losses for the major five crops in 2019, there is evidence that overall exposure to pathogens will increase (Bebber *et al.*, 2014; Yan *et al.*, 2017; Shukla *et al.*, 2019; Savary *et al.*, 2019; Ristaino *et al.*, 2021; Chaloner *et al.*, 2021). Recently, a report demonstrated the first sampling of the blast fungus *Magnaporthe spp.* in central Europe (Barragan *et al.*, 2022). Isolates which have been found on wild grass foxtail millet were able to infect crops like barley and wheat under laboratory conditions, highlighting an emerging risk for grain production in these areas (Barragan *et al.*, 2022).

To curtail this devastating trend, fundamental research on plant immunity has improved traditional breeding and given rise to a plethora of transgenic and non-transgenic “new plant breeding” technologies to improve pathogen resistance (Lusser & Davies, 2013). Among these, popular examples include marker-assisted breeding using resistance and susceptibility genes as molecular markers (Jena & Mackill, 2008; Hückelhoven *et al.*, 2013; Engelhardt *et al.*, 2018), targeting induced local lesions in genomes known as TILLING (McCallum *et al.*, 2000; Dong *et al.*, 2009; Slade & Moehs, 2012; Desiderio *et al.*, 2016), R gene enrichment sequencing-based breeding strategies (Jupe *et al.*, 2013; Steuernagel *et al.*, 2016; Witek *et al.*, 2016; Arora *et al.*,

2019), chemical immunity priming (Conrath *et al.*, 2015), spray-induced gene silencing (Qiao *et al.*, 2021; Niño-Sánchez & Sambasivam, 2022), genome engineering including editing of susceptibility genes (Li *et al.*, 2012; Steuernagel *et al.*, 2016; Wang *et al.*, 2016; Peng *et al.*, 2017) and introducing suites of receptors to introduce resistance (Foster *et al.*, 2009; Lacombe *et al.*, 2010; Horvath *et al.*, 2012). Recent advances in our understanding of NLRs through structural biology have enabled us to not only mutate receptors in order to alter or broaden their recognition spectrum, but also to *de novo* bioengineer immune receptors against new microbial target molecules (Kourelis *et al.*, 2021; Marchal *et al.*, 2022). While some of the approaches mentioned have been already successfully implemented into agricultural practice, global regulations concerning the legal definition of transgenic plant material and their introduction into fields has hampered the full exploitation of resistant germplasm (Langner *et al.*, 2018).

While most of this translational research is based on the huge progress that has been made on host perception of microbial proteins, several factors have impeded similar contributions from research on glycan perception. CW-related glycans as well as secreted glycan messengers commonly occur among many plant pathogens and symbionts from different kingdoms as well in plants themselves; they strongly vary in monomer composition, linkage pattern, and three-dimensional conformation (Wanke *et al.*, 2021). The complex chemo-physical properties glycans impede both their contamination-free purification from biological sources as well as *de novo* synthesis. While recent progress in automated approaches has pushed chemical synthesis of defined carbohydrates forward, this is mainly restricted to minor amounts of short glycans (Guberman & Seeberger, 2019; Ross & Farrell, 2021).

Fungal  $\beta$ -1,3-glucans illustrate well the difficulties outlined above. The general role of  $\beta$ -1,3-glucans as elicitors of plant immunity is widely acknowledged (Fesel & Zuccaro, 2016). However, a systematic survey of the correlation between  $\beta$ -1,3-glucan substrate and immunity activation is difficult as the use of substrates across studies is inconsistent. Furthermore, older studies use complex  $\beta$ -1,3-glucan extractions from different microbes that lack proper characterization.

To improve our understanding on the perception of  $\beta$ -glucans in plant-fungal interactions, we have reviewed the latest literature on the role of glycans in plant-microbe interactions (**Chapter 2**, Wanke *et al.*, 2021). Furthermore, we have

performed a systematic screen with two  $\beta$ -glucans of different length and branching pattern in selected monocot and dicot species (**Chapter 3**, Wanke *et al.*, 2020). Glycomic and proteomic analyses of the CW from plant-associated fungi have functionally characterized the outer  $\beta$ -glucan-enriched EPS matrix surrounding hyphae (**Chapter 4**, Chandrasekar *et al.*, 2022). Finally, we have investigated the role of host glucanases in the release of  $\beta$ -glucans (**Chapter 4**, Chandrasekar *et al.*, 2022) and fungal compatibility (**Chapter 5**, Wanke *et al.*, in preparation). While the individual results were discussed within the respective chapters, the following paragraphs summarize the findings presented in this thesis, contextualize them within a broader understanding of plant immunity and plant-microbe interactions, and outline future challenges in glycan immunity research.

### **Reassessing our understanding of the fungal CW structure: a three-layer model for plant-colonizing fungi**

Fungal CWs are among the first fungal structures that are in physical contact with the host immune system, therefore representing an important target for the host to detect the presence of a (potentially harmful) invader (Roy & Klein, 2012; Fesel & Zuccaro, 2016). Furthermore, CW composition and shape are crucial for successful colonization, for which reason they have been studied for decades to develop fungicide agents in both medicine and agriculture (Piotrowski *et al.*, 2015; Gow *et al.*, 2017; Revie *et al.*, 2018; García *et al.*, 2021). Most CW models were based on methodologies that require chemical extraction of carbohydrates (e.g. carbohydrate monomer and linkage analyses), providing only limited information on spatial architecture and biophysical properties of the CW (Fontaine *et al.*, 2000; François, 2006). Recent advances in non-destructive approaches like solid-state NMR spectroscopy (Kang *et al.*, 2018; Chakraborty *et al.*, 2021) as well as novel microscopic probes derived from secreted fungal lectins (Wawra *et al.*, 2016, 2019) have contributed relevant insights into fungal CW topology. Based on previous literature as well as observations in our lab, we propose a three-layer CW model for plant-colonizing fungi, i.e. a rigid inner chitin layer, a hydrated outer CW layer and a mobile,  $\beta$ -glucan-rich EPS layer only loosely connected to the mobile layer (**Chapter 2**, Figure 1). The hydrophobic chitin microfibrils serve as stiff scaffolds, which can be covalently linked to the  $\beta$ -1,3/1,4/1,6-glucans in the mobile phase (Fontaine *et al.*,

2000; Kang *et al.*, 2018). Compared to the inner skeletal layer, this outer layer undergoes more dynamic changes based on the environmental conditions, as for example observed in the plant-colonizing fungus *Colletrichum graminicola*. *C. graminicola* actively downregulates  $\beta$ -glucan content in its CW during biotrophic stages to conceal immunogenic fragments (Oliveira-Garcia & Deising, 2013, 2016). The exposed site of the outer CW layer often contains additional immunological inert glycan and protein decorations to further shield the outer CW layer (Pettolino *et al.*, 2009; Gow *et al.*, 2017; Geoghegan *et al.*, 2017; Mérida *et al.*, 2018). The inner and outer CW layers represent the fungal CW *sensu stricto*. In addition, cytological analyses with fluorescently labeled versions of the  $\beta$ -1,3/1,6-glucan-binding effectors FGB1 and WSC3 from *S. indica* have revealed that hyphae of phylogenetically unrelated fungi with different lifestyles are covered by a soluble  $\beta$ -1,3/1,6-enriched EPS matrix (Wawra *et al.*, 2016, 2019). While such EPS matrices have been studied in human pathogenic fungi (Gow *et al.*, 2017), only few reports are available for plant-colonizing fungi (Ruel & Joseleau, 1991; El Oirdi *et al.*, 2011; Scarpari *et al.*, 2017; Op De Beeck *et al.*, 2020). Our work on the EPS matrices of *S. indica* and *B. sorokiniana* provides the first comparative approach that uses glycomics, proteomics and immunological methodologies to functionally characterize both the CW *sensu stricto* and the EPS matrix (**Chapter 4**). Our analyses show that both CW layers represent separate CW compartments with distinct carbohydrate and protein signatures (**Chapter 4**; Figure 2). While both *S. indica* CW and EPS mainly consist of  $\beta$ -glucans, the CW exhibits a higher fraction of  $\beta$ -1,4-glucans and the EPS is dominated by  $\beta$ -1,3/1,6-glucans (**Chapter 4**; Figure 2C). These differential compositions are also reflected by the corresponding proteoms of those compartments. While the CW is enriched in lectins (e.g. FGB1, thaumatin), the EPS matrix associates with WSC-domain proteins and acts as an enzymatic scaffold for proteases and CAZymes (**Chapter 4**; Figure 2B, Supplementary Figure 2). Furthermore, we demonstrated that a GH17 glucanase that is secreted upon fungal colonization is hijacked by the fungus to release an immunologically inert, highly  $\beta$ -1,6-branched  $\beta$ -GD fragment that exhibits antioxidant activity and promotes fungal colonization (**Chapter 4**; Figures 3, 4 and 5). Altogether, our work stresses how these distinct CW compartments fulfil different roles in plant-fungal interactions. Reverse genetics of the corresponding EPS genes in *S. indica* would enable us to further investigate the role of the EPS matrix in fungal development, stress resilience to biotic and abiotic factors and plant colonization.



Altogether our work highlights the abundance and relevance of  $\beta$ -glucans in fungal cell walls across the fungal kingdom. Previous studies on *Candida albicans* EPS have revealed that CW and EPS synthesis are mediated by different genes and pathways (Taff *et al.*, 2012; Mitchell *et al.*, 2015).

### **Length does matter: principles behind DP-dependent, species-specific perception of $\beta$ -1,3-glucans**

Our systematic survey of short, unbranched  $\beta$ -1,3-glucans (i.e. laminarihexaose) and long, branched  $\beta$ -1,3/1,6-glucans (i.e. laminarin) revealed that the DP instead of branching pattern explains the observed differences in immunity activation among the screened plant species (**Chapter 3**). Receptor specificities for a defined DP range of glycan oligomers are common in glycan perception and can be observed for the perception of chitooligomers (Cao *et al.*, 2014; Bozsoki *et al.*, 2017; Feng *et al.*, 2019), cellooligomers (Aziz *et al.*, 2007; Johnson *et al.*, 2018), LPS O-chain-derived oligorhamnans (Bedini *et al.*, 2005), peptidoglycan (Liu *et al.*, 2014), mixed-linkage glucans (Rebaque *et al.*, 2021; Barghahn *et al.*, 2021) and oligogalacturonides (Côté & Hahn, 1994; Ferrari *et al.*, 2013). The optimal DP of a ligand for each of these ligand-receptor complexes is defined by the minimal chain length that is needed to assemble the receptor complex (consisting of one or few receptor proteins that physically interact with the ligand) and the maximal chain length that does not sterically hinder receptor complex assembly. Most elicitors from microbial cell surface glycans are released through host hydrolases and progressively digested into short oligomers or even monomers. This means that (mean) elicitor DPs in the apoplastic elicitor will vary throughout time, which has several implications for the perception of these glycan elicitors. In a scenario of constantly hydrolyzed elicitors, it is advantageous that most receptors bind ligands of a wide DP range because it increases the timespan of successful perception. Furthermore, continuous degradation of the produced glycans prevents overaccumulation of immunogenic fragments in the apoplast, which can cause harmful hyperimmunity (Benedetti *et al.*, 2018; Locci *et al.*, 2019). This highlights that hydrolase secretion must be well timed to produce the right amount of receptor ligand. A case study with the *Arabidopsis* peptidoglycan-degrading chitinase LYS1 has shown that both loss-of-function mutants as well as overexpression lines of LYS1 exhibit decreased peptidoglycan-triggered immune responses and

consequently increased susceptibility to the pytopathogenic bacterium *Pseudomonas syringae* pv. tomato DC300 (Liu *et al.*, 2014). This supports the claim that hydrolytic activity in the apoplast needs to be finely tuned for successful host defence.

We have demonstrated that recognition of short-chain and long-chain  $\beta$ -1,3-glucans depends on different perception machineries. Furthermore, we have shown that long-chain  $\beta$ -1,3-glucan perception in monocots and dicots is independent of the central carbohydrate co-receptor CERK1 (**Chapter 3**, Figures 4 and 5, Supplementary Figure 8). A possible explanation for this non-canonical perception pathway is the helical secondary structure of long  $\beta$ -1,3-glucans that promotes the association of three  $\beta$ -1,3-glucan molecules into a triple-helical quaternary structure (Deslandes *et al.*, 1980; Okobira *et al.*, 2008). This supramolecular structure was demonstrated to be important for  $\beta$ -1,3-glucan binding to insect  $\beta$ -glucan-binding proteins and GH81 family hydrolases (Takahasi *et al.*, 2009; Kanagawa *et al.*, 2011; Qin *et al.*, 2017; Pluvinage *et al.*, 2017). Moreover, the mammalian  $\beta$ -1,3-glucan receptor Dectin-1 preferably binds to longer  $\beta$ -1,3-glucans due to the formation of a secondary structure with increasing DP (Hanashima *et al.*, 2014). Notably, LPS-derived oligorhamnans and pectin-derived oligogalacturonides are other immunogenic glycans with supramolecular structures (secondary and quaternary structures) that are perceived in a CERK1-independent way. With increasing chain length, oligorhamnans form coils that enhance the induction of PR-1 gene expression in *Arabidopsis* (Bedini *et al.*, 2005). Oligogalacturonide oligomers form in presence of cations so-called egg box dimers, which enhance binding to the wall-associated kinase 1 (WAK1) receptor and promote extracellular alkalinization in *Arabidopsis* cell suspensions. Altogether, this prompts the notion that glycans with higher order structures are generally perceived in a non-canonical, CERK1-independent manner. This is further corroborated by crystallographic and computational approaches which demonstrate that CERK1 primarily mediates binding to linear glycan oligomers (Liu *et al.*, 2012; Hierro *et al.*, 2021).

To dissect the correlation between DP, higher order structure and activation of plant immunity, systematic analysis of a substrate set of  $\beta$ -1,3-glucans with DPs ranging from 3 to 30 would be insightful. Such a substrate set could be either generated by automated glycan synthesis or partial digestion of laminarin followed by preparative high performance liquid chromatography. Furthermore, chemical pretreatments (e.g.

with sodium hydroxide) that open the triple helical structure could be performed to assess whether  $\beta$ -1,3-glucan triplex formation is crucial for the perception of long-chain  $\beta$ -1,3-glucans in barley and *N. benthamiana*.

### Frequent branching of $\beta$ -1,3-glucans: a single solution for many problems

While  $\beta$ -1,3-backbones with  $\beta$ -1,6-substituted glucose are very commonly found in fungi and oomycetes, there is no report of  $\beta$ -1,6-linked glucans in plants. In fact, there is no genetic evidence that plants possess the enzymatic machinery to synthesize or degrade these types of linkages, making  $\beta$ -1,6-glucans a suitable target for plants to detect non-self pattern (Nars *et al.*, 2013). To our surprise, perception of long-chain  $\beta$ -1,3/1,6-glucans like laminarin is unaffected by the removal of its  $\beta$ -1,6-side chains, highlighting that the difference in perception pattern is due to chain length (and supramolecular structure) rather than branching pattern (**Chapter 3**). Since laminarin from *L. digitata* has a low degree of branching (approx. one branch every seven backbone units), we cannot exclude that  $\beta$ -1,3-glucans with higher branching frequencies are perceived via a machinery that relies on these substitutions. However, highly substituted short-chain  $\beta$ -1,3-glucans like the isolated  $\beta$ -GD laminarin from fungal EPS matrices and long-chain  $\beta$ -1,3-glucans like laminarin from *E. bicyclis* (both presenting a branch every second backbone unit) are not at all or only poorly perceived by barley (**Chapter 4 and 5**). The low immunogenic potential of laminarin from *E. bicyclis* can possibly be explained by the observation that the helical pitch of  $\beta$ -1,3-glucans proportionally decreases with increasing frequency of  $\beta$ -1,3-substitutions (Okobira *et al.*, 2008). This further supports the assumption that the supramolecular structure of long-chain  $\beta$ -1,3-glucans is important for its perception.

It was unexpected to see that  $\beta$ -GD does escape barley's immunity surveillance despite the similarity of its  $\beta$ -1,3-backbone to immunogenic laminariheptaose (**Chapter 4**, Figure 4, Supplementary Figure 13). Dense  $\beta$ -1,6-substitutions were shown to sterically interfere with the binding pockets of  $\beta$ -1,3-glucanases (Pluvinage *et al.*, 2017). Such sterical hindrance may well explain why  $\beta$ -GD can neither be perceived by the corresponding short-chain  $\beta$ -1,3-glucan receptor, nor further degraded by HvBGLUII. Furthermore, high  $\beta$ -1,6-substitution mediated the observed antioxidant properties of  $\beta$ -GD, enabling  $\beta$ -GD to scavenge host-produced ROS (**Chapter 4**, Figure 5). Our work therefore demonstrates that high frequency  $\beta$ -1,6-

substitutions of fungal CW  $\beta$ -1,3-glucans fulfill a dual role: they shield hydrolase-released MAMPs from host perception and facilitate fungal colonization due to its antioxidant activity. This principle seems to be conserved among plant-colonizing fungi since EPS matrices from evolutionary distant clades both presented similar  $\beta$ -1,6-substitution patterns (**Chapter 4**, Supplementary Figure 15-18). In this context, bacterial GH30 exo- $\beta$ -1,6-glucanases like FbGH30 that debranch laminarins could be an useful tool (Becker *et al.*, 2017). As a proof-of-principle experiment, it would be interesting to test whether overexpressing a secreted version FbGH30 in barley would be able to enhance fungal resistance (Becker *et al.*, 2017).

### **Perspectives on the elusive plant $\beta$ -1,3-glucan receptor(s)**

Previous work has demonstrated that the central carbohydrate co-receptor CERK1 is necessary for the recognition of the short-chain  $\beta$ -1,3-glucan laminarihexaose in *Arabidopsis* (Mélida *et al.*, 2018). Since laminarihexaose does not directly bind to CERK1, it remains unclear which receptor mediates the physical interaction with the substrate (Hierro *et al.*, 2021). As previously discussed, perception of long-chain  $\beta$ -1,3-glucans in *N. benthamiana* and rice is CERK1-independent (**Chapter 3**), demonstrating that there are at least two unrelated  $\beta$ -1,3-glucan receptor systems in plants. Previous work on an isolated oomycete CW heptagluco-side with a  $\beta$ -1,6-linked backbone and  $\beta$ -1,3-glucans branches showed that GBP from soybean was necessary to mount defense responses upon recognition of this heptagluco-side (Umemoto *et al.*, 1997). A GBP-specific antibody which abolished heptagluco-side binding prevented the production of phytoalexins. Since soybean GBP hydrolyzes  $\beta$ -1,3-glucans, it cannot be excluded that it is involved in tailoring the substrate for the downstream receptor rather than contributing as a direct receptor. As perception of the heptagluco-side is specific to legumes, a long-standing question in the field was whether GBPs in non-legumes mediate perception of other  $\beta$ -1,3-glucan-type elicitors (Fliegmann *et al.*, 2004). In this context, we have demonstrated that the only two GBP paralogs are not essential for short-chain and long-chain  $\beta$ -1,3-glucan perception in barley (**Chapter 5**, Supplementary Figure 12).

Another interesting candidate is the recently identified receptor for bacterial EPS, EPR3 (Kawaharada *et al.*, 2015, 2017). Together with the Nod factor receptors NFR1 and NFR5 in *Lotus japonicus*, EPR3 constitutes the second part of a two-step

surveillance mechanism to safeguard bacterial compatibility during the establishment of rhizobia-legume root nodule symbiosis. With its derived LysM domain secondary structures, EPR3 represents a promiscuous receptor for branched  $\beta$ -glucans with predominantly  $\beta$ -1,3/1,4/1,6-linked backbones (Wong *et al.*, 2020). Since EPR3 homologs can be detected in the genomes of non-nodulating plants, the authors speculate that EPR3 might be involved more generally in the perception of complex  $\beta$ -glucans across the plant kingdom (Wong *et al.*, 2020). Taking the observed decline in fungal compatibility in barley *gbp1 gbp2* mutants into account (Chapter 5, Figure 1C, Supplementary Figures 6 and 7), it would be interesting to address whether barley GBPs contribute to the release of a compatibility-relevant substrate for such an EPR3 homolog.

Intensive research in medicine has given rise to a plethora of  $\beta$ -1,3-glucan receptors in mammalian model systems, including humans (*e.g.* Dectin-1, Complement Receptor 3) (Brown & Gordon, 2003). Although sequence similarity approaches have not detected suitable receptor homologues in plants, recent advances in artificial intelligence-based protein structure prediction algorithms like AlphaFold will enable us to use large-scale structural information to mine plant genomes for putative receptor candidates (Jumper *et al.*, 2021). With the efforts of DeepMind and the European Bioinformatics Institute (EMBL-EBI) to catalog protein structural models of every predicted protein (Callaway, 2022), future approach in the field should use confirmed  $\beta$ -1,3-glucan-binding structural folds from non-plant receptors and  $\beta$ -1,3-glucan-binding enzymes to screen entire plant proteoms.

### **Complex roles of glucan hydrolases in plant immunity**

Plant  $\beta$ -1,3-glucanases have been known to be implicated in plant development and plant-microbe interactions for a long time. During plant development, they contribute to microspore and pollen development (Worrall *et al.*, 1992; Hird *et al.*, 1993; Bucciaglia & Smith, 1994; Wan *et al.*, 2011), pollen tube extension (Roggen & Stanley, 1969), seed development and germination (Vogeli-Lange *et al.*, 1994; Leubner-Metzger *et al.*, 1995; Leubner-Metzger, 2003; Petruzzelli *et al.*, 2003; Branco *et al.*, 2011), bud dormancy (Krabel *et al.*, 1993), plasmodesmata permeability (Wu *et al.*, 2018), abiotic stress response (Brederode *et al.*, 1991; Hinch *et al.*, 1997; Yaish *et al.*, 2006) as well as protection against invading filamentous microbes (Cutt & Klessig,

1992; Meins *et al.*, 1992; Boller, 1993). In the context of plant immunity,  $\beta$ -1,3-endoglucanases became popular as pathogenesis-related proteins group 2 (PR-2) crucial for plant defense. By intracellularly regulating callose turnover at plasmodesmata, they are involved in cell-to-cell movement of viruses (Beffa *et al.*, 1996; Iglesias & Meins, 2000; Zavaliev *et al.*, 2013; Chowdhury *et al.*, 2020). Furthermore, secreted  $\beta$ -1,3-endoglucanases do not only directly weaken invading fungi and oomycetes by processing their  $\beta$ -glucan-rich CW glycans but also release  $\beta$ -glucan fragments, which act as elicitors of plant defense responses (Perrot *et al.*, 2022). Disintegration of the microbial CW additionally exposes inner CW layers to other host hydrolases (e.g. chitinases) and increases the likelihood of MAMP release and microbial detection (Rovenich *et al.*, 2016; Wanke *et al.*, 2021).

The presented work in **Chapter 4** and **Chapter 5** further extends our understanding of  $\beta$ -1,3-glucanases and their contribution to plant immunity. We demonstrate that in addition to their canonical role as *apoplastic guardians* amplifying plant immunity,  $\beta$ -1,3-glucanases can positively contribute to fungal colonization. Barley BGLUIII is hijacked by phylogenetically distant fungi to release the antioxidant  $\beta$ -GD from their EPS matrices (**Chapter 4**), whereas barley GBP1/2 serves as a broad-range compatibility factor for fungal colonization (**Chapter 5**). While it seems counterintuitive that possible loopholes for pathogenic interactions are not lost throughout evolution, both  $\beta$ -1,3-glucanases equally contribute to colonization by beneficial fungi. Moreover, BGLUIII additionally hydrolyzed laminariheptaose into highly immunogenic fragments (**Chapter 4**, Supplementary Figure 13). To broaden the impact our findings, it would be important to test whether similar effects can be observed for the corresponding glucanase homologues in other monocots (e.g. *Brachypodium distachyon*, available T-DNA library) and dicots (e.g. Arabidopsis). Although plants secrete a multitude of  $\beta$ -glucanases with different substrate affinities and hydrolytic modes, all the experiments in this thesis have been performed with individual  $\beta$ -1,3-glucanases. A combined approach including proteomics, glycosidase activity profiling (Chandrasekar *et al.*, 2014) and glycomics on deconstructed *in vitro* (*i.e.* extracted apoplastic fluids and fungal CW and EPS fractions) and *in vivo* (*i.e.* apoplastic fluids during fungal colonization) samples would provide a comprehensive picture of the glycomic landscape during plant-fungal interactions

### Fungal EPS matrices - looking beyond plant-fungal interactions

EPS matrices with high  $\beta$ -1,3/1,6-glucan contexts are broadly conserved in plant-associated fungi, including Basidiomycetes and Ascomycetes (Wawra *et al.*, 2019). Since their phylogenetic divergence predates plant terrestrialization (Berbee & Taylor, 2010; James *et al.*, 2020), we can assume that their biological function extends beyond plant-fungal interactions. Previous studies revealed that lignocellulosic activity in the ectomycorrhizal Basidiomycete *Paxillus involutus* and the white rot fungus *Phanerochaete chrysosporium* are associated with the secretion of an EPS matrix that acts as scaffold for lignin peroxidases (Ruel & Joseleau, 1991; Op De Beeck *et al.*, 2020). Degradation of lignin is mediated by the generation of hydroxyl radicals. The authors speculate that these EPS matrices are relevant to accumulate the necessary enzymatic machinery for lignin degradation, to create a suitable microenvironment (e.g. pH, ionic strength) for the biochemical catalysis and to protect the fungus from oxidative damage through its radical scavenging activity (Op De Beeck *et al.*, 2020). These examples showcase that EPS matrices are functionally relevant for saprophytic lifestyles.

At the same time, EPS matrices represent a carbohydrate-rich, nutritious environment for other microbes that can hydrolytically degrade it into their building blocks. Since fungi and bacteria secrete  $\beta$ -1,3-glucanases (Gastebois *et al.*, 2010; Becker *et al.*, 2017), it is very likely that resilient branching patterns and antioxidant  $\beta$ -glucan oligomers in fungal EPS matrices were already relevant for microbe-microbe interactions before plants arrived in terrestrial ecosystems. Interestingly, we have observed that the fungal EPS matrix of *S. indica* drastically changes its architecture when colonized by root-associated bacteria (**Chapter 2**, Figure 2). This is further supported by the observation that inter-kingdom biofilms between bacteria and fungi jointly shape their surrounding EPS matrices, with each of the partners contributing their enzymatic toolkit to synthesize and degrade EPS material (Mitchell *et al.*, 2015; van Overbeek & Saikkonen, 2016; Miquel Guennoc *et al.*, 2018). Similar to the biofilm formation between the mycobiont and photobiont in lichen symbioses, these EPS-mediated assemblies could be relevant for the formation and resilience of compatible microbial consortia. Future studies should investigate the impact of EPS matrices in inter-kingdom biofilms on plant immunity. In particular, it will be important to assess



their contribution to microbiota assembly and stability, as well as their glycomic signatures that can be perceived by plants.

### **Final remarks**

The structural complexity of glycans creates a vast space of possibilities for biochemical dialog, ranging from bipartite communication between a single plant and microbe to interkingdom communication within a complex microbial community. Within the framework of this thesis, we have conceptually advanced our understanding of glycans in plant-microbe interactions, ranging from fungal CW architectures to their molecular perception. We have shown that in addition to the communicative potential of glycans, many glycan fragments come with biochemical activities that extend their function beyond simple messengers. Based on this groundwork, many future research directions emerge. Given the wide spread of EPS matrices in fungi and bacteria, derived glycan fragments might similarly function as carbohydrate effectors in microbe-microbe interactions. Furthermore, EPS matrices and their associated enzymatic capacity shapes the decomposition of organic matter, hence drastically shaping our soil ecosystems. Future studies will need to assess how agrochemicals like fertilizers and pesticides impact EPS production, composition, and reactivity. Understanding how glycans are processed and sensed within a complex microbiota context will contribute to an integrated view of plant-microbe-microbe interactions. This work has tremendous potential to inform our agricultural practices in the face of future environmental challenges.

## References

- Alexandratos, N. and Bruinsma, J.** (2012) World agriculture towards 2030/2050: the 2012 revision. Available at: <https://ageconsearch.umn.edu/record/288998/>.
- Arora, S., Steuernagel, B., Gaurav, K., et al.** (2019) Resistance gene cloning from a wild crop relative by sequence capture and association genetics. *Nat. Biotechnol.*, **37**, 139–143.
- Aziz, A., Gauthier, A., Bézier, A., Poinssot, B., Joubert, J.-M., Pugin, A., Heyraud, A. and Baillieul, F.** (2007) Elicitor and resistance-inducing activities of beta-1,4 cellodextrins in grapevine, comparison with beta-1,3 glucans and alpha-1,4 oligogalacturonides. *J. Exp. Bot.*, **58**, 1463–1472.
- Barghahn, S., Arnal, G., Jain, N., Petutschnig, E., Brumer, H. and Lipka, V.** (2021) Mixed Linkage  $\beta$ -1,3/1,4-Glucan Oligosaccharides Induce Defense Responses in *Hordeum vulgare* and *Arabidopsis thaliana*. *Front. Plant Sci.*, **12**, 682439.
- Bebber, D.P., Holmes, T. and Gurr, S.J.** (2014) The global spread of crop pests and pathogens. *Glob. Ecol. Biogeogr.*, **23**, 1398–1407.
- Bedini, E., De Castro, C., Erbs, G., Mangoni, L., Dow, J.M., Newman, M.-A., Parrilli, M. and Unverzagt, C.** (2005) Structure-dependent modulation of a pathogen response in plants by synthetic O-antigen polysaccharides. *J. Am. Chem. Soc.*, **127**, 2414–2416.
- Beffa, R.S., Hofer, R.M., Thomas, M. and Meins, F., Jr** (1996) Decreased Susceptibility to Viral Disease of beta-1,3-Glucanase-Deficient Plants Generated by Antisense Transformation. *Plant Cell*, **8**, 1001–1011.
- Berbee, M.L. and Taylor, J.W.** (2010) Dating the molecular clock in fungi – how close are we? *Fungal Biol. Rev.*, **24**, 1–16.
- Boller, T.** (1993) Antimicrobial Functions of the Plant Hydrolases, Chitinase and  $\beta$ -1,3-Glucanase. In B. Fritig and M. Legrand, eds. *Mechanisms of Plant Defense Responses*. Dordrecht: Springer Netherlands, pp. 391–400.
- Bozsoki, Z., Cheng, J., Feng, F., et al.** (2017) Receptor-mediated chitin perception in legume roots is functionally separable from Nod factor perception. *Proc. Natl. Acad. Sci. U. S. A.*, **114**, E8118–E8127.
- Branco, A.T., Dos Santos Ferreira, B., Lourenço, G.F., Lopes Marques, V.C., Tavares Machado, O.L., Pereira, M.G., Aquino Almeida, J.C. and Souza Filho, G.A. de** (2011) Induction of  $\beta$ -1,3-glucanase in seeds of maize defective-kernel mutant (827Kpro1). *Protein Pept. Lett.*, **18**, 651–657.
- Brederode, F.T., Linthorst, H.J. and Bol, J.F.** (1991) Differential induction of acquired resistance and PR gene expression in tobacco by virus infection, ethephon treatment, UV light and wounding. *Plant Mol. Biol.*, **17**, 1117–1125.
- Brown, G.D. and Gordon, S.** (2003) Fungal beta-glucans and mammalian immunity. *Immunity*, **19**, 311–315.
- Bucciaglia, P.A. and Smith, A.G.** (1994) Cloning and characterization of Tag 1, a tobacco anther beta-1,3-glucanase expressed during tetrad dissolution. *Plant Mol. Biol.*, **24**, 903–914.

- Cao, Y., Liang, Y., Tanaka, K., Nguyen, C.T., Jedrzejczak, R.P., Joachimiak, A. and Stacey, G.** (2014) The kinase LYK5 is a major chitin receptor in Arabidopsis and forms a chitin-induced complex with related kinase CERK1. *Elife*, **3**.
- Chakraborty, A., Fernando, L.D., Fang, W., Dickwella Widanage, M.C., Wei, P., Jin, C., Fontaine, T., Latgé, J.-P. and Wang, T.** (2021) A molecular vision of fungal cell wall organization by functional genomics and solid-state NMR. *Nat. Commun.*, **12**, 6346.
- Chaloner, T.M., Gurr, S.J. and Bebbler, D.P.** (2021) Plant pathogen infection risk tracks global crop yields under climate change. *Nat. Clim. Chang.*, **11**, 710–715.
- Chandrasekar, B., Colby, T., Emran Khan Emon, A., Jiang, J., Hong, T.N., Villamor, J.G., Harzen, A., Overkleef, H.S. and Hoorn, R.A.L. van der** (2014) Broad-range glycosidase activity profiling. *Mol. Cell. Proteomics*, **13**, 2787–2800.
- Chowdhury, R.N., Lasky, D., Karki, H., Zhang, Z., Goyer, A., Halterman, D. and Rakotondrafara, A.M.** (2020) HCPPro Suppression of Callose Deposition Contributes to Strain-Specific Resistance Against Potato Virus Y. *Phytopathology*, **110**, 164–173.
- Conrath, U., Beckers, G.J.M., Langenbach, C.J.G. and Jaskiewicz, M.R.** (2015) Priming for enhanced defense. *Annu. Rev. Phytopathol.*, **53**, 97–119.
- Côté, F. and Hahn, M.G.** (1994) Oligosaccharins: structures and signal transduction. *Plant Mol. Biol.*, **26**, 1379–1411.
- Cutt, J.R. and Klessig, D.F.** (1992) Pathogenesis-related Proteins. In T. Boller and F. Meins, eds. *Genes Involved in Plant Defense*. Vienna: Springer Vienna, pp. 209–243.
- Desiderio, F., Torp, A.M., Valè, G. and Rasmussen, S.K.** (2016) TILLING in plant disease control. In *Plant Pathogen Resistance Biotechnology*. Hoboken, NJ: John Wiley & Sons, Inc, pp. 365–384.
- Deslandes, Y., Marchessault, R.H. and Sarko, A.** (1980) Triple-Helical Structure of (1→3)-β-D-Glucan. *Macromolecules*, **13**, 1466–1471.
- Dietterich, L.H., Zanobetti, A., Kloog, I., et al.** (2015) Impacts of elevated atmospheric CO<sub>2</sub> on nutrient content of important food crops. *Scientific Data*, **2**, 1–8..
- Dong, C., Dalton-Morgan, J., Vincent, K. and Sharp, P.** (2009) A modified TILLING method for wheat breeding. *Plant Genome*, **2**, 39–47.
- El Oirdi, M., El Rahman, T.A., Rigano, L., El Hadrami, A., Rodriguez, M.C., Daayf, F., Vojnov, A. and Bouarab, K.** (2011) Botrytis cinerea manipulates the antagonistic effects between immune pathways to promote disease development in tomato. *Plant Cell*, **23**, 2405–2421.
- Feng, F., Sun, J., Radhakrishnan, G.V., et al.** (2019) A combination of chitooligosaccharide and lipochitooligosaccharide recognition promotes arbuscular mycorrhizal associations in *Medicago truncatula*. *Nat. Commun.*, **10**, 1–12.
- Fernando, N., Panozzo, J., Tausz, M., Norton, R.M., Neumann, N., Fitzgerald, G.J. and Seneweera, S.** (2014) Elevated CO<sub>2</sub> alters grain quality of two bread wheat cultivars grown under different environmental conditions. *Agric. Ecosyst. Environ.*, **185**, 24–33.
- Ferrari, S., Savatin, D.V., Sicilia, F., Gramegna, G., Cervone, F. and Lorenzo, G.D.** (2013) Oligogalacturonides: plant damage-associated molecular patterns and regulators of growth and development. *Front. Plant Sci.*, **4**, 49.

- Fesel, P.H. and Zuccaro, A.** (2016)  $\beta$ -glucan: Crucial component of the fungal cell wall and elusive MAMP in plants. *Fungal Genet. Biol.*, **90**, 53–60.
- Fliegmann, J., Mithofer, A., Wanner, G. and Ebel, J.** (2004) An ancient enzyme domain hidden in the putative beta-glucan elicitor receptor of soybean may play an active part in the perception of pathogen-associated molecular patterns during broad host resistance. *J. Biol. Chem.*, **279**, 1132–1140.
- Fontaine, T., Simenel, C., Dubreucq, G., Adam, O., Delepierre, M., Lemoine, J., Vorgias, C.E., Diaquin, M. and Latgé, J.-P.** (2000) Molecular organization of the alkali-insoluble fraction of *Aspergillus fumigatus* cell wall. *J. Biol. Chem.*, **275**, 27594–27607.
- Foster, S.J., Park, T.-H., Pel, M., Brigneti, G., Sliwka, J., Jagger, L., Vossen, E. van der and Jones, J.D.G.** (2009) Rpi-vnt1.1, a Tm-2(2) homolog from *Solanum venturii*, confers resistance to potato late blight. *Mol. Plant. Microbe. Interact.*, **22**, 589–600.
- François, J.M.** (2006) A simple method for quantitative determination of polysaccharides in fungal cell walls. *Nat. Protoc.*, **1**, 2995–3000.
- García, R., Itto-Nakama, K., Rodríguez-Peña, J.M., et al.** (2021) Poacic acid, a  $\beta$ -1,3-glucan-binding antifungal agent, inhibits cell-wall remodeling and activates transcriptional responses regulated by the cell-wall integrity and high-osmolarity glycerol pathways in yeast. *FASEB J.*, **35**, e21778.
- Gastebois, A., Mouyna, I., Simenel, C., Clavaud, C., Coddeville, B., Delepierre, M., Latgé, J.-P. and Fontaine, T.** (2010) Characterization of a new beta(1-3)-glucan branching activity of *Aspergillus fumigatus*. *J. Biol. Chem.*, **285**, 2386–2396.
- Geoghegan, I., Steinberg, G. and Gurr, S.** (2017) The Role of the Fungal Cell Wall in the Infection of Plants. *Trends Microbiol.*, **25**, 957–967.
- Guberman, M. and Seeberger, P.H.** (2019) Automated Glycan Assembly: A Perspective. *J. Am. Chem. Soc.*, **141**, 5581–5592.
- Hanashima, S., Ikeda, A., Tanaka, H., Adachi, Y., Ohno, N., Takahashi, T. and Yamaguchi, Y.** (2014) NMR study of short  $\beta$ (1-3)-glucans provides insights into the structure and interaction with Dectin-1. *Glycoconj. J.*, **31**, 199–207.
- Hincha, D.K., Meins, F., Jr and Schmitt, J.M.** (1997) [ $\beta$ ]-1,3-Glucanase Is Cryoprotective in Vitro and Is Accumulated in Leaves during Cold Acclimation. *Plant Physiol.*, **114**, 1077–1083.
- Hird, D.L., Worrall, D., Hodge, R., Smartt, S., Paul, W. and Scott, R.** (1993) The anther-specific protein encoded by the *Brassica napus* and *Arabidopsis thaliana* A6 gene displays similarity to beta-1,3-glucanases. *Plant J.*, **4**, 1023–1033.
- Horvath, D.M., Stall, R.E., Jones, J.B., Pauly, M.H., Vallad, G.E., Dahlbeck, D., Staskawicz, B.J. and Scott, J.W.** (2012) Transgenic Resistance Confers Effective Field Level Control of Bacterial Spot Disease in Tomato. *PLoS ONE*, **7**, e42036. Available at: h6.
- Hückelhoven, R., Eichmann, R., Weis, C., Hoefle, C. and Proels, R.K.** (2013) Genetic loss of susceptibility: a costly route to disease resistance? *Plant Pathol.*, **62**, 56–62.
- Iglesias, V.A. and Meins, F., Jr** (2000) Movement of plant viruses is delayed in a  $\beta$ -1, 3-glucanase-deficient mutant showing a reduced plasmodesmatal size exclusion limit and enhanced callose deposition. *Plant J.*, **21**, 157–166.

- IPBES** (2018) Summary for policymakers of the assessment report on land degradation and restoration of the Intergovernmental SciencePolicy Platform on Biodiversity and Ecosystem Services. Available at: <https://zenodo.org/record/3237411>.
- James, T.Y., Stajich, J.E., Hittinger, C.T. and Rokas, A.** (2020) Toward a Fully Resolved Fungal Tree of Life. *Annu. Rev. Microbiol.*, **74**, 291–313.
- Jena, K.K. and Mackill, D.J.** (2008) Molecular markers and their use in marker-assisted selection in rice. *Crop Sci.*, **48**, 1266–1276.
- Johnson, J.M., Thürich, J., Petutschnig, E.K., et al.** (2018) A Poly(A) Ribonuclease Controls the Cellotriose-Based Interaction between *Piriformospora indica* and Its Host Arabidopsis. *Plant Physiol.*, **176**, 2496–2514.
- Jumper, J., Evans, R., Pritzel, A., et al.** (2021) Highly accurate protein structure prediction with AlphaFold. *Nature*, **596**, 583–589.
- Kanagawa, M., Satoh, T., Ikeda, A., Adachi, Y., Ohno, N. and Yamaguchi, Y.** (2011) Structural Insights into Recognition of Triple-helical  $\beta$ -Glucans by an Insect Fungal Receptor. *J. Biol. Chem.*, **286**, 29158–29165. Available at: [Accessed February 6, 2023].
- Kang, X., Kirui, A., Muszyński, A., Widanage, M.C.D., Chen, A., Azadi, P., Wang, P., Mentink-Vigier, F. and Wang, T.** (2018) Molecular architecture of fungal cell walls revealed by solid-state NMR. *Nat. Commun.*, **9**, 2747.
- Kawaharada, Y., Kelly, S., Nielsen, M.W., et al.** (2015) Receptor-mediated exopolysaccharide perception controls bacterial infection. *Nature*, **523**, 308–312.
- Kawaharada, Y., Nielsen, M.W., Kelly, S., et al.** (2017) Differential regulation of the Epr3 receptor coordinates membrane-restricted rhizobial colonization of root nodule primordia. *Nat. Commun.*, **8**, 1–11. Available at: [Accessed February 10, 2023].
- Kourelis, J., Marchal, C. and Kamoun, S.** (2021) NLR immune receptor-nanobody fusions confer plant disease resistance. *bioRxiv*. Available at: <http://biorxiv.org/lookup/doi/10.1101/2021.10.24.465418>.
- Krabel, D., Eschrich, W., Wirth, S. and Wolf, G.** (1993) Callase-(1,3- $\beta$ -d-glucanase) activity during spring reactivation in deciduous trees. *Plant Sci.*, **93**, 19–23.
- Kummu, M., Heino, M., Taka, M., Varis, O. and Vavrioli, D.** (2021) Climate change risks pushing one-third of global food production outside the safe climatic space. *One Earth*, **4**, 720–729.
- Lacombe, S., Rougon-Cardoso, A., Sherwood, E., et al.** (2010) Interfamily transfer of a plant pattern-recognition receptor confers broad-spectrum bacterial resistance. *Nat. Biotechnol.*, **28**, 365–369.
- Langner, T., Kamoun, S. and Belhaj, K.** (2018) CRISPR Crops: Plant Genome Editing Toward Disease Resistance. *Annu. Rev. Phytopathol.*, **56**, 479–512.
- Leubner-Metzger, G.** (2003) Functions and regulation of  $\beta$ -1,3-glucanases during seed germination, dormancy release and after-ripening. *Seed Sci. Res.*, **13**, 17–34. Available at: [Accessed November 27, 2022].
- Leubner-Metzger, G., Frundt, C., Vogeli-Lange, R. and Meins, F., Jr** (1995) Class I [beta]-1,3-Glucanases in the Endosperm of Tobacco during Germination. *Plant Physiol.*, **109**, 751–759.

- Li, T., Liu, B., Spalding, M.H., Weeks, D.P. and Yang, B.** (2012) High-efficiency TALEN-based gene editing produces disease-resistant rice. *Nat. Biotechnol.*, **30**, 390–392.
- Liu, T., Liu, Z., Song, C., et al.** (2012) Chitin-induced dimerization activates a plant immune receptor. *Science*, **336**, 1160–1164.
- Liu, X., Grabherr, H.M., Willmann, R., et al.** (2014) Host-induced bacterial cell wall decomposition mediates pattern-triggered immunity in Arabidopsis. *eLife*, **3**. Available at: <http://dx.doi.org/10.7554/elife.01990>.
- Locci, F., Benedetti, M., Pontiggia, D., Citterico, M., Caprari, C., Mattei, B., Cervone, F. and De Lorenzo, G.** (2019) An Arabidopsis berberine bridge enzyme-like protein specifically oxidizes cellulose oligomers and plays a role in immunity. *Plant J.*, **98**, 540–554.
- Lusser, M. and Davies, H.V.** (2013) Comparative regulatory approaches for groups of new plant breeding techniques. *N. Biotechnol.*, **30**, 437–446.
- Marchal, C., Pai, H., Kamoun, S. and Kourelis, J.** (2022) Emerging principles in the design of bioengineered made-to-order plant immune receptors. *Curr. Opin. Plant Biol.*, **70**, 102311.
- McCallum, C.M., Comai, L., Greene, E.A. and Henikoff, S.** (2000) Targeted screening for induced mutations. *Nat. Biotechnol.*, **18**, 455–457.
- Meins, F., Sperisen, C., Neuhaus, J.-M. and Ryals, J.** (1992) The Primary Structure of Plant Pathogenesis-related Glucanohydrolases and Their Genes. In T. Boller and F. Meins, eds. *Genes Involved in Plant Defense*. Vienna: Springer Vienna, pp. 245–282.
- Mélida, H., Sopena-Torres, S., Bacete, L., Garrido-Arandia, M., Jordá, L., López, G., Muñoz-Barrios, A., Pacios, L.F. and Molina, A.** (2018) Non-branched  $\beta$ -1,3-glucan oligosaccharides trigger immune responses in Arabidopsis. *Plant J.*, **93**, 34–49.
- Mitchell, K.F., Zarnowski, R., Sanchez, H., Edward, J.A., Reinicke, E.L., Nett, J.E., Mitchell, A.P. and Andes, D.R.** (2015) Community participation in biofilm matrix assembly and function. *Proc. Natl. Acad. Sci. U. S. A.*, **112**, 4092–4097.
- Myers, S.S., Zanobetti, A., Kloog, I., et al.** (2014) Increasing CO<sub>2</sub> threatens human nutrition. *Nature*, **510**, 139–142.
- Nars, A., Lafitte, C., Chabaud, M., et al.** (2013) Aphanomyces euteiches cell wall fractions containing novel glucan-chitosaccharides induce defense genes and nuclear calcium oscillations in the plant host Medicago truncatula. *PLoS One*, **8**, e75039.
- Okobira, T., Miyoshi, K., Uezu, K., Sakurai, K. and Shinkai, S.** (2008) Molecular dynamics studies of side chain effect on the beta-1,3-D-glucan triple helix in aqueous solution. *Biomacromolecules*, **9**, 783–788.
- Oliveira-Garcia, E. and Deising, H.B.** (2016) Attenuation of PAMP-triggered immunity in maize requires down-regulation of the key  $\beta$ -1,6-glucan synthesis genes KRE5 and KRE6 in biotrophic hyphae of Colletotrichum graminicola. *Plant J.*, **87**, 355–375.
- Oliveira-Garcia, E. and Deising, H.B.** (2013) Infection structure-specific expression of  $\beta$ -1, 3-glucan synthase is essential for pathogenicity of *Colletotrichum graminicola* and evasion of  $\beta$ -glucan-triggered immunity in maize. *Plant Cell*, **25**, 2356–2378.

- Op De Beeck, M., Troein, C., Siregar, S., Gentile, L., Abbondanza, G., Peterson, C., Persson, P. and Tunlid, A.** (2020) Regulation of fungal decomposition at single-cell level. *ISME J.*, **14**, 896–905.
- Overbeek, L.S. van and Saikkonen, K.** (2016) Impact of Bacterial–Fungal Interactions on the Colonization of the Endosphere. *Trends Plant Sci.*, **21**, 230–242.
- Peng, A., Chen, S., Lei, T., Xu, L., He, Y., Wu, L., Yao, L. and Zou, X.** (2017) Engineering canker-resistant plants through CRISPR/Cas9-targeted editing of the susceptibility gene CsLOB1 promoter in citrus. *Plant Biotechnol. J.*, **15**, 1509–1519.
- Perrot, T., Pauly, M. and Ramírez, V.** (2022) Emerging Roles of  $\beta$ -Glucanases in Plant Development and Adaptive Responses. *Plants*, **11**. Available at: <http://dx.doi.org/10.3390/plants11091119>.
- Petruzzelli, L., Müller, K., Hermann, K. and Leubner-Metzger, G.** (2003) Distinct expression patterns of  $\beta$ -1,3-glucanases and chitinases during the germination of Solanaceous seeds. *Seed Sci. Res.*, **13**, 139–153. Available at: [Accessed November 27, 2022].
- Pettolino, F., Sasaki, I., Turbic, A., Wilson, S.M., Bacic, A., Hrmova, M. and Fincher, G.B.** (2009) Hyphal cell walls from the plant pathogen *Rhynchosporium secalis* contain (1,3/1,6)-beta-D-glucans, galacto- and rhamnmannans, (1,3;1,4)-beta-D-glucans and chitin. *FEBS J.*, **276**, 3698–3709.
- Piotrowski, J.S., Okada, H., Lu, F., et al.** (2015) Plant-derived antifungal agent poaic acid targets  $\beta$ -1,3-glucan. *Proc. Natl. Acad. Sci. U. S. A.*, **112**, E1490–7.
- Pluinage, B., Fillo, A., Massel, P. and Boraston, A.B.** (2017) Structural Analysis of a Family 81 Glycoside Hydrolase Implicates Its Recognition of  $\beta$ -1,3-Glucan Quaternary Structure. *Structure*, **25**, 1348–1359.e3.
- Qiao, L., Lan, C., Capriotti, L. and Ah-Fong, A.** (2021) Spray-induced gene silencing for disease control is dependent on the efficiency of pathogen RNA uptake. *Plant Biotechnol.*
- Qin, Z., Yang, D., You, X., Liu, Y., Hu, S., Yan, Q., Yang, S. and Jiang, Z.** (2017) The recognition mechanism of triple-helical  $\beta$ -1,3-glucan by a  $\beta$ -1,3-glucanase. *Chem. Commun.*, **53**, 9368–9371.
- Rebaque, D., Del Hierro, I., López, G., et al.** (2021) Cell wall-derived mixed-linked  $\beta$ -1,3/1,4-glucans trigger immune responses and disease resistance in plants. *Plant J.*, **106**, 601–615.
- Revie, N.M., Iyer, K.R., Robbins, N. and Cowen, L.E.** (2018) Antifungal drug resistance: evolution, mechanisms and impact. *Curr. Opin. Microbiol.*, **45**, 70–76.
- Ristaino, J.B., Anderson, P.K., Bebber, D.P., et al.** (2021) The persistent threat of emerging plant disease pandemics to global food security. *Proceedings of the National Academy of Sciences*, **118**, e2022239118.
- Roggen, H.P. and Stanley, R.G.** (1969) Cell-wall-hydrolysing enzymes in wall formation as measured by pollen-tube extension. *Planta*, **84**, 295–303.
- Ross, P. and Farrell, M.P.** (2021) The Road to Structurally Defined  $\beta$ -Glucans. *Chem. Rec.*, **21**, 3178–3193.
- Rovenich, H., Zuccaro, A. and Thomma, B.P.H.J.** (2016) Convergent evolution of filamentous microbes towards evasion of glycan-triggered immunity. *New Phytol.*, **212**, 896–901.



- Roy, R.M. and Klein, B.S.** (2012) Dendritic cells in antifungal immunity and vaccine design. *Cell Host Microbe*, **11**, 436–446.
- Ruel, K. and Joseleau, J.P.** (1991) Involvement of an Extracellular Glucan Sheath during Degradation of Populus Wood by *Phanerochaete chrysosporium*. *Appl. Environ. Microbiol.*, **57**, 374–384.
- Savary, S., Willocquet, L., Pethybridge, S.J., Esker, P., McRoberts, N. and Nelson, A.** (2019) The global burden of pathogens and pests on major food crops. *Nat Ecol Evol*, **3**, 430–439.
- Scarpari, M., Reverberi, M., Parroni, A., et al.** (2017) Tramesan, a novel polysaccharide from *Trametes versicolor*. Structural characterization and biological effects. *PLoS One*, **12**, e0171412.
- Shukla, P.R., Skea, J., Calvo Buendia, E., et al.** (2019) IPCC, 2019: Climate Change and Land: an IPCC special report on climate change, desertification, land degradation, sustainable land management, food security, and greenhouse gas fluxes in terrestrial ecosystems. Available at: <https://spiral.imperial.ac.uk/bitstream/10044/1/76618/2/SRCCL-Full-Report-Compiled-191128.pdf>.
- Steuernagel, B., Periyannan, S.K., Hernández-Pinzón, I., et al.** (2016) Rapid cloning of disease-resistance genes in plants using mutagenesis and sequence capture. *Nat. Biotechnol.*, **34**, 652–655. Available at: [Accessed February 2, 2023].
- Taff, H.T., Nett, J.E., Zarnowski, R., Ross, K.M., Sanchez, H., Cain, M.T., Hamaker, J., Mitchell, A.P. and Andes, D.R.** (2012) A *Candida* biofilm-induced pathway for matrix glucan delivery: implications for drug resistance. *PLoS Pathog.*, **8**, e1002848.
- Takahasi, K., Ochiai, M., Horiuchi, M., Kumeta, H., Ogura, K., Ashida, M. and Inagaki, F.** (2009) Solution structure of the silkworm  $\beta$ GRP/GNBP3 N-terminal domain reveals the mechanism for  $\beta$ -1,3-glucan-specific recognition. *Proceedings of the National Academy of Sciences*, **106**, 11679–11684.
- Tilman, D., Balzer, C., Hill, J. and Befort, B.L.** (2011) Global food demand and the sustainable intensification of agriculture. *Proc. Natl. Acad. Sci. U. S. A.*, **108**, 20260–20264.
- Toreti, A., Deryng, D., Tubiello, F.N., et al.** (2020) Narrowing uncertainties in the effects of elevated CO<sub>2</sub> on crops. *Nature Food*, **1**, 775–782. Available at: [Accessed January 31, 2023].
- Umemoto, N., Kakitani, M., Iwamatsu, A., Yoshikawa, M., Yamaoka, N. and Ishida, I.** (1997) The structure and function of a soybean beta-glucan-elicitor-binding protein. *Proc. Natl. Acad. Sci. U. S. A.*, **94**, 1029–1034.
- Vogeli-Lange, R., Frundt, C., Hart, C.M., Beffa, R., Nagy, F. and Meins, F.** (1994) Evidence for a role of beta-1,3-glucanase in dicot seed germination. *Plant J.*, **5**, 273–278.
- Wang, F., Wang, C., Liu, P., Lei, C., Hao, W., Gao, Y., Liu, Y.-G. and Zhao, K.** (2016) Enhanced Rice Blast Resistance by CRISPR/Cas9-Targeted Mutagenesis of the ERF Transcription Factor Gene OsERF922. *PLoS One*, **11**, e0154027.
- Wanke, A., Malisic, M., Wawra, S. and Zuccaro, A.** (2021) Unraveling the sugar code: the role of microbial extracellular glycans in plant-microbe interactions. *J. Exp. Bot.*, **72**, 15–35.
- Wan, L., Zha, W., Cheng, X., et al.** (2011) A rice  $\beta$ -1,3-glucanase gene Osg1 is required for callose degradation in pollen development. *Planta*, **233**, 309–323.

- Wawra, S., Fesel, P., Widmer, H., et al.** (2016) The fungal-specific  $\beta$ -glucan-binding lectin FGB1 alters cell-wall composition and suppresses glucan-triggered immunity in plants. *Nat. Commun.*, **7**, 1–11. Available at: [Accessed November 27, 2022].
- Wawra, S., Fesel, P., Widmer, H., Neumann, U., Lahrmann, U., Becker, S., Hehemann, J.-H., Langen, G. and Zuccaro, A.** (2019) FGB1 and WSC3 are in planta-induced  $\beta$ -glucan-binding fungal lectins with different functions. *New Phytol.*, **222**, 1493–1506.
- Witek, K., Jupe, F., Witek, A.I., Baker, D., Clark, M.D. and Jones, J.D.G.** (2016) Accelerated cloning of a potato late blight–resistance gene using RenSeq and SMRT sequencing. *Nat. Biotechnol.*, **34**, 656–660.
- Wong, J.E.M.M., Gysel, K., Birkefeldt, T.G., et al.** (2020) Structural signatures in EPR3 define a unique class of plant carbohydrate receptors. *Nat. Commun.*, **11**, 1–8. Available at: [Accessed February 5, 2023].
- Worrall, D., Hird, D.L., Hodge, R., Paul, W., Draper, J. and Scott, R.** (1992) Premature dissolution of the microsporocyte callose wall causes male sterility in transgenic tobacco. *Plant Cell*, **4**, 759–771.
- Wu, S.-W., Kumar, R., Iswanto, A.B.B. and Kim, J.-Y.** (2018) Callose balancing at plasmodesmata. *J. Exp. Bot.*, **69**, 5325–5339.
- Yaish, M.W.F., Doxey, A.C., McConkey, B.J., Moffatt, B.A. and Griffith, M.** (2006) Cold-active winter rye glucanases with ice-binding capacity. *Plant Physiol.*, **141**, 1459–1472.
- Yan, Y., Wang, Y.-C., Feng, C.-C., Wan, P.-H.M. and Chang, K.T.-T.** (2017) Potential distributional changes of invasive crop pest species associated with global climate change. *Appl. Geogr.*, **82**, 83–92.
- Zavaliev, R., Levy, A., Gera, A. and Epel, B.L.** (2013) Subcellular dynamics and role of Arabidopsis  $\beta$ -1,3-glucanases in cell-to-cell movement of tobamoviruses. *Mol. Plant. Microbe. Interact.*, **26**, 1016–1030.

## Abbreviations

AM	arbuscular mycorrhiza
BGLUII	$\beta$ -1,3-glucanase II
bp	base pair
Ca <sup>2+</sup>	calcium cation
CAZymes	carbohydrate active enzyme
CbG	cyclic $\beta$ -glucan
CC	coiled coil
CDPK	calcium-dependent protein kinase
CO	chitooligomers
ConA	Concanavalin A
CW	cell wall
CWA	cell wall appositions
CWDE	cell wall degrading enzyme
Da	Dalton
DAMP	damage-associated molecular pattern
DP	degree of polymerization
dpi	days post inoculation
elf18	peptide (12 amino acids) derived from bacterial elongation factor Tu
EPS	extracellular polysaccharide
ETI	effector-triggered immunity
ETS	effector-triggered susceptibility
flg22	peptide (22 amino acids) derived from flagelin
GAG	galactosaminogalactan
GalXM	glucuronoxylomanogalactan
GBP	glucan-binding protein
GH	glycoside hydrolase
Glc	glucose
GlcNAc	N-acetylglucosamine
GXM	glucuronoxylomannan
HPAEC-PAD	high-performance anion exchange chromatography with pulsed amperometric detection
JA	jasmonic acid
KO	knock out
LC-MS/MS	liquid chromatography with tandem mass spectrometry
LCO	lipochitooligosaccharide
LPS	lipopolysaccharide
LysM	lysine motif
MALDI-TOF	matrix-assisted laser desorption/ionization-time of flight

MAMP	microbe-associated molecular pattern
MAPK	mitogen-activated protein kinase
NLR	nucleotide-binding, leucine-rich repeat receptors
NMR	nuclear magnetic resonance
Nod factor	nodulation factor
ON	over night
PAMP	pathogen-associated molecular pattern
PGN	peptidoglycan
PR	Pathogenesis-related
PRR	pattern recognition receptor
PTI	pattern-triggered immunity
qPCR	quantitative PCR
RLS	rhizobia-legume symbiosis
RLU	relative light units
ROS	reactive oxygen species
RT-PCR	real time polymerase chain reaction
SA	salicylic acid
TIR	Toll/interleukin-1 receptor
TLC	thin-layer chromatography
TLE	<i>Trichoderma harzianum</i> lysing enzymes
TRV	tobacco rattle virus
UBI	ubiquitin
WGA	wheat germ agglutinin
WSC	cell wall integrity and stress response components
WT	wild-type
β-GD	β-1,3-glucan decaaccharide

## Author contributions

### Chapter 2:

Wanke, A., Malisic, M., Wawra, S., & Zuccaro, A. (2021). Unraveling the sugar code: the role of microbial extracellular glycans in plant-microbe interactions. *Journal of Experimental Botany*, 72(1), 15–35. <https://doi.org/10.1093/jxb/eraa414>

Contributions: A.W., M.M., and A.Z. developed the concept of this review. All authors wrote the manuscript, A.W. coordinated the writing process. A.W. and S.W. prepared the figures; S.W. performed the microscopy. A.Z. supervised the project and acquired the funding.

### Chapter 3:

Wanke, A.\*, Rovenich, H.\*, Schwanke, F., Velte, S., Becker, S., Hehemann, J.-H., Wawra, S., & Zuccaro, A. (2020). Plant species-specific recognition of long and short  $\beta$ -1,3-linked glucans is mediated by different receptor systems. *The Plant Journal*, 102(6), 1142–1156. <https://doi.org/10.1111/tpj.14688>

\* equal contribution

Contributions: A.W., H.R., J.-H.H., S.W. and A.Z. conceived and planned the experiments. A.W., H.R., F.S., S.V. and S.B. carried out the experiments and analyzed the results. A.W., H.R. and A.Z. wrote the manuscript.

### Chapter 4:

Chandrasekar, B.\* , Wanke, A.\*, Wawra, S.\* , Saake, P., Mahdi, L., Charura, N., Neidert, M., Poschmann, G., Malisic, M., Thiele, M., Stühler, K., Dama, M., Pauly, M., & Zuccaro, A. (2022). Fungi hijack a ubiquitous plant apoplastic endoglucanase to release a ROS scavenging  $\beta$ -glucan decasaccharide to subvert immune responses. *The Plant Cell*, 34(7), 2765–2784. <https://doi.org/10.1093/plcell/koac114>

\* equal contribution

Contributions: B.C., A.W., S.W., and A.Z. conceived the study. S.W. established the protocols for the CW and EPS matrix extraction and performed the proteomics of EPS, CW, and culture filtrates together with G.P. and K.S. B.C. performed carbohydrate analytics (glycosyl linkage analysis of EPS and CW, MALDI-TOF, purification of  $\beta$ -GD for  $^1\text{H}$  NMR, and ROS burst assay). A.W. performed DAB assays and gene expression

analysis. A.W. and B.C. performed  $\beta$ -GD oxidation assays. A.W., S.W., P.S., M.N., M.M., M.T., N.C. performed the ROS burst assays, EPS and CW preparations, and enzymatic digestions. L.M. performed the colonization assays. M.D. contributed to the  $^1\text{H}$  NMR result interpretation. M.P. directed and supervised the carbohydrate analytics. A.Z. supervised the project, designed the experiments, and wrote the paper with contribution of all the authors.

### **Chapter 5:**

Wanke, A., van Boerdonk, S., Mahdi, L.K., Stephan Wawra S., Miriam Neidert, M., Chandrasekar, B., Saake, P., Saur, I., Acosta, I.F, Pauly, M., Derbyshire, P., Zipfel, C., Zuccaro, A. (2023). A GH81-type  $\beta$ -glucan-binding protein facilitates colonization by mutualistic fungi in barley. *In preparation*.

Contributions: A.W. and A.Z. conceived the study. S.W., P.D. and C.Z. supervised and performed the protein pull-down. L.M., S.v.B. and I.S. performed the fungal colonization assays. A.W., M.N. and P.S. performed the biochemical experiments. A.W and I.F.A. generated the barley CRISPR/Cas9 mutants. B.C. and M.P. directed and supervised the carbohydrate analytics. A. W. and A.Z. supervised the project, designed the experiments, and wrote the paper with contribution of all the authors.

## Acknowledgements

To Alga Zuccaro, for selecting me back in the days at the IMPRS symposium, for providing me with this intriguing topic that sparked my interest in plant-fungal interactions, for this excellent environment to develop – as a person and as a scientist.

To Ruben Garrido-Oter and Jane Parker, for your guidance, your feedback and scientific support throughout my doctorate as thesis advisory members and mentors.

To Bart Thomma and Jan Riemer, for kindly accepting to be part of my thesis defense committee.

To Stephan Wagner, for being such a fantastic and engaged graduate school coordinator and solid support throughout this thesis.

To Margaret Kox, for all the (admin and non-admin) support during and after my time in Cologne.

To all the collaborators who supported the work performed in the context of this thesis.

To Sebastian Schornack, for being an incredibly understanding line manager and mentor in challenging times.

To Hanna Rövenich, for being a wonderful colleague, a dear friend, and a true inspiration, for me and many others in science.

To Florian Schwanke, for your hard work and great company, in lab and in life.

To all the other students that contributed so valuably with their work and spirit: Stefanie Velte, Daniela Niedeggen, Dennis Mahr, Meik Thiele, Pia Saake, Milena Malisic, Nyasha Charura and Miriam Neidert.

To the entire Zuccaro group, for all the laughter, the board game nights and the *Sonnendeck* fun.

To the Schornack group and the SLCU community, for all whiskeys, SLOSHs and the massive support I got from you in the last two years.

To Zoe Nahas, for listening, for our garden walks, for making me laugh, and generally for being such an important friend to me.



To Enrico Sandro Collizi, Renkse Vroomans and Sebastian Moreno, for all the valuable time inside and outside of the SLCU.

To Wei Kheng Teh, Dorka Nemes and Rhiannon Hobbs, for all the banter, trips and dancing. For being my second family in England, for caring about me.

To Camila Alday, for provoking and inspiring me at the same time.

To Hannah Kikwitzki, for the wonderful memories we share from our times in Münster and Cologne, for your love and warmth that have shown me what it truly means to feel at home. For challenging me and my principles, for encouraging me to develop.

To Eduard Huber, for our undoubted connection since more than 20 years – many more to come. Brace yourself for 2036!

To Carlo Fischer, for being an incredible flat mate, study fellow, mathematics team partner and sincere friend throughout the years.

To Jonathan Friedrich, for our interdisciplinary and endless science chats, for the small and not-so-small revolutions and riots, for our activism.

To Hanna Schmid and Tim Lochschmidt, for your honest and genuine friendship, for showing me that it does not need kinship to be family.

To Claudius Garten and Alina Windzio, for the many years of sincere friendship and warm neighborship.

To the entire Viva con Agua crew in Cologne, Münster, Hamburg and across the globe, for teaching me the impacts of positive communication and the power of joy.

To Julia, Mats and Malou Cortnumme, for your trust and your love. For being my extended family and support in times when I needed it the most (and beyond!).

To my parents Iwona and Eugeniusz Wanke, for letting me be myself (the “crazy bird”) and trusting in me and all my decision. Your respect for who I am, your unconditional love and your full acceptance of me as a person is the greatest thing a child can experience. With every year I grow and learn, I realize that none of what I am, none of what I achieved would have been possible without many of your sacrifices and efforts.

“I don’t know whether my life has been a success or a failure. But not having any anxiety about becoming one instead of the other, and just taking things as they come along, I’ve had a lot of extra time to enjoy life.”

Harpo Marx (*Harpo speaks!*, 1961)

## Eidstattliche Erklärung

Ich versichere, dass ich die von mir vorgelegte Dissertation selbständig angefertigt, die benutzten Quellen und Hilfsmittel vollständig angegeben und die Stellen der Arbeit – einschließlich Tabellen, Karten und Abbildungen –, die anderen Werken im Wortlaut oder dem Sinn nach entnommen sind, in jedem Einzelfall als Entlehnung kenntlich gemacht habe; dass diese Dissertation noch keiner anderen Fakultät oder Universität zur Prüfung vorgelegen hat; dass sie – abgesehen von unten angegebenen Teilpublikationen – noch nicht veröffentlicht worden ist, sowie, dass ich eine solche Veröffentlichung vor Abschluss des Promotionsverfahrens nicht vornehmen werde.

Die Bestimmungen der Promotionsordnung sind mir bekannt. Die von mir vorgelegte Dissertation ist von Prof. Dr. Alga Zuccaro betreut worden.

Cambridge, 23. February 2023  

---

(Ort/Datum)

A. Wanke  

---

(Alan Wanke)

## About the author

### Alan Wanke

120 Warren Close, CB2 1LE, Cambridge, United Kingdom  
alan.wanke@slcu.cam.ac.uk,  
LinkedIn: [www.linkedin.com/in/alan-wanke](http://www.linkedin.com/in/alan-wanke)  
Twitter: @alan\_wanke



## Education & Work Experience

---

- since 01/2021 **Research Assistant**  
**Sainsbury Laboratory, University of Cambridge (United Kingdom)**
- Research topic: "Establishing Mucoromycotina fine root endophytes as model organism for mycorrhization"  
Supervisor: Dr. Sebastian Schornack
- 10/2016 – 12/2020 **Graduate Student**  
**University of Cologne**  
**International Max Planck Research School Fellow at the Max Planck Institute for Plant Breeding**
- PhD topic: "Innate sensing of  $\beta$ -glucans in plants"  
Supervisor: Prof. Dr. Alga Zuccaro  
Advisors: Prof. Dr. Jane E. Parker, Dr. Ruben Garrido-Oter  
Thesis Defense Committee: Prof. Dr. Bart Thomma, Prof. Dr. Jan Riemer
- 10/2013 – 09/2016 **M.Sc. Biosciences**  
**Westfälische Wilhelms-Universität Münster**  
Final grade: 1.1 (excellent/ A-grade)
- Master thesis: "Characterization of the key enzymes involved in inulin synthesis in *Taraxacum koksaghyz*"**  
Supervisor: Prof. Dr. Dirk Prüfer, grade: 1.1 (excellent/ A-grade)
- 10/2010 - 09/2013 **B.Sc. Biosciences**  
**Westfälische Wilhelms-Universität Münster**  
Final grade: 1.2 (excellent minus/ A-grade)
- Bachelor thesis: „Characterization of an EF-hand/thioredoxin domain protein in *Chlamydomonas reinhardtii*“**  
Supervisor: Prof. Dr. Michael Hippler, grade: 1.0 (excellent/ A-grade)
- 10/2009 - 09/2010 **B.Sc. Electrical Engineering (discontinued)**  
**Rheinisch Westfälische Technische Hochschule Aachen**
- 09/2000 - 06/2009 **Abitur at Theodor-Heuss-Gymnasiums**  
Radevormwald, Abitur/ A-levels (grade: 1.7, B-grade)

## International Experience

---

- 10/2014 - 11/2014      **Research Internship at Pontifica Universidad Católica de Valparaíso/ Fraunhofer Research Center for Systems Biotechnology Chile**  
Project: "Development of an RNA I dependent vector for the expression of eGFP regulated by ISAV infection"  
Prof. Dr. Sergio Marshall (PUCV, Fraunhofer Institute Chile)
- 08/2012 - 01/2013      **Semester abroad at Linköping University (Sweden)**

## Volunteering and Extracurricular Activities

---

- **Outreach initiative: "I'm a Scientist, get me out here!" (March 2023):** Digital chat sessions with school classes on life as a plant scientist
- **Green Week Cambridge (September 2022):** Organiser of citizen science event on fungal networks
- **Plantae Fellow (2022):** Scientific communication & public outreach
- **SLCU outreach committee: The Great British Liverwort Hunt (2021)**
- **Member of candidate selection panel at NRW.Talente Region Aachen (since 2022)**
- **Member of candidate selection panel at German Academic Scholarship Foundation ("Studienstiftung des deutschen Volkes") (since 2020)**
- **Founder and board member of NGO "Viva Movimiento e.V." (since 2018)**
- **Internal representative of Max Planck Institute for Plant Breeding (2017 -2019)**  
Representative for Graduate School PhDs at the University of Cologne
- **Voluntary service at Viva con Agua (since 2013)**  
National volunteer representative (Germany, 2018-2020)  
Contact person for volunteer coordination (Cologne, 2017-2020)  
Contact person for charity events (Münster, 2015-2016)
- **Hobbies:** dancing (Lindy Hop), road cycling, hiking

## Core Competences

---

<b>Plant cultivation</b>	Hands-on experience with a wide range of plant species: <i>Chlamydomonas reinhardtii</i> , <i>Marchantia polymorpha</i> , <i>Marchantia paleacea</i> , <i>Lunularia cruciata</i> , <i>Taraxacum koksaghyz</i> , <i>Arabidopsis thaliana</i> , <i>Nicotiana benthamiana</i> , <i>Medicago truncatula</i> , <i>Lotus japonicus</i> , <i>Brachypodium distachyon</i> , <i>Hordeum vulgare</i> , <i>Oryza sativa</i>
<b>Protein biochemistry methods</b>	Heterologous protein production ( <i>Escherichia coli</i> , <i>Pichia pastoris</i> , <i>Nicotiana benthamiana</i> ) Protein purification and functional protein characterisation
<b>Plant microbe interactions</b>	Plant immunity assays Fungal and oomycete infection assays and quantification Generation of plant mutants <i>via</i> CRISPR/Cas (Immuno)Histochemistry Confocal microscopy

<b>Computational methods</b>	Next-Generation Sequencing data analysis De novo genome assembly of fungi and plants R and R/Bioconductor/(Bio)Python Adobe Illustrator
<b>Project management/teamwork.</b>	Supervision of wet lab interns (regularly since 2017) Supervision of a bachelor thesis (2018 and 2020, 3 months) Supervision of a master thesis (2018, 6 months) Supervision of practical courses (2017-2020, approx. 3 weeks per year) Organisation of a seminar on civil protest movements for 100 participants, German Academic Scholarship Foundation (2015) Regular organisation of charity events for Viva con Agua (2014-2020)
<b>Work-related responsibilities</b>	Organisation of institute retreat (SLCU) Co-initiation and -organisation of a live stream service for seminars at the Max Planck Institute for Plant Breeding to the University of Cologne
<b>Languages</b>	German (native) Polish (native) English (fluent, oral and written) Spanish (basic, oral and written)
<b>Career development</b>	<p><b><i>Statistics and Programming</i></b> Statistical literacy and data visualisation in R (2020) Statistical data analysis with R (2018) Introduction to RNA-seq data analysis and ChIP-seq data analysis (2016) NGS Summer School (Arhus, Denmark) (2016)</p> <p><b><i>Science-related courses</i></b> Academic Storytelling (2023) Voice Projection (2022) Masterclass Proposal Writing (2022) Patenting (2019) Population genetics and quantitative genetics (2018) Life Science Program (Lebenswissenschaftliches Kolleg), Biophysics group, German Academic Scholarship Foundation (2014-2016) Project leader certificate for genetic engineering facilities according to §15GenTSV (regional government Düsseldorf) (2013)</p> <p><b><i>Non-scientific courses</i></b> Political management certificate (GreenCampus) (2020) Entrepreneurship, Strategy and Leadership for MINT students (2019)</p>

## Achievements

---

### Publications

1. **Wanke, A., van Boerdonk, S., Mahdi, L.K., Wawra S., Neidert, M., Chandrasekar, B., Saake, P., Saur, I., Acosta, I.F, Pauly, M., Derbyshire, P., Zipfel, C., Zuccaro, A. (2023).** A GH81-type  $\beta$ -glucan-binding protein facilitates colonization by mutualistic fungi in barley. *In preparation*.
2. **Teulet, A., Quan, C., Evangelisti, E., Wanke, A., Yang, W., Schornack, S. (2022).** "A Pathogen Effector FOLD Diversified in Symbiotic Fungi." *BioRxiv*. <https://doi.org/10.1101/2022.12.16.520752>
3. **Chandrasekar, B.\*, Wanke, A.\*, Wawra, S.\*, Saake, P., Mahdi, L., Charura, N., Neidert, M., Poschmann, G., Malisic, M., Thiele, M., Stühler, K., Dama, M., Pauly, M., Zuccaro, A. (2022).** Fungi hijack a ubiquitous plant apoplastic endoglucanase to release a ROS scavenging  $\beta$ -glucan decasaccharide to subvert immune responses. *The Plant Cell*, 34(7), 2765–2784. <https://doi.org/10.1093/plcell/koac114>
4. **Vanacore, A., Vitiello, G., Wanke, A., Cavasso, D., Clifton, L. A., Mahdi, L., Campanero-Rhodes, M. A., Solís, D., Wuhrer, M., Nicolardi, S., Molinaro, A., Marchetti, R., Zuccaro, A., Paduano, L., Silipo, A. (2022).** Lipopolysaccharide O-antigen molecular and supramolecular modifications of plant root microbiota are pivotal for host recognition. *Carbohydrate Polymers*, 277, 118839. <https://doi.org/10.1016/j.carbpol.2021.118839>
5. **Wanke, A., Malisic, M., Wawra, S., Zuccaro, A. (2021).** Unraveling the sugar code: the role of microbial extracellular glycans in plant-microbe interactions. *Journal of Experimental Botany*, 72(1), 15–35. <https://doi.org/10.1093/jxb/eraa414>
6. **Wanke, A.\*, Rovenich, H.\*, Schwanke, F., Velte, S., Becker, S., Hehemann, J.-H., Wawra, S., Zuccaro, A. (2020).** Plant species-specific recognition of long and short  $\beta$ -1,3-linked glucans is mediated by different receptor systems. *The Plant Journal*, 102(6), 1142–1156. <https://doi.org/10.1111/tpj.14688>
7. **Stolze, A., Wanke, A., van Deenen, N., Geyer, R., Prüfer, D., Schulze Gronover, C. (2017).** Development of rubber-enriched dandelion varieties by metabolic engineering of the inulin pathway. *Plant Biotechnology Journal*, 15: 740-753. <https://doi.org/10.1111/pbi.12672>

### Fellowships & Awards

- 2022: Appointment to Plantae Fellow (American Society of Plant Biology)
- 2013-2016: Scholarship from "German Academic Scholarship Foundation" ("Studienstiftung des deutschen Volkes")

### Conferences and Meetings

- 2023: Endosymbiosis seminar, Cambridge, UK (oral presentation)
- 2022: Entangled Life Symposium, Cambridge, UK (oral presentation)
- 2022: Gordon Research Conference: Spatial *and* Temporal Dynamics in Plant Biology, Holderness, USA (2 poster presentations)
- 2022: SLCU internal seminar (oral presentation)
- 2022: SLCU/TSL/Imperial College Symposium on Plant Immunity, Cambridge, UK
- 2021: Endosymbiosis seminar, Cambridge, UK (oral presentation)
- 2020: VISCEA Plant Biotic Stresses and Resistance Mechanisms IV, Vienna, Austria (oral presentation)

- 2019: 18<sup>th</sup> IS-MPMI Congress, Glasgow, Scotland (poster presentation)
- 2019: PhD Retreat of the International Max Planck Research School, Hennef, Germany (oral presentation)
- 2019: 30<sup>th</sup> Fungal Genetics Conference, Pacific Grove, USA (poster presentation)
- 2018: PhD Retreat of the International Max Planck Research School, Hennef, Germany (poster presentation)
- 2018: Food for Future Conference, Cologne, Germany
- 2017: 12<sup>th</sup> Symposium of the VAAM special group “Molecular Biology of Fungi”, Jena, Germany (poster presentation)
- 2017: PhD Retreat of the International Max Planck Research School, Hennef, Germany (oral presentation)